International Journal on Advances in Intelligent Systems

2013 vol. 6 nr. 1&2

The *International Journal on Advances in Intelligent Systems* is Published by IARIA.
ISSN: 1942-2679
journals site: http://www.iariajournals.org
contact: petre@iaria.org

Sponsored by IARIA
www.iaria.org

International Journal on Advances in Intelligent Systems
Volume 6, Number 1 & 2, 2013

Phan Cong-Vinh, NTT University, Vietnam
Christophe Cruz, University of Bourgogne, France
Beata Czarnacka-Chrobot, Warsaw School of Economics, Department of Business Informatics, Poland
Claudia d'Amato, University of Bari, Italy
Sérgio Roberto P. da Silva, Universidade Estadual de Maringá - Paraná, Brazil
Mirela Danubianu, "Stefan cel Mare" University of Suceava, Romania
Dragos Datcu, Netherlands Defense Academy / Delft University of Technology , The Netherlands
Antonio De Nicola, ENEA, Italy
Claudio de Castro Monteiro, Federal Institute of Education, Science and Technology of Tocantins, Brazil
Noel De Palma, Joseph Fourier University, France
Jan Dedek, Charles University in Prague, Czech Republic
Zhi-Hong Deng, Peking University, China
Stojan Denic, Toshiba Research Europe Limited, UK
Vivek S. Deshpande, MIT College of Engineering - Pune, India
Sotirios Ch. Diamantas, Pusan National University, South Korea
Leandro Dias da Silva, Universidade Federal de Alagoas, Brazil
Jerome Dinet, Univeristé Paul Verlaine - Metz, France
Jianguo Ding, University of Luxembourg, Luxembourg
Yulin Ding, Defence Science & Technology Organisation Edinburgh, Australia
Alexiei Dingli, University of Malta, Malta
Mihaela Dinsoreanu, Technical University of Cluj-Napoca, Romania
Ioanna Dionysiou, University of Nicosia, Cyprus
Roland Dodd, CQUniversity, Australia
Nima Dokoohaki, Royal Institute of Technology (KTH)-Kista, Sweden
Suzana Dragicevic, Simon Fraser University- Burnaby, Canada
Mauro Dragone, University College Dublin (UCD), Ireland
Marek J. Druzdzel, University of Pittsburgh, USA
Carlos Duarte, University of Lisbon, Portugal
Raimund K. Ege, Northern Illinois University, USA
Jorge Ejarque, Barcelona Supercomputing Center, Spain
Larbi Esmahi, Athabasca University, Canada
Simon G. Fabri, University of Malta, Malta
Umar Farooq, Amazon.com, USA
Mehdi Farshbaf-Sahih-Sorkhabi, Azad University - Tehran / Fanavaran co., Tehran, Iran
Anna Fensel, Semantic Technology Institute (STI) Innsbruck and FTW Forschungszentrum Telekommunikation Wien, Austria
Stenio Fernandes, Federal University of Pernambuco (CIn/UFPE), Brazil
Oscar Ferrandez Escamez, University of Utah, USA
Florin Filip, Romanian Academy, Romania
Agata Filipowska, Poznan University of Economics, Poland
Ziny Flikop, Scientist, USA
Adina Magda Florea, University "Politehnica" of Bucharest, Romania
Francesco Fontanella, University of Cassino and Southern Lazio, Italy
Panagiotis Fotaris, University of Macedonia, Greece
Enrico Francesconi, ITTIG - CNR / Institute of Legal Information Theory and Techniques / Italian National Research Council, Italy

Rita Francese, Università di Salerno - Fisciano, Italy
Bernhard Freudenthaler, Software Competence Center Hagenberg GmbH, Austria
Sören Frey, University of Kiel, Germany
Steffen Fries, Siemens AG, Corporate Technology - Munich, Germany
Somchart Fugkeaw, Thai Digital ID Co., Ltd., Thailand
Naoki Fukuta, Shizuoka University, Japan
Mathias Funk, Eindhoven University of Technology, The Netherlands
Adam M. Gadomski**,** Università degli Studi di Roma La Sapienza, Italy
Alex Galis, University College London (UCL), UK
Crescenzio Gallo, Department of Clinical and Experimental Medicine - University of Foggia, Italy
Matjaz Gams, Jozef Stefan Institute-Ljubljana, Slovenia
Raúl García Castro, Universidad Politécnica de Madrid, Spain
Fabio Gasparetti, Roma Tre University - Artificial Intelligence Lab, Italy
Joseph A. Giampapa, Carnegie Mellon University, USA
George Giannakopoulos, NCSR Demokritos, Greece
David Gil, University of Alicante, Spain
Harald Gjermundrod, University of Nicosia, Cyprus
Angelantonio Gnazzo, Telecom Italia - Torino, Italy
Luis Gomes, Universidade Nova Lisboa, Portugal
Nan-Wei Gong, MIT Media Laboratory, USA
Francisco Alejandro Gonzale-Horta, National Institute for Astrophysics, Optics, and Electronics (INAOE), Mexico
Sotirios K. Goudos, Aristotle University of Thessaloniki, Greece
Victor Govindaswamy, Texas A&M University-Texarkana, USA
Gregor Grambow, University of Ulm, Germany
Fabio Grandi, University of Bologna, Italy
Andrina Granić, University of Split, Croatia
Carmine Gravino, Università degli Studi di Salerno, Italy
Dominic Greenwood, Whitestein Technologies, Switzerland
Michael Grottke, University of Erlangen-Nuremberg, Germany
Vic Grout, Glyndŵr University, UK
Maik Günther, Stadtwerke München GmbH, Germany
Francesco Guerra, University of Modena and Reggio Emilia, Italy
Alessio Gugliotta, Innova SPA, Italy
Richard Gunstone, Bournemouth University, UK
Fikret Gurgen, Bogazici University, Turkey
Ivan Habernal, University of West Bohemia, Czech Republic
Maki Habib, The American University in Cairo, Egypt
Till Halbach Røssvoll, Norwegian Computing Center, Norway
Jameleddine Hassine, King Fahd University of Petroleum & Mineral (KFUPM), Saudi Arabia
Ourania Hatzi, Harokopio University of Athens, Greece
Yulan He, Aston University, UK
Kari Heikkinen, Lappeenranta University of Technology, Finland
Cory Henson, Wright State University / Kno.e.sis Center, USA
Arthur Herzog, Technische Universität Darmstadt, Germany
Rattikorn Hewett, Whitacre College of Engineering, Texas Tech University, USA
Celso Massaki Hirata, Instituto Tecnológico de Aeronáutica - São José dos Campos, Brazil

Jochen Hirth, University of Kaiserslautern, Germany
Bernhard Hollunder, Hochschule Furtwangen University, Germany
Thomas Holz, University College Dublin, Ireland
Władysław Homenda, Warsaw University of Technology, Poland
Carolina Howard Felicíssimo, Schlumberger Brazil Research and Geoengineering Center, Brazil
Jingwei Huang , University of Illinois at Urbana-Champaign, USA
Weidong (Tony) Huang, CSIRO ICT Centre, Australia
Xiaodi Huang, Charles Sturt University - Albury, Australia
Eduardo Huedo, Universidad Complutense de Madrid, Spain
Marc-Philippe Huget, University of Savoie, France
Chi Hung, Tsinghua University, China
Chih-Cheng Hung, Southern Polytechnic State University - Marietta, USA
Edward Hung, Hong Kong Polytechnic University, Hong Kong
Muhammad Iftikhar, Universiti Malaysia Sabah (UMS), Malaysia
Prateek Jain, Ohio Center of Excellence in Knowledge-enabled Computing, Kno.e.sis, USA
Wassim Jaziri, Miracl Laboratory, ISIM Sfax, Tunisia
Hoyoung Jeung, SAP Research Brisbane, Australia
Yiming Ji, University of South Carolina Beaufort, USA
Jinlei Jiang, Department of Computer Science and Technology, Tsinghua University, China
Weirong Jiang, Juniper Networks Inc., USA
Hanmin Jung, Korea Institute of Science & Technology Information, Korea
Ilya S. Kabak, "Stankin" Moscow State Technological University, Russia
Eleanna Kafeza, Athens University of Economics and Business, Greece
Hermann Kaindl, Vienna University of Technology, Austria
Ahmed Kamel, Concordia College, Moorhead, Minnesota, USA
Faouzi Kamoun, University of Dubai, UAE
Rajkumar Kannan, Bishop Heber College(Autonomous), India
Teemu Kanstrén, VTT, Finland
Fazal Wahab Karam, Norwegian University of Science and Technology (NTNU), Norway
Dimitrios A. Karras, Chalkis Institute of Technology, Hellas
Koji Kashihara, The University of Tokushima, Japan
Nittaya Kerdprasop, Suranaree University of Technology, Thailand
Katia Kermanidis, Ionian University, Greece
Serge Kernbach, University of Stuttgart, Germany
Nhien An Le Khac, University College Dublin, Ireland
Malik Jahan Khan, Lahore University of Management Sciences (LUMS), Lahore, Pakistan
Reinhard Klemm, Avaya Labs Research, USA
Ah-Lian Kor, Leeds Metropolitan University, UK
Arne Koschel, Applied University of Sciences and Arts, Hannover, Germany
George Kousiouris, NTUA, Greece
Philipp Kremer, German Aerospace Center (DLR), Germany
Dalia Kriksciuniene, Vilnius University, Lithuania
Dariusz Król, AGH University of Science and Technology, ACC Cyfronet AGH, Poland
Roland Kübert, Höchstleistungsrechenzentrum Stuttgart, Germany
Markus Kunde, German Aerospace Center, Germany
Dharmender Singh Kushwaha, Motilal Nehru National Institute of Technology, India

Mary Luz Mouronte López, Ericsson S.A., Spain
Henning Müller, University of Applied Sciences Western Switzerland - Sierre (HES SO), Switzerland
Susana Munoz Hernández, Universidad Politécnica de Madrid, Spain
Adrian Muscat, University of Malta, Malta
Peter Mutschke, GESIS - Leibniz Institute for the Social Sciences - Bonn, Germany
Bela Mutschler, Hochschule Ravensburg-Weingarten, Germany
Deok Hee Nam, Wilberforce University, USA
Fazel Naghdy, University of Wollongong, Australia
Joan Navarro, Research Group in Distributed Systems (La Salle - Ramon Llull University), Spain
Saša Nešić, University of Lugano, Switzerland
Rui Neves Madeira, Instituto Politécnico de Setúbal / Universidade Nova de Lisboa, Portugal
Toàn Nguyên, INRIA Grenobel Rhone-Alpes/ Montbonnot, France
Andrzej Niesler, Institute of Business Informatics, Wroclaw University of Economics, Poland
Michael P. Oakes, University of Sunderland, UK
John O'Donovan, University of California - Santa Barbara, USA
Kouzou Ohara, Aoyama Gakuin University, Japan
Jonice Oliveira, Universidade Federal do Rio de Janeiro, Brazil
Ian Oliver, Nokia Location & Commerce, Finland / University of Brighton, UK
Michael Adeyeye Oluwasegun, University of Cape Town, South Africa
Sigeru Omatu, Osaka Institute of Technology, Japan
Sascha Opletal, University of Stuttgart, Germany
Flavio Oquendo, European University of Brittany/IRISA-UBS, France
Fakri Othman, Cardiff Metropolitan University, UK
Enn Õunapuu, Tallinn University of Technology, Estonia
Jeffrey Junfeng Pan, Facebook Inc., USA
Hervé Panetto, University of Lorraine, France
Malgorzata Pankowska, University of Economics, Poland
Harris Papadopoulos, Frederick University, Cyprus
Laura Papaleo, ICT Department - Province of Genoa & University of Genoa, Italy
Agis Papantoniou, National Technical University of Athens, Greece
Thanasis G. Papaioannou, École Polytechnique Fédérale de Lausanne (EPFL), Switzerland
Andreas Papasalouros, University of the Aegean, Greece
Eric Paquet, National Research Council / University of Ottawa, Canada
Kunal Patel, Ingenuity Systems, USA
Carlos Pedrinaci, Knowledge Media Institute, The Open University, UK
Juan C Pelaez, Defense Information Systems Agency, USA
Yoseba Penya, University of Deusto - DeustoTech (Basque Country), Spain
Cathryn Peoples, University of Ulster, UK
Asier Perallos, University of Deusto, Spain
Christian Percebois, Université Paul Sabatier - IRIT, France
Andrea Perego, European Commission, Joint Research Centre, Italy
Mark Perry, University of Western Ontario/Faculty of Law/ Faculty of Science - London, Canada
Willy Picard, Poznań University of Economics, Poland
Meikel Poess, Oracle, USA
Agostino Poggi, Università degli Studi di Parma, Italy
R. Ponnusamy, Madha Engineering College-Anna University, India

Dorin Popescu, University of Craiova, Romania
Stefan Poslad, Queen Mary University of London, UK
Wendy Powley, Queen's University, Canada
Radu-Emil Precup, "Politehnica" University of Timisoara, Romania
Jerzy Prekurat, Canadian Bank Note Co. Ltd., Canada
Didier Puzenat, Université des Antilles et de la Guyane, France
Sita Ramakrishnan, Monash University, Australia
Elmano Ramalho Cavalcanti, Federal University of Campina Grande, Brazil
Juwel Rana, Luleå University of Technology, Sweden
Martin Randles, School of Computing and Mathematical Sciences, Liverpool John Moores University, UK
Christoph Rasche, University of Paderborn, Germany
Ann Reddipogu, ManyWorlds UK Ltd, UK
Ramana Reddy, West Virginia University, USA
René Reiners, Fraunhofer FIT - Sankt Augustin, Germany
Paolo Remagnino, Kingston University - Surrey, UK
Sebastian Rieger, University of Applied Sciences Fulda, Germany
Andreas Riener, Johannes Kepler University Linz, Austria
Ivan Rodero, NSF Center for Autonomic Computing, Rutgers University - Piscataway, USA
Joel Rodrigues, Instituto de Telecomunicações / University of Beira Interior, Portugal
Alejandro Rodríguez González, University Carlos III of Madrid, Spain
Aitor Rodríguez-Alsina, University Autonoma of Barcelona (UAB), Spain
Paolo Romano, INESC-ID Lisbon, Portugal
Vicente-Arturo Romero-Zaldivar, Atos Origin SAE, Spain
Agostinho Rosa, Instituto de Sistemas e Robótica, Portugal
José Rouillard, University of Lille, France
Paweł Różycki, University of Information Technology and Management (UITM) in Rzeszów, Poland
Igor Ruiz-Agundez, DeustoTech, University of Deusto, Spain
Michele Ruta, Politecnico di Bari, Italy
Melike Sah, Trinity College Dublin, Ireland
Francesc Saigi Rubió, Universitat Oberta de Catalunya, Spain
Abdel-Badeeh M. Salem, Ain Shams University, Egypt
Yacine Sam, Université François-Rabelais Tours, France
Ismael Sanz, Universitat Jaume I, Spain
Ricardo Sanz, Universidad Politecnica de Madrid, Spain
Marcello Sarini, Università degli Studi Milano-Bicocca - Milano, Italy
Munehiko Sasajima, I.S.I.R., Osaka University, Japan
Minoru Sasaki, Ibaraki University, Japan
Hiroyuki Sato, University of Tokyo, Japan
Jürgen Sauer, Universität Oldenburg, Germany
Patrick Sayd, CEA List, France
Dominique Scapin, INRIA - Le Chesnay, France
Kenneth Scerri, University of Malta, Malta
Adriana Schiopoiu Burlea, University of Craiova, Romania
Rainer Schmidt, Austrian Institute of Technology, Austria
Bruno Schulze, National Laboratory for Scientific Computing - LNCC, Brazil
Wieland Schwinger, Johannes Kepler University Linz, Austria

Hans-Werner Sehring, T-Systems Multimedia Solutions GmbH, Germany
Paulo Jorge Sequeira Gonçalves, Polytechnic Institute of Castelo Branco, Portugal
Sandra Sendra Compte, Polytechnic University of Valencia, Spain
Kewei Sha, Oklahoma City University, USA
Hossein Sharif, University of Portsmouth, UK
Roman Y. Shtykh, Rakuten, Inc., Japan
Kwang Mong Sim, Gwangju Insitute of Science & Technology, South Korea
Robin JS Sloan, University of Abertay Dundee, UK
Vasco N. G. J. Soares, Instituto de Telecomunicações / University of Beira Interior / Polytechnic Institute of Castelo Branco, Portugal
Don Sofge, Naval Research Laboratory, USA
Christoph Sondermann-Woelke, Universitaet Paderborn, Germany
George Spanoudakis, City University London, UK
Vladimir Stantchev, SRH University Berlin, Germany
Claudius Stern, University of Paderborn, Germany
Mari Carmen Suárez-Figueroa, Universidad Politécnica de Madrid (UPM), Spain
Kåre Synnes, Luleå University of Technology, Sweden
Ryszard Tadeusiewicz, AGH University of Science and Technology, Poland
Yehia Taher, ERISS - Tilburg University, The Netherlands
Yutaka Takahashi, Senshu University, Japan
Azzelarabe Taleb-Bendiab, Liverpool John Moores University, UK
Dan Tamir, Texas State University, USA
Jinhui Tang, Nanjing University of Science and Technology, P.R. China
Yi Tang, Chinese Academy of Sciences, China
Said Tazi, LAAS-CNRS, Universite Toulouse 1, France
John Terzakis, Intel, USA
Sotirios Terzis, University of Strathclyde, UK
Vagan Terziyan, University of Jyvaskyla, Finland
Ioan Toma, STI Innsbruck/University Innsbruck, Austria
Lucio Tommaso De Paolis, Department of Innovation Engineering - University of Salento, Italy
Davide Tosi, Università degli Studi dell'Insubria, Italy
Raquel Trillo Lado, University of Zaragoza, Spain
Tuan Anh Trinh, Budapest University of Technology and Economics, Hungary
Simon Tsang, Applied Communication Sciences, USA
Theodore Tsiligiridis, Agricultural University of Athens, Greece
Antonios Tsourdos, Cranfield University, UK
José Valente de Oliveira, University of Algarve, Portugal
Cristián Felipe Varas Schuda, NIC Chile Research Labs, Chile
Eugen Volk, University of Stuttgart, Germany
Mihaela Vranić, University of Zagreb, Croatia
Chieh-Yih Wan, Intel Labs, Intel Corporation, USA
Jue Wang, Washington University in St. Louis, USA
Shenghui Wang, OCLC Leiden, The Netherlands
Zhonglei Wang, Karlsruhe Institute of Technology (KIT), Germany
Laurent Wendling, University Descartes (Paris 5), France
Maarten Weyn, Artesis University College of Antwerp, Belgium

International Journal on Advances in Intelligent Systems
Volume 6, Numbers 1 & 2, 2013

CONTENTS

The Activity Circle: Visualizing the Coordination Aspects of User Resistance Toward Workflow Technology

Marcello Sarini
Department of Psychology
University of Milano-Bicocca
Milano, Italy
Email: marcello.sarini@unimib.it

***Abstract*—The paper proposes a novel approach for addressing issues that are related to organizational changes that are induced by the introduction of an Information System within an organization. Specifically, we focus on the effects of a Workflow Technology because its introduction affects typical work practices, its use is mandatory, and Workflow Technology often makes it necessary to accomplish work activities in a more rigid way. Similar to other Information Systems, the consequence is that changes brought about because of Workflow Technology can trigger the phenomenon of user resistance. The Information Systems literature reports different strategies to limit the degree of user resistance toward Information Systems. Some of these strategies are based on the direct involvement of the designers of the technology, while others involve the managers of the organizations in which the technology is used. In this paper, we propose the *Workflow Evaluation Software*, a tool that actively involves the end users to reduce the effects of user resistance. In fact, this tool allows to simulate the use of Workflow Technology at an early stage of its implementation by focusing on the *coordination aspects* of user resistance that are related to how people coordinate their activities. Based on the data collected, the tool implements the Activity Circle, which is a social visualization mechanism that distributes the information related to the coordination aspects of user resistance among the users. We claim that the sharing of this information gives voices to the users and could represent one of the most promising strategies for reducing frustration and anger about any organizational change.**

***Keywords*-*Workflow Technology*, *Social Visualization*, *User Resistance*, *Organizational Change*.**

I. INTRODUCTION

The Activity Circle [1] is a general social visualization tool that displays information that is related to attitudes, opinions and possible trends in the behaviors of different people. It aims at making this information distributed among different people, with the idea that knowing this information about others who have some relationship with an individual is also relevant for that individual; furthermore, being aware of this information about others could also influence the individual's related attitudes, opinions and possible behaviors. The main idea is to design the Activity Circle to be as general as possible, considering that any information related to the possible interactions among different people could be displayed in terms of a dot that is capable of exhibiting different characteristics that are related to that information; for example, the distance from the center of the circle in the background could be related to the different strengths that are associated with the considered information. Specifically, the Activity Circle was designed while considering the reactions of users to the introduction of a new technology. The Activity Circle aims to make these reactions shared among a group of users, and this tool could hence be considered useful in the area of technology adoption research.

This paper focuses on the application of the Activity Circle when considering the possible reactions of users to the organizational changes that are induced by the introduction of an Information System [2], where an Information System (IS) is any technology that is aimed at supporting the management of interactions among people, processes and data within an organization [3]. Among the possible reactions of people to the introduction of an Information System, one of the most critical for its successful introduction is *user resistance*. User resistance is a complex phenomenon that is often associated with organizational change [4]. Information System research strongly emphasizes how the introduction of an IS could favor a form of organizational change and, consequently, how people react to changes that are induced by an IS [2].

Workflow Technology provides the infrastructure to design, execute, and manage business processes that are spread over a network of people and resources [5]. Among the many possible types of Information Systems, we focus on Workflow Technology (WT) because we think that the peculiarities of Workflow Technology (sometimes called Business Process Management Systems or Workflow Management Systems) are highly related to the theme of organizational change. In fact, this technology affects the usual work practices within an organization because it embeds a business process and, consequently, manages which activities must be performed, who is in charge of performing them, when the activities must be completed, and the order to be followed for the accomplishment of those activities. Furthermore, the use of this technology is mandatory for end users; this happens

because WT is used to support the implementation of organizational change that is aimed at making the accomplishment of work more standardized or its outcomes more determined and accountable [6]. Moreover, WT enables changes that make the accomplishment of work activities more rigid because the changes it promotes might impose fixed patterns of execution, which often harm the flexibility that is needed in work environments [7]. Consequently, the employees often consider the introduction of a Workflow Technology to be a source of frustration because of the perception of the power exerted by the organization, especially when employees are not directly involved in deciding the changes that affect their usual working practices. Accordingly, this aspect can raise user resistance to change either by users refusing to use the system or, less acutely, by users initiating coping strategies to re-appropriate their usual work practices and overcome the rigidity of the Workflow Technology with forms of production deviance [8], such as workaround [9]. According to the IS literature, in the following Related Work Section of this paper, we will summarize the main strategies that have been considered to overcome user resistance; these strategies mainly focus either on the designers of the technology or on the management of the organization in which the technology will be implemented. Usually, these strategies consider the phenomenon of organizational change as a generic monolithic process without considering the specificity of the change with regard to the business process that is affected by the change process itself. In this way, the identified strategies suggest using generic best practices, where these practices do not contemplate how the specific change of the business process affects consolidated local work practices and how this change could trigger the emergence of user resistance in the organization. We want to propose here an alternative strategy because we believe that reactions to change are not only attributable to the change itself but are also attributable to the specificity of the change in the considered business process. Hence, *local aspects of the change* must be accounted for because of the nature of the change that occurred in the specific business process and because the changes might affect the users' reactions. Consequently, there is a rise in the phenomenon of user resistance. This consideration is in line with what is advocated in a previous study [10], which claims that, in the research toward the adoption of business process change technology, it would be necessary to identify both generic and locally relevant process-centric constructs that could predict users' adoption of the related re-designed business process. In Section III, a tool is described, namely the *Workflow Evaluation Software* (WES), which is especially designed to involve directly the possible end users of a Workflow Technology in experiencing the effects of a Workflow technology–induced organizational change. To this aim, we propose using WES to simulate the management of a business process at both the design and execution times to collect and then make available information about the *coordination aspects* of user resistance at an early stage of development of a WT, where these coordination aspects are about the local aspects of the change on the specific process itself and are related to how people coordinate their activities about that process. This is because user resistance is a complex phenomenon and it is possible to isolate different components to partly explain the user resistance. From our perspective, we are interested in identifying aspects of user resistance related to the coordination efforts that are required by people when they are jointly called to accomplish the goals of a specific business process. Specifically with WES, we focus on business processes as they will be managed by Workflow Technology. Once the related information has been collected, we propose to display it with the Activity Circle in terms of a social proxy visualization approach to make all of the participants aware of the effects of their coordination efforts to reduce the possible disparities and frustration and to limit the emergence of user resistance.

Our challenge when proposing the WES tool is to limit the rise of user resistance during Workflow technology–induced organizational change i) by considering the local aspects of the change, and not the overall change process; ii) by isolating the effects of the introduction of a WT on the work practices without focusing on any specific implementation of a WT but instead focusing on the coordination aspects of user resistance; and iii) by simulating the effects organizational change as soon as possible to restrain the possible costs for the WT implementation.

The paper is organized as follows: Section II reports Related Work about the issue of user resistance to the introduction of an IS; Section III describes our proposal to manage the issue of user resistance at an the early stage of the introduction of a Workflow Technology; Section IV describes how to evaluate the effectiveness of our approach; and Conclusion and Future Work Section is presented at the end of the paper.

II. Related work

Because user resistance is a critical factor for the successful introduction of IS within organizations, most of the IS literature provides discussions for a better understanding of the complex phenomenon of user resistance (see [4] for a review on user resistance toward the use of Information Systems). Furthermore, some solutions are proposed in this literature to reduce the resistance to facilitating IS adoption. These solutions are usually described while considering either the involvement of the *management* of the organizations in which the IS should be used or the involvement of the *designers* of the new IS to be implemented.

Some authors remind the designers of a new Information System that its design should never be considered a neutral activity; the designers should consider that this activity will also bring an organizational change [4] along with the related

criticalities (such as the emergence of the phenomenon of user resistance to change). Consequently, most of the designers' effort during the design of a new system should be devoted to limit the possible user resistance. Other authors (e.g., [11]) state that the designers should implement a participative strategy with employees. In this strategy, employees should be involved in the development of the new system and should not be presented only the overall final result of the project; instead, this work should be conducted as a series of pilot studies to examine the impact of the change step by step. Following this strategy, the designers are also asked to develop and follow a clear implementation plan with the direct support of the management, who need to be informed in a detailed way about both the system and the related business process that is affected by the system. In this way, designers could also have the possibility of being informed by managers to better address the questions and concerns of the final users.

For the concerns of the management, the IS literature mainly considers two categories of strategy to address user resistance: *participative* and *directive* [12]. Participative strategies are devoted to involving final users in the development process for the new system, as when users perceive that they are an active part of the change process, their resistance toward the new system may be reduced. These strategies consider the phenomenon of user resistance either before the system is actually used, which suggests the incorporation of user participation into the design process, and the encouragement of open communication between management and employees. Alternatively, these strategies are generally implemented in a system that is already in use by considering the training of the users, giving users sufficient time to learn to use the system (without focusing on their performances during this transition period), or providing a clear documentation of the new standards that are related to the use of the new system [13][14][15]. Directive strategies, instead, are those that are imposed by the management and can be organized around two opposite perspectives: rewards and punishment. Most efforts of the management are devoted to the first type of perspective, as described in previous studies [12][15]. The authors suggest providing financial incentives for using the new system, a power redistribution among users using the system, and job title modifications. In addition, one study [15] also suggests that the management should give unions higher wage rates in return for a work rule change and should give one of their leaders, or someone they respect, a key role in designing or implementing a change. Punishment strategies are, for example, firing or transferring people who resist the change, and implicitly or explicitly threatening the loss of a job or promotion possibilities [15][12].

The theme of user resistance is relevant also for requirements engineering research (see e.g., [16]). However, requirements engineering is about the formulation of the software requirements related to the implementation of a technology (an Information System in this context). In this way, requirements engineering process is more focused on the implementation of the functionalities of the system and hence on the way people will accomplish their duties after its introduction; accordingly, higher user participation to the definition of the requirements will probably rise higher sense of belonging to the technology being implemented and this will reduce resistant behaviors [16]. However, we are more focused on less tangible aspects than the implementation of the system's functionalities; in fact, we are interested in the way people perceive the organization of their work after an organizational change. This would occur paradoxically even in case the procedures and processes related to the completion of a work are re-designed "on-paper" without the support of a technology. Obviously, the effects of the changes on the organization of work, and consequently also the possible resistant behaviors, would result amplified if the change is supported by a proper technology. For this reason, the identification of possible user resistance to IT–induced organizational change is more challenging.

The solutions reported within the body of the considered literature are mostly oriented toward providing suggestions, hints, indications, and rules of thumbs for managers and designers to limit the potential harm of user resistance by generally considering the overall process of organizational change. To our knowledge, the field lacks a practical tool that can be used to limit the negative influence of user resistance toward the adoption of a new WT by focusing instead on the specificity of the business process affected by the introduction of the WT. Therefore, taking our inspiration from the participative strategies that are suggested both to the designers and the management staff, we consider involving end users in the process of change to be extremely relevant. Specifically, the process of change would bring the users' participation to the design of the "re-engineered" business process [17] because it will then be implemented in the newly introduced Workflow Technology. In line with this suggestion, the solution that we propose is designed by accounting for the end-users' perspectives to make these potential users both aware and then able to express their voices about the change "imposed" by introducing the new WT. This scenario is in line with what was advocated by different scholars, e.g., by [18], who hope for the possibility to offer end-users alternative responses to reduce the likelihood of frustration in response to instances of power (such as how an organizational change that is related to the introduction of a new WT might be perceived by end users). In the next section, we describe our proposal for placing into practice a real shared channel with which alternative users' responses are voiced.

III. THE PROPOSAL

We propose a tool, the *Workflow Evaluation Software* (WES), to limit the effects of user resistance to the introduction of a Workflow Technology. The tool encompasses two main modules: the *Workflow Evaluation Module* (WEM) and the *Activity Circle Module* (ACM). The WEM allows users to manage both the modeling and execution of a workflow, which reflects the business process re-designed as a consequence of the introduction of the considered WT. The ACM makes possible the social visualization of information that is related to the possible user resistance from the Workflow Technology introduction, which causes the organizational change. Detailed description of these two modules will be provided in two dedicated subsections, while another subsection will describe the rationale of the model behind our tool.

A. The Workflow Evaluation Module

It is possible to find elsewhere a more detailed description of the WES tool and of its constituent modules [19]. The most important aspect to recall here is that the WEM implements what can be considered a *simulation tool* of a real Workflow Technology. A simulation tool not in the sense that the WEM fully implements the way how each activity has to be performed by any of the involved users, but rather in the sense that the WEM implements a sort of "workflow mockup tool" to assign to the involved users a placeholder for each of the activities they have to complete according to the right order of execution defined in the business process modeled using the module.

The main rationale behind this module is making possible to apply the WES tool in organizational settings in which an organizational change induced by the introduction of a WT is underway. Our idea is to anticipate the extent of the end-users' positions before both the implementation and use of the system to emphasize as soon as possible which are the possible forms of resistance to change before the costs of implementation will strongly impact the organization. In this way, the management can drive the change in a less traumatic way, thus reducing the possible negative impact of resistance by accounting for the reactions of the end-users who are in charge of making the WT introduction either a good or a bad investment for the organization. Obviously, this rationale is not free from criticism. In fact, our approach does not encompass all of the features that affect the possible success or non-success of the considered Workflow Technology. In fact, by using the WEM functionalities users focus only on the impact of change with respect to concerns about the new organization of the work. On the one hand, the module focuses on user interactions and the coordination of work activities; on the other hand, it focuses on how much the workload of each user has changed as a consequence of the introduction of the Workflow Technology. A more comprehensive evaluation of the effects of change from the considered WT will also require asking the users to evaluate how much the implemented system affects the completion of each activity that was assigned to them by considering, for example, the Perceived Ease of Use of the system [20], the technological integration with other applications and other characteristics that are related to the system as indicated, for example, in the DeLone and McLean Model of Information Systems Success [21] or in the BPM success model [22]. Though these last aspects are very relevant to address the issue of user resistance, they are more focused on the way the system is implemented and, hence, how it can be evaluated, only at a very later stage of the introduction of the new Workflow Technology. Conversely, we are more focused on the preliminary phase of WT introduction and on the coordination aspects of user resistance. To identify coordination aspects of user resistance, we defined a human-oriented meta-model of business processes, which we called the *Human-Oriented Meta-BUsiness Process* (HOMe-BUPro) model (see Figure 1 for the corresponding ER diagram).

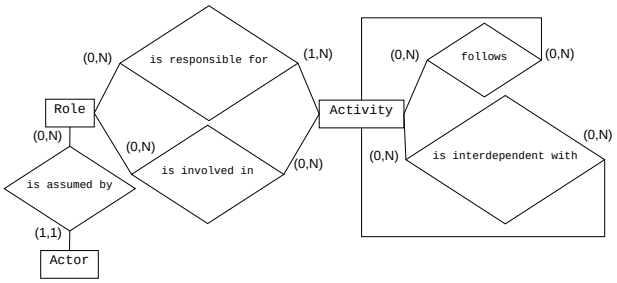

Figure 1. The ER diagram of the HOMe-BUPro model.

This model is not intended to fully design a business process, but it aims to be fairly general and complete to describe the interactions occurring among actors during a business process execution (and hence also to describe the coordination of the related activities). To this aim, it focuses on specifying the relevant constructs to capture the coordination efforts of the involved actors occuring during the unfolding of a business process, namely *Activities* (what has to be done), *Roles* (which functional role has the skills and the duties to accomplish an activity according to the organization's rules), and *Actors* (who is really in charge to perform an activity within the organization). The rationale of generality behind the HOMe-BUPro model was also guided by the idea of making this model easily mappable to any existing Workflow Technology and to any reasonable way of describing and representing a process model (even on paper). We conducted this effort while aiming to widen the possibility of applying the HOMe-BuPro model to different organizational settings, according to the local choices of Workflow Technology to be used or to any methodology used to represent internally a business process. Moreover, the rationale behind the HOMe-BUPro model is also to make it

appliable not only to the models that are employed by usual Workflow Technology (where this technology is usually built on imperative process models based on a very rigid control-flow approach) but also to richer workflow models. In fact, our aim is also to apply our model to other more flexible workflow approaches such as declarative, constraint-based approaches (e.g., the ESProNa engine [23] or the DECLARE tool [24]), to evaluate whether an improved flexibility during execution affects user resistance and the users' attitude toward the system. In other words, we want to identify whether the effects of change, and hence the possible resistance that arises as a consequence of this change, could be limited by a more flexible technology or whether the effects of change are basically always the same, irrespective of the technology used.

In order to make it possible the simulation of the co-ordination efforts related to the execution of a process, the WEM incorporates both a Process Designer functionality by which a Process Designer role can define all the aspects related to the modeling of the process, and a Human-driven Workflow Engine in which a Process Manager role can manually trigger the change of state of the Activities of the process, and to assign them to the related Actors in order to fully simulate the unfolding of a process during its execution.

We do not focus here on the details of the Process Designer functionality and on the Workflow Engine; rather we are interested to describe both the HOMe-BUPro model used to define the coordination of the Activities among the involved Actors and the way in which the related Actors' coordination efforts are measured.

B. The HOMe-BUPro model

We consider the application of the HOMe-BUPro model at two different stages of business process management: the design time and the enactment/run time as will be described in the next two subsections.

1) Design time: We based our model on the general characteristics of a business process to capture the coordination efforts among involved people, considering a process to be composed of a set of Activities. For each Activity, it is possible to specify the Roles that are involved in its accomplishment. We identified two types of relations that link Activities with Roles: a Role that is *responsible for* the accomplishment of the related Activity (at least one Role must be defined as being responsible for an Activity) and a Role that is *involved in* the accomplishment of the Activity (the presence of this relation is optional). The two different relations emphasize two possible positions in regards to the Activity to be completed: one is a position of full responsibility toward the overall accomplishment of the Activity; the second one, is a position indicating an optional involvement to support who is responsible to complete the Activity (e.g., to emphasize the difference between a Physician responsible for a Drug Administration activity and a Nurse supporting the Physician if we consider a subordinate relation, but also to emphasize the difference between a General Practictioner responsible for a Patient and a Specialist, when the General Practitioner asks the Specialist an opinion in regards to a Diagnosis). Figure 2 reports a sample process, as defined at the design time. This process was inspired by an insurance Claim Request process after a car accident considering only a subset of activities of the overall process. Role R_1 is responsible for Activity A_1, while Role R_4 is involved in its accomplishment. Roles R_2 and R_3 are both responsible for the accomplishment of A_2. The model allows us to define that the same Role, R_1, is both responsible for the accomplishment of an Activity, A_1, and is involved in the accomplishment of another Activity, A_3. Specifically for the case in example, Activity A_1 is about Claim Registration, under responsibility of an Agent (R_1) of the insurance company, who will follow then the entire evaluation process. Optionally, a Junior agent (R_4) could be involved to support the Agent responsible for the Claim Registration activity. A_2 is about the First Evaluation of the Claim (to identify a guesstimate amount of the request). This Activity is both under responsibility of an Accountant (R_2) and a Supervisor (R_3). After this first evaluation, the request passes through more formal steps, like the Document Collecting activity (A_3). This activity is under responsibility of a Document Collector (R_5), who in some cases could involve also the Agent following the Claim Request.

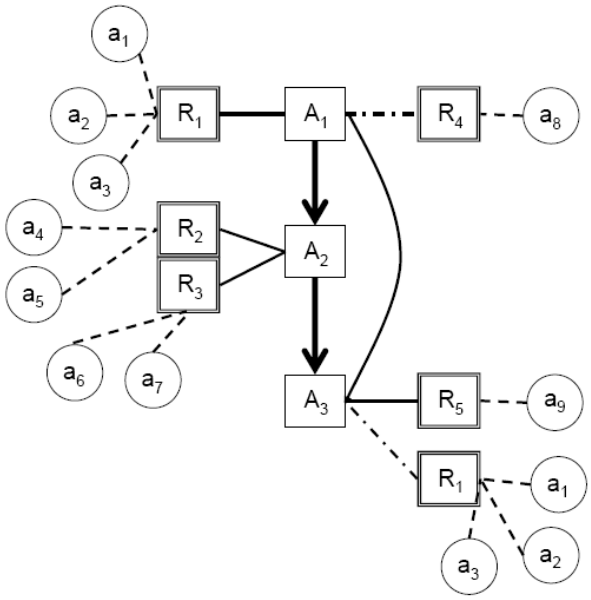

Figure 2. An example of a Claim Request process at the design time.

Then, at the design time, it is necessary to anticipate for each Role all of the Actors who could possibly assume that

Role and hence which Actors would be possibly involved in the accomplishment of the related Activities (even if the Actors who will actually accomplish an Activity during an instance of the process will be specified at the enactment time). To guarantee covering most of the possibilities of real work environments, the HOMe-BuPro model allows both to model collaboration among Actors with respect to a single Activity (e.g., modeling a pool of Actors who are involved in the accomplishment of the same Activity, as shown for Activity A_2, the First Evaluation of the Claim, in Figure 2, where both Accountant John, a_4, and Jim, a_5, have been involved to possibly collaborate for that Activity's accomplishment) and provide collaboration among the Actors who are involved in the accomplishment of different Activities (e.g., for the Agent Susan, a_1, and the Document Collector Joe, a_9, who are both involved in the accomplishment of the Claim Registration activity A_1 and the Document Collecting activity A_3).

Activities can be related as in the usual workflow models in terms of mandatory precedence (Claim Registration, A_1, which precedes the First Claim Evaluation, A_2, must end before the First Claim Evaluation can be executed, as shown by the arrow connecting A_1 and A_2 in Figure 2), but they can be related also in terms of interdependence (as shown in Figure 2 by a line connecting A_1 with A_3 indicating some form of interdependence among the Claim Registration and the Document Collecting activities). Interdependency describes a weaker relation, which indicates that the accomplishment of an Activity can be related to the accomplishment of another Activity without imposing a strict execution order. This construct also means that the Actors involved in the accomplishment of interdependent Activities, not just the Actors following a strict sequential order to complete two Activities one next to the other, can be considered as *mutually dependent* [25]. Accordingly, two Actors being mutually dependent means that an Actor relies positively on the work performed by the other to accomplish her duties, and vice versa. When two Actors are mutually dependent, this dependency could be described in terms of what has been defined as Coordination Requirements [26]. Coordination Requirements in fact describe an "objective" measure that is defined for the domain of large software development projects and express that the coordination efforts required for developers to complete their project could be defined according to the level of interdependence among the software modules of that project. The theme of interdependence is to be considered not only for software development, but also for business process management [25]; in this latter case, dependency rather than considering software module dependencies can be measured in terms of task interdependencies. An investigation of task interdependency can be found in a previous study [27], where a measure for representing the degree of task interdependency is defined. The authors of this study relate this measure to other process characteristics, such as the coordination mechanisms that are required for people to manage their coordination to get their job done according to a certain degree of Task Interdependence.

Measuring Interdependence: For measuring interdependence among Actors involved in the accomplishment of a process and hence to identify the related Coordination Requirements, we combined the concepts of Coordination Requirements with Task Interdependence. In fact, with respect to Task Interdependence, we considered that the coordination efforts needed to accomplish different activities are related to Task Interdependence: different degrees of task interdependency require people to adopt different coordination modes, from stricter, such as plans and rules for a high level of Task Interdependence, to weaker, such as unscheduled informal meetings for low interdependent tasks. Stricter coordination modes such as plans and rules require the involved Actors to perform a higher extra work effort to manage high Task Interdependence, i.e. to perform a huge amount of what has been called *articulation work* [25], while weaker coordination modes used for articulating low interdependent tasks require lesser articulation work than plans and rules. In regards to Coordination Requirements, we considered the idea behind Coordination Requirements to automatically computing them according to the degree of software module dependency. Accordingly, we defined the Coordination Requirements of Actors who are involved in the accomplishment of related Activities within a business process. The interest in identifying Coordination Requirements is based on the hypothesis that focusing on Coordination Requirements that arise among Actors to accomplish a business process (and hence on *local aspects of change*) will provide useful information to infer details about user resistance to change. Specifically, these aspects of resistance to change are not related to the measures that are based on individual differences [28] or to those based on general organizational measures about change. Instead, these aspects are related to the more objective measure of the coordination efforts that are imposed on Actors by the new organization of the work, i.e., on what we defined as the *coordination aspects of user resistance*. In this case, we argue than higher Coordination Requirements could be associated with increased work complexity and higher efforts of articulation work needed, which would result in a stronger form of user resistance or at least in a reduction of user satisfaction. This is in line with the study of [29], where it is shown that some job characteristics such as skill variety and autonomy are negatively related to satisfaction after the introduction of an organizational technology affecting the usual work practices. The choice of defining Coordination Requirements as objective measures of work complexity as an alternative to more complete scales to determine job characteristics, such us the scale described in a previous study [30], is motivated

by simplifying the measures that are related to identifying local aspects of change. The definition is also motivated by being more objective because Coordination Requirements are automatically generated by the business process model itself, and this generation does not require a longer subjective evaluation by the people who are involved.

Similarly to the formula proposed by Cataldo and colleagues [26], we defined Coordination Requirements as a measure that is computed using the following formula:

$$CR = T_A * T_D * T_A^T \quad (1)$$

where T_A represent the Task Assignment matrix, T_D represents the Task Dependency matrix and T_A^T is the transpose of the Task Assignment matrix. In the work of Cataldo and colleagues [26], T_A is built considering the developers who opened files related to a software modification request; T_D is identified by considering syntactic dependencies among the source code files of a system. In our case, the Task Assignment matrix identifies the Actors who are in charge of accomplishing each Activity in the process. The Task Dependency matrix describes the dependencies among the Activities of the considered process. We have different Task Assignment matrixes, which are defined at different stages of the management of the process: one matrix is defined at the design time, and one is designed at the enactment time. At the design time, the Task Assignment matrix is automatically generated from the process model, while at the enactment time the Task Assignment matrix considers only the Actors who were in charge of the accomplishment of an Activity for the specific instance of that process. The Task Dependency matrix is, instead, the same at both the design and run times, and it is automatically derived from the process model by extracting both the precedence and the interdependency relations among the Activities. Table I shows a Task Assignment matrix that is automatically generated from the process represented in Figure 2. The table is built as follows.

For each Actor:

- the Actor is assigned 2 each time that she can play the Role responsible for an Activity (e.g., in Table I, where a_1 is assigned the value 2 in correspondence with A_1 because, as shown in Figure 2, a_1 can play the Role R_1, which is responsible for A_1);
- the Actor is assigned 1 each time she can play a Role that is involved in the accomplishment of an Activity (e.g., in Table I, where a_3 is assigned 1 in correspondence with A_3 because, as shown in Figure 2, a_3 can play Role R_1, which is involved in A_3);
- the Actor is assigned 0, when there is no relation between the Role and the Activity.

These weights have been arbitrarily defined, and it is possible to consider smarter strategies for assigning them. In any case, the assignment follows a rationale that considers the effort requested in the accomplishment of an Activity to change according to the Role played by the Actor. Responsibility requires more effort than pure involvement, which is reflected in the values of the associated weights.

Table I
THE T_A TABLE GENERATED FOR THE CLAIM REQUEST PROCESS AT THE DESIGN TIME

Role	***Actor***	A_1	A_2	A_3
R_1	a_1	2	0	1
R_1	a_2	2	0	1
R_1	a_3	2	0	1
R_2	a_4	0	2	0
R_2	a_5	0	2	0
R_3	a_6	0	2	0
R_3	a_7	0	2	0
R_4	a_8	1	0	0
R_5	a_9	0	0	2

Table II presents a Task Dependency matrix that was automatically generated from the business process described in Figure 2. This Table reflects the static nature of the design of a process because the dependencies among the activities are fixed according to the model that was defined at the design time. The T_D is built as follows.

For each Activity:

- the Activity is assigned 2 when the column refers to the same Activity in a row. In other words, within the same Activity, the coordination effort requested for the Actors involved in the accomplishment of that Activity is the highest. For example, A_1 is assigned the value 2 in the column A_1;
- the Activity is assigned 1 when, in a column, the considered Activity follows the Activity considered in a row. For example, in Figure 2, it is clear that A_2 follows A_1; then, in Table II, the Activity A_1 is assigned 1 in correspondence with A_2. The precedence relation is not symmetrical (if A_2 follows A_1, it does not hold that A_1 follows A_2). Consequently, in Table II, A_2 is assigned 0 in correspondence with A_1;
- the Activity is assigned the value of 0.5 to emphasize the presence of an interdependency with the Activity of the corresponding column. In this case, in Table II, A_1 in correspondence with A_3 is assigned 0.5 because, as shown in Figure 2, A_1 is interdependent with A_3. Additionally in this case, interdependency is not symmetric, as shown in Table II, where for A_3 there is a zero value assigned with regard to A_1;
- the Activity is assigned 0, when there is no dependency among the Activities.

Additionally in this case, the weights have been arbitrarily defined, and it is possible to consider smarter strategies

Table II
THE T_D TABLE GENERATED FOR THE CLAIM REQUEST PROCESS AT THE DESIGN TIME

	A_1	A_2	A_3
A_1	2	1	0.5
A_2	0	2	1
A_3	0	0	2

to assign them. Nevertheless, a rationale is followed that considers the effort requested from Actors in the accomplishment of an Activity to change according to the degree of dependency among the Activities. This ranges from the highest effort among the Actors accomplishing the same Activity (the strongest dependency) to the lowest effort among the Actors who where involved in the accomplishment of the interdependent Activities (the weakest dependency).

According to Formula 1, it is possible to generate the Coordination Requirements table. Table III describes the Coordination Requirements that are associated with each pair of Actors according to the Claim Request process described in Figure 2. For each Actor (a single row, e.g., in Table III the first row refers to the Coordination Requirements of a_1), the Table reports the Coordination Requirements that are calculated with respect to all of the other possible Actors identified in the design phase. The last two columns, S_1 and S_2 aggregate the data about the Coordination Requirements that are related to a specific Actor. S_1 is about the sum of all of the Coordination Requirements of an Actor with respect to all of the other Actors involved in the process, and S_2 is about the sum of the Coordination Requirements for a Role, considering all of the possible Actors who play that Role. While the columns of the table with the names of other Actors identify the Coordination Requirements concerning Actor-Actor interactions, the last two colums (S_1 and S_2) are about a more general and comprehensive quantification of Coordination Requirements posed to each of the Actor involved in the process. This evaluation would be useful for example in comparing the coordination workloads requested to an Actor in regards to different processes: e.g., comparing the Coordination Requirements for the actual process (i.e., before the organizational change) with the requirements posed by the re-designed process as supported by the Workflow Technology (i.e., after the organizational change as simulated by means of the WES tool); in other cases, this evaluation would be useful also in giving the possibility to any involved Actor to compare her workload with the workloads of the others.

Consider for instance the case of John (a_4) and Jim (a_5), both Accountants responsible for the accomplishment of the First Evaluation of the Claim (A_2). Because of their competition for a promotion, they do not want to collaborate at all. Instead, as reported by Table III, a_4 and a_5 are enforced to possibly collaborate with one of the highest values of

Table III
THE CR TABLE GENERATED FOR THE CLAIM REQUEST PROCESS AT THE DESIGN TIME

	R_1	R_1	R_1	R_2	R_2	R_3	R_3	R_4	R_5		
	a_1	a_2	a_3	a_4	a_5	a_6	a_7	a_8	a_9	S_1	S_2
a_1	11	11	11	4	4	4	4	4	6	59	177
a_2	11	11	11	4	4	4	4	4	6	59	177
a_3	11	11	11	4	4	4	4	4	6	59	177
a_4	2	2	2	8	8	8	8	0	4	42	84
a_5	2	2	2	8	8	8	8	0	4	42	84
a_6	2	2	2	8	8	8	8	0	4	42	84
a_7	2	2	2	8	8	8	8	0	4	42	84
a_8	4.5	4.5	4.5	2	2	2	2	2	1	24.5	24.5
a_9	4	4	4	0	0	0	0	0	8	20	20

the identified Coordination Requirements (measured with the strength of eight, where eleven is the highest value) according to the new organization of work imposed by the new Claim Request process that is simulated by using the WES tool. So, in this case, more than other Actors, such as Steve (a_8), the Junior agent, with his highest Coordination Requirement set to 4.5, John and Jim might probably exhibit a resistant behavior toward the new organization of work as imposed by the Workflow Technology. In regards to S_1, the value of S_1 for both John and Jim is set, after the change of the considered process, to one of the highest values (42, where 59 is the highest value). Our hypothesis is that an increase of the Coordination Requirements for an Actor would correspond to a possible increase of a resistant behavior toward the organizational change induced by the introduction of a Workflow Technology.

The data about the columns in the CR table emphasize how much an Actor is involved in the coordination of Activities for a given process by considering that the measure of this involvement is based on what could occur according to the design of the process but it is not based on considering the specific instances of that process. The next step is to consider how these data could change for a specific instance of that process.

2) Enactment and Run time: At this time, among the possible Actors specified at the design time, the Actors actually involved in the execution of the Activities related to the current instance of the process will be chosen. Figure 3 depicts a possible instance of the Claim Request process that is considered in Figure 2. In this specific instance, Susan (a_1) is the only Agent who is responsible for the accomplishment of the Claim Registration activity A_1; John (a_4), an Accountant, and Paul (a_7), a Supervisor, are both responsible for the accomplishment of the First Evaluation of the Claim (A_2); Joe (a_9), a Document Collector, is responsible for the accomplishment of the Document Col-

lecting activity (A_3), while David (a_3), an Agent, is involved in the accomplishment of that Activity (see Figure 3, in which each assigned Actor is represented with a double-lined circle). Consequently, a new Task Activity matrix is automatically determined by accounting for only the Actors who are actually involved in the execution of that specific process instance. For the situation after the enactment has occurred, as depicted in Figure 3, Table IV is generated. To emphasize the differences with Table I, describing a static situation according to the design phase, in Table IV, the Actors underlined in the second column (named Actor) are the only Actors enacted for the considered instance of the process. Instead, the weights underlined are the weights that are changed in the T_A table, which reflect the change from the design time to the run time after enactment. Specifically, the values in Table IV are all at least equal to or at most less than the values in Table I because the table at the design time describes a wider set of possibilities to assign an Actor for the accomplishment of an Activity. Consequently, applying Formula 1 to the Task Activity matrix generated at the run time (Table IV) and to the Task Dependency matrix (Table II), it is possible to compute the Coordination Requirements table that is specific to that instance of the process (see Table V). Again, the Actors underlined in the first column are the only Actors enacted for the considered instance of the process. Instead, the weights underlined report the specific Coordination Requirements, which were changed according to the data reported by Tables IV and II. In this way, S_1 and S_2 in Table V describe, for each Actor enacted for that instance, the sum of the Coordination Requirements with respect to all of the other Actors and with respect to the Role played by that Actor. Again the values contained in Table V are all at least equal to or at most less than the values contained in Table III thus reflecting the different Coordination Requirements that occur at either the design or run times. In this specific instance of the Claim Request process, John (a_4) and Jim (a_5) are not enacted together, but only John is assigned for the completion of the First Evaluation of the Claim (A_2). Consequently, the Table V reflects this fact because both cells at the cross of a_4 and a_5 related rows/columns (and viceversa) equal zero (i.e., no Coordination Requirements among John and Jim are set for this instance). Obviously, this is the case for a single specific instance of the Claim Request process, so it is not possible to base the identification of possible resistant behaviors on a single case. For this reasons, our tool will refer either to data related to the design time (summarizing the set of all the possible cases) or to data related to the run time considering the single CR tables related to the instances of the considered process. The idea of considering two different sources of data to identify Coordination Requirements could be also used to implement forms of Socio-Technical Congruence [31] that is a way to measure the proportion of the Coordination Requirements

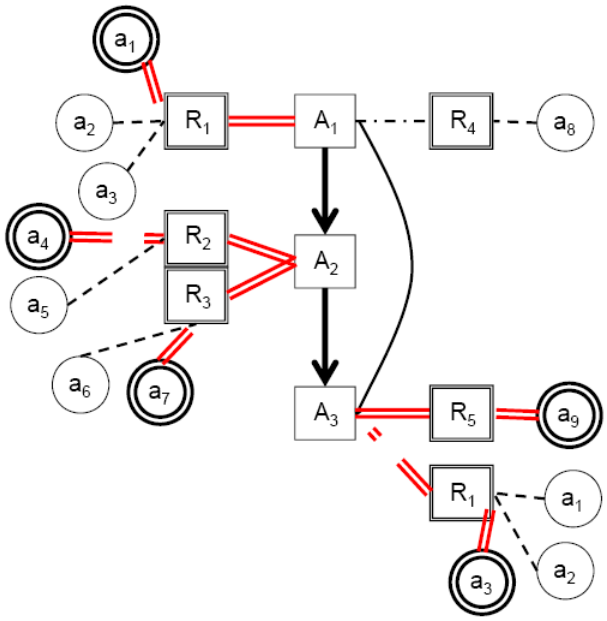

Figure 3. An example of instance of the Claim Request process after enactment.

Table IV
THE T_A TABLE ADAPTED FOR THE CLAIM REQUEST PROCESS AFTER ENACTMENT

Role	***Actor***	A_1	A_2	A_3
R_1	$\underline{a_1}$	2	0	$\underline{0}$
R_1	a_2	$\underline{0}$	0	$\underline{0}$
R_1	$\underline{a_3}$	$\underline{0}$	0	1
R_2	$\underline{a_4}$	0	2	0
R_2	a_5	0	$\underline{0}$	0
R_3	a_6	0	$\underline{0}$	0
R_3	$\underline{a_7}$	0	2	0
R_4	a_8	$\underline{0}$	0	0
R_5	$\underline{a_9}$	0	0	2

that actually emerged (at the run time) relative to the overall Coordination Requirements defined at the design time.

C. The Activity Circle Module

Once the information about a process and the related instances is collected, the *Activity Circle* (AC) is then used to make this information distributed (and hence shared) among the various participants who are involved in the business process. The Activity Circle relies on a social proxy approach [32] to social visualization [33], which is a way of visualizing any type of information that is related to the interactions that occur among people, by choosing to represent any of this information in terms of a social proxy (a graphical representation of that information). The visualization of the various social proxies involved then

Table V
THE CR TABLE GENERATED FOR THE CLAIM REQUEST PROCESS AT RUN TIME

	R_1	R_1	R_1	R_2	R_2	R_3	R_3	R_4	R_5		
	a_1	a_2	a_3	a_4	a_5	a_6	a_7	a_8	a_9	S_1	S_2
a_1	8	0	1	4	0	0	4	0	2	19	25
a_2	0	0	0	0	0	0	0	0	0	0	0
a_3	0	0	2	0	0	0	0	0	4	6	25
a_4	0	0	2	8	0	0	8	0	4	22	22
a_5	2	0	0	0	0	0	0	0	0	0	22
a_6	0	0	0	0	0	0	0	0	0	0	22
a_7	0	0	2	8	0	0	0	0	0	22	22
a_8	0	0	0	0	0	0	0	0	0	0	0
a_9	0	0	4	0	0	0	0	0	8	12	12

describes the trends in people's attitudes, opinions and behaviors. Because our focus is on WT acceptance, we mainly consider the information that can be shared among users of a Workflow Technology. In a previous study [1], we considered to distribute the information about how much a specific user intended to break the way of accomplishing her work with respect to the nature of the Workflow Technology that was imposed on her. Another study [19] focused on distributing information about perceived viscosity, i.e., about the perception that a user had of her increased or decreased effort requested to complete an activity after the introduction of a Workflow Technology. To this aim, Figure 4 describes an example of Activity Circle generated for a sample process of a Claim Request process. The process encompasses ten different Activities (the related dots in the Activity Circle shown in the figure). Each Activity is under responsibility of a Role (each Role is associated with a different color in the AC, for sake of readability in Figure 4 each Role responsible for an Activity is described using a different shape) and each Role could be played by a different Actor. For instance, the three pentagons are associated to three different Activities under responsibility of the Agents of the insurance company. The two triangles are related to two Activities under responsibility of the Supervisor role. As the triangle dots are closer to the center of the Activity Circle, the related Actors playing the Supervisor role perceived a stronger value of the viscosity as a consequence of the introduction of the Workflow Technology, while Agents, whose related dots are farther from the center of the AC, perceived a smaller effort requested to complete their activities. In fact, the closer a dot is to the center of the AC, the higher the perceived viscosity is, and vice versa, the farther a dot is from the center of the AC, the lowest the perceived viscosity is. Because this visualization is available to any of the involved users, the distribution of viscosity information makes each user aware of the others' perceptions, and this would mutually influence the attitudes toward the adoption of the new Workflow Technology. In particular, what are the possible reactions of the "Supervisors" (considered as a group, the group whose members are the Actors assuming the Role of Supervisor) in regards to the "Agents", because of their perception of the different efforts requested after the introduction of the technology? If we reason in terms of power, and power during IS implementation matters [34], Supervisors, perceiving higher viscosity than Agents, feel to be considered powerless than Agents in the new organization of work. This would have to be balanced with some strategy to limit the possible negative attitude toward WT by Supervisors.

In the current proposal, we focus instead on the visualization of the more objective measure of Coordination Requirements among the different users to provide a type of information that is possibly related to user resistance toward the new WT. The nature of Activity Circle is to make information about Coordination Requirements distributed and, hence, shared among the different users. Consequently, this goal makes each user aware of the possible differences in the related work complexities and the redistribution of work after the redesign of the process; hence, the AC can make evident possible cases of *relative deprivation* in the organizational setting [35]. Here, the relative deprivation refers to the discontent that each employee might feel when she compares her position to the positions of her colleagues and realizes that she has a higher burden of work; she believes that she does not deserve to have this higher burden of work compared with those around her. Relative deprivation could be then related to the perception of organizational injustice [36], and the level of this injustice would either favor or not favor the emergence of user resistance.

We provide here two different but related views: the *Actor view* and the *Role view*. The Actor view is about the visualization of Coordination Requirements among the different Actors who are involved in the same business process. The Role view is similar to the former view, but it focuses instead on providing the Coordination Requirements that are related to each of the involved Roles that the Actors have assumed. Considering here the case of data collected during the run time, the Actor view is related to the S_1 columns of the CR Tables that are associated with all of the instances of the same process. Specifically, each of the dots in the Activity Circle, where each dot is a proxy of one of the Actors involved in at least one of the instances of a given business process, is characterized by three different graphical aspects, each of which relates to some of the Actor's traits: the position, the size, and the transparency. The position of a dot is computed using the following formula:

$$position(a_i) = \sum_{j=1}^{N} S_1(a_i)_j / N \qquad (2)$$

where the Coordination Requirements of a_i with respect to all of the other involved Actors ($S_1(a_i)$) are added for any

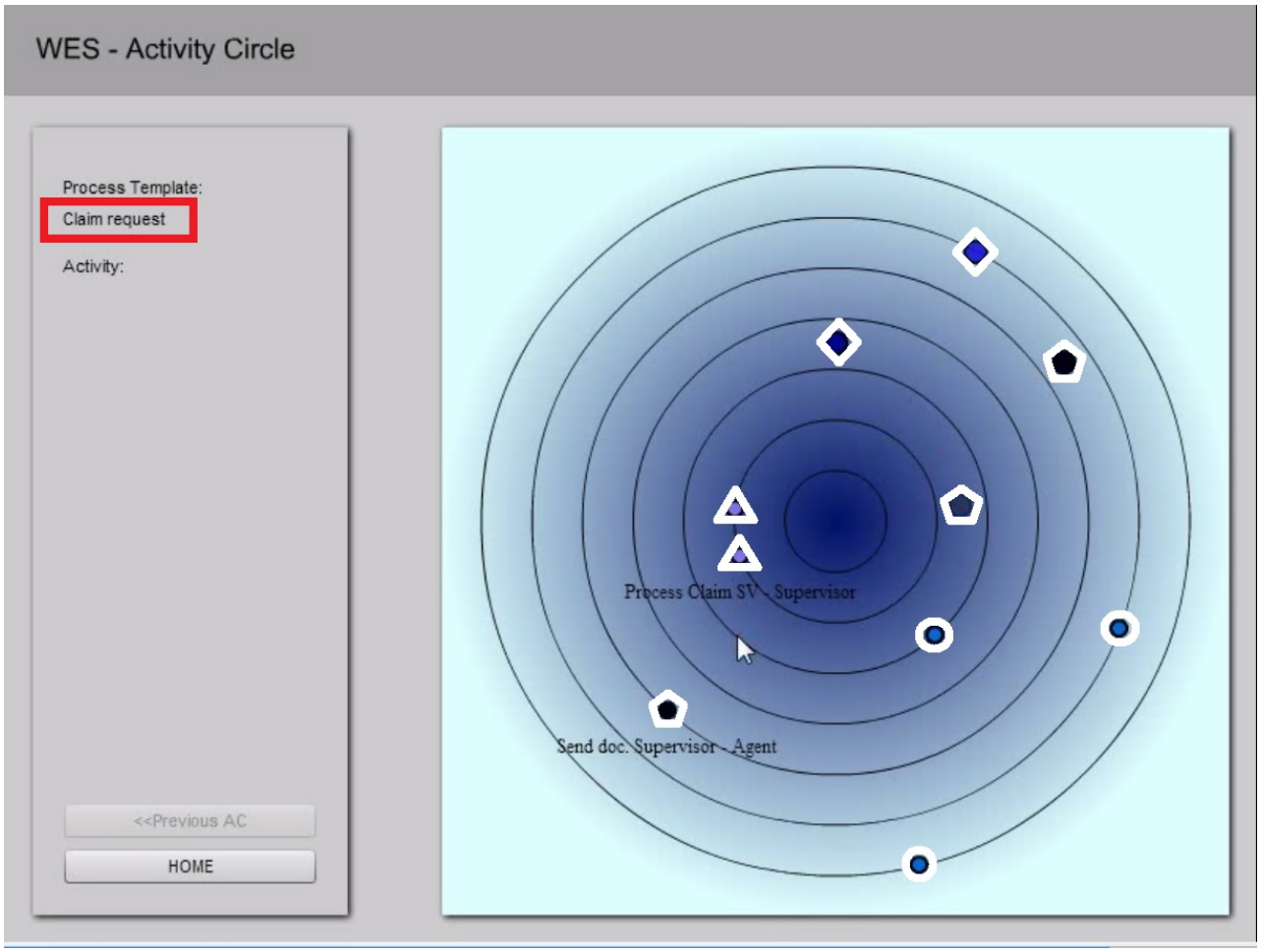

Figure 4. A sample of the Activity Circle showing the perceived viscosity for the activities of a Claim Request process.

of the j–specific instance of the process, and N represents the overall number of instances. The position of a dot is thus a clear indication of the Coordination Requirements of the related Actor: the farther a dot is from the center of the AC, the more Coordination Requirements the Actor has compared with the other Actors, and vice versa, the closer a dot is to the center of the AC, the fewer Coordination Requirements the Actor has with other Actors.

Size involves the dimension of the dot and is calculated according to the following formula:

$$size(a_i) = \sum_{j=1}^{N} enacted(a_i)_j / N \quad (3)$$

where $enacted(a_i)_j$ equals 1 if the Actor a_i was enacted in the accomplishment of instance j, and it equals 0 if not; N represents the overall number of instances of a process. This graphical aspect of the dot means that the size of the dot is defined proportionally to how much the value of size(a_i) is closer to 1. The larger the size of the dot is, the more the related Actor was enacted in most of the considered instances of the process. In other words, the size of the dot could be related to the experience of the corresponding Actor or, more specifically, to the accountability of that Actor within the considered organization.

The transparency of the dot is computed using the following formula:

$$transparency(a_i) = \sum_{j=1}^{N} (S_1(a_i)_j - position(a_i))^2 / N \quad (4)$$

where the closer to zero the transparency(a_i) is, the less the related dot is transparent. This arrangement means that the transparency reflects the variance of the Coordination Requirements of an Actor with respect to others. A dot that is not transparent means that the related Actor had the same Coordination Requirements with respect to other Actors for all of the different instances of the considered process.

Similarly, a Role view could be implemented by aggre-

gating, for each Role, all of the data about the Coordination Requirements for all of the Actors who played that Role. Consequently, the dots of this visualization would represent Roles (and not single Actors) to display how the Coordination Requirements are distributed among the different Roles that are involved in the execution of the considered business process.

It is possible to identify two scalability issues related to the AC visualization: first, the number of dots (associated to the number of Actors involved in a modeled process) which can be visualized within a single Activity Circle; this could raise an issue, if the number of dots is too high; second, the number of instances considered to generate each of the dot's characteristics; in fact, when too much instances are considered to generate the dots to be displayed on the Activity Circle, this might rise some problems especially in regards to the size of a single dot (too large) or to its position (too far from the center of the AC). We are confident that the solution of this second issue is also helpful to solve the first one. In fact, in order to deal with the possible issue due to a larger number of instances considered, we designed the system considering that each of the dot's characteristics will be normalized to a logaritmhic scale. This is useful both for large corpus of data, in order to limit the effects of the differences (giving the possibility of minimizing the differences among both dots' sizes and dots' positions) and also for small corpus of data (to emphasize the possible differences among the dots to be visualized when considering few data). The fact to reduce the effects of the dots differences considering large source of data makes also feasible to manage the visualization of a larger number of dots, contributing to the solution of the first scalability issue.

With both Actor and Role views, any Actor can visualize the Coordination Requirements about either the different Actors who are involved or the different Roles that are involved in the accomplishment of a process. Accordingly, this information makes clarification for the requesting user about the nature of the new arrangement with respect to the complexity of her work and the complexity of others' work. Hence, the related coordination aspects of user resistance can be elucidated. Consequently, if any form of user resistance has occurred, with the AC, we have built a mechanism that promotes social influence to reduce the impact of the resistance. However, we must evaluate whether this mechanism can effectively reduce the impact of user resistance toward WT adoption. In any case, if it is not possible to reduce user resistance, then the AC contributes to making different users aware of the aspect of resistance that is related to coordination efforts. The AC accomplishes this goal in a measurable fashion, giving the involved users voices and allowing the management to hear this voice clearly. In addition, this is done in an anonymous form to address users' fears of possible retaliation. To socialize information about the Coordination Requirements makes relative deprivation explicit and can bring about a reduction in the perception of organizational injustice [36]. With regard to the procedural justice that is advocated because of participation in the definition of new procedures [37] or because of the goal to reduce employees' frustration in response to instances of organizational power [18], the AC can represent an alternative channel to provide voices for users, especially in the presence of perceived procedural injustice [38]. The AC can also facilitate vicarious learning [39] about situations that are related to the new organization of the work by allowing users to learn from each other by observing the other colleagues' workloads and by making it possible to find users who use forms of unintentional "employee silence" [40].

IV. Evaluation of the WES tool

The next step is to evaluate the real effectiveness of the WES tool in limiting the possible negative effects that are related to the coordination aspects of user resistance. To do this, it is necessary to study the WES adoption in real cases in which a Workflow technology–induced organizational change is occurring. To evaluate the effectiveness of the WES tool, a set of experimental studies needs to be implemented. First of all, a study to demonstrate, even if some indirect evidences are available (see e.g., [29]), that Coordination Requirements are positively related to user resistance: i.e., the more the Coordination Requirements for a user are, the more probably she will exhibit a resistant behavior and viceversa. In addition, it would be useful also to identify other job characteristics related to user resistance such as autonomy [30] to enrich the WES tool. However, this considering only the job characteristics which could be easily incorporated into the WES tool because they could be automatically generated from the workflow model designed using the WES tool. Next, it is necessary to implement a set of longitudinal studies comparing measures related to user resistance *before* and *after* the change induced by the new organization of work as a consequence of the introduction of a Workflow Technology; this has to be done considering both generic organizational measures such as organizational commitment and locally relevant constructs associated to the re-designed process [10]. The comparison of the values measured before and after the change, could be used to describe at what extent the change possibly determined the rising of resistant behaviors.

While it is clear when to set the "before" time, i.e., before the change process has been initiated, to set the "after" time is more critical. In other words, when will it be convenient to measure the effects of the change? The risk is that the later the "after" is set in time, the more the effects of the change are radical and most of all the more the costs of WT implementation have been risen. Conversely, the risk is that the sooner the "after" is set in time, and the lesser the effects of the change might be perceived by the involved users; consequenlty, what is measured would not precisely

predict the rising of resistant behaviors. It is so necessary to find an acceptable trade-off to set the "after" time. What is an acceptable trade-off is however still a research question. Some authors [29] considered to set the "after" time during what is called the "shakedown" phase of the technology deployment. This phase is considered as lasting from the point the Workflow Technology is functional and accessible by users until normal use is achieved. This is considered as the most shocking phase for the users, who have to deal with the new technology and hence with the real consequences of its introduction; so, during this time, it is more possible than users will exhibit resistant behaviors. Though we consider this reasonable, we claim that however to set the "after" time in the shakedown phase might result too later in time, that is, in this case, the costs for the implementation of the technology have been already risen, and also the time needed to implement the Workflow Technology has been already spent. What if all users during this phase would resist to the adoption of the new technology? Perhaps is it better to have a less realistic measure of resistance (e.g., to identify a probability of resistance less accurately) but to limit the costs of implementation? We believe that anticipating as much as possible the setting of the "after" time would be the right answer, and this is our challenge in proposing the WES tool. Obviously, we need an experimental proof that to anticipate the "after" time by using the WES tool gives however a good approximation to predict the possibility of resistant behaviors. To demonstrate this, we need to implement an experimental study in which a group will be assessed to measure constructs related to user resistance in the shakedown phase, while another group will be assessed with the WES tool in a very preliminary phase of the change, that is by providing users with a simulation of the change occuring with the re-designed process. The comparison of the measures collected at the two different times by considering the two different groups will provide some useful information about the feasibility of the WES approach. Another point to investigate is about the effectiveness of the WES in communicating the consequences of the change, because we claim that socializing the information about consequences of the change by means of social visualization techniques should mitigate the emergence of resistant behaviors. In this respect, another study should compare two (or possibly more) groups in which the same change at the same "after" time is communicated. With this design of the study, it is possible to compare the measures related to user resistance between the two (or more) groups in order to identify whether the use of the WES tool is more effective or not to limit the possible rise of resistant behaviors than other strategies used to manage an organizational change induced by the redesign of a work process.

V. Conclusion and Future work

The paper presented the WES, a tool for anticipating the possible effects of user resistance toward the introduction of a Workflow Technology at an early stage of its implementation. In fact, with WES, it is possible to design a business process and to simulate its execution by involving the possible Actors. Actors can be made aware of the Coordination Requirements with respect to the other mutual Actors through the Activity Circle. The AC implements a social visualization approach in which the position of each dot on a circle represents the strength of the Coordination Requirement of the related Actor. The visualization of the Coordination Requirements associated with each Actor then allows for sharing the coordination aspects of the user resistance among the involved people. This visualization is intended to give voices to real users about the organization of the work (as imposed by the Workflow Technology) at an early stage of the implementation in an attempt to limit their possible frustration and provide managers with information that allows them to address, as soon as possible, any user resistance. This approach limits the possible ramifications that result from (at worst) a "sabotage" of the system [15] or that limit the costs for redesigning the system. The WES encompassing the HOMe-BUPro model and the visualization of Coordination Requirements is being implemented as a part of a research project of the author by integrating these new features within the existing WES system [41]. Future work will focus first on the evaluation of the effectiveness of the WES tool (see Section IV); second, future work will focus on evaluating the possibility to integrate in the WES tool different "organizational" measures that are related to user resistance and to find the way to visualize them with the Activity Circle in a coherent way.

References

[1] M. Sarini, "The Activity Circle: Building a Bridge Between Workflow Technology and Social Software," in *Proceedings of the Advances in Human-Oriented and Personalized Mechanisms, Technologies and Services (CENTRIC), 2010 Third International Conference on*. IEEE Press, pp. 22 –27, 2010.

[2] S. Laumer, "Resistance to IT-induced Change - Theoretical Foundation and Empirical Evidence," Ph.D. dissertation, University of Bamberg. Germany, 2012.

[3] G. Marakas and J. O'Brien, *Introduction to Information Systems-16th edition*. McGraw-Hill, 2012.

[4] R. Hirschheim and M. Newman, "Information Systems and User Resistance: Theory and Practice," *The Computer Journal*, vol. 31, no. 5, pp. 398–408, 1988.

[5] K. R. Abbott and S. K. Sarin, "Experiences with Workflow Management: Issues for the Next Generation." Chapel Hill, NC, USA: ACM Press, pp. 113–120, 1994.

[6] P. Dourish, "Process Description as Organisational Accounting Devices: the Dual Use of Workflow Technologies," in *Proceedings of the 2001 Conference on Supporting Group Work (GROUP '01)*. ACM, New York, pp. 52–60, 2001.

[7] J. Bowers, G. Button, and W. Sharrock, "Workflow from Within and Without: Technology and Cooperative Work on the Print Industry Shopfloor," in *Proceedings of the Fourth European Conference on Computer-Supported Cooperative Work (ECSCW'95)*. Kluwer Academic Publishers, pp. 51–66, 1995.

[8] S. Robinson and R. Bennett, "A Typology of Deviant Workplace Behaviors: A Multidimensional Scaling Study," *The Academy of Management Journal*, vol. 38 (2), pp. 555–572, 1995.

[9] P. Koopman and R. R. Hoffman, "Work-arounds, Make-work, and Kludges," *IEEE Intelligent Systems*, vol. 18, no. 6, pp. 70–75, 2003.

[10] V. Venkatesh, "Where to Go from Here? Thought on Future Directions for Research on Individual-level Technology Adoption with a Focus on Decision Making," *Decision Science*, vol. 37, no. 4, pp. 497–518, 2006.

[11] C. Wen, U. Remus, and A. M. Mills, "Understanding and Addressing User Resistance to IS Implementation in a Lean Context," in *Proceedings of the 19th European Conference on Information Systems, ECIS 2011*, 2011.

[12] J. J. Jiang, W. A. Muhanna, and G. Klein, "User Resistance and Strategies for Promoting Acceptance Across System Types," *Information & Management*, vol. 37, no. 1, pp. 25–36, 2000.

[13] H. Kim and A. Kankanhalli, "Investigating User Resistance to Information Systems Implementation: a Status Quo Bias Perspective," *MIS Quarterly*, vol. 33, no. 3, pp. 567–582, 2009.

[14] S. ThaoPhia, "User Resistance to Information Technology: A Case Study of the Hmong American Partnership," Ph.D. dissertation, Capella University, USA, 2008.

[15] S. Shang and T. Su, "Managing User Resistance in Enterprise Systems Implementation." in *Proceedings of the Tenth Americas Conference on Information System AMCIS*. ,pp. 149–153, 2004.

[16] C. Folkerd and G. Spinelli, "User exclusion and fragmented requirements capture in publicly-funded IS projects," *Transforming Government: People, Process and Policy*, vol. 3, no. 1, pp. 32–49, 2009.

[17] M. Hammer, "Reengineering Work: Don't Automate, Obliterate," *Harvard Business Review*, vol. July-August, pp. 104–112, 1990.

[18] T. Lawrence and S. Robinson, "Ain't Misbehavin: Workplace Deviance as Organizational Resistance," *Journal of Management*, vol. 33, pp. 378–394, 2007.

[19] M. Sarini, "The Activity Circle: A Social Proxy Interface to Display the Perceived Distributed Viscosity about Workflow Technology," in *Cognitively Informed Intelligent Interfaces: Systems Design and Development*. IGI global, 2012.

[20] F. Davis, "A Technology Acceptance Model for Empirically Testing New End-user Information Systems : Theory and Results," Ph.D. dissertation, Sloan School of Management, 1986.

[21] W. H. Delone and E. R. McLean, "The Delone and McLean model of Information Systems Success: A Ten-year Update," *Journal of Management Information Systems*, vol. 19, no. 4, pp. 9–30, 2003.

[22] S. Poelmans and H. A. Reijers, "Assessing Workflow Management Systems a Quantitative Analysis of a Workflow Evaluation Model," in *Proceedings of International Conference on Enterprise Information Systems (ICEIS 2009)*, 2009.

[23] M. Igler, P. Moura, M. Zeising, and S. Jablonski, "ESProNa: Constraint-based Declarative Business Process Modeling," in *Proceedings of the IEEE International Enterprise Distributed Object Computing Conference Workshops (EDOCW)*, pp. 91–98, 2010.

[24] M. Pesic and W. M. P. van der Aalst, "A Declarative Approach for Flexible Business Processes Management," in *Proceedings of Business Process Management Workshops*, pp. 169–180, 2006.

[25] K. Schmidt and L. Bannon, "Taking CSCW Seriously: Supporting Articulation Work," *Computer Supported Cooperative Work, The Journal of Collaborative Computing*, vol. 1, no. 1, pp. 7–40, 1992.

[26] M. Cataldo, P. A. Wagstrom, J. D. Herbsleb, and K. M. Carley, "Identification of Coordination Requirements: Implications for the Design of Collaboration and Awareness Tools," in *Proceedings of the 2006 20th anniversary conference on Computer supported cooperative work*, ser. CSCW '06. New York, NY, USA: ACM, pp. 353–362, 2006.

[27] A. H. Van De Ven, A. L. Delbecq, and R. Koenig, "Determinants of Coordination Modes within Organizations," *American Sociological Review*, vol. 41, no. 2, pp. 322–338, 1976.

[28] S. Oreg, "Resistance to Change: Developing an Individual Differences Measure," *Journal of Applied Psychology*, vol. 88, pp. 680–693, 2003.

[29] M. G. Morris and V. Venkatesh, "Job Characteristics And Job Satisfaction: Understanding The Role Of Enterprise Resource Planning System Implementation, ", *MIS Quarterly*, vol. 34, no. 1, pp. 143–161, 2010.

[30] R. Hackman and G. Oldham, *Work Redesign*. Addison Wesley, 1985.

[31] M. Cataldo, J. D. Herbsleb, and K. M. Carley, "Socio-Technical Congruence: A Framework for Assessing the Impact of Technical and Work Dependencies on Software Development Productivity," in *Proceedings of the Second ACM-IEEE international symposium on Empirical software engineering and measurement (ESEM'08)*, pp. 2–11, 2008.

[32] T. Erickson, "'Social' Systems: Designing Digital Systems that Support Social Intelligence," *AI & Society*, vol. 23, no. 2, pp. 147–166, 2008.

[33] K. G. Karahalios and F. B. Viégas, "Social Visualization: Exploring Text, Audio, and Video Interaction," in *Proceedings of the CHI '06 extended abstracts on Human factors in computing systems*. New York, NY, USA: ACM, pp. 1667–1670, 2006.

[34] M. L. Markus, "Power, politics, and MIS implementation," *Communications of the ACM*, vol. 26, no. 6, pp. 430–444, 1983.

[35] F. Crosby, "Relative Deprivation in Organizational Settings," *Research in Organizational Behavior*, vol. 6, pp. 51–93, 1984.

[36] J. Greenberg, "A Taxonomy of Organizational Justice Theories," *The Academy of Management Review*, vol. 1, pp. 9–22, 1987.

[37] J. Colquitt, "On the Dimensionality of Organizational Justice: A Construct Validation of a Measure." *Journal of Applied Psychology*, vol. 86, no. 3, pp. 386–400, 2001.

[38] J. Thibaut and L. Walker, *Procedural Justice: A Psychological Analysis*. Erlbaum, Hillsdale, 1975.

[39] L. Trevino and S. Youngblood, "Bad Apples in Bad Barrels: A Causal Analysis of Ethical Decision Making Behavior," *Journal of Applied Psychology*, vol. 75(4), pp. 378–385, 1990.

[40] M. Knoll and R. Dick, "Do I Hear the Whistle? A First Attempt to Measure four Forms of Employee Silence and their Correlates," *Journal of Business Ethics*, pp. 1–14, 2012.

[41] R. Armenio, "Implementazione di un sistema per la visualizzazione e la valutazione della perceived distribuited viscosity relativa ad una workflow technology (in Italian)." Master's thesis, University of Milano-Bicocca, 2011.

A Framework for Exploratory Analysis of Extreme Weather Events Using Geostatistical Procedures and 3D Self-Organizing Maps

Jorge Gorricha, Victor Lobo
CINAV
Escola Naval
Almada, Portugal
lourenco.gorricha@marinha.pt, vlobo@isegi.unl.pt

Ana Cristina Costa
ISEGI-UNL
Universidade Nova de Lisboa
Lisboa, Portugal
ccosta@isegi.unl.pt

***Abstract*— Extreme weather events such as heavy precipitation can be analyzed from multiple perspectives such diverse as the daily intensity or the number of consecutive wet days. Thus, it is necessary to get an overall view of the problem in order to characterize the extreme precipitation occurrence along time and space. Extreme precipitation indices, estimated from the empirical distribution of the daily observations, are increasingly being used not only to investigate trends in observed precipitation records, but also to examine scenarios of future climate changes. However, each of the indices, by itself, shows only a part of the phenomenon and there are multiple examples where one single index is not sufficient to characterize the occurrence of extreme precipitation. Therefore, a high dimensional approach should be considered. In this paper, we propose a framework for characterizing the spatial patterns of extreme precipitation that is based on two types of visualization approaches. The first one uses linear models, such as Ordinary Kriging and Ordinary Cokriging, to produce continuous surfaces of five extreme precipitation indices. The second one uses a three-dimensional Self-Organizing Map to visualize the phenomenon from a global perspective, allowing identification and characterization of spatial patterns and homogeneous areas. Also, to allow an easy interpretation of spatial patterns, a pattern matrix is proposed, where variables and color patterns are ordered using a one-dimensional Self-Organizing Map. The proposed framework was applied to a set of precipitation indices, which were computed using daily precipitation data from 1998 to 2000 measured at nineteen meteorological stations located in Madeira Island. Results show that the island has distinct climatic areas in relation to extreme precipitation events. The northern part of the island and the higher locations are characterized by heavy precipitation events, whereas the south and northwest parts of the island exhibit low values in all indices. The promising results from this study indicate that the proposed framework, which combines linear and nonlinear approaches, is a valuable tool to deepen the knowledge on local spatial patterns of extreme precipitation.**

Keywords-Climate; Kriging; Precipitation patterns; Self-Organizing Map; 3D Self-Organizing Map.

I. INTRODUCTION

The occurrence of extreme weather events, such as extreme precipitation, is usually associated to an increase of risk for some human activities. Therefore, the monitoring of risk associated with such phenomena is a key element in ensuring safety, economic development and sustainability of human activities.

Some extreme weather events, such as heavy precipitation, can be analyzed from multiple perspectives as diverse as the daily intensity of precipitation or the number of consecutive wet days. Moreover, those perspectives often have overlapping effects. Thus, when characterizing the occurrence of extreme precipitation, it is necessary to get a synoptic perspective of the phenomenon, considering all its dimensions. This work extends our earlier work on extreme precipitation in Madeira Island [1] regarding the use of Geostatistical Procedures and a Three-Dimensional (3D) Self-Organizing Map (SOM) [2-5] to visualize multidimensional spatial data.

To get a uniform view on observed changes in precipitation extremes, a core set of standardized indices was defined by the joint working group CCI/CLIVAR/JCOMM Expert Team on Climate Change Detection and Indices (ETCCDI) [6]. Some of these indices correspond to the enunciated perspectives of extreme precipitation. This kind of climate data has, at least, two major problems: first, as stated before, each of the indices, by itself, shows only a part of the problem; second, precipitation indices are typically measured in meteorological stations and, therefore, it is necessary to estimate the values of those indices in areas that are not covered by meteorological stations.

Extreme precipitation events can be characterized and analyzed using multiple approaches. Numerous studies of changes in extreme weather events focus on linear trends in the indices, aiming to determine whether there has been a statistically significant shift in such indices [7-10], but only a few focus on their local spatial patterns [11].

In this paper, we propose a framework for the exploratory analysis of extreme precipitation events that is based on two types of approaches: the first one uses linear models, such as Ordinary Kriging and Ordinary Cokriging, to produce continuous surfaces of five extreme precipitation indices; the second one uses a 3D SOM to visualize the phenomenon from a global perspective, i.e., in all its dimensions, allowing the identification and characterization of homogeneous areas and the detection of spatial patterns.

To illustrate the effectiveness of the proposed framework, we present a case study of precipitation events in Madeira Island, which is a Portuguese subtropical island located in the North Atlantic. It is considered a

Mediterranean biodiversity 'hot-spot' and is especially vulnerable to climate change [12]. During the winter season, eastward moving Atlantic low-pressure systems bring precipitation to the island and stationary depressions can cause extreme precipitation events [12]. The characterization of precipitation in Portuguese islands has been less studied than in mainland Portugal [8].

The work reported herein investigates the spatial patterns of extreme precipitation in Madeira Island during three hydrological years (1998-2000). Amongst the eleven precipitation indices proposed by the ETCCDI, five indices were selected, hoping to achieve a global characterization of the phenomenon in its different perspectives. The selected indices capture not only the precipitation intensity, but also the frequency and length of heavy precipitation events. Although the period chosen is not significant for a robust characterization of extreme precipitation events in Madeira Island, it is sufficient to test the proposed framework and provide an exploratory analysis of the phenomenon.

First, for spatial interpolation purposes, the spatial continuity models of the five precipitation indices were computed using geostatistical procedures, such as Ordinary Kriging (OK) and Ordinary Cokriging (OCK). Finally, the estimated surfaces of all the precipitation indices were analyzed using a clustering tool especially adapted for visualizing multidimensional data: the SOM.

This paper is organized into five sections as indicated: Section II presents the related work; Section III presents the framework; Section IV provides an example covering the proposed framework; Section V reports some concluding remarks.

II. RELATED WORK

Looking for spatial patterns and homogeneous zones is an important field of study in climatology. The aim of this paper is demonstrate that 3D SOM can be a valuable tool when it is used together with some well known geostatistical procedures, such as Kriging, in order to detect homogeneous zones and spatial patterns associated to some extreme weather events, such as heavy precipitation.

The use of SOM has brought a new approach to climate analysis that allows us to circumvent some limitations of traditional approaches [13], such as Principal Component Analysis (PCA). A typical example of this was demonstrated by comparing SOM and PCA in the extraction of spatial patterns in Reusch et al. [14]. In fact, that work demonstrates that PCA can fail to extract spatial patterns in cases where SOM performs well.

Identifying homogeneous zones and spatial patterns is one of the major fields of application of SOM in climate analysis and we can find multiple examples of such applications in the literature. For instance, in Hsu and Li [15], SOM is used to recognize homogeneous hydrologic regions and for the identification of the associated precipitation characteristics. Guèye et al. [16] propose the use of SOM, combined with a hierarchical ascendant classification to compute, using the mean sea level pressure and 850 hPa wind field as variables, the main synoptic weather regimes relevant for understanding the daily variability of rainfall. In more recent work, SOM is applied to, objectively, identify spatially homogeneous clusters [15]. In Gorricha and Lobo [17], the use of SOM is proposed for the visualization of homogeneous zones using border lines computed according to the distances in the input data space. In Lin et al. [18], the SOM is applied to identify the homogeneous regions for regional frequency analysis, showing that the SOM can identify them more accurately when compared to other clustering methods.

However, the use of SOM in climate analysis is not restricted to spatial patterns recognition. The literature is also rich in other examples, such as the use of the SOM to classify atmospheric patterns related with extreme rainfall [19], the use of SOM to identify synoptic systems causing extreme rainfall [20] and some other examples of using the SOM in climate studies, such as analysis of circulation variability, evolution of the seasonal climate and climate downscaling [13, 21].

Because the SOM converts the nonlinear statistical relationships that exist in data into geometric relationships, able to be represented visually [3, 4], it can be considered as a visualization method for multidimensional data, especially adapted to display the clustering structure [22, 23], or in other words, as a diagram of clusters [3]. When compared with other clustering tools, the SOM is characterized mainly by the fact that, during the learning process, the algorithm tries to guarantee the topological ordering of its units, thus allowing an analysis of proximity between the clusters and the visualization of their structure [24].

Typically, a clustering tool must ensure the representation of the existing patterns in data, the definition of proximity between these patterns, the characterization of clusters and the final evaluation of the output [25]. In the case of spatial data, the clustering tool should also ensure that the groups are made in line with geographical closeness [24]. The geo-spatial perspective is, in fact, a crucial point that makes the difference between spatial clustering and clustering in common data. Recognizing this, there are several approaches, including some variants to the SOM algorithm [26], proposed to visualize the SOM in order to deal with geo-spatial features. In this context, an alternative way to visualize the SOM taking advantage of the very nature of geo-referenced data can be reached by coloring the geographic map with label colors obtained from SOM units [24]. One such approach is the "Prototypically Exploratory Geovisualization Environment" [27] developed in MATLAB®. This prototype incorporates the possibility of linking SOM to the geographic representation by color, allowing dealing with data in a geo-spatial perspective.

In this study, we propose to use a clustering method for spatial data based on the visualization of the output space of a 3D SOM [28]. The proposed approach is based on the association of each of the three orthogonal axes (x, y and z) that define the SOM grid output space to one of the three primary colors: red, green and blue (RGB scheme). The results obtained in Gorricha and Lobo [28] point to a significant increase in the clustering quality due to use of 3D SOMs, when compared with the most usual SOMs, i.e., defined with a regular two-dimensional (2D) grid of nodes.

III. DATA ANALYSIS FRAMEWORK

The framework used in this study integrates two main steps: first, the values of each index (variable) at unsampled locations are estimated using geostatistical procedures; second, the indices (variables) are visualized using the SOM.

A. Geostatistical modeling of precipitation indices

As the ultimate goal is to get an insight of the spatial patterns of extreme precipitation, the first step is the spatial interpolation of each primary variable (index averaged over the study period). Geostatistical methods, known as Kriging, are usually preferred to estimate unknown values at unsampled locations because they account for the attribute's spatial continuity.

In this study, we will focus on two particular cases of this group of linear estimators: the OK and the OCK. The main difference between these two Kriging variants is that OCK explicitly accounts for the spatial cross-correlation between the primary variable and secondary variables [29].

A key step of Kriging interpolation is the spatial continuity modeling, which corresponds to fitting an authorized semivariogram model (e.g., Exponential, Spherical, Gaussian, etc.) to the experimental semivariogram cloud of points [29]. This procedure is extremely important for structural analysis and is essential to get the Kriging parameters [30]. The modeling results of this stage will be detailed in the next Section.

The methodology used to model the spatial continuity of each index can be summarized as follows:

- Determine the experimental semivariogram for the two main directions of the island's relief orientation (if there is significant evidence of geometric anisotropy). Isotropy can be assumed only if the semivariogram is not dependent on direction [31];
- In the remaining cases assume isotropy;
- If there is evidence of strong correlation and linear relationship between some primary variable and the existing secondary information (i.e., elevation), the model of co-regionalized variables is considered in the semivariogram modeling phase.

After modeling the experimental semivariograms, the OK/OCK methods are applied. The interpolation model selected to describe each index will be chosen based on the Mean Error (ME) of the cross-validation (or "leave-one-out" cross-validation) results. This criterion is especially appropriate for determining the degree of bias in the estimates [32], but it tends to be lower than the real error [33]. Therefore, the final decision will also consider the Root Mean Square Error (RMSE) of the cross-validation results, which is an error statistic commonly used to check the accuracy of the interpolation method.

B. Using the SOM to Visualize the Precipitation Indices

After producing the spatial surface of each averaged precipitation index, the main goal is to visualize this set of variables in order to identify areas with similar patterns of occurrence of extreme precipitation. To achieve this, we propose the use of the SOM, a data visualization tool that has been proposed for visualizing spatial data [34, 35].

The SOM is an artificial neural network based on an unsupervised learning process that performs a gradual and nonlinear mapping of high dimensional input data onto an ordered and structured array of nodes, generally of lower dimension [4]. In its most usual form, the SOM algorithm performs a number of successive iterations until the reference vectors associated to the nodes of a bi-dimensional network represent, as far as possible, the input patterns that are closer to those nodes (vector quantization). In the end, every input pattern in the data set is mapped to one of the network nodes (vector projection). As a result of this process, by combining the properties of an algorithm for vector quantization and vector projection, the SOM compresses information and reduces dimensionality [36].

After this optimization process, topological relations amongst input patterns are, whenever possible, preserved through the mapping process, allowing the similarities and dissimilarities in the data to be represented in the output space [3]. Therefore, the SOM algorithm establishes a nonlinear mapping between the input data space and the map grid that is called the output space.

Formally, let us consider a 3D SOM defined with three dimensions [u v w] and a rectangular topology. The SOM grid or the output space (N) is a set of ($u \times v \times w$) units (nodes) defined in R^3, such that:

$$N = \{n_i = [x\ y\ z]^T \in R^3 : i = 1, 2, ..., (u \times v \times w)\} \quad (1)$$

where x, y and z are the unit coordinates in the output space, such that:

$$\begin{aligned} x &= 0,1,...,(u-1) \\ y &= 0,1,...,(v-1) \\ z &= 0,1,...,(w-1) \end{aligned} \quad (2)$$

These coordinates must be adjusted to fit the RGB values, which typically vary between 0 and 1. The new coordinates (R,G,B) of the unit n_i in RGB space can be obtained through the range normalization of the initial values:

$$R = \frac{x}{u-1}; \quad G = \frac{y}{v-1}; \quad B = \frac{z}{w-1} \quad (3)$$

As a result, each of the three dimensions of the 3D SOM will be expressed by a change in tone of one particular primary color (RGB) and, hence, each SOM unit will have a distinct color label. This process allows that each geo-referenced element can receive the color of its Best Matching Unit (BMU), i.e., the SOM unit where each geo-referenced element is mapped. Fig. 1 represents schematically a SOM with 27 units (3×3×3) in the RGB space followed by the geographical representation of several geo-referenced elements painted with the color labels of their BMU's.

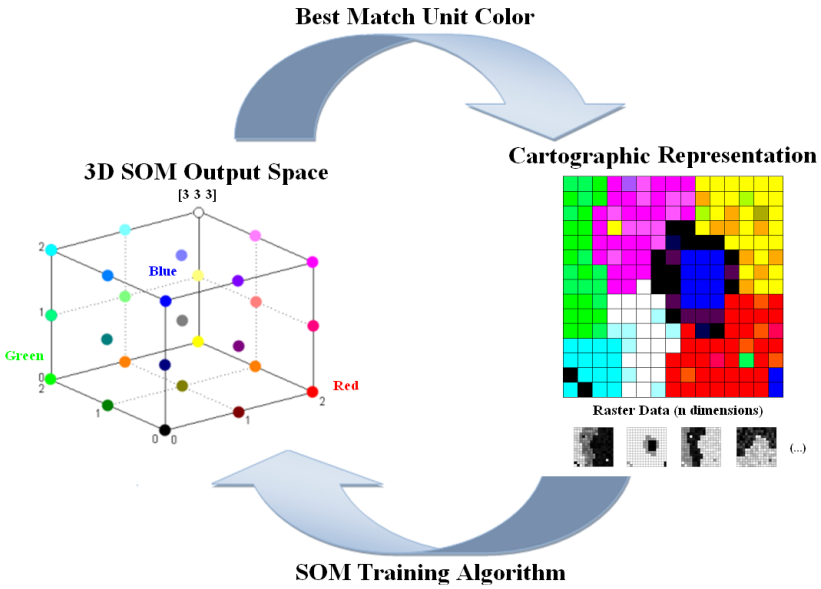

Figure 1. Linking SOM's knowledge to cartographic representation. A color is assigned to each SOM unit (following the topological order). Then the geo-referenced elements are colored with the color of their BMU's.

The visualization strategy proposed in Fig. 1 is also adaptable to explore the SOM output space of SOMs defined with only two dimensions, indeed the most usual form. However, this visualization strategy, based on the association of an RGB color to each output space dimension of the SOM, clearly won with the use of 3D SOMs.

C. Framework Diagram

In this subsection, we present a diagram (Fig. 3) that summarizes the proposed framework for exploratory analysis of extreme weather events that are characterized by several variables measured in some meteorological stations along time (several years).

The framework will encompass three major phases:

- Data extraction and preprocessing;
- Estimation of values at unsampled locations using OK and OCK, including the Geo-statistical modeling of variables along space;
- Visualization of the high dimensional spatial data using the SOM.

IV. The Case of Madeira Island

A. Study Region And Data

This subsection provides a description of the study region and of the data used to characterize extreme precipitation patterns in Madeira Island in order to illustrate the framework proposed in Section II.

1) Madeira Island

The study area corresponds to Madeira Island, which is located in the Atlantic Ocean between latitudes 32° 30' N – 33° 30' N and longitudes 16° 30' W – 17° 30' W. The island has an area of approximately 737 km^2 distributed over a mountain range of 58 km oriented in the direction WNW-ESE (Fig. 2).

The climate of the island is extremely influenced by the Atlantic Azores anticyclone and also by its own characteristics of altitude and relief direction [37]. In fact, the island's topography orientation causes a barrier, almost perpendicular to the most frequent wind direction (northeast). As a result of this natural barrier, there is a continuous ascent of moist air masses from the Atlantic, causing frequent precipitation in the northern part of the island [37].

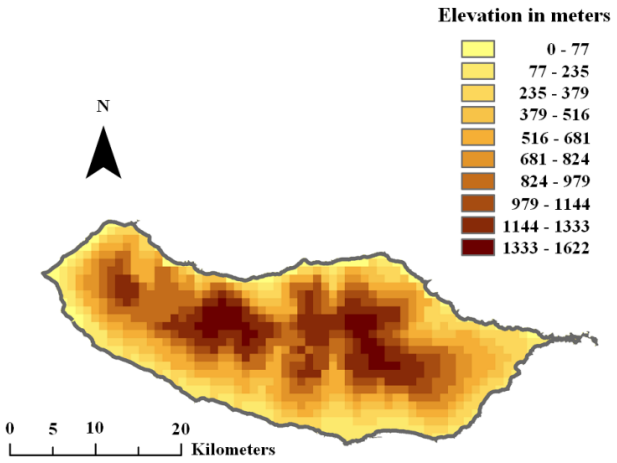

Figure 2. Madeira's island elevation model.

Despite the small size of the island, there are significant differences in the climate of its two halves [38]: the northern part of the island is colder and wetter; the southern part is warmer and drier. Also, as expected, the precipitation on the island increases with altitude but presents significant differences between those two halves.

FRAMEWORK DIAGRAM

1. DATA PREPROCESSING PHASE

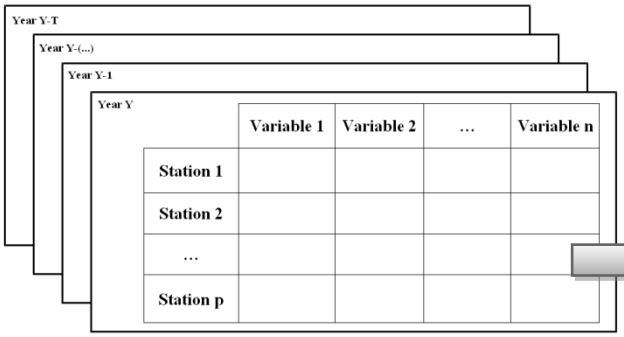

In this phase it is necessary to identify the variables that allow characterizing the phenomenon and the meteorological stations where those variables are measured along time.

The final data matrix is obtained with the mean values of each variable measured at the *p* meteorological stations.

Mean Values of variables at stations	Variable 1	Variable 2	...	Variable n
Station 1				
Station 2				
...				
Station p				

2. ESTIMATION OF VALUES AT UNSAMPLED LOCATIONS

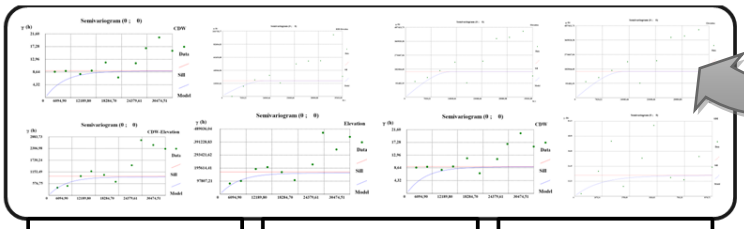

Experimental Semivariogram Assuming Isotropy

Experimental Semivariogram Assuming Anisotropy (if there is significant evidence of geometric anisotropy)

Experimental Semivariogram for the model of co-regionalized variables (if there is evidence of strong correlation between primary variable and secondary information)

For each variable it is necessary to choose the best model for spatial interpolation. The spatial continuity models will be found through the experimental semivariograms.

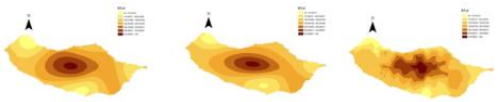

One model per variable will be chosen using cross validation methods generating a raster model.

3. VISUALIZATION OF SPATIAL DATA

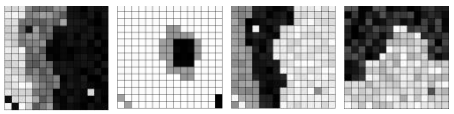

Variable 1 **Variable 2** **(…)** **Variable n**

The raster model of each variable will be used in a 3D SOM

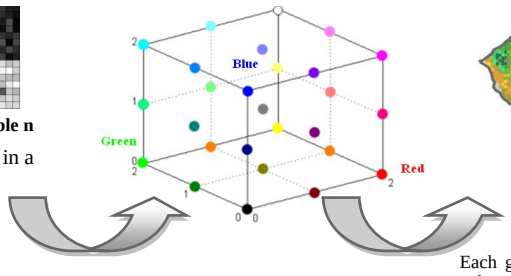

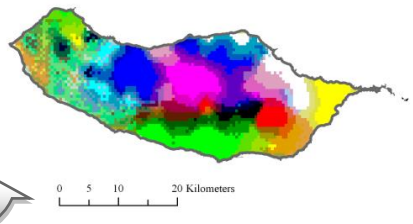

Each geo-referenced element (raster cell) receives the color of its Best Matching Unit (3D SOM Output space)

Color\Index	CWD	SDII	R1	Rx1d	Rx5d
Yellow	6,6	13,7	91	100	125
Green	7,5	14,6	73	95	132
Red	9,6	17	76	101	206
Dry Green	8,9	15	92	105	188
Brown	7,9	15,5	95	111	185
White	9,5	14	110	106	199
Blue	12,9	15,6	116	115	302
Violet	10	19,9	93	138	336

To allow an easy interpretation a pattern matrix is proposed where variables and color patterns are ordered using a 1D SOM. Also, by applying a color scheme to the values of each variable we can easily identify the colors that represent high (red), mean (yellow) and low (green) values of each variable.

Figure 3. Diagram of the proposed framework for exploratory analysis of extreme weather events that are characterized by several variables.

The highest annual precipitation occurs in the highest parts of the island and the lower rainfall amounts are observed in lowland areas, such as *Funchal* and *Ponta do Sol* [39].

2) Precipitation indices

The daily precipitation data used to compute the indices were observed at 19 meteorological stations of the National Information System of Hydric Resources (NISHR) in the period 1998–2000 (Fig. 4) and downloaded from the NISHR database (http://snirh.pt). In the present study, only annually specified indices are considered. A wet day is defined as a day with an accumulated precipitation of at least 1.0 mm. The precipitation indices computed on an annual basis can be described as follows:

- R1 is the number of wet days (in days);
- Rx1d is the maximum 1-day precipitation (in mm);
- CWD is the maximum number of consecutive wet days (in days);
- SDII is named simple daily intensity index and is equal to the ratio between the total rain on wet days and the number of wet days (in mm/day);
- Rx5d is the highest consecutive 5–day precipitation total (in mm).

Some of the selected indices are part of a variable set that is widely used in rainfall-extremes analysis and for recognition of the associated spatio-temporal patterns [40].

The precipitation data used in the subsequent analysis corresponds to the simple annual average of each index from October 1998 to September 2000, at each station location. Summary statistics of these data are presented in Table I. The combined analysis of the 5 indices allows characterizing extreme precipitation situations under different perspectives, namely considering the intensity, length and frequency of the precipitation events.

The data and ancillary information used in this study, particularly the island map and its Terrain Digital Elevation Model (Fig. 2) were downloaded from the Instituto Hidrográfico website and from the GeoCommunity™ portal, respectively.

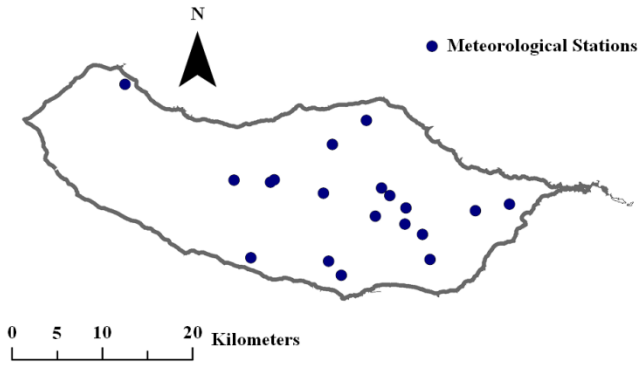

Figure 4. Distribution of meteorological stations over the island (NISHR network).

TABLE I. SUMMARY STATISTICS OF THE PRECIPITATION INDICES VALUES AVERAGED IN THE PERIOD 1998–2000

Variable	CWD (days)	R1 (days)	Rx1d (mm)	SDII (mm/day)	Rx5d (mm)
Min	5	52	50	8	64
Median	9	104	114	15.00	216
Max	15	141	169	26	390
Mean	9.53	94.95	114.74	15.48	218.2
Standard-deviation	3.1	27.47	35.0	4.26	92.9
Skewness	0.44	-0.25	-0.06	1.11	0.18
Kurtosis	-0.77	-1.22	-1.22	2.15	-0.63

B. Results

In this subsection, we present the spatial interpolation of the precipitation indices and the spatial patterns of extreme precipitation obtained using the methodology proposed in the previous Section.

Deterministic interpolation methods, such as Inverse Distance Weighting (IDW), were not considered because these methods produce inaccurate results when applied to clustered data [32]. Actually, not only the number of stations is small, but also the stations are not distributed equally over the island.

One possible way to try to reduce the problem is through the use of secondary information. In this study, we used the elevation model of Madeira Island as secondary information since some primary variables are strongly correlated with elevation.

1) Spatial interpolation of precipitation indices

The semivariogram modeling was conducted using the GeoMS® software and the spatial prediction models were obtained using ARCGIS®. The final visualization of the extreme precipitation was produced through routines and functions implemented in MATLAB®.

Not surprisingly, the most correlated indices are Rx1d and Rx5d. The remaining indices are moderately or weakly correlated, which indicates their suitability to characterize different features of the precipitation regime in Madeira Island. Moreover, Rx5d and CWD are moderately correlated with elevation (Table II).

TABLE II. CORRELATION MATRIX BETWEEN INDICES AND ELEVATION (ELEV.)

Variables	Elev.	CWD	R1	Rx1d	SDII	Rx5d
Elev.	1					
CWD	0.768	1				
R1	0.424	0.684	1			
Rx1d	0.393	0.242	0.489	1		
SDII	0.308	-0.134	-0.098	0.627	1	
Rx5d	0.616	0.440	0.542	0.804	0.62	1

Taking into account the results obtained in the exploratory analysis (IDW models not shown), several

modeling strategies were compared considering the spatial continuity behavior assumed for each index and its correlation with elevation (Table III). Although the relief of the island has a WNW-ESE direction, the analysis of the estimated surfaces obtained with IDW shows no evidence of anisotropy, except for variable Rx5d. This means that the spatial variability of all other indices was assumed identical in all directions (i.e., isotropic).

TABLE III. EXPERIMENTAL SEMIVARIOGRAM MODELING STRATEGIES

Index model number	Semivariogram	Spatial behavior assumed
CWD-1	Omnidirectional	Isotropic
CWD-2	Linear model of co-regionalization with elevation	Isotropic
R1	Omnidirectional	Isotropic
Rx1d	Omnidirectional	Isotropic
SDII	Omnidirectional	Isotropic
Rx5d-1	Omnidirectional	Isotropic
Rx5d-2	Semivariogram models for the azimuth directions 100º and 10º	Anisotropic
Rx5d-3	Linear model of co-regionalization with elevation	Isotropic

Table IV summarizes the semivariogram parameters estimated for the models indicated in Table III through the experimental semivariograms. An example of fitting a model to an experimental semivariogram to choose the model of spatial continuity is shown in Fig. 5.

TABLE IV. SEMIVARIOGRAM PARAMETERS ESTIMATED FOR THE MODELS INDICATED IN TABLE III

Index model number	Model type	Nugget	Partial sill	Spatial range (Km)
CWD-1	Spherical	6	3	11.7
CWD-2	Exponential (Exp.)	0	9 (CWD) 940 (CWD-Elevation) 166272 (Elevation)	13.4
R1	Exp.	0	714	12.6
Rx1d	Exp.	0	1157	8.2
SDII	Exp.	0	17	5.3
Rx5d-1	Gaussian	1165	6992	12.7
Rx5d-2	Gaussian	1371	6794	14.3 (major) 8.2 (minor)
Rx5d-3	Spherical	0	6440 (Rx5d) 23891 (Rx5d-Elevation) 166380 (Elevation)	12.6

OCK with elevation was used in the spatial interpolation of the averaged Rx5d and CWD, whereas all other variables were interpolated through OK (Figs. 6-9).

The final interpolation model selected to describe the spatial distribution of Rx5d and CWD depends on the error statistics of the cross-validation presented in Table V. In this case, we opted for a "leave-one-out" cross-validation strategy, where sample values are deleted from the dataset, one at the time. Then, the interpolation method is applied to estimate the missing value using the remaining observed values. Once the process is complete, the estimation errors were calculated as the differences between estimated and observed values. ME values close to zero indicate a small bias in the estimation. Hence, the best interpolation strategy for both variables is OCK with the semivariogram models Rx5d-3 and CWD-2, respectively.

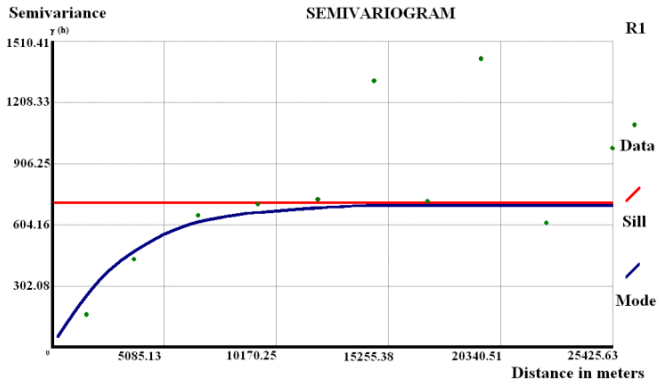

Figure 5. Example of a Semivariogram: variable R1 assuming isotropic behaviour.

TABLE V. CROSS-VALIDATION ERROR STATISTICS OBTAINED IN THE VARIOUS SPATIAL INTERPOLATION STRATEGIES (SELECTED MODELS ARE IN BOLD)

Indices	Spatial interpolation model	ME	RMSE
CWD	OK with the semivariogram model CWD-1	0.045	3.13
	OCK with the semivariogram model CWD-2	**-0.02**	**3.214**
R1	**OK**	**0.529**	**20.77**
Rx1d	**OK**	**2.68**	**31.67**
SDII	**OK**	**-0.01**	**5.012**
Rx5d	OK with the semivariogram model Rx5d-1	5.647	59.52
	OK with the semivariogram model Rx5d-2	4.493	56.5
	OCK with the semivariogram model Rx5d-3	**-0.853**	**69.04**

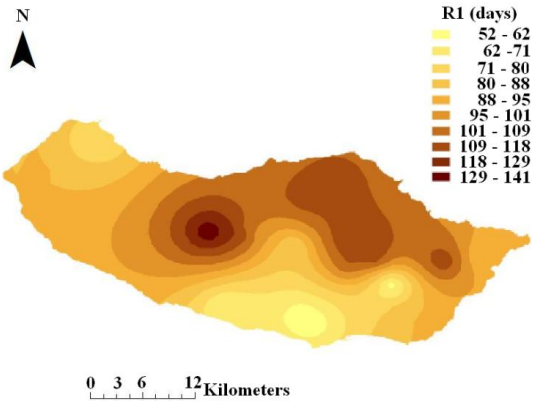

Figure 6. OK interpolation of the averaged R1 index.

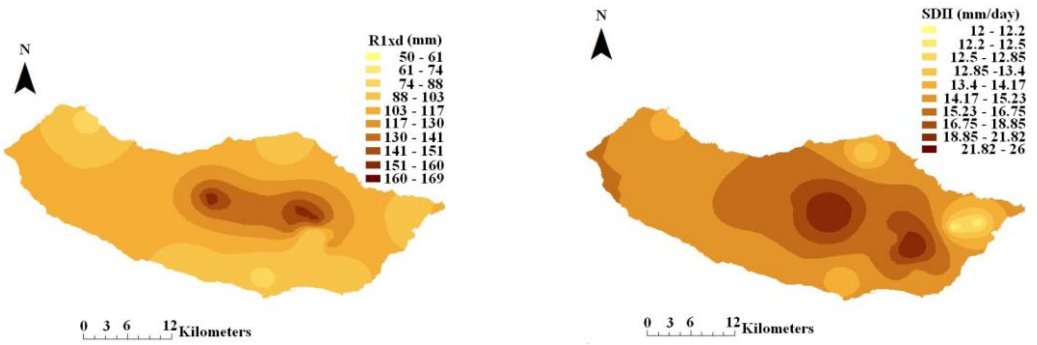

(a) (b)

Figure 7. OK interpolation: (a) Averaged Rx1d index; (b) Averaged SDII index.

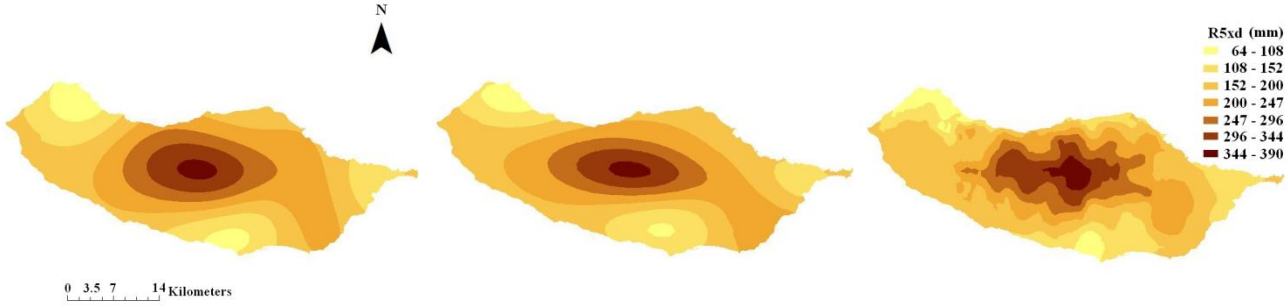

(a) (b) (c)

Figure 8. Interpolation of the averaged Rx5d index using: (a) OK and the semivariogram model Rx5d-1; (b) OK and the semivariogram model Rx5d-2; (c) OCK and the semivariogram model Rx5d-3.

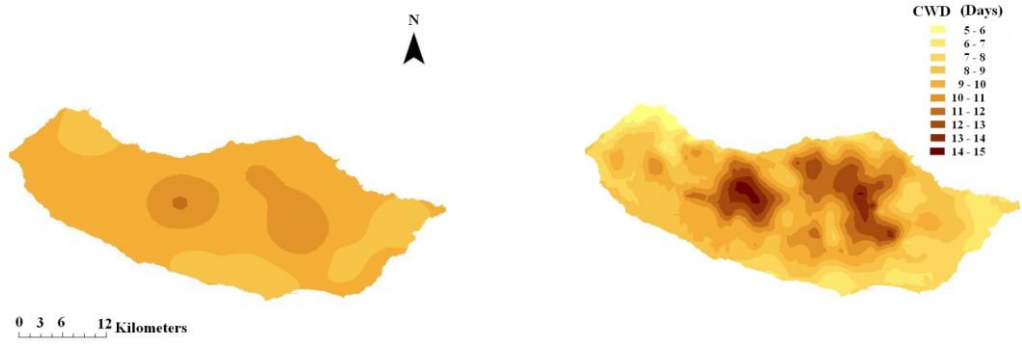

(a) (b)

Figure 9. Interpolation of the averaged CWD index using: (a) OK and the semivariogram model CWD-1; (b) OCK and the semivariogram model CWD-2.

2) Spatial patterns of extreme precipitation

In order to visualize the spatial patterns of extreme precipitation from a global perspective, a 3D SOM was applied to the indices surfaces obtained through Kriging. First, the selected models (Table V), obtained in raster format, were converted back to point data, sampled at regular intervals. Afterwards, the indices values were normalized to ensure equal variance in all variables and the SOM was parameterized as follows:

- The output space was set with 3 dimensions [4 × 4 × 4], which corresponds to 64 units in total;
- The neighborhood function selected was Gaussian;
- The length of the training was set to "long" (8 epochs);
- Random initialization.

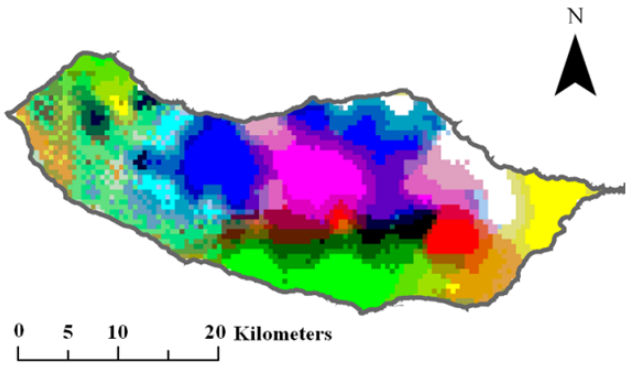

(a)

Color\Index	CWD (days)	SDII (mm/day)	R1 (days)	Rx1d (mm)	Rx5d (mm)
Yellow	6.6	13.7	91	100	125
Green	7.5	14.6	73	95	132
Red	9.6	17	76	101	206
Dry Green	8.9	15	92	105	188
Brown	7.9	15.5	95	111	185
White	9.5	14	110	106	199
Blue	12.9	15.6	116	115	302
Violet	10	19.9	93	138	336

(b)

Figure 10. Visualization of the five precipitation indices: (a) Cartographic representation of data using the output of the SOM mapped to a 3D RGB space. Areas with similar colors have similar characteristics. (b) Matrix of Patterns. This representation of the values in table VII allows to interpret the colors of spatial patterns and is obtained by the ordination of variables and patterns (colors) according to the euclidean distance between those variables and patterns and by using a color schemma to express high/low values of the variable (green-yellow-red).

As the final results depend on the initialization of the SOM, 100 models were obtained and the best model was chosen according to the criterion of best fit, i.e., the lowest quantization error (Table VI).

TABLE VI. 3D SOM RESULTS (100 MODELS)

	Quantization Error	Topological Error
Selected Model	**0.117**	**0.010**
Average Model	0.123	0.045

A RGB color was assigned to each unit of the SOM (output space of the network) according to its output space coordinates. In turn, each raster cell was represented cartographically with the color assigned to the unit of the SOM where that cell is mapped, i.e., its BMU (Fig. 10 (a)). This means that each color corresponds to a homogeneous zone in terms of the various indices values.

Table VII summarizes the characteristics of each area identified in Fig. 10. There are significant differences between the different areas (colors). Table VII allows comparing the predicted mean values for the whole island.

Although the colors in Fig. 10 (a) have a precise meaning, it is recognized that reading Fig. 10 (a) simultaneously with the values of Table VII is not easy. In fact, it will be much more difficult if many variables (and colors) are available for analysis. With this in mind, we also propose the matrix pattern in Fig. 10 (b), based on Table VII, to facilitate the interpretation of the map in Fig. 10 (a).

This matrix is the result of a one-dimensional ordering of the variables and color patterns that characterize each of the areas shown in Fig.10 (a). Within the array of patterns each cell receives one color depending on the value of the variable: low values of the variable are represented by a green color, average values are represented by a yellow color and high values are represented by a red color.

TABLE VII. SUMMARY OF THE AVERAGE VALUES FOR EACH AREA

Color\Index	CWD (days)	R1 (days)	Rx1d (mm)	SDII (mm/day)	Rx5d (mm)
Yellow	**6.6**	**91**	**100**	**13.7**	**125**
Violet	**10**	**93**	**138**	**19.9**	**336**
Red	**9.6**	**76**	**101**	**17**	**206**
Blue	**12.9**	**116**	**115**	**15.6**	**302**
White	**9.5**	**110**	**106**	**14**	**199**
Dry Green	**8.9**	**92**	**105**	**15**	**188**
Green	**7.5**	**73**	**95**	**14.6**	**132**
Brown	**7.9**	**95**	**111**	**15.5**	**185**

Thus, by applying a color scheme to the values of each variable we can easily identify the colors that represent high (red), mean (yellow) and low (green) values of each variable.

To perform the ordering of the variables and color patterns we also used SOM. However, in this case, the SOM was defined only with a single output space dimension. In fact, because of its own features, SOM is not only a clustering method; it performs an ordering that depends on its output space dimension. If the SOM is defined with one single dimension, colors will be represented by one single SOM unit in the output space as represented in Fig. 11. Thus colors will be ordered. The same strategy applies to variables; each variable will be mapped to one single SOM unit that has a specific order in the output space.

The colors and variables of the matrix pattern in Fig. 10 (b) are ordered according to the results in Table VIII.

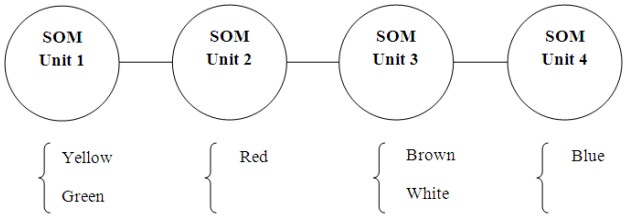

Figure 11. This figure represents schematically an example of a SOM with an output space definied with one single dimension with four units. All colors (or variables) will be mapped to one single unit so they will be ordered in the output space of the SOM.

TABLE VIII. ORDINATION PROCESS OF VARIABLES AN COLOR PATTERNS REPRESENTED IN FIG. 10

Color	SOM unit (best match unit)
Yellow	1
Violet	3
Red	6
Blue	8
White	10
Dry Green	13
Green	16
Brown	20
SOM definied with one single dimension (1X20)	

Variables	SOM Unit (best match unit)
CWD	1
R1	5
Rx1d	10
SDII	15
Rx5d	20
SOM definied with one single dimension (1X20)	

Thus, interpreting the matrix pattern in Fig. 10 (b), we can say that despite its small size, Madeira Island has distinct zones in relation to extreme precipitation events. The violet area and blue area correspond to the higher regions of the island characterized by higher values in all indices, whereas the yellow area (in the far east of the island) is characterized by the lowest values in all indices. The north of the island, which is colored blue and white, corresponds to high values in all indices (although much smaller than in the violet colored area), with particularly high R1 index values. Finally, the area colored in green is characterized by low values in all indices and broadly corresponds to Funchal city. The dry green area is very close to the average values (a phenomenon that is partly explained by the lack of information in the area). There are no significant differences between the green and brown zones.

Another important aspect that can be extracted from Fig. 10 (a) is the transition zone between green and violet/blue area. In fact, if we had used a traditional clustering method we would probably get the distinct areas but not the transition zones.

V. CONCLUSION

In this paper, we propose a framework for characterizing the spatial patterns of extreme weather events exemplified by the exploratory analysis of extreme precipitation events in Madeira Island. This framework combines two different approaches: the first one is based on geostatistical procedures and the second one is based on the 3D SOM. The first approach is used to estimate spatial surfaces of extreme precipitation indices. The second one allows visualizing the phenomenon from a global perspective, thus, enabling the identification of homogeneous areas in relation to extreme precipitation events.

The proposed framework is specially adapted to an exploratory analysis of high dimensional spatial data via visualization. The results show that it is possible to identify the relevant spatial patterns that exist in data, thus allowing gaining new knowledge about data. Another important issue is that the proposed framework does not impose a priori hypothesis about the number of clusters. In fact, the clustering structure emerges naturally without any previous definition. Moreover, not only the clusters emerge visually but also the transition zones between homogeneous zones became evident. This is, in fact, a crucial point and is actually a huge advantage since it is going to match exactly the reality of the area: spatial changes occur but gradually, not abruptly.

The spatial and temporal resolution of the data set considered in this example is too small to thoroughly characterize the extreme precipitation phenomenon in Madeira Island. Nevertheless, the results indicate the proposed framework as a valuable tool to provide a set of maps that can effectively assist the spatial analysis of a phenomenon. It can have multiple perspectives and deal with high dimensional data requiring a global view. The results of this particular application open perspectives for new applications not only in the climate context, but also in other domains where it is necessary to analyze high dimensional spatial patterns.

REFERENCES

[1] J. Gorricha, V. J. A. S. Lobo, and A. C. Costa, "Spatial Characterization of Extreme Precipitation in Madeira Island Using Geostatistical Procedures and a 3D SOM," in *Proceedings of the 4th International Conference on Advanced Geographic Information Systems, Applications, and Services - GEOProcessing 2012*, Valencia, Spain, 2012, pp. 98-104.

[2] T. Kohonen, "The self-organizing map," *Proceedings of the IEEE*, vol. 78, pp. 1464 -1480, 1990.

[3] T. Kohonen, "The self-organizing map," *Neurocomputing*, vol. 21 pp. 1-6, 1998.

[4] T. Kohonen, *Self-organizing Maps*, 3rd ed. New York: Springer, 2001.

[5] T. Kohonen, "Essentials of the self-organizing map," *Neural Networks*, vol. 37, pp. 52-65, 2013.

[6] A. M. G. K. Tank, F. W. Zwiers, and X. Zhang, "Guidelines on Analysis of extremes in a changing climate in support of informed decisions for adaptation," WMO2009.

[7] A. C. Costa and A. Soares, "Trends in extreme precipitation indices derived from a daily rainfall database for the South of Portugal," *International Journal of Climatology*, vol. 29, pp. 1956-1975, 2009.

[8] M. I. P. de Lima, S. C. P. Carvalho, and J. L. M. P. de Lima, "Investigating annual and monthly trends in precipitation structure: an overview across Portugal," *Nat. Hazards Earth Syst. Sci.*, vol. 10, pp. 2429-2440, 2010.

[9] G. M. Griffiths, M. J. Salinger, and I. Leleu, "Trends in extreme daily rainfall across the South Pacific and relationship to the South Pacific Convergence Zone,"

International Journal of Climatology, vol. 23, pp. 847-869, 2003.

[10] M. Haylock and N. Nicholls, "Trends in extreme rainfall indices for an updated high quality data set for Australia, 1910–1998," *International Journal of Climatology*, vol. 20, pp. 1533-1541, 2000.

[11] A. C. Costa, R. Durão, M. J. Pereira, and A. Soares, "Using stochastic space-time models to map extreme precipitation in southern Portugal," *Nat. Hazards Earth Syst. Sci.*, vol. 8, pp. 763-773, 2008.

[12] M. J. Cruz, R. Aguiar, A. Correia, T. Tavares, J. S. Pereira, and F. D. Santos, "Impacts of climate change on the terrestrial ecosystems of Madeira," *International Journal of Design and Nature and Ecodynamics*, vol. 4, pp. 413-422, 2009.

[13] B. C. Hewitson, "Climate Analysis, Modelling, and Regional Downscaling Using Self-Organizing Maps," in *Self-Organising Maps: applications in geographic information science*, A. Skupin and P. Agarwal, Eds. Chichester, England: John Wiley & Sons, 2008, pp. 137-153.

[14] D. B. Reusch, R. B. Alley, and B. C. Hewitson, "Relative performance of Self-Organizing Maps and Principal Component Analysis in pattern extraction from synthetic climatological data," *Polar Geography*, vol. 29, pp. 188-212, 2005.

[15] K.-C. Hsu and S.-T. Li, "Clustering spatial-temporal precipitation data using wavelet transform and self-organizing map neural network," *Advances in Water Resources*, vol. 33, pp. 190-200, 2010.

[16] A. K. Guèye, S. Janicot, A. Niang, S. Sawadogo, B. Sultan, A. Diongue-Niang, and S. Thiria, "Weather regimes over Senegal during the summer monsoon season using self-organizing maps and hierarchical ascendant classification. Part II: interannual time scale," *Climate Dynamics*, vol. 39, pp. 2251-2272, 2012.

[17] J. Gorricha and V. Lobo, "Improvements on the visualization of clusters in geo-referenced data using Self-Organizing Maps," *Computers & Geosciences*, vol. 43, pp. 177-186, 2012.

[18] G.-F. Lin and L.-H. Chen, "Identification of homogeneous regions for regional frequency analysis using the self-organizing map," *Journal of Hydrology*, vol. 324, pp. 1-9, 2006.

[19] T. Cavazos, "Large-Scale Circulation Anomalies Conducive to Extreme Precipitation Events and Derivation of Daily Rainfall in Northeastern Mexico and Southeastern Texas," *Journal of Climate*, vol. 12, p. 1506, 1999.

[20] G. Schädler and R. Sasse, "Analysis of the connection between precipitation and synoptic scale processes in the Eastern Mediterranean using self-organizing maps," *Meteorologische Zeitschrift*, vol. 15, pp. 273-278, 2006.

[21] B. C. Hewitson and R. G. Crane, "Self-organizing maps: applications to synoptic climatology," *Climate Research*, vol. 22, pp. 13-26, August 08, 2002 2002.

[22] J. Himberg, "A SOM based cluster visualization and its application for false coloring," in *Proceedings of the IEEE-INNS-ENNS International Joint Conference on Neural Networks*, Como, Italy, 2000, pp. 587- 592.

[23] S. Kaski, J. Venna, and T. Kohonen, "Coloring that reveals high-dimensional structures in data," in *Proceedings of 6th International Conference on Neural Information Processing*, Perth, WA, 1999, pp. 729-734.

[24] A. Skupin and P. Agarwal, "What is a Self-organizing Map?," in *Self-Organising Maps: applications in geographic information science*, P. Agarwal and A. Skupin, Eds. Chichester, England: John Wiley & Sons, 2008, pp. 1-20.

[25] A. K. Jain, M. N. Murty, and P. J. Flynn, "Data Clustering: A Review," *ACM Computing Surveys*, vol. 31, pp. 264-323, 1999.

[26] F. Bação, V. Lobo, and M. Painho, "The self-organizing map, the Geo-SOM, and relevant variants for geosciences," *Computers & Geosciences*, vol. 31, pp. 155-163, 2005.

[27] E. L. Koua and M. Kraak, "An Integrated Exploratory Geovisualization Environment Based on Self-Organizing Map," in *Self-Organising Maps: applications in geographic information science*, P. Agarwal and A. Skupin, Eds. Chichester, England: John Wiley & Sons, 2008, pp. 45-86.

[28] J. Gorricha and V. Lobo, "On the Use of Three-Dimensional Self-Organizing Maps for Visualizing Clusters in Georeferenced Data " in *Information Fusion and Geographic Information Systems*. vol. 5, V. V. Popovich, C. Claramunt, T. Devogele, M. Schrenk, and K. Korolenko, Eds.: Springer Berlin Heidelberg, 2011, pp. 61-75.

[29] P. Goovaerts, *Geostatistics for natural resources evaluation*. New York: Oxford University Press, 1997.

[30] P. A. Burrough and R. A. McDonnell, *Principles of Geographical Information Systems*. Oxford: Oxford University Press, 1998.

[31] A. D. Hartkamp, K. D. Beurs, A. Stein, and J. W. White, "Interpolation Techniques for Climate Variables," CIMMYT, Mexico1999.

[32] E. H. Isaaks and R. M. Srivastava, *An introduction to applied geostatistics*. New York: Oxford University Press, 1989.

[33] I. A. Nalder and R. W. Wein, "Spatial interpolation of climatic Normals: test of a new method in the Canadian boreal forest," *Agricultural and Forest Meteorology*, vol. 92, pp. 211-225, 1998.

[34] E. L. Koua, "Using self-organizing maps for information visualization and knowledge discovery in complex geospatial datasets," in *Proceedings of 21st International Cartographic Renaissance (ICC)*, Durban, 2003, pp. 1694-1702.

[35] F. Bação, V. Lobo, and M. Painho, "Applications of Different Self-Organizing Map Variants to Geographical Information Science Problems," in *Self-Organising Maps: applications in geographic information science*, A. Skupin and P. Agarwal, Eds. Chichester, England: John Wiley & Sons, 2008, pp. 22-44.

[36] J. Vesanto, J. Himberg, E. Alhoniemi, and J. Parhankangas, *SOM Toolbox for Matlab 5*. Espoo, Finland: Helsinki University of Techology, 2000.

[37] S. Prada, M. Menezes de Sequeira, C. Figueira, and M. O. da Silva, "Fog precipitation and rainfall interception in the natural forests of Madeira Island (Portugal)," *Agricultural and Forest Meteorology*, vol. 149, pp. 1179-1187, 2009.

[38] J. J. M. Loureiro, "Monografia hidrológica da ilha da Madeira," *Revista Recursos Hídricos*, vol. 5, pp. 53-71, 1984.

[39] S. Prada, "Geologia e Recursos Hídricos Subterrâneos da Ilha da Madeira." vol. PhD: Universidade da Madeira, 2000.

[40] H. J. Fowler and C. G. Kilsby, "A regional frequency analysis of United Kingdom extreme rainfall from 1961 to 2000," *International Journal of Climatology*, vol. 23, pp. 1313-1334, 2003.

Distributed Evolutionary Optimisation for Electricity Price Responsive Manufacturing using Multi-Agent System Technology

Tobias Küster, Marco Lützenberger, Daniel Freund, and Sahin Albayrak
DAI-Labor, Technische Universität Berlin
Ernst-Reuter-Platz 7, 10587 Berlin, Germany
{tobias.kuester, marco.luetzenberger, daniel.freund, sahin.albayrak}@dai-labor.de

***Abstract*—With the recent uptake in renewable energies, such as wind and solar, often comes the apprehension of unreliable energy supply due to variations in the availability of those energy sources, also resulting in severe fluctuations in the price of electricity at energy exchange spot markets. However, those fluctuations in energy costs can also be used to stimulate industry players to shift energy intense processes to times when renewable energies are abundant, not only saving money but at the same time also stabilising the power grid. In previous work, we presented a software framework that can be used to simulate and optimise industrial production processes with respect to energy price forecasts, using a highly generic meta-model and making use of evolutionary algorithms for finding the best process plan, and multi-agent technology for distributing and parallelising the optimisation. In this paper, we want to wrap up our work and to aggregate the results and insights drawn from the EnEffCo project, in which the system has been developed.**

***Keywords*—production planning; energy efficiency; evolutionary computing; multiagent systems**

I. Introduction

The transition towards sustainable energy provision must be regarded as one of the most urgent global challenges of the upcoming decades. Regulatory and technological solutions must be developed to pursue the goal of decreasing the environmental impact, and supplying reliable, secure and affordable energy nevertheless. The amount of integrated Renewable Energy Sources (RES) on the one hand and the enhancement of primary energy efficiency on the other are crucial dimensions for a successful transition. However, without the implementation of intelligent technological and regulatory mechanisms, intermittency of regenerative sources will affect primary energy efficiency of global energy networks and markets.

In this paper, building upon previous work [1], we present a system for simulating production processes and for optimising those processes w.r.t. local energy production and variable energy prices.

From an economic point of view, the energy price in particular has sparked fierce debates, and its impact becomes apparent when looking at the most recent incidents in Bulgaria, where increased energy prices caused political disturbances [2]. Fossil and nuclear generation technologies currently appear to bear economic advantages over still emergent photovoltaic and wind generation. In 2009, 5.8% of the globally produced energy was generated by nuclear power plants [3]. In industrialised nations, this share is significantly higher: In the United States and in the European Union, the amount of energy that was produced by nuclear power plants ranged between 10.0% and 14.1% [3].

However, the Fukushima Daiichi nuclear incident has painfully fostered an increasing awareness for the insecurity of nuclear power and convinced many governments to adopt phase-out legislations. The German government, for instance, adopted a similar legislation and intends to shut down all nuclear power plants before the year 2023. As laudable as this endeavour is, the complete nuclear phase-out entails difficulties, not least because the ceasing amount of controllable base load electricity has to be replaced.

Now, looking at already high energy costs, and having in mind that 10 to 14 percent of our today energy production will cease over the next years, it is most likely that energy costs will increase even more in the foreseeable future.

Regarding the intermittency of generation, especially in the electricity grid, primary energy efficiency and affordable electricity can only be provided together with electricity storage or powerful demand response mechanisms.

The industrial sector in particular will be in need of these to remain competitive in the presence of significant energy price increase and price fluctuations. Considering the amount of energy the industry procures, even slight changes in the energy pricing may entail large amounts of additional costs.

A. The Industry

In Germany, the industry requires roughly 42% of the overall energy demand [4]. Industrial players are well aware of the chances and obstacles related to the 'Energiewende'. One approach to counter the dependency from energy providers and energy prices is to install local power generation facilities, such as gas- or coal-fired power plants or block heating stations on site. In most cases, energy still has to be procured from external providers, yet, as opposed to private customers, industrial players have flexible options in doing so. Energy can be either procured in the long-term at fixed prices, or short-term strategies can be applied, procuring energy only hours before it is actually needed. These short-term purchases of

energy are done at energy exchanges, such as the *European Energy Exchange AG, EEX* [5]. Following the principle of demand and response, electricity prices at energy exchanges are highly flexible and time-dependent – at times, the price can even become negative. Whenever there is a low demand for energy (e.g., at night times or sometimes right in the middle of the day), and, at the same time, an usually high amount of available energy (e.g., as a result to sunny or stormy weather and energy that is produced by solar panels or by wind turbines, respectively), the resulting price drops. Conversely, when there is a high demand for energy and there is less intermittent energy available, the price increases. The flexibility in purchasing energy allows industrial players to optimise their energy costs by means of complex investment strategies and production planning. Besides, the European legislation allows industries not only to purchase energy, but also to offer surpluses of energy at the energy exchange. This additional option further increases the potential of industries to minimise energy costs, though it aggravates the production planning likewise.

B. Production Planning and Energy Costs

Fluctuating energy prices allow industries to significantly decrease energy costs. To put it simple: In order to utilise periods with low energy costs, energy consuming parts of the process have to be shifted. As simple as this sounds, today production processes comprise a large number of sub-processes, which are also frequently interconnected and code-pendent. Thus, shifting parts of a process most likely requires other parts of the process to be shifted, as well. As an example, consider the welding of automotive bodies. Welding is considered an energy expensive production step and to shift welding processes to periods with low energy prices may yield significant savings, yet, welding is also one of the first processes in automotive production lines and shifting may require a complete reconfiguration of the entire production schedule, including material delivery and personnel planning. If one now considers the shifting of processes not as the only option, but as one of many options of industrial players to optimise their energy costs (e.g., to use local energy production, to procure and to sell energy at flexible prices, to use intermediate storage, or to reconfigure the production schedule), the complexity of the optimisation problem becomes apparent.

C. The EnEffCo Project

Within the project *EnEffCo* (**En**ergy **Eff**iciency **Co**ntrolling in the automotive industry), we were confronted with this exact problem, namely to optimise primary energy efficiency of industrial production facilities. In a joint project our goal was to develop an optimisation framework for short term energy procurement.

We decided to use stochastic optimisation, or more specifically evolutionary algorithms for this problem. We implemented an optimisation routine based on Evolution Strategy [6], considering production schedules as partially optimised phenotypes, which were continuously measured and mutated until some steady state occurred. The approach yielded good results most of the time; however, as with most stochastic algorithms, it could also get stuck in local optima. To counter this problem, and at the same time to make use of today's distributed computing infrastructure, we extended our approach by means of multi-agent technology [1]. Instead of using one single optimiser, we deployed many optimisation agents simultaneously, and overcame the problem of local optima by using different initial populations.

In this article, we summarise and conclude our work by presenting collected experiences in optimising energy costs of production processes by means of artificial intelligence.

We start with introducing the reader to the concepts used within this work, describing the domain model used for representing production processes and schedules in Section II. Then, in Section III, we describe in detail how the production processes are simulated and how the process schedule is optimised in terms of the prospected energy costs. Afterwards, in Section IV, we present a first evaluation of this optimisation using three different example processes. Subsequently, in Section V, we elaborate our approach in distributing the optimisation process among software agents, and how it fares compared to the centralised optimisation. Finally, we have a look at related approaches in Section VI and conclude our work in Section VII, where we also motivate the application of our framework in other domains.

II. Concept and Process Representation

In our approach, we use evolutionary algorithms to rearrange individual processing steps to make the best use of times of cheap energy, for instance due to variations in the availability of renewable energies, like wind, or solar.

Of course, this approach is only feasible if the production facilities are not used to their full capacity at all times, but only if there is potential for variations. This may also be the case if some machines can be used for multiple tasks, only one of which can be carried out at a time, or in case of variable shifts and break times. Another requirement is the availability of storage area for intermediate products, so that their production can be brought forward, or be deferred, to make use of times of low energy costs. Locally installed energy sources, energy storages and co-generation units can also be taken into account.

In preparation of the optimisation, the first thing to do is to create a model of the production process, including the several activities, the machinery, resources, and (intermediate) products involved. We decided on employing a very simple model, being inspired by Petri nets and adding only a bit of domain-specific information on top of that. Basically, the model consists only of *activities*, representing the individual steps in the production as well as supportive processes, and *resources*, representing all physical entities in the factory, i.e., products and by-products as well as machinery.

This model of the production process – the individual activities and how they are connected – can then be simulated, executing the several activities and consuming and producing resources accordingly. The result of the simulation is used as a quality measure for the actual optimisation algorithm, which will eventually return the process plan with the highest quality,

which can then be used to re-schedule the execution of the individual activities in the process.

Besides finding the optimal process plan for a given production process, the simulation and optimisation can also be used for investigating the effect of variations in the process model, e.g., higher storage capacities.

In the following, we will introduce the production process meta model; in the next section, simulation and optimisation are explained.

A. Production Process Meta-Model

The production process is modelled as a bipartite graph of *activities* and *resources*, similar to a Petri net [7]: Activities correspond to transitions, and resources correspond to places. Consequently, activities are "activated", or executable, if both the resources to be consumed by that activity as well as enough capacities for the resources to be produced are available. Other than in a classical Petri net, activities are not executed instantaneously but have a certain duration. Also, there are different types of resources with specific characteristics.

A slightly simplified diagram of the meta-model is shown in Figure 1. In the following, the individual elements of the model are described in detail.

- The *ProcessGraph* represents the process as a whole, made up of activities and resources. The attribute `secPerStep` specifies the number of seconds each atomic time step takes.
- An *Activity* is an individual action in the production process, having the given `duration` (multiples of the atomic time step). Activities can have `input` and `output` resources and an `energyConsumption` (one value per time step), which can also be negative.
- *Resources* represent items involved in the production, e.g., raw materials, products, machinery, or even waste heat. Depending on what they represent, their `type` is either *primary*, *secondary*, or *inventory*. Each resource has an initial `stock`, a maximum `capacity`, and may also have associated `costs`.
- *Linkings* represent the `input/output` relation between activities and resources. The `quantity` specifies the amount to consume or to produce of that resource. Consequently, they indirectly act as a precedence constraint between activities.
- *Constraints* can be used to handle a variety of additional conditions that are difficult to check otherwise, like time windows when activities must (not) be executed, e.g., for break times.

The classification of resources is based on these rules:

1) *Primary Resources* are more or less directly integrated into the final product, e.g., raw materials, pre-fabricated parts, and intermediate products.
2) *Secondary Resources* have a role in the production, without being an actual part of the product, e.g., pressurised air and gasoline for machines, waste heat, or a battery's state of charge.
3) *Inventory Resources* are part of the inventory of the factory, e.g., machines and tools. (Consequently, we think of inventory resources as not being actually consumed or produced, but merely allocated and deallocated.)

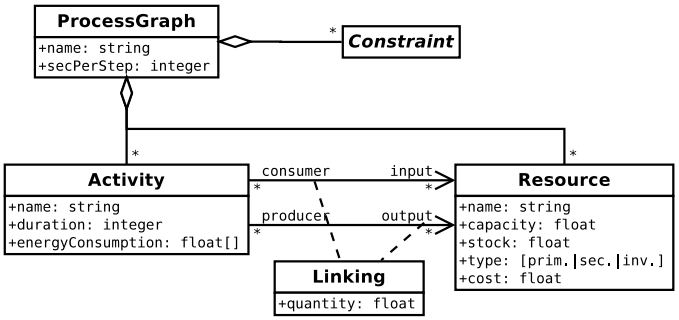

Fig. 1. Process meta-model, slightly simplified.

Conversely, activities that are producing or consuming one or more primary resources, and are thus directly involved in the production, are considered *primary activities*; otherwise, we will speak of *secondary activities*.

Electrical energy, being the main concern of the optimisation, is not regarded as a resource, but treated separately. Unlike resources, which have to be produced by activities of the process itself, electrical energy can be retrieved in (for all practical purposes) unlimited quantities and at any time. Moreover, the price for electrical energy can vary over the course of the day, based on the energy market. Surplus energy can be sold, as well.

When an activity is executed, its input resources are consumed and its output resources are produced, and it adds to the overall energy consumption of the production process. Primary and inventory resources are consumed in the first step and produced in the last step of the activity's execution; both secondary resources and energy are consumed and/or produced in *each* step of the activity.

Using this simple meta-model, a wide range of production processes can be modelled. At the same time its generality also allows for the simulation and optimisation of energy-related processes in other domains, such as creating charging schedules for electric vehicle fleets [8].

B. Implementation of Process Model and Modelling Tool

The process meta-model and a simple graphical editor for creating and configuring process models have been implemented as extensions to the Eclipse development environment. Following the usual notation for Petri nets, activities are represented by rectangles and resources by circles, using line style and colour to distinguish the different types of activities and resources (Figure 2).

Besides the basic modelling capabilities, the editor provides means for validating the process graph, for browsing and importing energy consumption data from a data base, and for passing the process graph to the optimisation system.

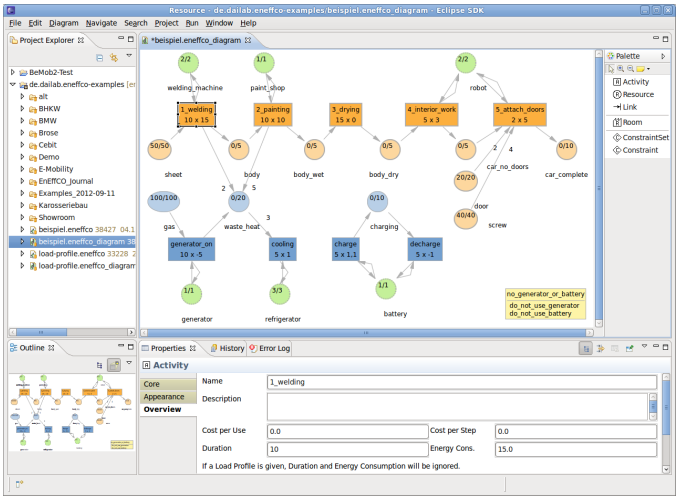

Fig. 2. Graphical process editor showing an example process.

C. Acquisition of Energy Consumption and Price Prognosis Data

One important prerequisite for optimising production processes with respect to their energy consumption is, of course, the measurement of the energy consumption of the several activities making up the production process. To this end, a number of sensors have to be installed in the production facilities to measure and record the energy consumption of the individual machines.

However, while this yields the energy consumption of e.g., a certain industrial robot, this does not correspond directly to any of the activities. For instance, an activity can require the work of different machines, and one machine can serve different activities. Instead, an activity's energy consumption is usually a section of the combined energy consumption of multiple machines.

For this purpose, a special data base client has been integrated into the process modelling tool. Using this client, the user can choose energy consumption profiles for one or more machines from the data base and select the section corresponding to a certain activity from a diagram. The combined energy consumption data for that period is then set to be the energy consumption of that activity.

III. Simulation and Optimisation

The purpose of the optimisation is to find the best possible *production schedule* for a given process model [6]. That schedule is defined by the times the individual activities are executed.

The optimisation process consists of three major aspects:

1) the simulation of a given production schedule,
2) measuring the quality of that schedule, based on the result of the simulation, and
3) finding the schedule with the highest quality.

In the following, we will look at each of these aspects in detail.

A. Simulation

The simulation of a production schedule keeps track of the resource stocks and the energy consumption in each step of the process, checking which activities are to be started, which activities are still running, and which activities are to be ended in the current step, producing and consuming resources and energy accordingly:

- For each activity to be started, the given quantity of *primary* and *inventory* input resources are consumed.
- For each activity that is currently running, the given quantities of both *secondary* resources (input and output) and *energy* are consumed and/or produced.
- For each activity to be finished, the given quantity of *primary* and *inventory* output resources are produced.

Concerning energy consumption and cost, two parameters of the simulation can be adjusted to reflect different determining factors: First, an *energy price curve* can be provided, for instance based on the prognosis given by the day-ahead energy market – in the implementation at hand, cost optimisation is conducted based on day-ahead price forecasts, e.g., for the EEX electricity spot market. Second, a *base energy* level can be specified, being the amount of energy the facility acquires via a flat fee. Energy consumption up to this level has already been paid for, so the *energy price curve* does not apply for that.

Once the simulation has terminated, it yields a record of the energy consumption and the resource stocks for each individual step in the execution of the process. These numbers, combined with the resources' capacities, the energy price curve, and other constraints, can now be used to determine the *quality* of that production schedule.

B. Quality Measurement

The *quality* of a production schedule p is determined by a sigmoid function of its *defect*, such that a high defect results in a quality close to -1, and a defect close to zero gives a quality close to zero (see Equation 1). A negative defect will result in a positive quality (this is possible in some situations, e.g., in case of negative energy prices, or energy-producing activities).

$$quality(p) = \frac{-defect(p)}{\sqrt{1 + defect(p)^2}} \quad (1)$$

The *defect* of p is the weighted sum of the energy costs $(e(p,i) \cdot w_e)$ and the defects (over- and under-shootings) of the several resources' stocks $(s_r(p,i) \cdot w_r i)$ over all steps i of the simulation (see Equation 2).

$$defect(p) = \sum_{i \in steps} [e(p,i)\ w_e + \sum_{r \in res.} s_r(p,i)\ w_r(i)] \quad (2)$$

In this equation, the energy consumption, stocks and weights are represented as functions. Different weights w can (and should) be used for resource stocks being too low and those being too high and for the different kinds of resources.

Production schedules that exceed the maximum or minimum capacities of a resource are not discarded immediately, but

are merely given a lower quality rating. This is beneficial in overcoming local optima.

C. Optimisation

Finding an energy- and cost-efficient arrangement of the several activities in the process for a given energy price curve is both a constraint-satisfactory problem and an optimisation problem: on the one hand, there must be no violations of the resources' capacities; on the other hand, the production schedule has to be as cost-efficient as possible.

Due to the large number of degrees of freedom in the process plans – with many different activities that can be started or stopped in each step of the process – the search space is much too big for exhaustive search to be applicable.

In our approach, we make use of *Evolution Strategy* (ES), a stochastic optimisation method originally introduced by Rechenberg [9], which is similar to Genetic Algorithms [10]. Besides Evolution Strategy, both *Simulated Annealing* and *Ant Colony Optimisation* have been tried, as well. However, of the three algorithms ES yielded by far the best results.

1) The ES Algorithm: As the name implies, Evolution Strategy is inspired by natural evolution: Using a $(\mu/\rho + \lambda)$ strategy, an initial "population" of μ individuals is generated. Based on these μ "parents", λ "offspring" are created by recombining and mutating a random selection of ρ parents. The quality of each of the parents and offspring is determined and the μ best individuals are selected to be the parents of the next generation. This process is repeated until the quality of the best individual does not improve for a certain number of generations.

Algorithm 1 EVOLUTION STRATEGY(μ, ρ, λ)

```
current ← INITPOPULATION(μ)
repeat
  next ← ∅
  for i ∈ {1..λ} do
    parents ← rand. select ρ indiv. from current
    offspring ← MUTATE(RECOMBINE(parents))
    next ← next ∪ {offspring}
  end for
  current ← select μ best from current ∪ next
until quality stagnates
return best individual from current
```

2) Applying ES to Manufacturing Schedules: In the system at hand, each individual represents a possible production schedule. To this end, three functions have to be implemented for production schedules, next to the quality measurement: (i) How to create the initial population of individuals, (ii) how to mutate an individual, and optionally (iii) how to recombine individuals.

The initial population is created by a very simple scheduler, chaining primary activities as long as and as early as the primary resources and inventory resources permit, or until a desired quantity of products has been produced. Thus, the initial production schedule already constitutes a valid (but naive) schedule for all the primary activities, but without taking secondary resources or energy costs into account.

There are several possibilities for mutating an individual, one of which is chosen at random: (a) a randomly chosen secondary activity can be inserted into or removed from the schedule, (b) an activity or a group of activities (primary or secondary) can be moved to another place in the process plan, i.e., being executed earlier or later, or (c) the execution times of two activities can be swapped.

For recombination, one can randomly select activities from one of the two parents, or take the activities up to some specific step from one parent, and the rest from another – of course always taking care that the right number of primary activities is selected to complete the task at hand. However, due to the many dependencies among the individual activities of a production schedule – the ordering of primary activities as well as secondary activities being executed at times relatively to some other activities – recombination does not yet work well for this domain. Thus, in practice, the parameter ρ was always assumed to be 1.

D. Implementation of the Optimisation Framework

A generic optimisation framework was created that can be used for optimising different domains using different optimisation algorithms. The actual Evolution Strategy algorithm as well as the process model domain have been implemented as plug-ins for this framework [6].

The optimisation is controlled via a simple graphical user interface (GUI, Figure 3). Like the rest of the optimisation framework, the GUI has both generic and domain- or algorithm dependent parts. For the manufacturing domain, the optimisation GUI features a large domain-specific area, providing controls for configuring the simulation and optimisation (e.g., the energy price curve to use) and for showing the best production schedule found so far in a Gantt chart-like diagram. The process chart is continuously updated as the optimisation proceeds, and also allows to 'rewind' to previous steps in the optimisation.

Once the optimisation has come to an end, additional charts are available, showing the energy consumption and resource stocks for each step in the final production schedule, as well as the development of these numbers over the course of the entire optimisation as a three-dimensional plot. Finally, the optimised production schedule can be saved to file.

IV. EVALUATION

In this section, we will discuss a number of application examples of the process optimisation algorithm. Our first example describes the ideal manufacturing process, providing enough capacities – in both time and space – to shift primary activities so that parts of the production can be handled at times of cheap energy. The scenario shown in the second example may be more realistic w.r.t. today's manufacturing processes: Here, the production activities can not be changed, but only secondary activities (such as cooling, co-generation units and buffer batteries) may be used for shifting energy consumption. Finally, the third example demonstrates both the flexibility of

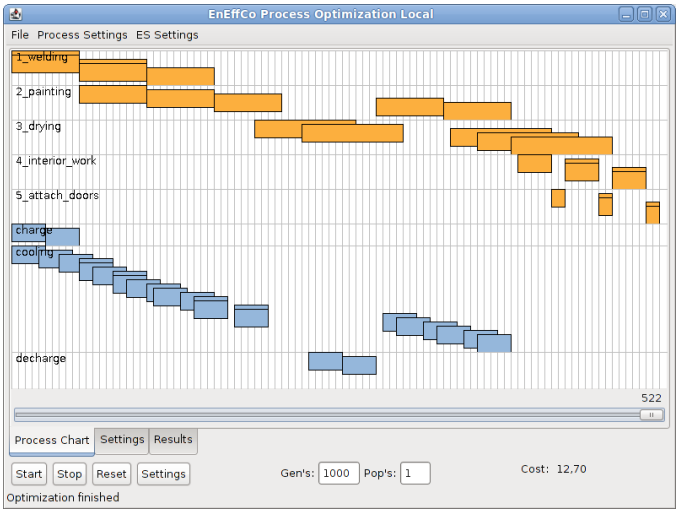

Fig. 3. Prototypical user interface for controlling the optimisation and viewing the results.

the process model and the prospects of our approach, as we use the optimisation for creating optimal charging schedules for large electric vehicle fleets.

A. Example 1: Use of Functional Storage

In this example, a simple, fictional car manufacturing process is pictured (see Figure 2).

1) Example Process: The process starts with two energy-intensive activities that induce high amounts of waste-heat: welding and painting the car chassis. Once the paint has dried, some interior works are performed, and finally the doors are attached to the chassis. For each of the intermediate products, a specific primary resource was created. The resulting production process graph is supplemented with utility activities and resources such as cooling, on-site electricity storage and a gas-powered co-generation unit. The latter two elements can be used to temporarily decrease the energy consumption, but costs for the consumed gas will in turn add to the production schedule's defect.

While the process surely is not too realistic, it demonstrates many of the aspects that can be realised in the process model, for example

- modelling the basic production chain,
- inventory resources used by multiple activities,
- resources associated with a cost, and
- cooling facilities and other supporting processes.

2) Optimisation Results: The resulting schedule can be seen in Figure 3. Here, the process has been optimised against a hypothetical hill-shaped energy price curve, i.e., with highly-priced energy in the mid of the day and low-priced energy in the morning and evening.

As can be seen, most of the energy-intensive activities (*welding* and *painting*) are taken care of in the morning, with the exception of one instance of the *painting* activity, which has been deferred to the afternoon. The high-price period is spend entirely with the *drying* activity, which consumes no electric energy at all. The remaining activities are positioned as late as possible, to get the lowest possible price for the required energy. Note also, that among the several instances of the *cooling* activity in the morning there are also two instances of the charging activity, *charging* the aforementioned in-house energy storage when energy is cheap, and *discharging* it again when the energy price is highest.

B. Example 2: Shifting Secondary Activities

The second example deals with a more realistic setting: Here, the core manufacturing process is fixed in time; no primary activities can be shifted. The straightforward motivation for this scenario is that in most industries, energy consumption is not the key cost driver. Hence, the goal for energy cost minimisation is to optimise energy consumption, given a specific production schedule. In this scenario, no primary activities are shifted. Instead, secondary activities, such as ventilation or even the generation of electricity and heat through combined heat and power stations (CHP) are viable means to approximate an optimum energy load curve. In fact, secondary processes may contribute significantly to the overall energy consumption of industrial sites.

1) Example Process: The example chosen describes a site configuration, where wind energy will be provided on site and a 24 hour wind generation forecast is incorporated into the calculations. Additionally, local energy generation comprises a combined heat and power station, which can be either idle or operate with half or full generation capacity. All primary production processes are combined into a single, day-long activity with a specific load curve, since, as mentioned before, modifications are not eligible for them. As a shiftable secondary activity, ventilation is modelled for load shifting purposes. It can be operated on standard capacity or can alternatively be increased or decreased to adjust its load level. However, a sufficient amount of fresh air must be provided at all times.

The schedule is now optimised according to a 24 hour day-ahead electricity price forecast. Local energy production is assumed to be very cost efficient. Wind generation is merely characterised by maintenance costs for the turbines, CHP related costs are calculated from maintenance and gas expenses and are attributed to heat and electricity proportionally. The costs for ventilation load shifting are assumed to be higher than wind generation costs but lower than CHP expenses in this example.

2) Optimisation Results: Figure 4 shows the resulting load curves for this optimisation example. The abscissa shows the time of the optimisation period. The first ordinate on the left shows electrical load in megawatts. The second ordinate on the right shows electricity market price forecasts in euro per kWh. Six different graphs describe the optimisation results. The area graph shows the wind generation forecast for the site. The dotted line, which is related to the second y axis on the right, depicts the external electricity price forecast. The dashed line and the solid line show the external electricity procurement

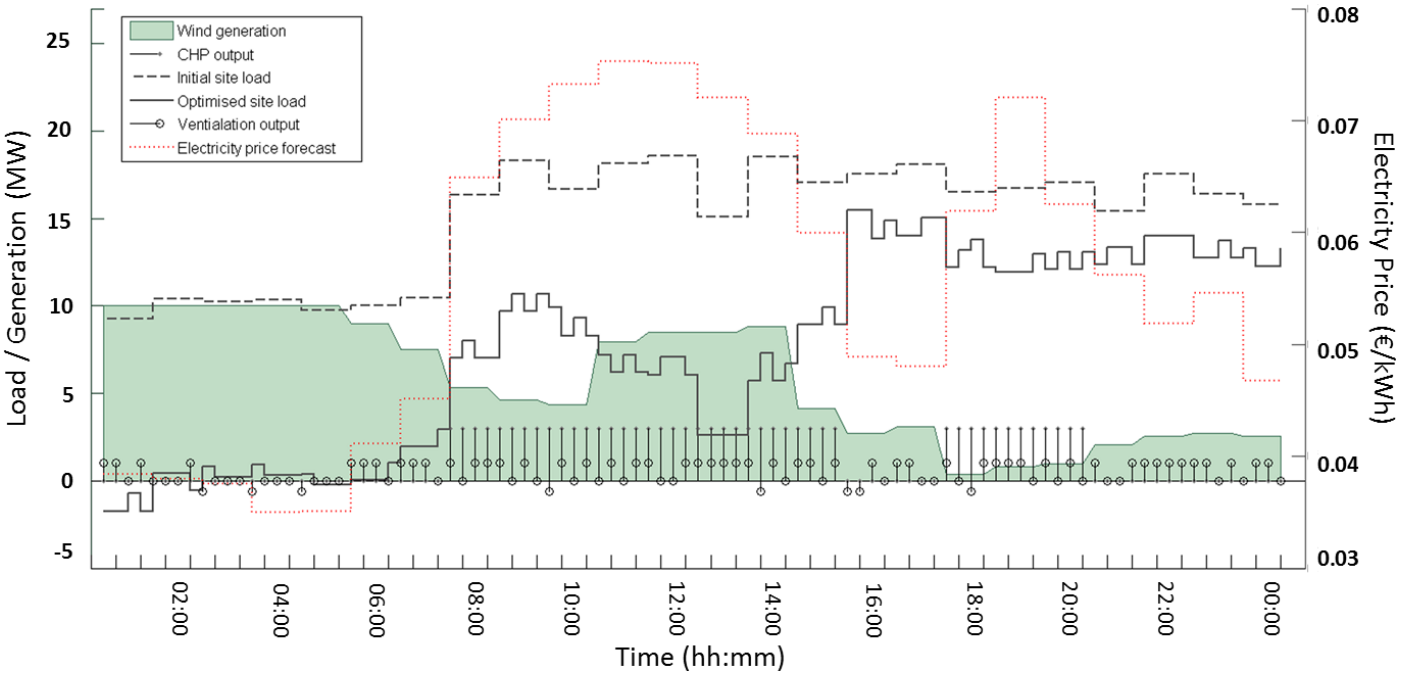

Fig. 4. Load optimisation from shifting secondary activities on an industry site.

of the site before and after the optimisation respectively. Energy consumption before the automation (dashed line) does not incorporate any local wind generation and is assumed to be covered by the external grid only. Shiftable loads are presented as stem graphs in this figure. Stem graphs with a solid point marker present the operation of the combined heat and power station, stem graphs with circle markers present ventilation. Negative ventilation load occurs when an increase of operation capacity is enforced to maintain the amount of fresh air within the predefined boundaries. Positive ventilation load occurs when operation capacity is reduced to decrease external electricity procurement.

Since wind forecast, site consumption from primary activities, and electricity market price are assumed to be non-variable, the attention should be drawn to the shiftable activities. It can be seen that the combined heat and power are strictly dependent on the market price and generation is curtailed when the price drops below about 0.059 Euros per kWh. Load shedding from ventilation control also depends upon the electricity market price but is less costly than CHP, so it is only excluded when the electricity price is at its lowest point during the high price interval between 8:00 and 21:00. To keep the amount of fresh air within the necessary boundaries, additional ventilation is injected from time to time. This occurs primarily when the electricity price is low.

To sum up these results, the optimisation tool clearly adjusts load profiles to external electricity price forecast and internal electricity generation costs to decrease the overall energy procurement costs.

C. Example 3: EV Fleet Charging Schedules

In the third and final example, the meta-model is applied to a different domain: creating charging schedules for electric vehicle (EV) sharing fleets in a micro smart grid (MSG) [8]. Here, the challenge is to schedule long-running charging activities so that no bookings are at risk while at the same time making use of locally produced energy and times of low energy prices. Further, the EVs can be used as temporary energy storages for load balancing.

1) Example Process: Here, the process graph is not created by hand, using the graphical editor, but instead is derived automatically from another model, describing the setup of the MSG, including among others the various *electric vehicles* and their current state of charge, a number of *bookings* for those EVs, and different *prosumers* representing both locally installed regenerative energy sources as well as the facility's own prospected power consumption.

For each prosumer, a day-long primary activity with an energy consumption curve reflecting the prognosis is created. Each EV is represented by a small subgraph featuring an inventory resource for the storage (the EV's battery), a secondary resource for its current capacity, and one or more charging activities reflecting the different possibilities for charging and discharging the battery, dependent on the charging station. Finally, each booking is represented by another primary activity, linked to the respective storage resource, and fixed in time at the booking's starting time. Figure 5 depicts one of those segments.

2) Optimisation Results: This optimisation was carried out two times: Once with the above described process model using

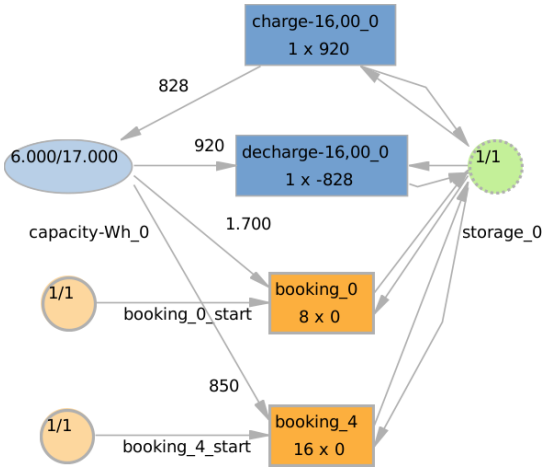

Fig. 5. Segment of process graph showing activities and resources for a single electric vehicle and associated bookings.

the meta-model and optimisation described in this paper, and once using a domain-specific meta-model developed specifically for this task (still using the same optimisation algorithm).

The results of the optimisation are promising: Charging activities are scheduled such that all bookings can be fulfilled (i.e., the storage of the respective electric vehicle is sufficiently charged) while at the same take making best use of locally produced energy and periods of low energy prices. The resulting charging schedules closely resemble those created using the domain-specific model.

However, we also found some limitations in our meta-model. For instance, using inventory resources to "lock" electric vehicles while charging or being rented does not allow for bookings that are not bound to a specific vehicle (e.g., bookings for *any* vehicle).

Nevertheless, first results convinced us to extend our approach to the domains of electro mobility and smart grids.

V. Agent-based Optimisation and Distribution

While evolutionary algorithms yield good results most of the time, it is also possible, as with other stochastic optimisation algorithms, that the optimisation gets stuck in local optima. To increase the chances of arriving at a solution close to the global optimum, the optimisation should be applied to more than one "population", and since the individual populations are optimised independently from each other, they can easily be parallelised and distributed.

To this end, the optimisation framework has been embedded into a distributed multi-agent system, allowing for the transparent and dynamic distribution of an arbitrary number of optimisation clients and servers.

Admittedly, the strength of the agent paradigm is less the transparent distribution but rather the comprehensive support that facilitates the development of autonomous, reactive, proactive and social competent entities, namely agents. As mentioned above, our current implementation is focused on distribution rather than on exploiting the latter attributes of agency. Yet, we justify the use of agent technology with our future intentions. The presented optimisation framework was well planned and its development was subdivided into different stages. In the first stage it was our intention to implement a distributed system and to ensure reliable and robust communication between the system's entities. Right now we find ourselves at this very point. For the future, however, we plan to exploit agent capabilities more comprehensively. Based on the robust and reliable distribution we want to allow agents to exchange partially optimised process plans and to recombine these plans for a more effective mutation mechanism. The recombination process, however, challenges agency far beyond distributional aspects and for this exact reason we decided to make use of agent technology right from the beginning. We consider the current application as first step towards a far more efficient and complex multi-agent based optimisation software. For a complete overview of our future intention, however, the reader is referred to Section VII.

In the following, we describe the interaction protocol, which makes a number of optimisation servers ("agents" conducting the optimisation) available to one or more optimisation clients [1]. Afterwards, we explain how the protocol and the surrounding multi-agent system have been implemented using the JIAC V agent framework.

A. Interaction Protocol

Two roles are involved in the protocol:

- *optimisation client*, requesting an optimisation
- *optimisation server*, conducting the optimisation

Obviously, there should be more than one optimisation server agent for the distribution to provide any benefit at all, but there may be multiple clients, as well, sharing those servers. An interaction diagram of the protocol is shown in Figure 6. It is composed of the following steps:

1) The protocol starts with a client broadcasting a REQUEST message to all the servers.
2) Each server receiving the message checks whether it already has an "employer", i.e., whether it is currently running an optimisation. If not, it replies with an OKAY message.
3) The client receives the OKAY message, and if it still requires the server (i.e., if there have not been enough replies from other servers yet), it replies by sending the actual MODEL to be optimised to that server. The number of remaining optimisation runs is reduced. (The full model, including energy consumption curves, price curves, etc., is not sent until now, to reduce network traffic.)
4) On receiving the MODEL message, the server will check again whether it already has an employer, as in the case of multiple clients, it might have sent OKAY messages to other clients, which may already have sent their MODEL messages.
   - If so, the server replies with a TOO LATE message. The client received this messages and corrects the number of remaining optimisations.

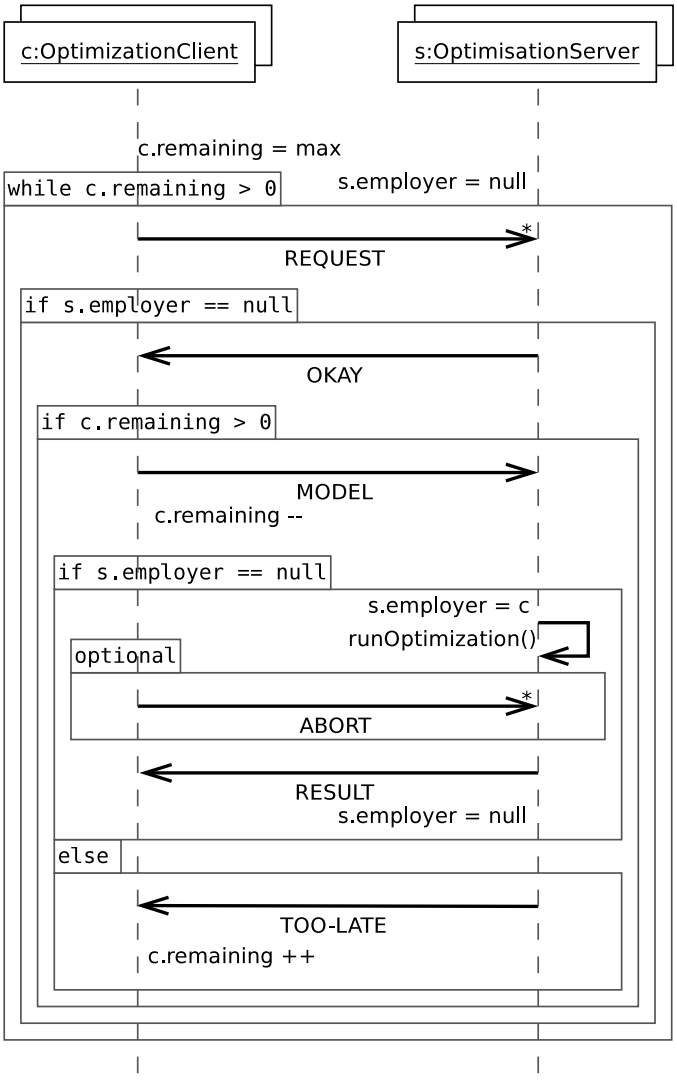

Fig. 6. Interaction protocol used in the distributed optimisation. Messages marked with an '*' are sent to all servers.

- Otherwise, the server accepts the client as its new employer and starts the optimisation run, and finally sends a message holding the RESULT back to the client.
- At any time, the client can send an ABORT message, stopping the optimisation.

5) The client continues sending out REQUEST messages until the desired number of optimisations has been conducted.

Using this interaction protocol, each of the populations of a $(\mu/\rho + \lambda)$ optimisation can be distributed to another agent. Since each run of the optimisation, or each population respectively, is independent from the others, this does not introduce any noteworthy communication overhead.

B. Implementation using JIAC V

JIAC V (Java Intelligent Agent Componentware, Version 5) is a Java-based multi-agent development framework and runtime environment [11], [12]. Among others, JIAC features communication, tuple-space based memory, transparent distribution of agents and services, as well as support for dynamic reconfiguration in distributed environments, such as component exchange at runtime. Individual JIAC agents are situated within Agent Nodes, i.e., runtime containers, which also provide support for strong migration. The agents' behaviours and capabilities are defined in a number of so-called *Agent Beans*, which are controlled by the agent's life cycle.

The protocol has been implemented by means of two JIAC Agent Beans, namely the *Optimisation Client Bean* and *Optimisation Server Bean*. Just like the optimisation framework introduced in Section III, the Agent Beans were kept generic so that the protocol can just as well be used with domain-models other than the one presented in this work, and even with different optimisation algorithms.

The implementation with JIAC (or a similar multi-agent framework) has some advantages over traditional approaches using remote procedure calls or web services:

- Both the Client Nodes and the Server Nodes can be distributed to any computer in the local network, with no need to configure IP addresses or ports. Consequently, if one of the server agents drops out, it can seamlessly be replaced by another one.
- With each JIAC agent running in a separate thread, a node with multiple agents being deployed to a multi-core server computer will automatically make best use of the several CPUs.
- Using asynchronous messaging, optimisations can be aborted ahead of time. Also, servers can send back intermediate results, to provide a trend for long-running optimisations.

Besides agents holding the Optimisation Client and Server Beans, a number of additional agents have been added to the system to represent and to connect the different components, as shown in Figure 7.

- A *DB Agent* provides an interface to the data base holding the measured energy consumption values, making them available to the other agents.
- Integrated into the Eclipse IDE is a *Plugin Agent*, which connects to the *DB Agent* to acquire energy consumption data to be imported into the current process graph. Further, this agent can send the process graph created in the editor to an *Optimisation Client Agent*.
- The *Optimisation Client Agents* carries out the distributed optimisation, sending individual optimisation jobs to different *Optimisation Server Agents*.
- The result of the optimisation can then be sent to the *Web GUI Agent*, showing the resulting process plan and its properties in a number of diagrams and graphs.

Using the same optimisation algorithms, the distributed system performs as well as the local system. It yields good results in reasonable time and the variability of results quickly decreases with an increased number of populations.

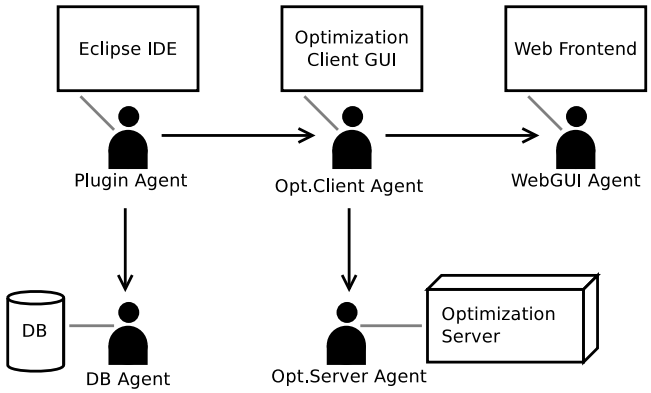

Fig. 7. Agent, components, and interactions in the distributed system.

C. Evaluation

Complementary to the evaluation of the optimisation approach in general, as discussed in Section IV, in this section we want to evaluate specifically the benefits of the distributed and parallelised version of the algorithm using the agent-based setup [1].

We evaluated the benefits of distribution and parallelisation using the first example process from Section IV, a production goal of five completed cars, a hill-shaped energy price curve and an evolution strategy with $\mu = 3$ and $\lambda = 8$.

The example process was optimised several times with different numbers of populations. The number of populations ranged from one to thirteen, and ten runs of the optimisation were performed in each case. The results are shown in the logarithmic plot in Figure 8. Note that at the time this evaluation was conducted [1], the quality function was $quality(p) = \frac{1}{1+defect(p)}$, resulting in a different range in quality values. As can easily be seen, the results of the evaluation are still valid using the new quality function.

As can be seen in Figure 8 (left), using only one population, the quality of the optimised process plan varies greatly. While there are some results with near-optimal quality, many populations apparently get stuck in local optima and obtain a low overall-quality. For up to four populations, results start to look better, but are still noticeably scattered. For five and more populations, the results become reliable, with almost each optimisation run resulting in near-optimal quality.

It may be noticed that the maximum quality reached – around 0.05 – is still far from the theoretically possible. The reason for this is that energy costs, no matter whether they could be improved any further, still add to the defect of the process schedule. Thus, with minimum energy costs of around 20 (in no specific currency), the quality can not be much greater than 0.05.

Also to be noted is the gap in quality between around 0.015 and 0.045. This gap separates results, which still have resource conflicts, and those merely suffering from less-than-optimal energy costs. In the evaluation, the weight of resource conflicts was set to add greatly to the overall result's defect, making the quality look almost discrete.

Further, we discovered that there is little to none correlation between the time an individual optimisation run takes, and the resulting quality (see Figure 8, right): the result of a quick optimisation run can be just as good (or bad) as that of a longer running optimisation, and vice versa. Thus, one possibility to improve the performance could be to start a large number of optimisations in parallel, and to abort the remaining optimisation runs once the first few results to choose from have arrived.

VI. Related Work

Industry has long since discovered, that the optimisation of manufacturing processes is able to significantly increase revenues. As a result to the continuous demand for optimisation frameworks, there are many sophisticated applications available today. In this section we outline the current spearhead of optimisation tools and concepts; yet, due to the broad range of existing approaches it is difficult to present a comprehensive survey and for this reason we decided to put emphasis on approaches and concepts that influenced our own work the most. We open this section with an analysis of academic approaches that apply evolutionary algorithms for the optimisation of manufacturing processes and proceed by presenting commercially distributed optimisation software. Here we distinguish between general purpose frameworks, visual approaches, manufacturing- and business process optimisation tools. Finally, we discuss the significance of our work against the backdrop of contemporary applications.

A. Evolutinary Algorithms and Process Optimisation

The idea to use evolutionary algorithm for the optimisation of manufacturing processes is not entirely new, as the complexity of many optimisation problems has strongly promoted their use.

Highly interesting for our work is the approach of *Santos et al.* [13], as it puts focus on energy related criteria. Yet, as opposed to our objective, the aim of *Santos et al.* is to reduce energy consumption in general, while we try to adapt our manufacturing schedules to a given energy price curve. *Bernik et al.* [14] developed a similar approach, although they do not account for energy criteria. The approach is capable to propose manufacturing schedules that are able to satisfy a given production target. In addition to the manufacturing schedule, resource requirements are calculated and assigned to the production depots. *Schreiber et al.* [15] describe a similar application, which optimises manufacturing schedules towards a given production target. As opposed to the work of *Bernik et al.*, the application is able to calculate so called lot-sizes, which are defined as the number of pieces that are processed at the same time at one workplace with one-off (time) and at the same costs investment for its set up [15].

To summarise, while there are some approaches that account for energy related factors, dynamic pricing is currently not covered although the markets offer such possibility.

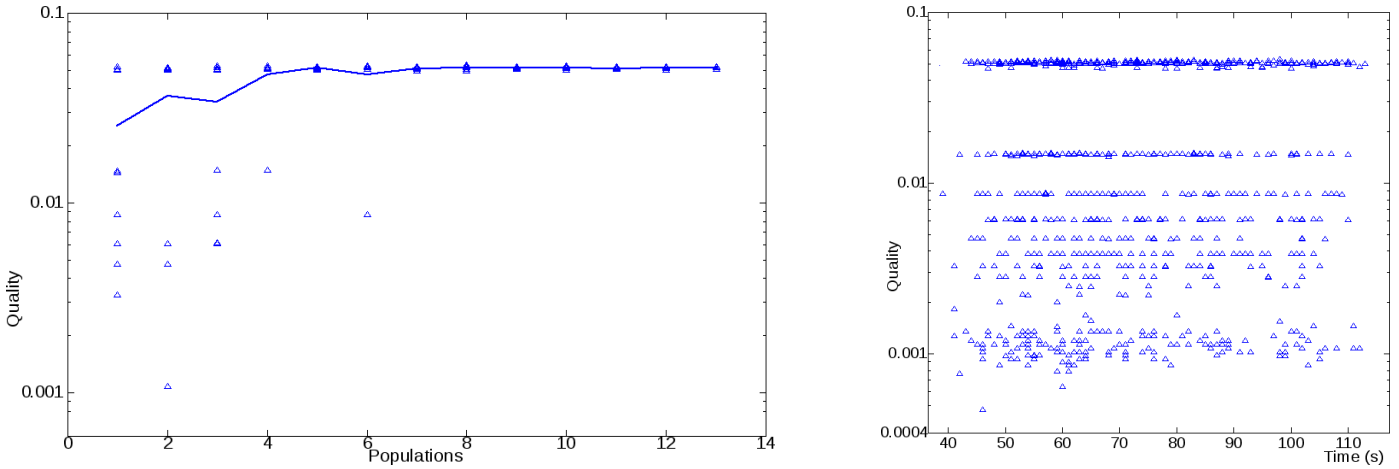

Fig. 8. Left: Correlation of number of populations to expected result quality. The graph indicates average quality values. Right: Correlation of time of optimisation run to result quality. [1]

B. Optimisation Frameworks for Production Processes

Next to frameworks that apply evolutionary algorithms in order to optimise manufacturing processes, there are of course applications that apply other methods for the same objective.

The *Siemens Plant Simulation Software* [16] for instance facilitates the simulation based optimisation of production systems and controlling strategies, while business- and logistic-processes may be supported as well. The *SIMUL8* framework [17] (Figure 9), *Arena* [18] and *GPSS/H* [19] provide similar features and are able to simulate entire production processes, from warehouse capacities and equipment utilisation to logistics, transportation, military and mining applications. *SIMUL8* additionally accounts for real life requirements, such as maintenance intervals and shift patterns. Further, *SIMUL8* uses an agent-based simulation for the optimisation of production processes.

Other types of software packages as for instance *Simio* [20] and *ShowFlow* [21] do not explicitly focus on the optimisation of production processes, but on their visualisation. For this purpose, most of the mentioned applications apply sophisticated 3D engines.

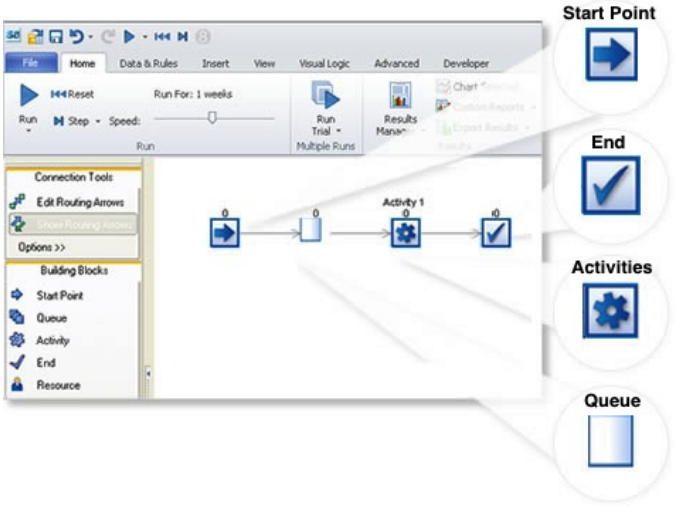

Fig. 9. The *SIMUL8* production process configuration tool, showing a palette (bottom left) and a canvas (bottom right) element as well as an exemplary process structure, including a start-, a queue-, an activity- and an end object. [17]

C. General Purpose Frameworks

Thus far, we have exclusively analysed approaches that have been developed for the optimisation of manufacturing processes. Yet, over the last years, the idea of general purpose frameworks emerged. Instead of focusing on a particular domain or problem, general purpose frameworks are able to optimise general processes, such as monetary flow, quality- and organisation management, allocation scenarios, logistics, transports and many more. Foundation to these frameworks is a generic meta-model, which is able to capture process structures, and which is usually based on established concepts.

The *PACE* framework of Eichenauer [22] and the work of Siebers et al. [23] for instance feature an arbitrary level of detail for process design. While *PACE* uses hierarchically arranged *High-Level-Petri-Nets* for this purpose, Siebers et al., using *AnyLogic*, apply an object-oriented meta-model for its processes and uses a multi-agent based model for the simulation of process configurations. *AnyLogic* further comprises a graphical user frontend, which provides information on simulated processes similar to the representation that we use for our own process configuration tool. However, *AnyLogic* integrates information on the current simulation procedure and allows for the real-time adjustment of simulation parameters, such as throughput rates or storage capacities. As an example, this feature can be used in order to simulate and observe the impact of sudden machine failures. An illustration of the visual representation of the simulated processes is given in Figure 10.

SLX [24] takes a layered approach to process modelling.

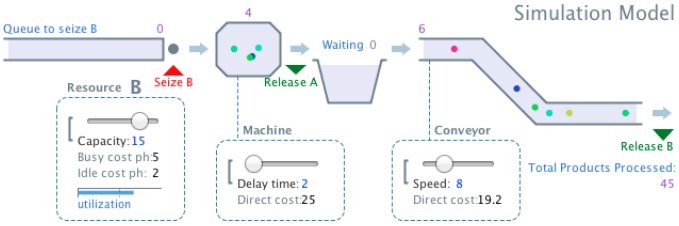

Fig. 10. The *AnyLogic* visualisation of simulated processes ([23], cut-out). Not only displays the tool the current state of simulation processes, but also allows for the adjustment of simulation parameters, such as throughput rates and capacities.

Most commonplace processes are handled in *SLX*'s upper layers, while more complex problems can be captured with *SLX*'s lower layers. The *Microsaint* [25] package avoids hierarchical structures and facilitates readability as well as easy comprehensibility. The framework entirely relies on flow charts as meta process language. In most analysed frameworks, process design is usually supported by visual editing tools. The *ADONIS* framework [26] for instance provides an impressive graphical editor for the design and manipulation of the examined process system.

In summary, we can state that general purpose tools apply a generic meta-model in order to facilitate a broad range of problems. For this meta-model, established concepts such as Petri nets [7] or flow charts are used. The analysed frameworks facilitate process design by graphical editing tools.

D. Optimisation Frameworks for Business Processes

In addition to applications that explicitly account for the optimisation of production processes, we want to attend focus on those that have been developed for other reasons. Business processes for instance have a striking resemblance to manufacturing processes and as there are optimisation frameworks for business processes, we want to mention the most prominent members of this realm as well.

To start with, *ProcessModel* [27] is a business process optimisation software, which supports optimisation from problem analysis to efficiency evaluation. The tool is able to visualise many aspects such as money savings or the efficiency of analysed processes to serve customers. A similar application is *SIMPROCESS* [28]. In addition to the capabilities of *ProcessModel*, *SIMPROCESS* is able to handle hierarchical process structures and comes with a set of sophisticated tools for the process design. Both applications apply means of simulation in order to verify optimised processes and to estimate their overall quality.

E. Lessons Learned

In this section, we gave a comprehensive overview on state of the art concepts and applications. We have already mentioned, that there are many sophisticated applications available today. Some of them have been explicitly developed in order to optimise production processes, others were designed in a generic fashion and yet feature similar capabilities.

The idea of optimising production with respect to dynamic energy tariffs is adopted by none of the examined applications, and energy related criteria in general are currently not comprehensively covered by state-of-the-art solutions, as only the approach of *Santos et al.* supports such factors.

We learned that evolutionary algorithms can be used to increase the performance of optimisation algorithms and thus selected such principle for our own application. For this purpose, we applied an established concept [9] whose performance we further enhanced by distributing our computation units.

Also, our survey did not indicate distributed computing to be widely used in process optimisation frameworks. Only the *AnyLogic* framework provides an according feature, for which the developers make use of the agent paradigm.

For our implementation we use the exact same view, only that we apply a rather comprehensive agent model as we use our agents as autonomous problem solvers while *AnyLogic* agents can be understood as simulated autonomous entities, such as persons or vehicles.

The analysis of general purpose frameworks inspired us to use a very simple and generic domain model in order to support a large number of process structures and also to provide functionality beyond the scope of optimising manufacturing processes.

To sum up, we can say that currently there are neither concepts nor frameworks, which account for the optimisation of manufacturing processes with respect to variable energy prices.

VII. Conclusion and Future Work

In this paper, we presented an optimisation framework that was developed within the government- and industry funded project EnEffCo. The main objective of the EnEffCo project was to develop software that facilitates to increase the primary energy efficiency in production and to evaluate the software with the involved industry partners.

The optimisation framework exploits the fact that industrial users are able to purchase energy with a short lead and at highly flexible prices, e.g., at the European Energy Exchange, EEX. The energy prices at the energy exchange comply with the principle of demand and response. As such, time periods with surpluses of energy (e.g., caused by an increase in wind or sunshine and the resulting energy from wind engines or solar collectors) and low grid demand (e.g., right in the middle of the day or during night times) result in low and possibly negative energy prices, while periods with only little energy from renewable energy sources and an increased grid demand result in high energy prices.

In order to capture the arrangement of production lines, we have developed a suitable domain model. The model is similar to a Petri net and comprises only two main types, namely activities and resources. A link type is used to indicate a connection between activities and resources. The generic design of the domain model allowed us to consider scenarios beyond the originally intended scope of the project. As an example, we were able to optimise charging procedures of electric vehicles.

An instance of this model, representing the different machines and tasks found in a production process, is then passed to the optimisation framework, together with an energy price forecast obtained from the energy exchange.

Due to the many options in optimising production processes (e.g., randomly shifting, adding- or removing individual activities within extensive timeframes), we decided to use stochastic optimisation. Besides other approaches, such as Simulated Annealing and Ant Colony Optimisation, the best results were achieved using Evolution Strategies, where a population of individuals (process plans) is gradually mutated and (optionally) recombined until a satisfying quality is reached.

While the quality of the results may vary, the optimisation process generally produces reliable results in a timely manner, allowing industries to quickly act even on short-term energy price fluctuations. Making use of today's distributed computing architectures, the optimisation can be distributed to multiple clients and servers, using the JIAC V multi-agent framework. This way, the reliability of the outcomes increases further, while on average taking no longer than a single run of the optimisation. Additional JIAC agents are used to integrate the optimisation with other components of the system, e.g., the process modelling tool and the user frontend.

The EnEffCo Project officially ended in December 2012. Nevertheless, we intend to further refine our approach and to extend the capabilities to other domains.

Currently, we are transferring our findings from the EnEffCo project to ongoing projects, for instance for load-balancing in micro smart grids and for optimising the charging schedules of large electric vehicle car sharing fleets [8]. While some extensions to the domain model and the optimisation framework had to be introduced, so far, the results look promising.

Furthermore, it is our intention to enhance the optimisation process by allowing agents to exchange and recombine partially optimised production schedules. This requires agents to autonomously query intermediate results from other optimisation agents and to select suitable parts from these results for the mutation process. Where our current implementation is focused on distributional aspects only, this extension will exploit the agent paradigm more comprehensively and pave the way for a high-performance agent-based optimisation framework.

ACKNOWLEDGMENT

This work was developed in the project "Energieeffizienzcontrolling am Beispiel der Automobilindustrie" (*EnEffCo*) (Eng.: Energy Efficiency Controlling in the automotive industry), funded by the *Federal Ministry of Economics and Technology* under the funding reference number 0327843B.

REFERENCES

[1] T. Küster, M. Lützenberger, and D. Freund, "Distributed optimization of energy costs in manufacturing using multi-agent system technology," in *Proc. of 2nd Int. Conf. on Smart Grids, Green Communications and IT Energy-aware Technologies (ENERGY 2013), St. Maarten, St. Maarten*, P. Lorenz and K. Nygard, Eds. IARIA, March 2012, pp. 53–59.

[2] "Bulgaria government to resign, pm boiko borisov says," BBC NEWS Europe, March 2013, accessed: 21.5.2013. [Online]. Available: http://www.bbc.co.uk/news/world-europe-21516658

[3] "Energymix EU–USA–China," Bundeszentrale für politische Bildung, March 2013, accessed: 21.5.2013. [Online]. Available: http://www.bpb.de/nachschlagen/zahlen-und-fakten/europa/75143/energiemix

[4] "Auswertungstabellen zur Energiebilanz für die Bundesrepublik Deutschland 1990 bis 2011 – Berechnungen auf Basis des Wirkungsgradansatzes," Arbeitsgemeinschaft für Energiebilanzen e.V., September 2012.

[5] "EEX Website," European Energy Exchange AG, accessed: 21.5.2013. [Online]. Available: http://www.eex.com

[6] T. Küster, M. Lützenberger, and D. Freund, "An evolutionary optimisation for electric price responsive manufacturing," in *Proceedings of the 9th Industrial Simulation Conference, Venice, Italy*, S. Balsamo and A. Marin, Eds. EUROSIS-ITI, June 2011, pp. 97–104.

[7] T. Murata, "Petri nets: Properties, analysis and applications," in *Proceedings of the IEEE*, april 1989, pp. 541–580.

[8] D. Freund, A. F. Raab, T. Küster, S. Albayrak, and K. Strunz, "Agent-based integration of an electric car sharing fleet into a smart distribution feeder," in *3rd IEEE PES Innovative Smart Grid Technologies Europe (ISGT Europe)*, 2012.

[9] I. Rechenberg, *Evolutionsstrategie : Optimierung technischer Systeme nach Prinzipien der biologischen Evolution*, ser. Problemata. Stuttgart-Bad Cannstatt: Frommann-Holzboog, 1973.

[10] A. Eiben and J. Smith, *Introduction to Evolutionary Computing*, ser. Natural Computing. Springer-Verlag, Berlin, 2003.

[11] B. Hirsch, T. Konnerth, and A. Heßler, "Merging agents and services – the JIAC agent platform," in *Multi-Agent Programming: Languages, Tools and Applications*, R. H. Bordini, M. Dastani, J. Dix, and A. El Fallah Seghrouchni, Eds. Springer, 2009, pp. 159–185.

[12] M. Lützenberger, T. Küster, T. Konnerth, A. Thiele, N. Masuch, A. Heßler, M. Burkhardt, J. Tonn, S. Kaiser, J. Keiser, and S. Albayrak, "JIAC V – a MAS framework for industrial applications," in *Proc. of the 12th Int. Conf. on Autonomous Agents and Multiagent Systems (AAMAS 2013), Saint Paul, MN, United States of America*, T. Ito, C. Jonker, M. Gini, and O. Shehory, Eds., 2013.

[13] A. Santos and A. Dourado, "Global optimization of energy and production in process industries: a genetic algorithm application," *Control Engineering Practice*, vol. 7, no. 4, pp. 549–554, 1999.

[14] I. Bernik and M. Bernik, "Multi-criteria scheduling optimization with genetic algorithms," in *Proceedings of the 8th WSEAS International Conference on Evolutionary Computing*. Stevens Point, Wisconsin, USA: World Scientific and Engineering Academy and Society (WSEAS), 2007, pp. 253–258.

[15] P. Schreiber, P. Vazan, P. Tanuska, and O. Moravcik, "Production optimization by using of genetic algorithms and simulation model," in *DAAM International Scientific Book 2009*, B. Katalinic, Ed. DAAM International, 2009.

[16] Siemens, "Plant simulation – plant, line and process simulation and optimization," Project Broschure, 2010, accessed: 21.5.2013. [Online]. Available: http://www.plm.automation.siemens.com/en_us/Images/7541_tcm1023-4957.pdf

[17] K. Concannon, M. Elder, K. Hunter, J. Tremble, and S. Tse, *Simulation Modeling with SIMUL8*, 4th ed. Visual Thinking International Ltd., 2003.

[18] M. D. Rossetti, *Simulation Modeling and Arena*, 1st ed. Wiley, 2009.

[19] R. C. Crain, "Simulation using GPSS/H," in *Proceedings of the 29th Winter Simulation Conference*, December 1997, pp. 567–573.

[20] J. A. Joines and S. D. Roberts, *Simulation Modeling with SIMIO: A Workbook*. Simio LLC, 2010.

[21] I. S. Solutions, "The ShowFlow website," 2011, accessed: 21.5.2013. [Online]. Available: http://www.showflow.com/

[22] B. Eichenauer, "Optimizing business processes using attributed petri nets," in *Proceedings of the 9th Symposium about Simulation as Commercial Decision Help*, March 2004, pp. 323–338.

[23] P.-O. Siebers, U. Aickelin, H. Celia, and C. W. Clegg, "Understanding

retail productivity by simulating management practices," in *Proceedings of the Eurosim 2007, Ljubljana, Slovenia*, 2007, pp. 1–12.

[24] J. O. Henriksen, "SLX: The X is for extensibility," in *Proceedings of the 32nd Winter Simulation Conference*, 2000, pp. 183–190.

[25] D. W. Schunk, W. K. Bloechle, and K. R. L. Jr., "Micro saint: Micro saint modeling and the human element," in *Proceedings of the 32nd Winter Simulation Conference*, 2002, pp. 187–191.

[26] S. Junginger, H. Kühn, R. Strobl, and D. Karagiannis, "Ein Geschäftsprozessmanagement-Werkzeug der nächsten Generation – ADONIS: Konzeption und Anwendungen," *Wirtschaftsinformatik*, vol. 42, no. 5, pp. 392–401, 2000.

[27] ProcessModel, Inc., "The ProcessModel website," 2011, accessed: 21.5.2013. [Online]. Available: http://www.processmodel.com/

[28] CACI, "The SIMPROCESS website," 2011, accessed: 21.5.2013. [Online]. Available: http://simprocess.com/

Estimating Disaggregated Employment Size from Points-of-Interest and Census Data: From Mining the Web to Model Implementation and Visualization

Filipe Rodrigues, Ana Alves, Evgheni Polisciuc
Department of Informatics Engineering
University of Coimbra
Portugal
Email: {fmpr,ana}@dei.uc.pt,
evgheni@student.dei.uc.pt

Shan Jiang, Joseph Ferreira
Massachusetts Institute of Technology
Boston, USA
Email: {shanjiang,jf}@mit.edu

Francisco C. Pereira
Singapore-MIT Alliance
for Research and Technology
Singapore
Email: camara@smart.mit.edu

***Abstract*—The global spread of internet access and the ubiquity of internet capable devices has lead to an increased online presence on the behalf of companies and businesses, namely in collaborative platforms called local directories, where Points-of-Interest (POIs) are usually classified with a set of categories and tags. Such information can be extremely useful, especially if aggregated under a common (shared) taxonomy. This article proposes a complete framework for the urban planning task of disaggregated employment size estimation based on collaborative online POI data, collected using web mining techniques. In order to make the analysis possible, we present a machine learning approach to automatically classify POIs to a common taxonomy - the North American Industry Classification System. This hierarchical taxonomy is applied in many areas, particularly in urban planning, since it allows for a proper analysis of the data at different levels of detail, depending on the practical application at hand. The classified POIs are then used to estimate disaggregated employment size, at a finer level than previously possible, using a maximum likelihood estimator. We empirically show that the automatically-classified online POIs are competitive with proprietary gold-standard POI data. This fact is then supported through a set of new visualizations that allow us to understand the spatial distribution of the classification error and its relation with employment size error.**

***Keywords*—machine learning, spatial analysis, points-of-interest, urban planning, GIS.**

I. INTRODUCTION

With the increasing number of mobile devices and social networks in the latest years, the amount of geo-referenced information available on the Web is growing at an astonishing rate. Capture devices such as camera-phones and GPS-enabled cameras can automatically associate geographic data with images, which is significantly increasing the number of geo-referenced data available online. Social networks also have an important role. They are a great medium where users can share information they collect with their mobile devices. As a consequence, the amount of online descriptive information about places has reached reasonable dimensions for many cities in the world.

A point of interest, or POI for short, is a specific point location that someone may find useful or interesting. POIs can be used in navigation, characterization of a place, sociological studies, city dynamics analysis, geo-reference of texts, etc [1]. Such a simple information structure can be used and enriched such that context-aware systems behave more intelligently.

In spite of their importance, the production of POIs is scattered across a myriad of different websites, systems and devices, thus making it extremely difficult to obtain an exhaustive database of such wealthy information. There are hundreds, if not thousands, of POI directories in the Web like Yahoo![1], Manta[2] and Yellow Pages[3], each one using its own taxonomy of categories or tags. Therefore, it is essential to unify these different sources by mapping them to a common taxonomy. Otherwise, their application as a whole becomes impractical.

In this article, we propose the use of machine learning techniques to automatically classify POIs from different sources to a standard taxonomy such as NAICS [2] (U.S., Canada and Mexico) or ISIC[4] (United Nations), thereby allowing a proper analysis and visualization of the POI data, especially when the latter comes from different sources. A good example is land use analysis, a central pillar in urban planning. If the POIs do not share a common taxonomy then we are not able to determine, for instance, how many POIs of universities exist in a given area, since a POI source can classify them as "schools" while others classify them as "higher education." This makes the whole analysis unreliable. In the particular case that we explore in this article, we are interested in classifying POIs according to the North American Industry Classification System (NAICS). The NAICS is the standard used by Federal statistical agencies in classifying business establishments for the purpose of collecting, analyzing, and publishing statistical data related to the U.S. business economy [2]. NAICS was developed under the auspices of the Office of Management and Budget (OMB), and was adopted in 1997 to replace the old Standard Industrial Classification (SIC) system.

NAICS is a two to six-digit hierarchical classification code system, offering five levels of detail. Each digit in the code is part of a series of progressively narrower categories, and more digits in the code signify greater classification detail.

[1] http://local.yahoo.com
[2] http://www.manta.com
[3] http://www.yellowpages.com
[4] http://unstats.un.org/unsd/cr/registry/isic-4.asp

The first two digits designate the economic sector, the third digit designates the sub-sector, the fourth digit designates the industry group, the fifth digit designates the NAICS industry, and the sixth digit designates the national industry. A complete and valid NAICS code contains six digits [3]. By having different levels of detail, NAICS codes allow us to perform analysis at different granularities depending on the practical application at hand.

Figure 1 shows part of the NAICS hierarchy for the retail economic sector.

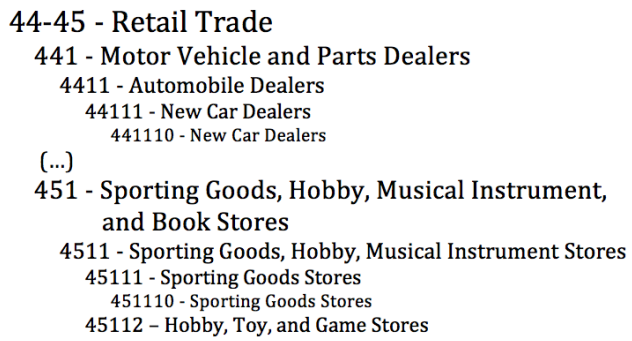

Fig. 1. Example of the NAICS hierarchy for the retail economic sector.

In order to make learning possible, a POI matching technique is proposed, allowing the establishment of golden dataset from which various typical machine learning models are then estimated. After comparing several classification methods, we apply the results to the urban modeling task of estimating employment size at a disaggregated level. This task is traditionally made at a coarser level (Traffic Analysis Zone, Census Tract or Block Group level) than what could be now possible, through the use of POI data.

Finally, we explore innovative visualization techniques to (1) understand the POI distribution across space, (2) identify spatial areas of POI classification error, and (3) relate the latter with the accuracy of employment size estimation model.

In summary, the main contributions of this article are:

- A POI matching algorithm;
- A machine learning approach to automatically classify POIs to standard classification system (NAICS);
- A model to estimate employment at a disaggregated level;
- A collection of visualization techniques that allow a deeper understanding of the geographical data and the models developed.

The remainder of this article is organized as follows. Section II presents previous related studies. Section III explains our data analysis and modeling methodology, from data preparation to model generation and validation. Section IV shows the obtained results. In Section V we describe the application of this methodology to the field of urban planning. Section VI presents a collection of visualization techniques of the data used and the models produced. We finish the article with conclusions and future work.

II. State of the Art

The applications of machine learning algorithms in classification tasks are vast and cover diverse areas that range from Speech Recognition to Medicine, including forecasting in Economics and Environmental Engineering or Road Traffic Prediction. In urban planning, land-use/land-cover information has long been recognized as a very important material [4]. However, as Fresco [5] claimed, accurate data on actual land-use cannot be easily found at both global/continental and national/regional scales.

In order to cope with these problems, automatic approaches to classify land use are being developed using distinct techniques.

A common approach to infer land-use/land-cover is to use satellite imagery. However, while these approaches have already proven to get good results, they are more suited to land-cover inference which is considered somehow different from land-use by many authors. Campbell [6], for example, considers land-cover to be concrete whereas land-use is abstract. That is, land-cover can be mapped directly from images, while land-use requires land-cover and additional information on how the land is used. Danoedoro [7] tries to improve land-use classification via satellite imagery by combining spectral classification, image segmentation and visual interpretation. Although he showed that satellite imagery could be used for generating socio-economic function of land-use at 83.63% accuracy, he is the first to recognize that applying such techniques to highly populated areas would be problematic.

Li et al. [8] use data mining techniques to discover knowledge from GIS databases and remote sensing image data that could be used for land use classification. In the field of remote sensing, Bayes classification (or maximum likelihood classification) is most widely used and, for most multi-spectral remote sensing data, the Bayes method classifies the coarse classes correctly, such as water, residential area, green patches, etc. But usually more detailed classification is required in land use classification. In order to subdivide some of the classes, Li et al. proposes the use of inductive learning techniques, particularly the C5.0 algorithm. By using these techniques they were able to get an overall accuracy of 89%. Comparing their final result with the result produced only by Bayes classification, the overall accuracy increased 11%.

An alternative to satellite imagery is the POI data. Using a large commercial POI database, Santos and Moreira [9] create and classify location contexts using decision trees. They identify clusters by means of a density-based clustering algorithm (Shared Nearest Neighbor algorithm) which allow them to define areas (or regions) through the application of a concave hull algorithm they developed to the POIs within each cluster. Finally, making use of the C5.0 algorithm, they classify a given location according to such characteristics as the number of POIs in a cluster, the size of the area of the cluster and the categories of the POIs within the cluster.

In order to use POI data for the classification of places and land-use analysis, POI classification is an essential task. Griffin et al. [10] use decision trees to classify GPS-derived POIs. However, they refer to POIs as “personal” locations to a given individual (i.e., home, work, restaurant, etc.). The main goal of their approach is then to automatically classify trips. In

their approach, they start by determining clusters of trip-stops (i.e., stops that took more than 5 minutes) using a density-based clustering algorithm (Dbscan). Then, they make use of the C4.5 algorithm to classify the generated clusters as being "home", "work", "restaurant", etc., based on the time of the day and the length of the stay. However, to our best knowledge, no previous approaches have been made to classify POIs to a classification system such as NAICS. The latter is widely used for industry classification and has already been used, for instance, to classify Web Sites through machine learning techniques [11].

Spatial analysis has long been a topic of interest for researchers, who seek a comprehensive understanding on how the city behaves in different perspectives and its impact in the economy. Methods for analyzing spatial (and space-time) data have already been well developed by statisticians [12] and econometricians [13].

Visualization of geo-referenced data is one effort in such understanding. Instead of simply presenting information on a map, visualization facilitates the recognition of patterns in data by preprocessing and applying statistical filtering (e.g., average, deviation, clustering) over large datasets. Keim et al. [14] were pioneers in using visual approaches to explore heterogeneous and noisy large amount of spatial data. The authors showed how visualizations offered a qualitative overview of the data and allowed unexpectedly detected phenomena to be pointed out and explored using further quantitative analysis. Later, Costa and Venturini [15] improved these methodologies in order to give the possibility to interact with such artifacts. The authors applied them to a large POI database and showed with linear computation time it would be possible to present and interact with up to one million spatial points.

Currid et al. [16] try to understand the importance of agglomeration economies as a backbone to urban and regional growth, by identifying clusters of several "advanced" service sectors (professional, management, media, finance, art and culture, engineering and high technology) and comparing them in the top ten populous metropolitan areas in the U.S. They concluded that there are three spatial typologies of growth in the advanced services within U.S. urban regions. These typologies allowed them to understand qualities of place in general and of places specifically that drive the agglomeration of advanced services.

On a particular case study of the biotech industry in the U.S., Sambidi and Harrison[17] also analyze factors affecting site-selection of industries, testing the hypothesis of spatial agglomeration economies in that industry and confirm it using spatial econometrics. In the same topic, Arbia[18] classifies the spatial processes of individual firms into a birth process (new firms) and a growth process (existing firms) and proposes a model of economic activities on a continuous space also with the purpose of studying the geographical concentration of economic activities and analyze the economic behavior of individual firms.

III. Approach

In this section, we describe our approach, particularly what are the sources of our POI data, how we generate the training data, what methods we use for classification and how we perform validation.

A. POI Sources

Our data consists of a large set of POIs extracted from Yahoo! through their public API, another set acquired to Dun & Bradstreet (D&B) [19], a consultancy company that specializes in commercial information and insight for businesses, and a third one from InfoUSA[5] provided by the Harvard Center for Geographic Analysis (ESRI Business Analyst Data). In the first data set (from Yahoo!), the database is essentially built from user contributions. In the other two, the data acquisition process is semi-automatic and involves integration of official and corporate databases, statistical analysis and manual evaluation [19]. The POIs from D&B and InfoUSA have a NAICS code assigned (2007 version), which is not present in Yahoo!. However, each POI from Yahoo! is assigned, in average, roughly two arbitrary categories from the Yahoo! categories set. These categories are specified by the user, when adding a new POI, through a textfield and can be rather disparate since Yahoo! forces no restrictions over them. Considering that every POI source provides either some categories or tags associated with their POIs, we take advantage of this information to classify them to NAICS, where a single unifying code is assigned to each POI.

We have 156364 POIs from Yahoo!, 29402 from D&B and 196612 from InfoUSA for the area of Boston, Massachusetts. We also used 331118 POIs from Yahoo! and 16852 from D&B for the New York city area to see how our previously trained model would perform in a different city. We estimate that the Yahoo!'s categories taxonomy has more than 1300 distinct categories distributed along a 3-level hierarchy. On the other hand, NAICS has a total of 2332 distinct codes distributed along their 6-level hierarchy (1175 only in the sixth level).

Given its nature, the growth of the Yahoo! database (or any other user content platform) is considerably faster than D&B and InfoUSA, and the POI categorization follows less strict guidelines, which in some cases, as mentioned before, may become subjective. Our hypothesis is that there is considerable coherence between Yahoo! categories and NAICS codes, such that a model can be learned that automatically classifies incoming Yahoo! POIs.

In order to generate training data for the machine learning algorithms we use a *POI Matching* algorithm.

B. POI Matching and Data Preparation

When we are comparing POIs from different sources, it is important to have a way to identify similar POIs in order to correlate both databases. This requires a way to identify similarities based, not only in proximity, but also in name likeness. Our matching algorithm compares POIs according to their name, Web Site and distance. It makes use of the JaroWinklerTFIDF class from the SecondString project [20] to identify close names, ignoring misspelling errors and some abbreviations. Taking this into account, two POIs will be considered similar by our algorithm if they fit into one of the following groups:

[5] www.infousa.com

TABLE I. SOME STATISTICS OF DATASETS A AND B

	Dataset A	Dataset B
NAICS source	D&B	InfoUSA
Total POIs	7289	44634
Distinct NAICS	504	689
Distinct Yahoo! categories	802	1109
Distinct Yahoo! category combinations	569	1002
Category combinations that appear only once	136	92
Categories that appear only once	181	107
NAICS that appear only once	115	96

- The distance between the two POIs is less than 80 meters, the name similarity is above 0.70 and one or both POIs do not have website information.
- The distance between the two POIs is less than 80 meters, the name similarity is above 0.70 and the website similarity is higher than 0.60.
- The distance between the two POIs is less than 80 meters, the name similarity is above 0.60 and the website similarity is higher than 0.95.

We set the similarity thresholds to high values in order to get only high confidence matches. By manually validating a random subset of the POI matches identified (6 sets of 50 random POIs assigned to 6 volunteers), we concluded that the percentage of correct similarities identified was above 98% ($\sigma = 1.79$). Differently to validations later mentioned in this article, this is an extremely objective one, not demanding external participants or a very large sample[6].

After matching Yahoo! POIs to D&B and InfoUSA, we built two different geographic databases, where each POI contains a set of categories from Yahoo! and a NAICS classification provided by D&B and InfoUSA respectively. From this point on, we shall refer to the initial dataset, which results from POI matches between Yahoo! and D&B, as dataset A, and to the dataset resultant from the POI matching between Yahoo! and InfoUSA as dataset B. The later is six times larger than the former, due to larger coverage of InfoUSA in Boston.

Table I shows some statistic details of both datasets used.

The dataset A contains 7289 POIs for Boston and Cambridge and 2415 for New York. In comparison with the original databases, these are much smaller sets due to a very conservative POI matching approach (string similarity of at least 80%, max distance of 80 meters). However the POI quantities are high enough to build statistically valid models. We performed a detailed analysis of this data and identified 569 different category combinations which included only 802 distinct categories from the full set (of over 1300). From D&B, our data covers 504 distinct six-digit NAICS codes. However, the 2007 NAICS taxonomy has a total of 1175 six-level categories, meaning that our sample data only covers some of the most common NAICS codes, which only represents about 43% of the total number of NAICS categories. Nevertheless, the remaining ones are more exotic in our context and hence less significant for posterior analyses.

[6]Using the central limit theorem, the standard error of the mean should be near 0.73. Assuming an underestimation bias for n=6 of 5% (by the [21]), accuracy keeps very high, yielding a 95% confidence interval of [96.5%, 98.7%]

TABLE II. MOST COMMON NAICS IN THE DATASET A

NAICS code	Description	Occurrences
423730	Warm Air Heating and Air-Conditioning Equipment and Supplies Merchant Wholesalers	707
446130	Optical Goods Stores	200
314999	All Other Miscellaneous Textile Product Mills	193
493120	Refrigerated Warehousing and Storage	136
332997	Industrial Pattern Manufacturing	123

TABLE III. MOST COMMON YAHOO! CATEGORIES IN THE DATASET A

Yahoo! category	Occurrences
Salons	157
All Law Firms	129
Government	116
Trade Organizations	115
Architecture	86

Figure 2 shows the distribution of POIs along the different NAICS codes for dataset A. As we can see in the chart, the distribution is far from being uniform, which further complicates the classification task for NAICS codes with few training examples.

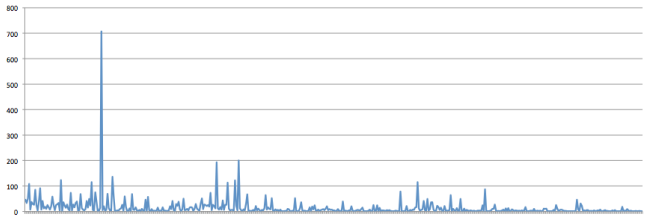

Fig. 2. Distribution of the POIs in dataset A along the different NAICS codes

Further analyses on the coherence between NAICS and Yahoo! show that only in 80.2% of the POIs in dataset A the correspondent NAICS was consistent with the most common one for that given set of categories, which means that about one fifth of the POIs are incoherent with the rest of the sample. This fact highlights the problem of allowing users to add arbitrary categories to their POIs without restrictions. For different NAICS levels, particularly for two-digit and four-digit NAICS, the same analyses showed, as expected, a higher level of coherency. For the two and four-digit NAICS, 87.1% and 83.4% of the POIs, respectively. Therefore, by having the same set of Yahoo! categories mapping to different NAICS codes in different occasions, it is not expectable that we obtain a perfect model that classifies correctly all test cases. In order to understand the impact of these inconsistencies in the results, we also modified the POI dataset so that the NAICS code of a given POI would match the NAICS codes of the other POIs with the same category set, assigning to each POI the most common NAICS code for that given category set in the dataset. The results of this experiment are also presented in Section IV.

Tables II and III show, respectively, the five most common NAICS and Yahoo! categories we identified in dataset A.

Regarding dataset B, we identified 689 distinct NAICS codes and 1109 distinct categories of the more than 1300 that we found in Yahoo!. The latter are in larger number

TABLE IV. BRIEF DESCRIPTION OF THE ALGORITHMS TESTED

Implementation	Description
ID3	Unpruned decision tree based on the ID3 algorithm.
C4.5	Pruned or unpruned C4.5 decision tree.
C4.5graft	Grafted C4.5 decision tree.
RandomForest	Forest of random trees.
RandomTree	Tree with K randomly chosen attributes at each node. Performs no pruning. Also has an option to allow estimation of class probabilities based on a hold-out set (backfitting).
JRip	Propositional rule learner, Repeated Incremental Pruning to Produce Error Reduction (RIPPER), as proposed by W. Cohen as an optimized version of IREP.
IBk	K-nearest neighbors classifier. Can select appropriate value of K based on cross-validation. Can also do distance weighting.
IB1	1 - nearest-neighbor classifier. Simplification of IBk.
K*	K* is an instance-based classifier. The class of a test instance is determined from the class of similar training instances . It uses an entropy-based distance function.
BayesNet	Bayesian Network
NaiveBayes	Naive Bayes model

than the ones from dataset A (only 802) and therefore dataset B provides a better coverage of the source taxonomy. The number of distinct category combinations almost doubled when compared to dataset A, which leads to more diversity in the training data and more accurate classifiers.

Figure 3 shows the distribution of POIs from dataset B along the different NAICS codes. Similarly to the distribution of dataset A, it is an irregular distribution.

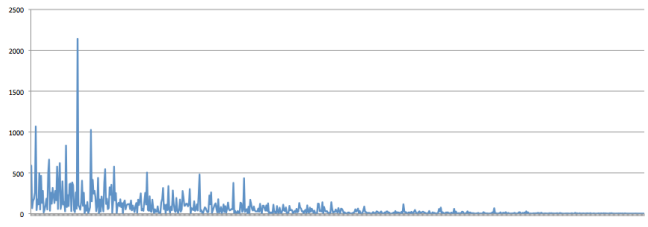

Fig. 3. Distribution of the POIs in dataset B along the different NAICS code

C. Flat Classification

The "flat classification" task corresponds to directly assigning a NAICS code to a POI given its "bag" of Yahoo! categories. It is "flat" because the inherent hierarchy of NAICS is not taken into account in the classification model. Each NAICS code is simply seen as an isolated string "tag" that is assigned to a POI.

We experimented various machine learning algorithms for this particular classification task. Table IV provides a brief description of the algorithms we tested. It is not the scope of this article to describe any of the algorithms in detail. The interested reader is redirected to dedicated literature [22], [23].

In our experiments, we built classifiers for different NAICS levels (i.e., NAICS categories with different granularities), particularly two, four and six-digit NAICS codes. This choice is typical in urban planning depending on the study at hand (e.g., level 2 allows to analyze economic sectors, while level 6 goes to the level of the establishment specificities).

For validation purposes we use ten-fold cross-validation [23]. We also performed validation with an external test set (data from a another city, New York) to understand the dependency of the generated models on the study area.

D. Hierarchical Classification

In this approach, we take advantage of the hierarchical structure of NAICS, thus the overall classifier is itself a hierarchy of classifiers. In this hierarchy, each classifier decides what classifier to use next, narrowing down the NAICS code possibilities on each step, until a final 6-digit code (or 4-digit code, depending on the goal) is achieved. Figure 4 depicts one possible hierarchy.

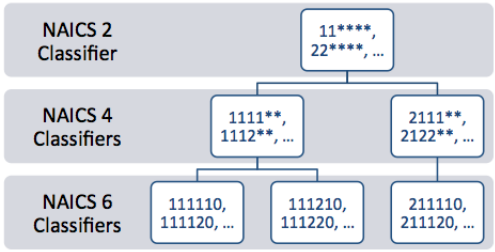

Fig. 4. A possible hierarchy of classifiers

By looking at the hierarchy above, we can see that it has 3 levels (2, 4 and 6-digit NAICS). The first level always consists of a single classifier that decides which NAICS economic sector (2-digit code) the POI belongs to. Taking the sector into account, the algorithm then decides which classifier to use next at the second level. After that, the same process repeats until a leaf node is achieved in the tree structure of the hierarchy of classifiers. To provide an example consider a POI that has the following NAICS code: 111110. According to Figure 4 the top-level classifier will decide that it belongs to sector 11 ("Agriculture, Forestry, Fishing and Hunting") and the left-most level 2 classifier will be used next. Then, this classifier will determine that the 4-digit NAICS code of the POI is 1111 ("Oilseed and Grain Farming") and, based on this decision, the left-most classifier in the third level of the Figure 4 will be used, and will supposedly classify the POI with the NAICS code 111110 ("Soybean Farming"). Of course, along this top-down process a mistake can be made by one classifier. In this case, the error would propagate downwards and there would be no way to recover from it, and hence the final NAICS code would be wrong.

Our hypotheses is that by using a hierarchy of classifiers, the classification task will be divided into several classification models, each one less complex, more accurate and dealing with a simpler problem. If we consider, for example, the ID3 algorithm, the entropy values for the different features will be computed according to a smaller class subset, and therefore the selection of the next feature to use (which is based on the entropy calculation) will be different and the resulting tree will also be different. Hopefully, the generated classifier will be more suited to that particular classification (like deciding for a POI if it belongs to the subcategory 531, 532, etc, knowing that it belongs to NAICS sector 53).

In our experiments, we use three different hierarchies of classifiers, two with 2 levels:

- NAICS 2 and NAICS 4
- NAICS 2 and NAICS 6

and other one with 3 levels:

- NAICS 2, NAICS 4 and NAICS 6

As we did for the flat classification, we also tried to test different types of machine learning algorithms: bayesian networks, tree-based learners, instance-based learners, rule-based learners. Neural networks were not possible to test due to their computational demands, both in processing power and memory.

For the hierarchical approaches we also perform ten-fold cross-validation, but the data splitting between training/testing is more prone to biased results than with standard flat classification. As in normal ten-fold cross-validation, we also start by leaving 10% of the data out for test and use the remaining 90% for training, repeating this process ten times. However, each classifier in a given level only receives the part of those 90% of training data that respects to it. For instance, a level two classifier for deciding which sub-category of NAICS sector 53 a given POI belongs to would only be trained with POIs that belong to that NAICS sector. Hence, the only classifier that receives all the training data (90%) would be the top-level classifier (i.e., the one that decides which NAICS sector a POI belong to). After the training phase, the hierarchy is tested with the 10% of the data left out. This process is repeated ten times, and the average accuracy over the ten iterations is determined.

IV. RESULTS

Table V shows the results obtained using different machine learning algorithms for different NAICS levels (two, four and six-digit codes) for dataset A. There are some missing results in the cases where the algorithm took over 72 hours to run. We can see that the tree-based (e.g., ID3, RandomForest) and instance-based learning approaches (e.g., IBk, K*) are the ones that perform better in this classification task, especially the latter. Notice that only 80.2% of data is classified in a totally non-ambiguous way. The most successful algorithm is IBk (with k=1), which essentially finds the similar test case and assigns the same NAICS code. The difference in accuracy between tree-based and instance based approaches is too small to conclude which one outperforms the other, however we could expect that instance based models bring better results since the distribution of the different Yahoo! categories is relatively even among examples of the same NAICS code (implying no clear "dominance" of some categories over others). Understandably, the Naive Bayes algorithm performs badly because the assumption that different Yahoo! categories for the same NAICS classification are independently distributed is obviously false (e.g., "Doctors & Clinics, Laboratories, Medical Laboratories" are correlated). Such assumption is not fully necessary in Bayesian Networks, which actually brings better results. Unfortunately, we could not find a model search algorithm that performs in acceptable time (less than 72 hours) and produces a more accurate model. We used Simulated Annealing and Hill Climbing.

TABLE V. RESULTS OBTAINED FOR THE DIFFERENT MACHINE LEARNING ALGORITHMS WITH POIS FROM DATASET A FOR THE BOSTON AREA

Algorithm	NAICS2(kappa)	NAICS4(kappa)	NAICS6(kappa)
ID3	85.495 (0.842)	77.955 (0.776)	74.015 (0.737)
C4.5	84.241 (0.828)	77.630 (0.772)	73.071 (0.727)
Random Forest	86.174 (0.849)	79.298 (0.789)	74.753 (0.744)
Random Tree	85.303 (0.840)	77.763 (0.774)	74.192 (0.739)
JRip	81.334 (0.795)	74.340 (0.737)	69.264 (0.686)
IB1	82.736 (0.812)	74.266 (0.738)	68.644 (0.683)
IBk	86.646 (0.854)	79.475 (0.791)	75.343 (0.750)
K*	85.702 (0.844)	79.726 (0.794)	75.387 (0.751)
BayesNet	80.950 (0.790)	56.721 (0.554)	45.064 (0.438)
NaiveBayes	74.399 (0.715)	40.446 (0.382)	30.264 (0.283)

TABLE VI. RESULTS OBTAINED FOR THE DIFFERENT MACHINE LEARNING ALGORITHMS USING A RE-CLASSIFIED VERSION OF DATASET A

Algorithm	NAICS2	NAICS4	NAICS6
ID3	92.975	89.728	88.680
RandomForest	93.609	90.805	89.846
IBk	94.170	91.189	89.979

As expected, we obtained better results classifying POIs to the two-level NAICS than for the six-level NAICS, since the noise due to ambiguous classifications in the POI dataset is smaller (we now have 87.1% of non-ambiguous cases).

In Table VI, we can see the results obtained by changing the POI dataset A so that the NAICS codes of POIs where ambiguities arise are grouped together in the same "super-category", eliminating the inconsistencies.

By comparing the results in Table VI with the results in Table V, we realize that the NAICS labeling inconsistencies in the POI data have a major negative effect in the performance of the machine learning algorithms, reducing the accuracy in more than 16% in some cases for the six-level NAICS codes. This also gives indications for future versions of NAICS, where some categories may become aggregated according to these "super-categories".

It would be expectable to obtain accuracies closer to 100% for the results in Table VI. However, that does not happen since 115 of the 514 NAICS codes covered by our dataset A only occur once. Therefore, when we split the dataset to perform the ten-fold cross-validation, a significative number of the test cases will have NAICS codes that the algorithm was not trained for, causing it to incorrectly classify them.

Table VII shows the results we obtained by training the machine learning approaches with dataset A from Boston and Cambridge and testing them with New York POI data. As we can see in the results, if we apply the generated model to a different city, it still performs well, even though the accuracy drops a small amount in some cases. This is understandable since even the Yahoo! taxonomy differs slightly from city to city.

Table VIII shows the results obtained for the different machine learning algorithms using dataset B.

TABLE VII. RESULTS OBTAINED FOR THE DIFFERENT MACHINE LEARNING ALGORITHMS USING POI DATA FROM BOSTON FOR TRAINING AND POI DATA FROM NEW YORK FOR TESTING

Algorithm	NAICS2	NAICS4	NAICS6
ID3	85.061	75.586	70.209
RandomForest	85.488	76.867	71.318
IBk	85.360	76.909	71.276

TABLE VIII. RESULTS OBTAINED FOR THE DIFFERENT MACHINE LEARNING ALGORITHMS WITH POIS FROM DATASET B FOR THE BOSTON AREA

Algorithm	NAICS2(kappa)	NAICS4(kappa)	NAICS6(kappa)
ID3	90.567 (0.897)	85.459 (0.852)	82.091 (0.819)
C4.5	90.113 (0.800)	85.085 (0.849)	81.831 (0.816)
RandomForest	90.758 (0.899)	85.710 (0.855)	82.436 (0.823)
RandomTree	90.500 (0.896)	85.275 (0.851)	81.818 (0.817)
JRip	85.748 (0.844)	80.998 (0.807)	78.495 (0.780)
IB1	87.224 (0.861)	81.495 (0.812)	76.826 (0.766)
IBk	91.024 (0.902)	85.974 (0.858)	82.553 (0.824)
K*	90.227 (0.893)	85.849 (0.856)	82.522 (0.824)
BayesNet	88.961 (0.880)	77.964 (0.776)	67.877 (0.675)
NaiveBayes	87.910 (0.868)	70.250 (0.696)	56.052 (0.554)

TABLE IX. COMPARISON BETWEEN THE RESULTS FOR DATASET B USING FLAT CLASSIFICATION (4-DIGIT NAICS) AND HIERARCHICAL CLASSIFICATION WITH 2 LEVELS (NAICS 2 AND 4)

	Flat classification	Hierarchical classification	
Algorithm	accuracy	Level1 acc.	Level2 acc.
ID3	85.459	90.659	85.620
C4.5	85.085	90.172	84.901
RandomForest	85.710	90.959	85.969
RandomTree	85.275	90.509	85.315
JRip	80.998	85.806	80.440
IB1	81.495	87.637	81.126
IBk	85.974	91.080	86.097
K*	85.849	90.305	85.244
BayesNet	77.964	88.002	74.243
NaiveBayes	70.250	30.688	20.091

By analyzing the results from Table VIII we can see that the results have significantly improved over dataset A, which shows the importance of the training data in the performance of the machine learning algorithms.

Finally, Tables IX to XI show the results obtained using the different hierarchical classification schemes for various types of machine learning algorithms.

Our intuition was that hierarchical classification would perform generally better than standard flat classification. However, only in some algorithms the results improved. Therefore, we will not argue that hierarchical classification of POIs into NAICS is always a better solution. In fact, as shown before by comparing the datasets A and B, the quality and the dimensions of the dataset seems to have a much bigger impact on the results than whether we apply hierarchical or flat classification.

Another interesting fact in the results from the hierarchical classification is that the accuracies vary considerably with the hierarchy type used. For instance, when classifying POIs with 6-digit NAICS codes, we can see that using a two-level hierarchy the RandomForest algorithm improved over the flat classification, while using a three-level hierarchy it became worse (although the differences in accuracy are small).

TABLE X. COMPARISON BETWEEN THE RESULTS FOR DATASET B USING FLAT CLASSIFICATION (6-DIGIT NAICS) AND HIERARCHICAL CLASSIFICATION WITH 2 LEVELS (NAICS 2 AND 6)

	Flat classification	Hierarchical classification	
Algorithm	accuracy	Level1 acc.	Level2 acc.
ID3	82.091	90.659	82.100
C4.5	81.831	90.173	81.484
RandomForest	82.436	90.959	82.477
RandomTree	81.818	90.509	81.654
JRip	78.495	85.806	76.398
IB1	76.826	87.637	76.826
IBk	82.553	91.080	82.551
K*	82.522	90.305	81.661
BayesNet	67.877	89.059	69.336
NaiveBayes	56.052	88.002	59.885

TABLE XI. COMPARISON BETWEEN THE RESULTS FOR DATASET B USING FLAT CLASSIFICATION (6-DIGIT NAICS) AND HIERARCHICAL CLASSIFICATION WITH 3 LEVELS (NAICS 2, 4 AND 6)

	Flat classification	Hierarchical classification		
Algorithm	accuracy	Level1 acc.	Level2 acc.	Level3 acc.
ID3	82.091	90.659	85.620	82.111
C4.5	81.831	90.172	84.901	81.341
Random Forest	82.436	90.959	85.969	82.398
Random Tree	81.818	90.509	85.315	81.694
JRip	78.495	85.806	80.440	76.889
IB1	76.826	87.637	81.126	76.826
IBk	82.553	91.080	86.097	82.539
K*	82.522	90.305	85.244	81.486
BayesNet	67.877	-	-	-
NaiveBayes	56.052	-	-	-

V. AN APPLICATION IN URBAN PLANNING

In this section, we describe a practical application of Yahoo! POIs classified to NAICS using a non-hierarchical approach with the k-nearest neighbor classifier (see Section III-C for more details).

In the field of urban planning, urban simulation models have evolved significantly in the past several decades. For instance, the travel demand modeling approach has been evolving from the traditional Four-Step Model (FSM) to the Activity-Based Model (ABM) [24]. Consequently, requirements for disaggregated data increase greatly, ranging from population data, employment data, to travel survey data. The employment data (on the travel destination side) is usually obtained from proprietary sources, which adds another layer of barriers to widely applying the Activity-Based Modeling approach, let alone the expensive travel-survey data acquisition. In order to study this issue, researchers are trying to develop new methods of estimating disaggregated employment size and location by category.

In our case, we intend to develop a set of new methods and demonstrate their applications for estimating activities, incorporating them into travel demand and urban simulation models. This will be beneficial for cities that lack detailed

survey data for building Activity-Based Models but wish to test the sensitivity of travel behavior to policy changes such as Intelligent Transportation Systems (ITS) implementations that are likely to alter activity patterns. An important step to achieve these goals is to obtain a disaggregated employment distribution by POIs of an area. For the case of Cambridge, MA, we have official data at the Block Group (BG) level (obtained from the U.S. Census Transportation Planning Package 2000), which essentially describes the total size of employees by economic sector at that spatial resolution. We need to distribute these totals into Block or Parcel level.

For demonstration purposes we only use POIs from the "Retail Trade" sector of the NAICS taxonomy, i.e., categories whose code starts by 44 or 45. Figures 5 and 6 show the aggregated retail employment density at the Block Group level and distribution of our POI data from Yahoo! at the Census Block level for Cambridge, respectively.

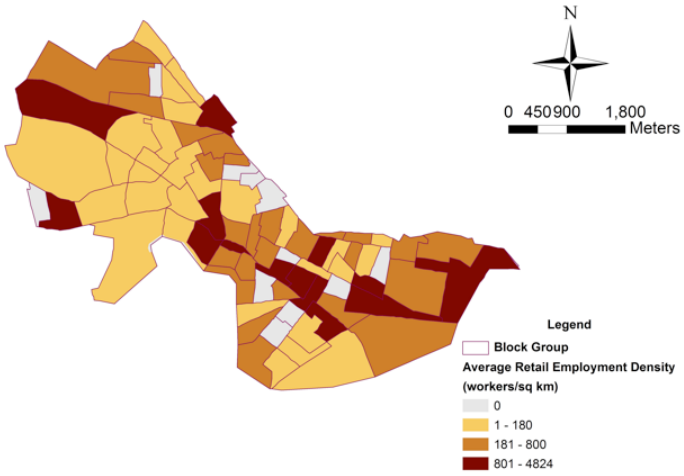

Fig. 5. Aggregated retail employment density at the Block Group level (pl/sq km= employed people per square kilometer).

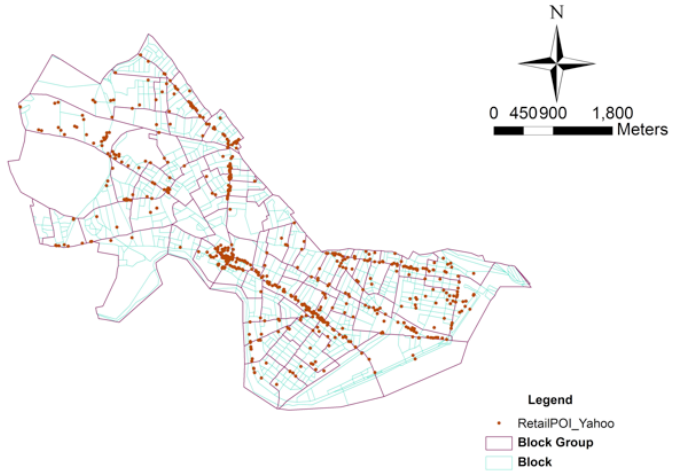

Fig. 6. Cambridge retail POI distributions from Yahoo!

By using the business establishment survey data (from InfoUSA, 2007) which is believed to be close to the population, we are able to obtain a benchmark estimate of employment size by category at the Census Block level for the study areas. This will function as a ground truth to test our algorithm. Notice however that the dates for each of the databases are quite distinct (2000 for Census, 2007 for InfoUSA and 2010 for Yahoo!) therefore some error is expected to happen.

We employ the local maximum likelihood estimation (MLE) method as described below to derive the disaggregated destination estimation at Block level.

1) We calculate the total number of POIs (destinations) by category c in each Block b.
2) We assume that the employment size at destination d in Block Group g of category c is proportional to some function f of its associated block area $a_{d,c,g}$, which means the effective area of the destination d in Block Group g of category c. The form of function f will be explored based on the empirical data, and we also allow the possibility that $f(a_{d,c,g}) = a_{d,c,g}$ which is the natural benchmark case. Mathematically, assume that for employment category c, there are $n_{c,g}$ destinations at Block Group g. For $d = 1, 2, \ldots, n_{c,g}$, let random variable $e_{d,c,g}$ be the employment size of category c at destination d in Block Group g.
3) We assume that $e_{d,c,g}(d = 1, 2, \ldots, n_{c,g})$ are i.i.d.$(f(a_{d,c,g}) \cdot \alpha_{c,g}, \sigma^2_{c,g})$, where $\alpha_{c,g}$ is the employment size of category c per unit of effective area at Block Group g; $\alpha_{c,g}$ and $\sigma_{c,g}$ are positive constants independent of d. $E(e_{d,c,g}) = f(a_{d,c,g}) \cdot \alpha_{c,g}$ and $Var(e_{d,c,g}) = \sigma^2_{c,g}$. We then estimate $\alpha_{c,g}$ by employing the maximum likelihood method locally at Block Group g for employment category c. Thus we obtain an estimate of employment size $e_{d,c,g}$ of category c at destination d in Block Group g.
4) Finally, we sum up the employment size in category c in Census Block b in Census Block Group g.

By employing the same local maximum likelihood method described above and using the business establishment survey data (e.g., ESRI Business Analysis package) which is believed to be close to the population POIs, we obtain a benchmark estimate of employment size by category at the Block level for the study area, $E^*_{b,c,g}$. By using the derived POI information (obtained from the machine learning algorithm), we obtain an estimate of employment size by category c at Block b for the study area, $\hat{E}_{b,c,g}$.

Then the mean squared error (MSE), weighted mean squared error (WMSE), and the relative weighted mean squared error (RWMSE) can be calculated to evaluate the goodness of fit of the model (see Equations 1, 2, 3, and 4).

$$\text{MSE}(\hat{E}_{b,c,g}, E^*_{b,c,g}) = \sum_{b,c,g} (\hat{E}_{b,c,g} - E^*_{b,c,g})^2 \quad (1)$$

$$\text{WMSE}(\hat{E}_{b,c,g}, E^*_{b,c,g}) = \sum_{b,c,g} w_{b,c,g} (\hat{E}_{b,c,g} - E^*_{b,c,g})^2 \quad (2)$$

$$\text{RWMSE}(\hat{E}_{b,c,g}, E^*_{b,c,g}) = \frac{\sum_{b,c,g} w_{b,c,g} (\hat{E}_{b,c,g} - E^*_{b,c,g})^2}{\sum_{b,c,g} w_{b,c,g} (\bar{E}_{b,c,g} - E^*_{b,c,g})^2} \quad (3)$$

$$\bar{E}_{b,c,g} = \frac{w'_{b,g} \sum_q E^*_{q,c,g}}{\sum_q w'_{q,g}} \quad (4)$$

Weights $\{w_{b,c,g}\}$ are normalized to reflect the proportion of each Census Block in the whole map. In Equation 2, when we take the weight $w_{b,c,g} = 1$ for any subscripts b, c, and g, the corresponding WMSE becomes MSE. In Equation 4, $w'_{b,g} =$ area of Block b in Block Group g, and $\bar{E}_{b,c,g}$ is the estimated employment size in Block b of category c, using the traditional disaggregation approach, assuming that the employment is uniformly distributed across blocks in each Block Group g.

If RWMSE is less than 1, it means that the quality of the derived POIs is reliable, so is the new method; the smaller the RWMSE, the more accurate is the method. If WMSE or RWMSE equals to 0, it means that the derived POIs from the Internet match exactly with the trusted proprietary POIs (treated as the population POIs). However, if RWMSE is greater than 1, it means that the derived POIs cannot well reflect the distribution of the population POIs.

Figures 7 and 8 show the estimation results of the disaggregated retail employment density at Block level in Cambridge, MA, by using POIs from infoUSA and Yahoo! respectively. By comparing the estimation results, we find that the disaggregated employment estimations by using the POIs captured from the Internet using Yahoo! and those obtained from the proprietary source (infoUSA 2007) are very close.

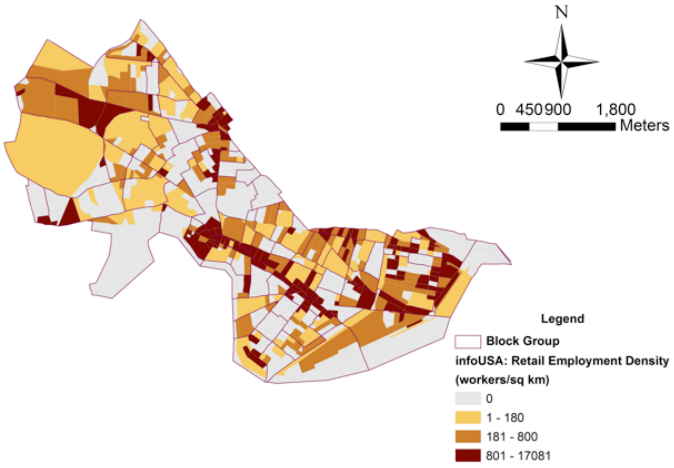

Fig. 7. Disaggregated retail employment densities at the Block level, in Cambridge, MA, by using POIs from infoUSA

Employing Equation 3, the disaggregated employment estimation at the Block level using Yahoo! POI gives RMSE = 0.312. The RMSE is significantly smaller than 1, which means that using the extracted Yahoo! online POIs to estimate the disaggregated employment sizes at the Block level has reduced the mean squared error by around 69% compared to the traditional average disaggregation approach.

VI. Model Performance Analysis with Visual Techniques

In this section, we explore visualization techniques to further assess the performance of the developed models. Furthermore, by making use of these visualization techniques we are able to identify possible ways to improve the models' performance and establish future work directions.

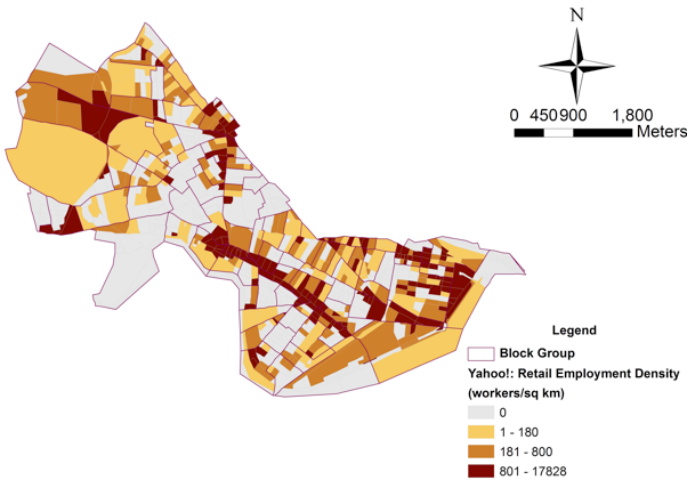

Fig. 8. Disaggregated retail employment densities at the Block level, in Cambridge, MA, by using POIs from Yahoo!

We start by visualizing the errors of the learned POI classifier. Due to the hierarchical structure of the NAICS taxonomy, there are 6 types of error depending on the level at which classifier fails first. Therefore, we define the error level $\xi(p)$ of some POI p as the first index, from right to left, where the predicted NAICS code is different from the true one. So, for example, if the classifier mislabels a POI from NAICS 921130 as 921120, we say it made a level 2 error ($\xi(p) = 2$). On there other hand, if it mislabels it as 238320 we say it made a level 6 error ($\xi(p) = 6$). Correctly classified POIs are said to have an error level of 0. Hence, the higher the error level, the worst its consequences are for practical applications that use the classified POI data. In particular, errors of levels 5 and 6 are especially bad, since they mean the classifier was unable to correctly identify the economic sector of the POI, thus invalidating analysis even at the coarsest level of granularity.

With this in mind, we developed a colour-based representation scheme, where different colours represent different error levels. Figures 9 and 10 show this visualization method applied to the Boston metropolitan area and Cambridge respectively. Figure 10 shows that the majority of the POIs are correctly classified, and that most of the errors that occur correspond to higher level errors (i.e., level 5 and 6). These findings are coherent with the results presented in Table VIII. However, we can now observe that these errors are not uniformly distributed across space. Contrarily, we can see that, regardless of the error level, the higher the POI density is in a given region, the more likely it is to have high quantities of misclassified POIs. Although intuitive, notice that this observation is of vital importance for practical uses of the classified POI data.

Despite the possibility to visualize the spatial distribution of the error of the POI classifier, the visualization method described above has some limitation when it comes to comparing different error level. This led us to the idea of using small multiples - a technique commonly used to compare various versions of data sets with the same structure in order to show shifts in relationship [25]. In other words, the different layers were separated and afterwards composed in sequenced order. The resulting artefact can be seen in Figure 11. Apart from the

Fig. 10. Spatial distribution of the POI classification error in the area of Cambridge, MA.

fact that most of the times the POIs are correctly classified, as the figure evidences, the distribution of the misclassified POIs is not uniform even at the individual error levels. Furthermore, we can see that level 6 errors are the most frequent ones.

The small multiples visualization allowed us to visualize and compare the spatial distribution of different error levels. However, it is hard to really understand the relation between classification error and POI density from these methods. In order to better understand this relation, a new visualization method was developed. The first step consists in constructing a modular grid over the map, whose size can be manipulated, which then reflects on the resulting visual impact. Then, the average error level $\overline{\xi_j}$ of a grid cell j is simply calculated as follows:

$$\overline{\xi_j} = \frac{1}{|P_j|} \sum_{p \in P_j} \xi(p) \quad (5)$$

where P_j denotes the set of all POIs in the grid cell j. The value of $\overline{\xi_j}$ is then used to visually represent how severe the misclassification is in that grid cell. By having a single-value representation of the misclassification error for a given region, we can now easily overlay this information with POI density. Figure 12 shows an example of this visualization method for the Boston metropolitan area. The radius of the black circles represent the values of ξ_j and the different intensities of red represent the POI density.

The visualization from Figure 12 allows us to compare POI density and average error per cell. Hence, we can see that saturated red cells with small circles in it represent optimal areas in terms of the reliability of the POI data, since the average classification error is small even with high POI densities. On the other hand, the cells with large circles and almost white background colour represent areas with many classification errors, even though the number of POIs is small. The worst case would be for a cells to have large circles and red saturated colours. That would mean that there are many incorrectly classified POIs. As Figure 12 evidences, there are no such regions in our classified data. Furthermore, we can see that the regions where misclassification is more severe, correspond to regions of low POI density. Thus, from a perspective of the "functional regions" of space, where each region is defined by the economical activities that take place there, these are the areas where the resultant analysis would be less reliable.

The visualization method described above can easily be extended to include the performance of practical application of the POI data - in this case, the employment size estimation model from Section V. Figure 13 shows the resulting visual-

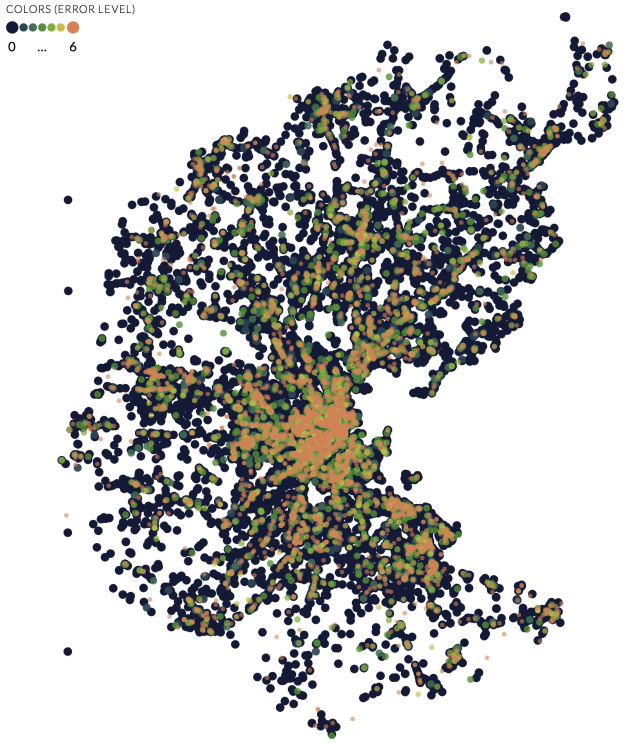

Fig. 9. Spatial distribution of the POI classification error in the Boston metropolitan area.

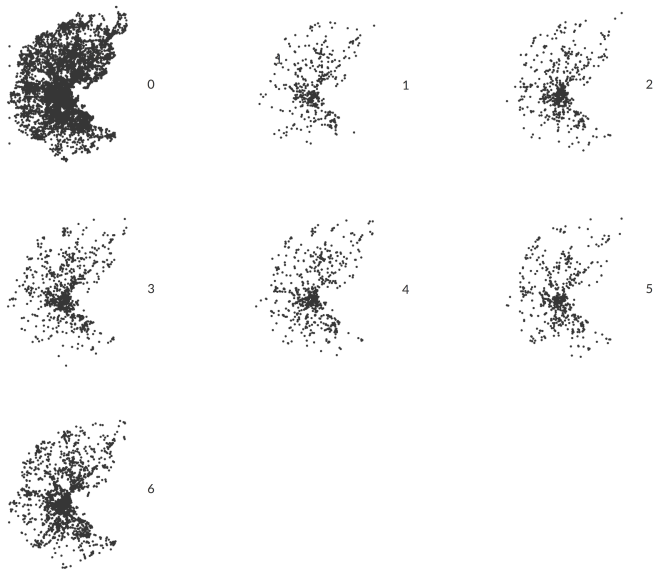

Fig. 11. Distribution of the classification error through space for different error levels ξ.

ization for the study area of Cambridge. As we can see from this figure, there is some relation between POI classification error and estimated employment size error. In fact, a closer look at this relation shows a Spearman correlation of 0.179 (p-value = 0.006). Hence, a future work direction should be on improving the classifier's performance. But, more importantly,

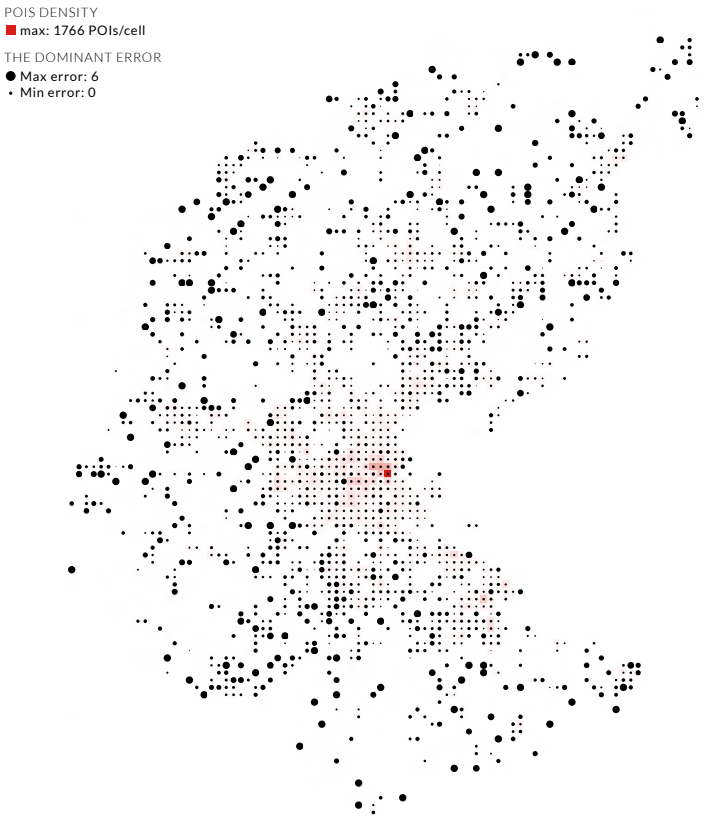

Fig. 12. Visualization of the relation between POI density and average POI classification error level $\overline{\xi_j}$ for the Boston metropolitan area. High intensity red squared represent zones high POI density. Circle radius represent the value of the average error level $\overline{\xi_j}$.

Figure 13 suggests the hypothesis that regions with lower POI densities are more likely to have higher estimated employment size errors, which in turn favors the idea that building a more comprehensive POI database, through the aggregation of multiple online sources of data, constitutes a very important future work direction.

VII. Conclusion and Future Work

In this paper, a complete framework for employment size estimation at a disaggregated level based on online collaborative POI data mined from the Web was proposed. We empirically showed that it possible to classify POI to the widely used NAICS taxonomy with several different machine learning algorithms using only the categories or tags that are commonly associated with them. We matched two different POI databases (InfoUSA and Dun & Bradstreet) to Yahoo!, in order to build two reliable training sets that have POIs with user provided bags of categories classified with NAICS codes. We tested several classification algorithms and the results show that the best approaches for this particular task are inductive based algorithms, namely instance based and tree based learning. These allow for an accuracy as high as 82% in the most complex task (classification with 6-digit NAICS codes). We also tried to perform classification in a hierarchical way, however the results did not showed many improvements

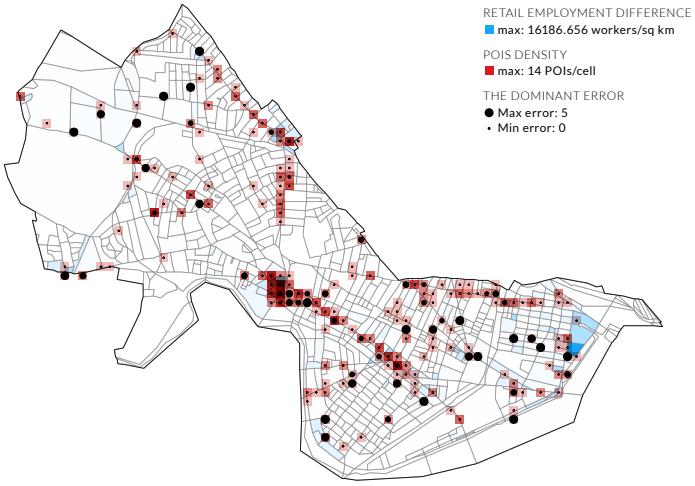

Fig. 13. Relation between POI density (red), estimated disaggregated employment size error (blue), and POI classification error (black circles) for the area of Cambridge, MA.

over the flat approaches, leading us to the conclusion that the size of the training set and its consistency/quality can have a larger impact on the results than the classification algorithm itself (except maybe for Bayesian approaches).

The classified POIs were applied to the urban planning task of employment size and location disaggregation from Block Group level to Block level and the results show encouraging quality. This strengthens the idea that well classified POI data to a convenient taxonomy like the NAICS is of great use and can have many distinct applications.

To the authors best knowledge, this is the only work that proposes an automatic approach for classifying POIs to the NAICS, and, therefore, a comparison with other works is not possible. Thus, we contribute with a novel approach to this important problem that has high impact in urban planning and space classification.

Furthermore, we propose several visualization techniques to help improve the overall quality of the proposed framework, by helping us to (1) identify regions of high classification error, (2) understand the relationship between POI classification error and POI density, (3) comprehend how POI classification error relates with estimated employment size error, (4) visualize how all these aspect distribute among space, and many other interesting aspects of the models and the data.

Future work will investigate the use of semantic enrichment of the POI data in order to help improve the POI classification accuracy. Furthermore, we also intend to explore other sources of online data, so that a more comprehensive POI dataset could be built.

References

[1] F. Rodrigues, F. Pereira, A. Alves, S. Jiang and J. Ferreira. Automatic Classification of Points-of-Interest for Land-use Analysis. Proceedings of the Fourth International Conference on Advanced Geographic Information Systems, Applications, and Services (GEOProcessing), pp. 41–49, 2012.

[2] U. C. Bureau. North american industry classification system (naics): Introduction, February 2010. http://www.census.gov/eos/www/naics/.

[3] N. Association. Naics association: Frequently asked questions, February 2010. http://www.naics.com/faq.htm.

[4] D. T. Lindgren. *Land-use Planning and Remote Sensing*. Martinus-Nijhoff, Boston, MA, 1985.

[5] L. O. Fresco. *The Future of the Land – Mobilizing and Integrating Knowledge for Land-use Options*. John Wiley & Sons, Chichester, 1997.

[6] J. B. Campbell. *Mapping the Land – Aerial Imagery for Land use Information*. Association of American Geographers, Washington, D.C., 1983.

[7] P. Danoedoro. Extracting land-use information related to socio-economic function from quickbird imagery: A case study of semarang area, indonesia. *Map Asia 2006*, 2006.

[8] D. Li, K. Di, and D. Li. Land use classification of remote sensing image with gis data based on spatial data mining techniques. *Geo-Spatial Information Science*, 3:30–35, 2000.

[9] M. Santos and A. Moreira. Automatic classification of location contexts with decision trees. *CSMU-2006 : Proceedings of the Conference on Mobile and Ubiquitous Systems, Guimares, Portugal*, 2006.

[10] T. Griffin, T. Huang, and R. Halverson. Computerized trip classification of gps data. *Proceedings of 3rd International Conference on Cybernetics and Information Technologies, Systems and Applications (CITSA 2006)*, 2006.

[11] J. Pierre. On the automated classification of web sites. *Linkoping Electronic Articles in Computer and Information Science*, 6, 2001.

[12] R. P. Haining. *Spatial data analysis in the social and environmental sciences*. Cambridge University Press, Cambridge, 1990.

[13] L. Anselin and R. Florax. *New directions in spatial econometrics*. Springer, New York, 1995.

[14] D. Keim, C. Panse, M. Sips and S. North. Pixel based visual mining of geo-spatial data. *Computers & Graphics (CAG)*, 2004, vol. 28.

[15] D. Costa and G. Venturini. A Visual and Interactive Data Exploration Method for Large Data Sets and Clustering. *Advanced Data Mining and Applications, Lecture Notes in Computer Science*, 2007, vol. 4632, pp. 553–561.

[16] E. Currid and J. Connolly. Patterns of knowledge: The geography of advanced services and the case of art and culture. *Annals of the Association of American Geographers*, 98:414–434, 2008.

[17] P. Sambidi and W. Harrison. Spatial clustering of the u.s. biotech industry. 2006 Annual meeting, July 23-26, Long Beach, CA 21360, American Agricultural Economics Association (New Name 2008: Agricultural and Applied Economics Association), 2006.

[18] G. Arbia. Modelling the geography of economic activities on a continuous space. *Papers in Regional Science*, 80(4):411–424, 2001.

[19] D. . Bradstreet. D & b website, February 2010. http://www.dnb.com/.

[20] W. Cohen, P. Ravikumar, and S. Fienberg. A comparison of string distance metrics for name-matching tasks. *Proceedings of the IJCAI-2003 Workshop on Information Integration on the Web (IIWeb-03), Acapulco, Mexico*, pp. 73–78, 2003.

[21] J. Gurland and R. Tripathi. A simple approximation for unbiased estimation of the standard deviation. *American Statistician*, 25(4):30–32, 1971.

[22] I. H. Witten and E. Frank. *Data Mining: Practical machine learning tools and techniques, 2nd Edition*. Morgan Kaufmann, 2005.

[23] T. M. Mitchell. *Machine Learning*. McGraw-Hill, New York, 1997.

[24] M. McNally and C. Rindt. *The Activity-Based Approach*. Handbook of Transportation Modeling. Elsevier, Amsterdam, London, 2008.

[25] E. Tufte. Visual Display of Quantitative Information. pp. 170–175, 2001.

Inverse Kinematics with Dual-Quaternions, Exponential-Maps, and Joint Limits

Ben Kenwright
Newcastle University
School of Computing Science
United Kingdom
b.kenwright@ncl.ac.uk

***Abstract*—We present a novel approach for solving articulated inverse kinematic problems (e.g., character structures) by means of an iterative dual-quaternion and exponential-mapping approach. As dual-quaternions are a break from the norm and offer a straightforward and computationally efficient technique for representing kinematic transforms (i.e., position and translation). Dual-quaternions are capable of represent both translation and rotation in a unified state space variable with its own set of algebraic equations for concatenation and manipulation. Hence, an articulated structure can be represented by a set of dual-quaternion transforms, which we can manipulate using inverse kinematics (IK) to accomplish specific goals (e.g., moving end-effectors towards targets). We use the projected Gauss-Seidel iterative method to solve the IK problem with joint limits. Our approach is flexible and robust enough for use in interactive applications, such as games. We use numerical examples to demonstrate our approach, which performed successfully in all our test cases and produced pleasing visual results.**

Keywords-Inverse Kinematics; Gauss-Seidel; Articulated Character; Games; Joint Limits; Iterative; Dual-Quaternion; Jacobian; Exponential-Map

I. Introduction

Generating fast reliable Inverse Kinematic (IK) solutions in real-time with angular limits for highly articulated figures (e.g., human bipeds including hands and feet) is challenging and important [1, 2, 3, 4, 5]. The subject is studied across numerous disciplines, such as graphics, robotics, and biomechanics, and is employed by numerous applications in the film, animation, virtual reality, and game industry

However, articulated models (e.g., bipeds and hands) can be highly complex; even the most simplified models of 20-30 joints can generate a vast number of poses [6, 7]. Whereby producing a simple pose to achieve a solitary task can produce ambiguous solutions that make the problem highly nonlinear and computationally expensive to solve. For example, even a straightforward task of reaching to pickup an object can be accomplished by means of any number of motions.

This paper focuses using dual-quaternions and quaternion exponential-maps with an iterative Gauss-Seidel algorithm [8] to solve an articulated IK problem; such as the hand model shown in Figure 2. The Gauss-Seidel algorithm is an iterative, efficient, low memory method of solving linear systems of equations of the form $Ax = b$. Hence, we integrate the Gauss-Seidel iterative algorithm with an articulated IK problem to produce a flexible whole system IK solution for time critical systems, such as games. This method is used as it offers a flexible, robust solution with the ability to trade accuracy for speed and give good visual outcomes.

Furthermore, to make the Gauss-Seidel method a practical IK solution for an articulated hand structure, it needs to enforce joint limits. We incorporate joint limits by modifying the update scheme to include an iterative projection technique. Additionally, to ensure real-time speeds we take advantage of spatial coherency between frames as a warm starting approximation for the solver. Another important advantage of the proposed method is the simplicity of the algorithm and how it can be easily configured for custom IK problems.

The main contribution of the paper is the practical demonstration and discussion of using the Gauss-Seidel method for real-time articulated IK problem with joint limits, dual-quaternions [9], and exponential-quaternion mapping [10]. Furthermore, we discuss constraint conditions, speedup approaches and robustness factors for solving highly non-linear IK problems in real-time.

The roadmap for rest of the paper is organized as follows. Firstly, we briefly review existing work in Section II. Section III describes the articulated model, we use for our simulations. Then in Section IV, we present essential mathematical algorithms and principles for the paper (e.g., dual-quaternion algebra). We follow on by explaining the IK problem in Section V. While in Section VI, we explain the Jacobian matrix, then in Section VII we discuss our approach for solving the IK problem with the Gauss-Seidel algorithm. Finally, we present results in Section IX, then Section X discusses limitations, followed by the closing conclusion and discussion in Section XI.

II. Related Work

Inverse kinematics is a popular problem across numerous disciplines (e.g., graphical animation, robotics, biomechan-

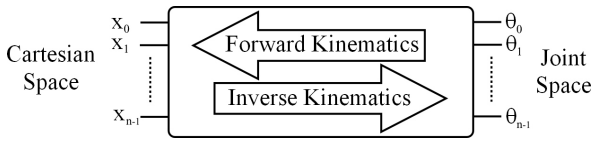

Figure 1. Forward & Inverse Kinematics. Illustrating the relationship between forward and inverse kinematics parameters.

ics). IK is a vital component that can be implemented using a wide range of solutions. We give a brief overview of existing, current, and cutting-edge approaches to help emphasise the different ways of approaching the problem; enabling the reader to see where our method sits.

In general, however, for very simple problems with just a few links, analytical methods are employed to solve the IK problem. Alternatively, for larger configurations, iterative numerical methods must be employed due to the complexity of the problem.

The articulated IK problem of finding a solution for poses that satisfy positional and orientation constraints has been well studied, e.g., [11, 3, 12, 7]. The problem is highly nonlinear, meaning there can be numerous solutions; hence, multiple poses fulfilling the constraint conditions. In practical situations, there can even be cases where no solution exists due to the poor placement of end-effectors. IK systems typically use cut down models, e.g., merely performing IK on individual limbs (as in body, arms, legs) [13, 14, 6]. This makes the problem computationally simpler and less ambiguous.

Numerous solutions from various fields of research have been implemented to solving the IK problem. The Jacobian-based matrix approach is one of the most popular methods and the method upon which we base our iterative solution [7, 15, 16]. The Jacobian matrix method aims to find a linear approximation to the problem by modelling the end-effectors movements relative to the instantaneous systems changes of the links translations and orientations. Numerous different methods have been presented for calculating the Jacobian inverse, such as, Jacobian Transpose, Damped Least-Squares (DLS), Damped Least-Squares with Singular Value Decomposition (SVD-DLS), Selectively Damped Least-Square (SDLS) [17, 5, 18, 19, 20, 15].

An alternative method uses the Newton method; whereby the problem is formulated as a minimization problem from which configuration poses are sought. The method has the disadvantage of being complex, difficult to implement and computationally expensive to computer-per-iteration [16].

The Cyclic Coordinate Descent (CCD) is a popular real-time IK method used in the computer games industry [21]. Originally introduced by Wang et al. [22] and then later extended to include constraints by Welman et al. [3]. The CCD method was designed to handle serial chains and is thus difficult to extend to complex hierarchies. It has the advantage of not needing to formulate any matrices and has a lower computational cost for each joint per iteration. Its downside is that the character poses even with constraints can produce sporadic and unrealistic poses. However, further work has been done to extend CCD to work better with human based character hierarchies [4, 6, 23].

A novel method recently proposed was to use a Sequential Monte Carlo approach but was found to be computationally expensive and only applicable for offline processing [24, 25].

Data driven IK systems have been presented; Grochow et al. [26] method searched a library of poses to determine an initial best guess solution to achieve real-time results. An offline mesh-based for human and non-human animations was achieved by learning the deformation space; generating new shapes while respecting the models constrains [27, 28].

A method known as ”Follow-The-Leader” (FTL) was presented by Brown et al. [29] and offered real-time results using a non-iterative technique. However, this approach was later built upon by Aristidou et al. [30] and presented an iterative version of the solver known as FABRIK.

The Triangular IK method [31, 32], uses trigonometric properties of the cosine rule to calculate joint angles, beginning at the root and moving outwards towards the end-effectors. While the algorithm can be computationally fast, due to it being able to propagate the full hierarchy in a single iteration, it cannot handle multiple end-effectors well and is primarily based around singly linked systems.

The advantages of an iterative IK system for articulated structures, such as character, was also presented by the interesting paper by Tang et al. [33] who explored IK techniques for animation using a method based on the SHAKE algorithm. The SHAKE algorithm is an iterative numerical integration scheme considered similar to the Verlet method [34], which can exploit substantial step-sizes to improve speed yet remain stable when solving large constrained systems. The algorithm is also proven to have the same local convergence criterion as the Gauss-Seidel method we present here as long as the displacement size is kept sufficiently small.

The paper by Arechavaleta et al. [35] presents a well written explanation of using iterative methods (primarily the Gauss-Seidel technique) for computing fast and accurate solutions for ill-conditioned LCP problems.

We use the iterative Gauss-Seidel approach presented by Kenwright [1], however, we store the joint angles as quaternion-exponent and employ dual-quaternion algebra [9] for solving forward and inverse kinematic problems. As unit-quaternions are an ideal tool for orientations of rigid transforms, however, they do not contain any translation information about the location of points in 3D space. Hence, dual-quaternions are an extension of quaternion by means of dual-number theory as a compact, efficient, and smart approach of representing both rotation and translation in a single vector with its own algebraic rules (e.g., calculating

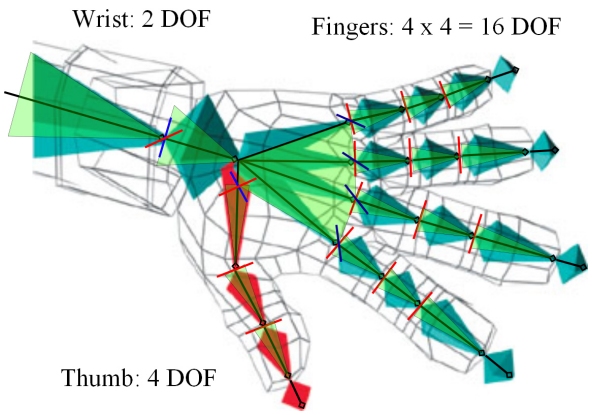

Figure 2. Articulated Hand Model. The articulated hand model (including the wrist) was used for the simulations and possessed 22 degrees of freedom (DOF). The structure comprised of 17 links and 16 joints.

differences, inverting, interpolating). The robotic community has exploited dual-quaternions to solve IK problems; for example, Hoang-Lan et al. [36] solved IK problem by formulating a dual-quaternion metric error measurement for constructing the Jacobian.

III. Articulated Model

The articulated model used for our simulations and evaluation of our approach is shown in Figure 2. The mechanical functioning is of a human hand and is constructed using a series of interconnected rigid segments (or links) connected by joints (also, note, an interconnected series of links is also called a kinematic chain). As shown in Figure 2, we represent the hand as a collection of 17 rigid body segments connected using 16 primary joints. The character's hand gives us 22 degrees of freedom (DOF). Joints such as the wrist have three DOF corresponding to abduction/adduction, flexion/extension and internal/external rotation (i.e., rotation around the x, y, and z axis). Where complex joints such as the ball-and-socket (i.e., with 3 DOF) can be formed from multiple simpler joints (i.e., 3 single DOF joints). So a joint with n DOF is equivalent to n joints of 1 DOF connected by n-1 links of length zero. Thus, for example, the wrist joint can be described as a sequence of 2 separate joints of 1 DOF, where 1 of the joints connecting links has a zero length, as done by Kenwright [1]. Euler angles are an intuitive and straightforward means of representing orientation, since they are easy to visualize and enforce upper and lower boundary limits. However, we store each joint rotation as a quaternion-exponential (i.e., axis-angle combination), as it offers a similarly compact parameterization as Euler angles but without the gimbals lock problem. We combine the exponential-mapping with quaternion and dual-quaternion algebra to solve the IK solution, while clamping angular limits through a twist-and-swing decomposition of the orientation.

As shown in Figure 2, the single DOF connected joints were colored in accordance with their axis type; the x, y, and z representing the colors red, green and blue. The foot was set as the base for the IK with five end-effectors (i.e., head, pelvis, right-hand, left-hand and left-foot). We developed an application for an artist to interrogate and experiment with the skeletal IK system; setting end-effectors locations and viewing the generated poses. Each end-effector has a 6 DOF constraint applied to it; representing the target position and orientation. The ideal end-effectors are drawn in red, and the current end-effectors are drawn in green. This can be seen clearly in Figure 5, where the target end-effectors are located at unreachable goals.

IV. Mathematical Background

We give a brief introduction to the essential mathematical definitions on quaternion and dual-quaternion algebra. For a more detailed introduction and an overview of their practical advantages, see Kenwright [9]. Since quaternions have proven themselves in many fields of science and computing as providing an unambiguous, un-cumbersome, computationally efficient method of representing rotational information. We combine dual-number theory to extend quaternions to dual-quaternions, so we can use them to represent rigid transforms (i.e., translations and rotations).

A. Definitions

To reduce ambiguity and make the paper as readable as possible, we define variable symbol definitions:

$$\begin{array}{rlrl} q & \text{quaternion} & \hat{q} & \text{unit-quaternion} \\ \underline{q} & \text{dual-quaternion} & \underline{\hat{q}} & \text{unit dual-quaternion} \\ \vec{v} & \text{vector} & \hat{v} & \text{unit-vector} \end{array} \quad (1)$$

While we mostly represent quaternions and dual-quaternions with the letter q, there are instances where we use the letter t to indicate that the dual-quaternion or quaternion is a pure translation component.

B. Quaternions

The quaternion was introduced by Hamilton [37] in 1860 and has the following form:

$$\mathbf{q} = q_s + q_x\mathbf{i} + q_y\mathbf{j} + q_z\mathbf{k} \quad (q_s, q_x, q_y, q_z \in \mathbb{R}) \quad (2)$$

where $\mathbf{ii} = \mathbf{jj} = \mathbf{kk} = \mathbf{ijk} = -1$.

While w is sometimes used to represent the scalar component in quaternions, we us the letter s, to avoid ambiguity with exponential-mapping variable ($\vec{w}$). Alternatively, it is more commonly defined as a pair $(s, \vec{v})$ with $s \in \mathbb{R}$ and $\vec{v} \in \mathbb{R}^3$.

A *unit-quaternion* has a unit-length with $q_s^2 + q_x^2 + q_y^2 + q_z^2 = 1$ and the inverse of a unit-quaternion is its conjugate

$q^* = q_s - \vec{v}$. Given an axis and angle of rotation a unit-quaternion can be calculated using:

$$\begin{aligned} q_s &= cos(\theta/2), \quad & q_x &= n_x sin(\theta/2) \\ q_y &= n_y sin(\theta/2), \quad & q_z &= n_z sin(\theta/2) \end{aligned} \tag{3}$$

where $\hat{n} = n_x, n_y, n_z$ is a unit-vector representing the axis of rotation and θ is the angle of rotation. Whereby, given a point in 3D space $\vec{x}$ we can rotate to give $\vec{x}'$ using:

$$\vec{x}' = \hat{q}\vec{x}\hat{q}^* \tag{4}$$

Addition, subtraction, and the product of two quaternions, is defined by:

$$\begin{aligned} \mathbf{q_0} + \mathbf{q_1} &= (s_0 + s_1, \vec{v_0} + \vec{v_1}) \\ \mathbf{q_0} - \mathbf{q_1} &= (s_0 - s_1, \vec{v_0} - \vec{v_1}) \\ \mathbf{q_0 q_1} &= (s_0 s_1 - \vec{v_0}\vec{v_1}, s_0\vec{v_1} + s_1\vec{v_0} + \vec{v_0}\vec{v_1}) \end{aligned} \tag{5}$$

A crucial fact that we exploit in this paper is that the exponential of a unit-quaternion is the combined axis-angle component:

$$\begin{aligned} exp(\hat{q}) &= [0, \hat{n}\theta] \\ &= [0, \vec{w}] \end{aligned} \tag{6}$$

where $\hat{n}$ is the unit-vector representing the axis of rotation and θ is the angle magnitude in radians. The logarithm of a quaternion is the inverse of the exponential enabling us to convert to and from the axis-angle component. The exponential of a unit-quaternion is often called the *exponential map*, which we denote as $\vec{w}$.

$$\begin{aligned} \theta &= ||\vec{w}|| \\ \hat{v} &= \frac{\vec{w}}{||\vec{w}||} \end{aligned} \tag{7}$$

The exponential-map can be computed robustly, even in the neighborhood of the origin [10].

C. Dual-Numbers

Dual-number theory was introduced by Clifford [38] in 1873 and is defined as:

$$\hat{z} = r + \epsilon d \quad \text{with } \epsilon^2 = 0 \text{ but } \epsilon \neq 0 \tag{8}$$

where r is the real-part, d is the dual-part, and ϵ is the dual operator. While dual-number theory can be used to represent different quantities (e.g., dual-vectors), we are primarily interested in dual-quaternions because it gives us the ability of unifying rigid transform space into a single state-space variable (i.e., position and translation).

D. Dual-Quaternions

A dual-quaternion is defined as a dual-number with quaternion components and has the ability to represent 3D Euclidean coordinate space (i.e., rotation and translation) as a single parameter.

$$\underline{q} = q_r + \epsilon q_d \tag{9}$$

where q_r and q_d are quaternions. Additionally, since the dual-quaternion consists of two quaternion components it can be represented as: $\underline{q} = [q_0, q_1, q_2, q_3, q_4, q_5, q_6, q_7]^T$. The common algebraic operations are defined as:

$$\begin{aligned} \alpha\underline{q} &= \alpha q_r + \alpha\epsilon q_d \\ \underline{q}_0 + \underline{q}_1 &= q_{r0} + q_{r1} + \epsilon(q_{d0} + q_{d1}) \\ \underline{q}_0\,\underline{q}_1 &= q_{r0}q_{r1} + \epsilon(q_{r0}q_{d1} + q_{d0}q_{r1}) \end{aligned} \tag{10}$$

The conjugate of a dual-quaternion $\underline{q}^* = q_r^* + \epsilon q_d^*$ with the norm (or length) of a dual-quaternion given by $||\underline{q}|| = \underline{q}\underline{q}^*$ and the unity condition (i.e., for unit dual-quaternions) is:

$$\underline{q}\,\underline{q}^* = 1 \quad q_r^* q_d + q_d^* q_r = 0 \tag{11}$$

A **unit dual-quaternion** can be used to represent any rigid transformation (i.e., position and rotation); we construct a unit dual-quaternion rigid transformation using:

$$\begin{aligned} \hat{\underline{q}} &= q_{rot} + \epsilon\frac{1}{2}q_{rot}q_{pos} \qquad \text{(rotation then translation)} \\ &\text{or} \\ \hat{\underline{q}} &= q_{rot} + \epsilon\frac{1}{2}q_{pos}q_{rot} \qquad \text{(translation then rotation)} \\ &= (1 + \epsilon\frac{1}{2}q_{pos})q_{rot} \end{aligned} \tag{12}$$

where q_{rot} and q_{pos} are the rotation and translation quaternions respectively, with the translation quaternion $q_{pos} = [0, t_x, t_y, t_z]$.

V. Forward and Inverse Kinematics

Forward and inverse kinematics is the process of calculating positions and orientations either from joint space (i.e., using interconnected positions and orientations of the joints) or from Cartesian space (i.e., the world positions and orientations) as shown in Figure 1.

A. Forward Kinematics (FK)

The FK problem is straightforward to calculate and has no ambiguity or singularities. For an articulated structure, we can concatenate the dual-quaternion transforms through multiplication to generate the final positions and orientations of the interconnected links. For example, a serial chain of n links would be:

$$\hat{\underline{q}} = \hat{\underline{q}}_0\hat{\underline{q}}_1\hat{\underline{q}}_2 ... \hat{\underline{q}}_{n-1} \tag{13}$$

where $\hat{\underline{q}}_0 ... \hat{\underline{q}}_{n-1}$ define each individual joints rotation and translation.

B. Inverse Kinematics (IK)

IK is the reverse of FK. While FK remains fast and simple for large interconnected structures, IK solutions can be computationally expensive, possess singularity problems and contain multiple solutions. However, in practice, we attempt to find a best fit approximation that will meet the desired constraints. For example, in Equation (13), we know $\hat{q}$ and would seek to find the orientation (and/or translation) for each link ($\hat{q}_0..\hat{q}_{n-1}$), and $\hat{q}$ is the position and orientation of the combined links (i.e., for the end-effector).

C. Pure Rotation and Pure Translation

A dual-quaternion's transformation can be represented by two pure dual-quaternions, i.e., a *pure rotation* and *pure translation*:

$$\begin{aligned} \hat{q}_{tra} &= 1 + \epsilon\frac{1}{2}\hat{q}_{pos} \quad \text{(pure translation)} \\ \hat{q}_{rot} &= \hat{q}_{rot} + \epsilon\hat{0} \quad \text{(pure rotation)} \end{aligned} \tag{14}$$

where we concatenate the pure dual-quaternion transforms by multiplication to calculate the combined set of transforms, as shown in Equation (12); however, be warned the order of multiplication determines if translation or rotation is performed first. For example, we represent the FK problem as:

$$\begin{aligned} \hat{q} &= \hat{q}_0\hat{q}_1\hat{q}_2\cdots\hat{q}_{n-1} \\ &= (\hat{q}_0^t\hat{q}_0^r)(\hat{q}_1^t\hat{q}_1^r)(\hat{q}_2^t\hat{q}_2^r)\ldots(\hat{q}_{n-1}^t\hat{q}_{n-1}^r) \end{aligned} \tag{15}$$

where the superscript letter r and t indicates a pure rotation or pure translation dual-quaternion transform respectively (as defined in Equation (14)).

VI. Jacobian Matrix

The Jacobian $\mathbf{J}$ is a matrix that represents the change in joint orientations to displacement of end-effectors. Each frame we calculate the Jacobian matrix from the current angles and end-effectors. We assume a right-handed coordinate system. To illustrate how we calculate the Jacobian for an articulated system, we consider the simple example shown in Figure 3. For a more detailed description see [17, 5, 18, 19, 20, 15]. The example demonstrates how we decompose the problem and represent it as a matrix for a sole linked chain with a single three DOF end-effector. We then extend this method to multiple linked-chains with multiple end-effectors (each with six DOF) to represent the character hierarchy.

Each joint is stored as an axis-angle component ($w = \hat{n}\theta$):

$$\mathbf{w} = \begin{bmatrix} \vec{w}_0 \\ \vec{w}_1 \\ \vec{w}_2 \\ \ldots \\ \vec{w}_n \end{bmatrix} \tag{16}$$

where $\vec{w}_i$ is the rotation (i.e., axis-angle) of joint i relative to joint $i-1$, and e for the end-effectors global position. From these matrices, we can determine that the end-effectors, and the joint angles are related. This leads to the forward kinematics definition, defined as:

$$\mathbf{e} = \begin{bmatrix} e_x \\ e_y \\ e_z \end{bmatrix} \tag{17}$$

The end-effectors and the joint orientation (i.e., quaternion-exponent) are related and is defined by:

$$\mathbf{e} = f(\ \mathbf{w}\ ) \tag{18}$$

We can differentiate the kinematic equation for the relationship between end-effectors and joint orientation. This relationship between a change in joint orientation and a change in end-effectors location is represented by the Jacobian matrix and is given by:

$$\dot{\mathbf{e}} = \mathbf{J}\dot{\mathbf{w}} \tag{19}$$

The Jacobian $\mathbf{J}$ is the partial derivatives for the change in end-effectors locations by change in joint angles.

$$\mathbf{J} = \frac{\partial \mathbf{e}}{\partial \mathbf{w}} \tag{20}$$

If we re-arrange the kinematic problem:

$$\mathbf{w} = f^{-1}(\mathbf{e}) \tag{21}$$

We can conclude a similar relationship for the Jacobian:

$$\dot{\mathbf{w}} = \mathbf{J}^{-1}\dot{\mathbf{e}} \tag{22}$$

For small changes, we can approximate the differentials by their equivalent deltas:

$$\Delta\mathbf{e} = \mathbf{e}_{target} - \mathbf{e}_{current} \tag{23}$$

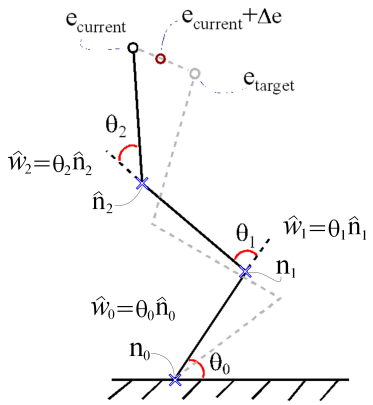

Figure 3. Forward & Inverse Kinematics Example. Illustrating the relationship between the different parameters, e.g., end-effector error and joint orientations. $\vec{w}$ quaternion exponential-map for each joint (i.e., axis-angle combination $\vec{w} = \hat{n}\theta$).

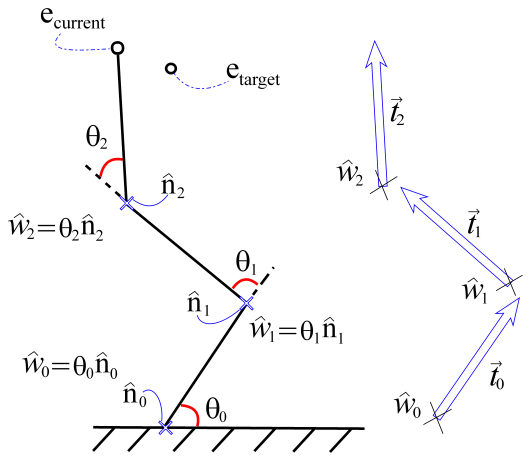

Figure 4. A simple three link serial chain example, where $\vec{w}$ is the axis-angle combination (i.e., quaternion- exponential-map), $\vec{t}$ is the translation vector, $\hat{n}$ is the unit-length axis of rotation, and θ is the angle. For a simple 2D case (i.e., only in the x-y axis) the axis of rotation is $\hat{n} = [0, 0, 1]$..

For these small changes, we can then use the Jacobian to represent an approximate relationship between the changes of the end-effectors with the changes of the joint angles.

$$\Delta \mathbf{w} = \mathbf{J}^{-1} \Delta \mathbf{e} \tag{24}$$

We can substitute the result back in:

$$\mathbf{w}_{current} = \mathbf{w}_{previous} + \Delta \mathbf{w} \tag{25}$$

For a step-by-step explanation of the process of calculating the Jacobian for the quaternion-exponent see Appendix B-B. For example, calculating the Jacobian for Figure 4 gives:

$$\mathbf{J} = \begin{bmatrix} \frac{\partial \mathbf{e}}{\partial w_0} \\ \frac{\partial \mathbf{e}}{\partial w_1} \\ \frac{\partial \mathbf{e}}{\partial w_2} \end{bmatrix} \tag{26}$$

and

$$\mathbf{e} = \mathbf{e}_{current} - \mathbf{e}_{target}$$

The Jacobian matrix is calculated for the system so that we can calculate the inverse and hence the solution. Alternatively, a good explanation of the Jacobian and its applications is also presented by Buss [15], who gives an introduction to IK methods using the Transpose, Pseudoinverse, and Damped Least-Square method.

VII. Gauss-Seidel Algorithm

We set up the IK problem into a particular arrangement, so that we can solve for the unknowns using the Gauss-Seidel method. Whereby, we construct the IK formulation using the Jacobian matrix with the linear equation format of the form:

$$\text{Linear Equation: } \mathbf{Ax} = \mathbf{b} \tag{27}$$

The IK problem is then composed as:

$$\mathbf{J}^T \mathbf{J} \Delta \mathbf{q} = \mathbf{J}^T \Delta \mathbf{e} \tag{28}$$

Equating equivalent variables:

$$\begin{aligned} \mathbf{A} &= \mathbf{J}^T \mathbf{J} \\ \mathbf{b} &= \mathbf{J}^T \Delta \mathbf{e} \\ \mathbf{x} &= \Delta \mathbf{q} = unknown \end{aligned} \tag{29}$$

A. Damping and Stability

1) Damping: With the Gauss-Seidel iterative method, we solve for the unknown x value. To prevent singularities and make the final method more stable and robust we incorporated a damping value:

$$\mathbf{A} = (\mathbf{J}^T \mathbf{J} + \delta \mathbf{I}) \tag{30}$$

where δ is a damping constant (e.g., $\sim$0.0001), and $\mathbf{I}$ is an identity matrix.

2) Singularities: The exponential-map of a quaternion (i.e., the axis-angle combination) is parameterized in $\in \mathbb{R}^3$ and hence contains singularities similar to Euler angles possessing gimbals lock singularities. However, for our IK iterative situation, we take small incremental steps (i.e., angular change is less than π) we can avoid the singularity problem, since we can shift the exponential-map singularity away from the safe working region [10]. The exponenential-map has singularities at a radius of $2n\pi$ (for $n = 1, 2, 3..$). Hence, if the exponential-map angle $||\vec{w}||$ is close to π we replace $\vec{w}$ by $(1 - 2\pi/||\vec{w}||)\vec{w}$, which is the same rotation but shifted away from the singularity problem.

B. Gauss-Seidel Implementation

The Gauss-Seidel iterative algorithm is a technique developed for solving a set of linear equations of the form $Ax = b$. The method has gained a great deal of acclaim in the physics-based community for providing a computationally fast robust method for solving multiple constraint rigid body problems [39, 40, 41]. The iterative algorithm is based on matrix splitting [42], and its computational cost per iteration is O(n), where n is the number of constraints. Furthermore, the number of constraints and the number of iterations is what dominates the performance of the algorithm. Algorithm 1 is the basic Gauss-Seidel method for a generic linear system of equations of the form $Ax = b$; for the unknowns, an initial guess is needed. Naively this value could be zero and result in the system having a cold start. Then the algorithm would proceed, while at each iteration, the corresponding elements from A, b and x (current) act as a feedback term to move x (next) closer to the solution.

Algorithm 1 Gauss-Seidel iterative algorithm to solve $Ax = b$ given x^0

```
x = x^0
for iter=1 to iteration limit do
    for i=1 to n do
        Δx_i = [b_i − Σ_{j=1}^{n} A_ij x_j] / A_ii
        x_i = x_i + Δx_i
    end for
end for
```

The conditions for the Gauss-Seidel iterative Algorithm 1 terminating are:

- If a maximum number of iterations has been reached
- If the error $||Ax-b||$ drops below a minimum threshold
- If $||\Delta x_i||$ falls below a tolerance
- If $||\Delta x_i||$ remains the same as the previous frame (within some tolerance)

It is essential that the coefficients along the diagonal part of the matrix be dominant for the Gauss-Seidel method to converge on a solution.

C. Angular Limits - Twist-and-Swing

Any practical character-based IK system needs to have the ability to enforce angular joint limits before it can be considered a viable real-world solution. We incorporate angular joint limits into the simple iterative algorithm by clamping the modified angle orientations at each iteration update (see Equation (31)). While this can be accomplished easily with Euler angles by setting a minimum and maximum angle. For the exponential-map (i.e., the axis-angle combination) parameterization, we use the twist-and-swing decomposition [10], since it presented a fast, robust, and simple technique for robustly calculating angular errors and enforcing limits (as demonstrated and shown by Kallmann [43]).

$$\mathbf{w} = \begin{cases} lower & : \ if\ (\mathbf{w} + \mathbf{J}^{-1}\Delta\mathbf{e}) \ < lower \\ upper & : \ if\ (\mathbf{w} + \mathbf{J}^{-1}\Delta\mathbf{e}) \ > upper \\ \mathbf{w} + \mathbf{J}^{-1}\Delta\mathbf{e} & : \ otherwise \end{cases} \quad (31)$$

For complex joint models, such as the ball-and-socket joint, the twist-and-swing decomposition presents a practical and intuitive representation. The twist-and-swing allows us to define and enforce joint limits intuitively. The twist is around the 'x-axis' while the swing is around the 'yz-plane'. We can decompose a quaternion orientation into its twist and swing components shown in Equation 32. This is in world space but can easily be converted to local space (e.g., joint space).

$$\begin{aligned} \mathbf{q}_{twist_x} &= \left(\frac{q_s}{\sqrt{q_s^2 + q_x^2}}, \frac{q_x}{\sqrt{q_s^2 + q_x^2}}, 0, 0 \right) \\ \mathbf{q}_{swing_{yz}} &= \left(\sqrt{q_s^2 + q_x^2}, 0, \frac{q_s q_y - q_x q_z}{\sqrt{q_s^2 + q_x^2}}, \frac{q_s q_z + q_x q_y}{\sqrt{q_s^2 + q_x^2}} \right) \\ \mathbf{q} &= \mathbf{q}_{swing_{yz}} \mathbf{q}_{twist_x} \end{aligned} \quad (32)$$

$$\begin{aligned} \mathbf{q}_{twist_y} &= \left(\frac{q_s}{\sqrt{q_s^2 + q_y^2}}, 0, \frac{q_y}{\sqrt{q_s^2 + q_y^2}}, 0 \right) \\ \mathbf{q}_{swing_{xz}} &= \left(\sqrt{q_s^2 + q_y^2}, 0, \frac{q_s q_x + q_y q_z}{\sqrt{q_s^2 + q_y^2}}, \frac{q_s q_z - q_x q_y}{\sqrt{q_s^2 + q_y^2}} \right) \\ \mathbf{q} &= \mathbf{q}_{swing_{xz}} \mathbf{q}_{twist_y} \end{aligned} \quad (33)$$

$$\begin{aligned} \mathbf{q}_{twist_z} &= \left(\frac{q_s}{\sqrt{q_s^2 + q_z^2}}, 0, 0, \frac{q_z}{\sqrt{q_s^2 + q_z^2}} \right) \\ \mathbf{q}_{swing_{xy}} &= \left(\sqrt{q_s^2 + q_z^2}, 0, \frac{q_s q_x - q_y q_z}{\sqrt{q_s^2 + q_z^2}}, \frac{q_s q_y - q_x q_z}{\sqrt{q_s^2 + q_z^2}} \right) \\ \mathbf{q} &= \mathbf{q}_{swing_{xz}} \mathbf{q}_{twist_y} \end{aligned} \quad (34)$$

where q_x, q_y, and q_z are the rotations around the x-, y-, and z-axis respectively, and q_{xy}, q_{xz}, and q_{yz} are the rotations a vector in the xy-, xz-, and yz-plane respectively (see Appendix A for proof). We can validate the twist-and-swing decomposition by multiplying them together and reconstructing the original quaternion.

This extension of the basic Gauss-Seidel algorithm to handle constraint limits for the unknowns is called the Projected Gauss-Seidel (PGS) algorithm. The angular limits form bounds that are in form of upper and lower joint angles that are easily enforced through clamping. Furthermore, the PGS algorithm has O(n) running time and convergence is guaranteed as long as the matrix is positive definite [8]. In practice, we have found the algorithm to provide promising visual and numerical results.

VIII. Spatial and Temporal Coherency

We give the iterative solver a warm-start approximation at the start of each iteration update by taking advantage of spatial and temporal coherency of the problem. Since the PGS solver is iterative by design and without a warm-start approximation, its convergence rate can be very slow (i.e., depending upon the eigenvalues of the matrix it is solving). However, by caching the result between updates (i.e., use previous solution as the start for the next update), we can considerably reduce the number of iterations, especially for cases when there are only minuscule changes for the system.

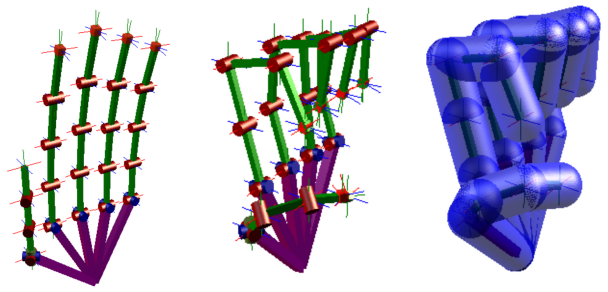

Figure 5. Simulation Screenshots A. Experimental poses for our articulated hand.

IX. Experimental Results

On average, the small spatial coherent transitions between frame updates resulted in the Gauss-Seidel method requiring only two or three iterations for the end-effectors to reach acceptable answers. This resulted in the IK solver being able to easily maintain a low-computational overhead and run at real-time frame-rates. While our Gauss-Seidel implementation was straightforward it was implemented in a single threaded program and did not exploit any parallel architecture speed ups (e.g., using a multi-core CPU or GPU); however, numerous methods were demonstrated by Courtecuisse et al. [44] for exploiting multi-core architectures to achieve much improved performance using the Gauss-Seidel algorithm.

The performance of our iterative Gauss-Seidel IK implementation was computationally fast and ran at real-time frame-rates enabling the IK problem to be modified on the fly. For cases when little or no movement occurred the solver would perform 1 to 2 iterations at most, while for sporadic changes in the articulated posture resulted in approx. 10 or more iterations. Furthermore, our Gauss-Seidel method would only require a few milliseconds to compute the solution. However, the cost of calculating the IK solution can vary greatly depending upon the starting assumption. Our implementation performed at real-time rates and maintained a consistent frame-rate well above a 100Hz. Simulations were performed on a machine with the following specifications: Windows7 64-bit, 16Gb Memory, Intel i7-2600 3.4Ghz CPU. Compiled and tested with Visual Studio 2012.

One important criteria was that the IK solver remained stable, e.g., when the end-effectors are placed out of reach, so that no solution exists. In practice, when no result was obtainable, a best reach condition was always presented, stretching to obtain the end-effectors but remaining stable (i.e., not oscillating or jittering). Furthermore, when end-effectors were started at radically different locations, the resulting solution would haphazardly jerk; however, the result always converged on acceptable poses.

We experimented with a diverse range of poses of generally unpredictable and chaotic finger movement to explore the stability and flexibility of our approach. For example, we did random on the spot compositions of the hand opening, closing, stretching, and so on, and always converged on a solution. It should be pointed out that the hand has less problems with angular limits and singularity conditions compared to a full body articulated structure. However, the hand has enough degrees of freedom and flexibility to perform a suitably detailed set of tests.

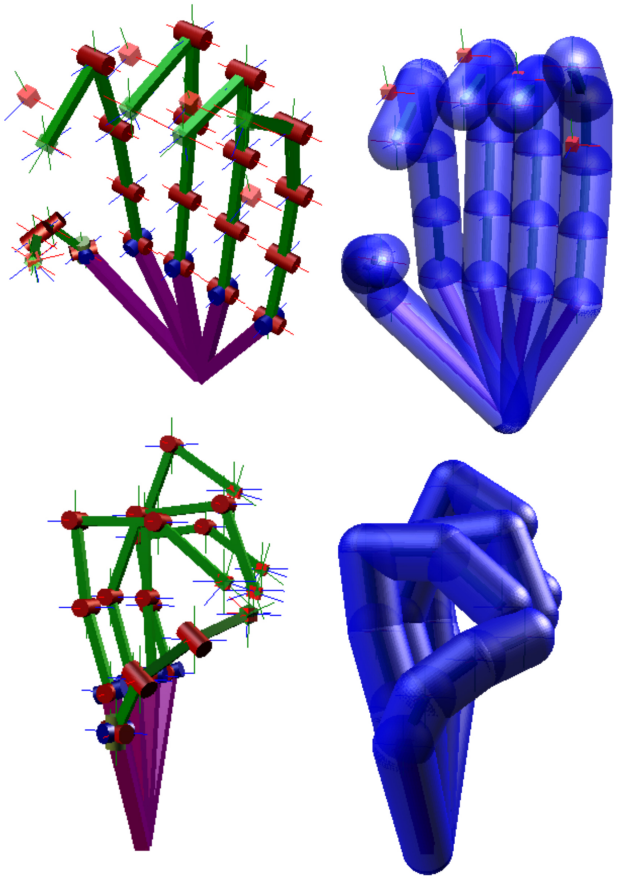

Figure 6. Simulation Screenshots B. Experimental poses for our articulated hand.

X. Limitations

We did not include any inter-link collision detection so it was possible for fingers to pass through one another. During situations when joints were against their angular limits, it would take longer for the iterative IK solver to converge on a solution, since joints that could not move further would be constantly pushed back. Finally, we did not weight or couple any of the angular joints; hence, the final pose could look uncomfortable and unnatural while still being physically-plausible. For example, in a real-world human hand, if the index finger is pulled downwards towards the wrist, it should

affect its neighboring fingers.

XI. Conclusion and Discussion

We presented the Gauss-Seidel technique as a method for solving real-time articulated IK problems with quaternion-exponential maps and dual-quaternions. We used temporal caching to reduce the computational cost and gain real-time performance speeds. The results of the IK system performed well enough to be used in time critical systems (such as games). With the angular limits, the method can suffer from singularity problems if the end-effectors jump; however, due to the end-effectors following small spatial transitions singularities are mostly avoided. All in all, the algorithm is simple to implement, computationally fast, little memory overhead, and is fairly robust. The IK solution can work with multiple end-effectors to produce poses with smooth movement with and without constraints.

While we demonstrated the practical aspect of using the Gauss-Seidel method as a valid real-time method for a articulated IK system, further work still needs to be done for a more detailed statistical comparison between the aforementioned IK solutions; comparing memory, complexity and computational costs.

A further area of study would be combining the IK solver with a physics-based system (i.e., rigid body constraint solver) and explore object interaction (e.g., picking up a ball or a pencil). Furthermore, to enable greater simulation speeds, the possible investigation and exploration of making the solver more parallel, for example, Poulsen [45] demonstrated a Parallel Projected Gauss-Seidel Method.

This paper exploited the Gauss-Seidel iterative method in conjunction with a set of highly non-linear equations to solve an inverse kinematic problem for an articulated structure. While we demonstrated the practical viability of the Gauss-Seidel method with exponential-maps, we did not implement and compare our approach with the many different numerical techniques(e.g., Newton or Broyden approach) and is an area of further investigation.

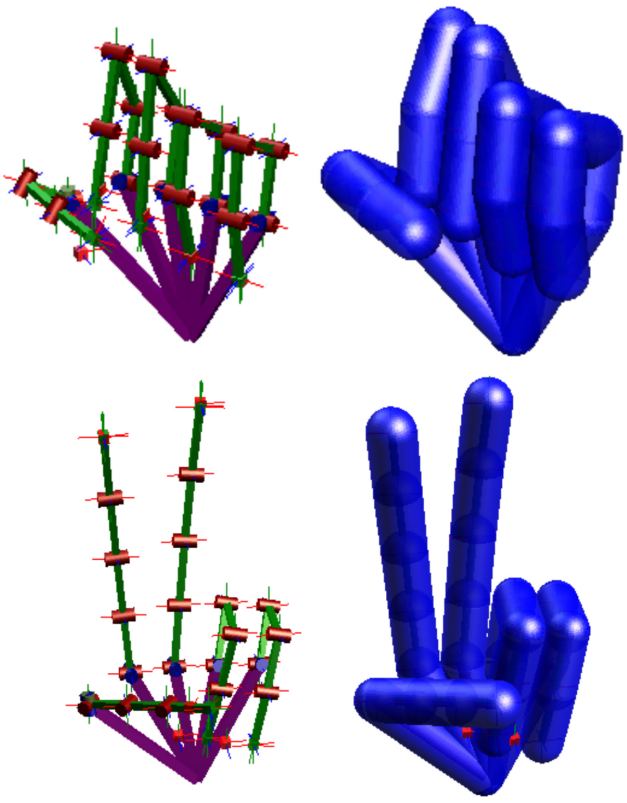

Figure 7. Simulation Screenshots C. Experimental poses for our articulated hand.

Acknowledgment

The authors would like to thank the reviewers for taking time out of their busy schedules to provide valuable, helpful, and insightful feedback that has contributed towards making this better paper more clear, concise, and correct.

References

[1] B. Kenwright, "Real-time character inverse kinematics using the gauss-seidel iterative approximation method," *CONTENT 2012, The Fourth International Conference on Creative Content Technologies*, pp. 63–68, 2012. 1, 2, 3

[2] B. Kenwright, "Synthesizing balancing character motions," *Workshop on Virtual Reality Interaction and Physical Simulation VRIPHYS 2012*, pp. 87–96, 2012. 1

[3] C. Welman, *Inverse kinematics and geometric constraints for articulated figure manipulation*. PhD thesis, 1993. 1, 2

[4] L. Unzueta, M. Peinado, R. Boulic, and A. Suescun, "Full-body performance animation with Sequential Inverse Kinematics," *Graphical Models*, vol. 70, pp. 87–104, Sept. 2008. 1, 2

[5] W. Wolovich and H. Elliott, "A computational technique for inverse kinematics," in *The 23rd IEEE Conference on, Decision and Control, 1984*, vol. 23, pp. 1359–1363, IEEE, 1984. 1, 2, 5

[6] R. Kulpa and F. Multon, "Fast inverse kinematics and kinetics solver for human-like figures," *IEEE Humanoid Robots*, vol. December, no. 5, pp. 38–43, 2005. 1, 2

[7] J. Zhao and N. Badler, "Inverse kinematics positioning using nonlinear programming for highly articulated figures," *ACM Transactions on Graphics (TOG)*, vol. 13, no. 4, pp. 313–336, 1994. 1, 2

[8] W. R. Cottle, J.-S. Pang, and E. R. Stone, *The Linear Complementarity Problem*. Academic Press, 1992. 1,

7

[9] B. Kenwright, "A beginners guide to dual-quaternions: What they are, how they work, and how to use them for 3d character hierarchies," pp. 1–13, 2012. WSCG 2012 Communication Proceedings, Conference June. 2012. 1, 2, 3

[10] F. S. Grassia, "Practical parameterization of rotations using the exponential map," *J. Graph. Tools*, vol. 3, pp. 29–48, Mar. 1998. 1, 4, 6, 7

[11] M. Girard and A. Maciejewski, "Computational modeling for the computer animation of legged figures," in *ACM SIGGRAPH Computer Graphics*, vol. 19, pp. 263–270, ACM, 1985. 2

[12] B. Rose, S. Rosenthal, and J. Pella, "The process of motion capture: Dealing with the data," in *Computer Animation and Simulation*, vol. 97, pp. 1–14, Citeseer, 1997. 2

[13] K. Yamane and Y. Nakamura, "Natural motion animation through constraining and deconstraining at will," *IEEE Transactions on Visualization and Computer Graphics*, vol. 9, pp. 352–360, July 2003. 2

[14] L. Zhao, "Gesticulation behaviors for virtual humans," *Pacific Graphics '98. Sixth Pacific Conference on Computer Graphics and Applications*, pp. 161–168, 1998. 2

[15] S. R. Buss and J.-S. Kim, "Selectively damped least squares for inverse kinematics," *Journal of Graphics Tools*, vol. 10, pp. 37–49, 2004. 2, 5, 6

[16] R. Fletcher, *Practical methods of optimization, Volume 1*. Wiley, 1987. 2

[17] A. Balestrino, G. D. Maria, and L. Sciavicco, "Robust control of robotic manipulators," *Proc. Of the 9th IFAC World Congress*, vol. 5, pp. 2435–2440, 1984. 2, 5

[18] J. Baillieul, "Kinematic programming alternatives for redundant manipulators," in *Robotics and Automation. Proceedings. 1985 IEEE International Conference on*, vol. 2, pp. 722–728, IEEE, 1985. 2, 5

[19] C. Wampler, "Manipulator inverse kinematic solutions based on vector formulations and damped least-squares methods," *Systems, Man and Cybernetics, IEEE Transactions on*, vol. 16, pp. 93–101, Jan. 1986. 2, 5

[20] Y. Nakamura and H. Hanafusa, "Inverse kinematic solutions with singularity robustness for robot manipulator control," *Journal of Dynamic Systems, Measurement, and Control*, vol. 108, no. 3, pp. 163–171, 1986. 2, 5

[21] J. Lander, "Making kine more flexible," *Game Developer Magazine*, no. November, 1998. 2

[22] L. Wang, "A combined optimization method for solving the inverse kinematics problems of mechanical manipulators," *Robotics and Automation, IEEE*, vol. 1, no. 4, 1991. 2

[23] R. Boulic, J. Varona, L. Unzueta, M. Peinado, A. Suescun, and F. Perales, "Evaluation of on-line analytic and numeric inverse kinematics approaches driven by partial vision input," *Virtual Reality*, vol. 10, pp. 48–61, Apr. 2006. 2

[24] N. Courty and E. Arnaud, "Inverse kinematics using sequential monte carlo methods," *Articulated Motion and Deformable Objects*, pp. 1–10, 2008. 2

[25] C. Hecker, B. Raabe, R. W. Enslow, J. DeWeese, J. Maynard, and K. van Prooijen, "Real-time motion retargeting to highly varied user-created morphologies," *ACM Transactions on Graphics*, vol. 27, p. 1, Aug. 2008. 2

[26] K. Grochow, S. Martin, A. Hertzmann, and Z. Popović, "Style-based inverse kinematics," in *ACM Transactions on Graphics (TOG)*, vol. 23, pp. 522–531, ACM, 2004. 2

[27] R. Sumner, M. Zwicker, C. Gotsman, and J. Popović, "Mesh-based inverse kinematics," in *ACM Transactions on Graphics (TOG)*, vol. 24, pp. 488–495, ACM, 2005. 2

[28] K. Der, R. Sumner, and J. Popović, "Inverse kinematics for reduced deformable models," in *ACM Transactions on Graphics (TOG)*, vol. 25, pp. 1174–1179, ACM, 2006. 2

[29] J. Brown, J. Latombe, and K. Montgomery, "Real-time knot-tying simulation," *The Visual Computer*, vol. 20, no. 2, pp. 165–179, 2004. 2

[30] A. Aristidou and J. Lasenby, "FABRIK: A fast, iterative solver for the Inverse Kinematics problem," *Graphical Models*, vol. 73, pp. 243–260, Sept. 2011. 2

[31] R. Mukundan, "A robust inverse kinematics algorithm for animating a joint chain," *International Journal of Computer Applications in Technology*, vol. 34, no. 4, p. 303, 2009. 2

[32] R. Muller-Cajar and R. Mukundan, "Triangualation-a new algorithm for inverse kinematics," *Proc. of the Image and Vision Computing New Zealand*, pp. 181–186, 2007. 2

[33] W. Tang, M. Cavazza, and D. Mountain, "A constrained inverse kinematics technique for real-time motion capture animation," *The Visual Computer*, vol. 15, pp. 413–425, Nov. 1999. 2

[34] L. Verlet, "Computer experiments on classical fluids. I. Thermodynamical properties of Lennard-Jones molecules," *Physical Review*, vol. 159, no. 1, pp. 98–103, 1967. 2

[35] G. Arechavaleta, E. Lopez-Damian, and J. Morales, "On the use of iterative lcp solvers for dry frictional contacts in grasping," in *Advanced Robotics, 2009. ICAR 2009. International Conference on*, pp. 1–6, June. 2

[36] H.-L. Pham, V. Perdereau, B. V. Adorno, and P. Fraisse, "Position and orientation control of robot manipulators using dual quaternion feedback," in *IROS*, pp. 658–663, 2010. 3

[37] W. R. Hamilton, "Elements of quaternions," *Reprinted by Chelsea Pub, New York in 1969*, 1860. 3

[38] Clifford, "Preliminary sketch of biquaternions," *In Oxford Journals, Proceedings London Mathematical Society, 1-4,*, pp. 381–395, 1873. 4

[39] F. Jourdan, P. Alart, and M. Jean, "A Gauss-Seidel like algorithm to solve frictional contact problems," *Computer Methods in Applied Mechanics and Engineering*, vol. 155, pp. 31–47, Mar. 1998. 6

[40] T. Liu and M. Wang, "Computation of three-dimensional rigid-body dynamics with multiple unilateral contacts using time-stepping and gauss-seidel methods," *Automation Science and Engineering, IEEE Transactions on*, vol. 2, no. 1, pp. 19–31, 2005. 6

[41] E. Catto, "Iterative dynamics with temporal coherence," in *Game Developer Conference*, pp. 1–24, 2005. 6

[42] H. G. Gene and F. V. L. Charles, *Matrix Computations*. The Johns Hopkins University Press, 3rd editio ed., 1996. 6

[43] M. Kallmann, "Analytical inverse kinematics with body posture control," *Computer Animation and Virtual Worlds*, vol. 19, pp. 71–91, May 2008. 7

[44] H. Courtecuisse and J. Allard, "Parallel Dense Gauss-Seidel Algorithm on Many-Core Processors," *2009 11th IEEE International Conference on High Performance Computing and Communications*, no. 1, pp. 139–147, 2009. 8

[45] M. Poulsen, "Parallel projected gauss-seidel method," Master's thesis, University of Copenhagen, 2010. 9

[46] M. Bartelink, "Global inverse kinematics solver for linked mechanisms under joint limits and contacts," Master's thesis, Universiteit Utrecht (European Design Centre), 2012. 12

Appendix A. Proof of Twist-and-Swing Decomposition Equation

We show through quaternion algebra the mathematical proof for Equation 32, which can similarly be applied to Equation (33) and Equation (34), and how a 3D unit-quaternion can be decomposed into two parts: the *twist* and *swing* components. We start with a unit-quaternion rotation shown in Equation 35.

$$\mathbf{q} = (q_s, q_x, q_y, q_z) \tag{35}$$

where is the vector component, and is the scalar component. We can calculate a quaternion from an axis-angle using Equation 36.

$$\begin{aligned} q_s &= c_{xyz} = \cos\left(\frac{\theta}{2}\right) \\ q_x &= s_x = v_x \sin\left(\frac{\theta}{2}\right) \\ q_y &= s_y = v_y \sin\left(\frac{\theta}{2}\right) \\ q_z &= s_z = v_z \sin\left(\frac{\theta}{2}\right) \end{aligned} \tag{36}$$

where v is a unit-vector representing the axis of rotation, and is the angle of rotation. Hence, we can say since the twist is only around the x-axis we can deduce that the yz-axis components will be zero and give us Equation 37.

$$\mathbf{q}_{twist} = \mathbf{q}_x = (c_x, s_x, 0, 0) \tag{37}$$

Furthermore, we can also deduce that the swing x-axis component will be zero in the resulting quaternion as shown in Equation 38.

$$\mathbf{q}_{swing} = \mathbf{q}_{yz} = (c_{yz}, 0, s_y, s_z) \tag{38}$$

where c and s represent the scalar cos and sin component of the half angles (i.e., see Equation 36). A unit-quaternion must obey Equation 39.

$$q_s^2 + q_x^2 + q_y^2 + q_z^2 = 1 \tag{39}$$

Hence, from Equation 37 and Equation 38 we can derive Equation 40.

$$\begin{aligned} c_x^2 + s_x^2 &= 1 \\ c_{yz}^2 + s_y^2 + s_z^2 &= 1 \end{aligned} \tag{40}$$

Subsequently, if we multiply the individual twist and swing quaternions together we can reconstruct the original quaternion as shown in Equation 41.

$$\begin{aligned} \mathbf{q}_{xyz} &= \mathbf{q}_{yz}\mathbf{q}_x \\ &= (c_{yz}, 0, s_y, s_z)(c_x, s_x, 0, 0) \\ &= ((c_x c_{yz}), (s_x c_{yz}), (c_x s_y + s_x s_z), (c_x s_z - s_x s_y)) \end{aligned} \tag{41}$$

Hence, from Equation 37 and knowing the vector sum of the two non-zero components from Equation 41 sums up to one, we can derive q_{twist}, as shown in Equation 42.

$$\begin{aligned} \mathbf{q}_{twist} &= q_s^2 + q_x^2 \\ &= (c_x c_{yz})^2 + (s_x c_{yz})^2 \\ &= c_{yz}^2(c_x^2 + s_x^2) \qquad (knowing, \quad \cos^2 + \sin^2 = 1) \\ &= c_{yz}^2 \end{aligned} \tag{42}$$

Therefore, we have Equation 43.

$$c_{yz} = \sqrt{q_s^2 + q_x^2} \tag{43}$$

We can multiply Equation 41 by the inverse of Equation 43 to remove the quaternion swing component and leave the quaternion twist part (shown in Equation 44).

$$\begin{aligned} \mathbf{q}_{twist} &= \mathbf{q}_x \\ &= (c_x, s_x, 0, 0) \\ &= ((c_x c_{yz}), (s_x c_{yz}), 0, 0)\frac{1}{c_{yz}} \\ &= (q_s, q_x, 0, 0)\frac{1}{\sqrt{q_s^2 + q_x^2}} \end{aligned} \tag{44}$$

We extract the swing component by multiply the quaternion by the inverted (conjugated) twist quaternion (shown in Equation 45).

$$\begin{aligned} \mathbf{q}_{swing} &= \mathbf{q}_{xyz}\mathbf{q}_{twist}^* \\ &= (q_s, q_x, q_y, q_z)(q_s, -q_x, 0, 0)\frac{1}{\sqrt{q_s^2 + q_x^2}} \\ &= (c_{yz}, 0, s_y, s_z) \\ &= ((q_s^2 + q_x^2), 0, (q_s q_y - q_x q_z), (q_s q_z + q_x q_y))\frac{1}{\sqrt{q_s^2 + q_x^2}} \end{aligned} \tag{45}$$

Whereby, Equation 44 and Equation 45 sums-up our algebraic proof. Similarly the twist-and-swing can be proved for the y-, and z-axis (as shown in Equation (33) and Equation (34)).

Appendix B. Calculating the Jacobian

The joint-space and Cartesian space are the two state space variables for the kinematic system (shown in Figure 1). The Jacobian matrix relates the changes in joint angles θ with change in position or orientation $\mathbf{X}$ of some point on the connected hierarchy of links (i.e., Cartesian space) and is defined as:

$$J = \frac{\partial \mathbf{X}}{\partial \theta} \tag{46}$$

A. Finite-Difference Method

The finite-difference method is an approximation technique given by Equation (47). The error is proportional to the δ step and is limited by numerical accuracy (e.g., a 32-bit floating point) and the computational speed of the system. The method is idea for situations where it is difficult or impossible to find an analytical solution for the kinematic system due to its complexity and size. However, the method is a good solution for estimating an approximate Jacobian solution.

$$\frac{dy}{dx} \approx \frac{y(x+\delta) - y(x)}{\delta} \tag{47}$$

The finite-difference implementation for calculating an approximate Jacobian is given in Algorithm 2.

Algorithm 2 Finite-Different Method for Approximating the Jacobian

```
p = f(q)
for n = 0 to n − 1 do
    p_δ = f(q + e_n δ)
    J_n = (p_δ − p)/δ
end for
return J
```

B. Analytical Formulation of the Jacobian using Dual-Quaternions and Quaternion Exponentials

As step-by-step derivation of the Jacobian Dual-quaternion to Quaternion Exponential Mapping from the work by Bartelink [46] is presented below in Figure 8.

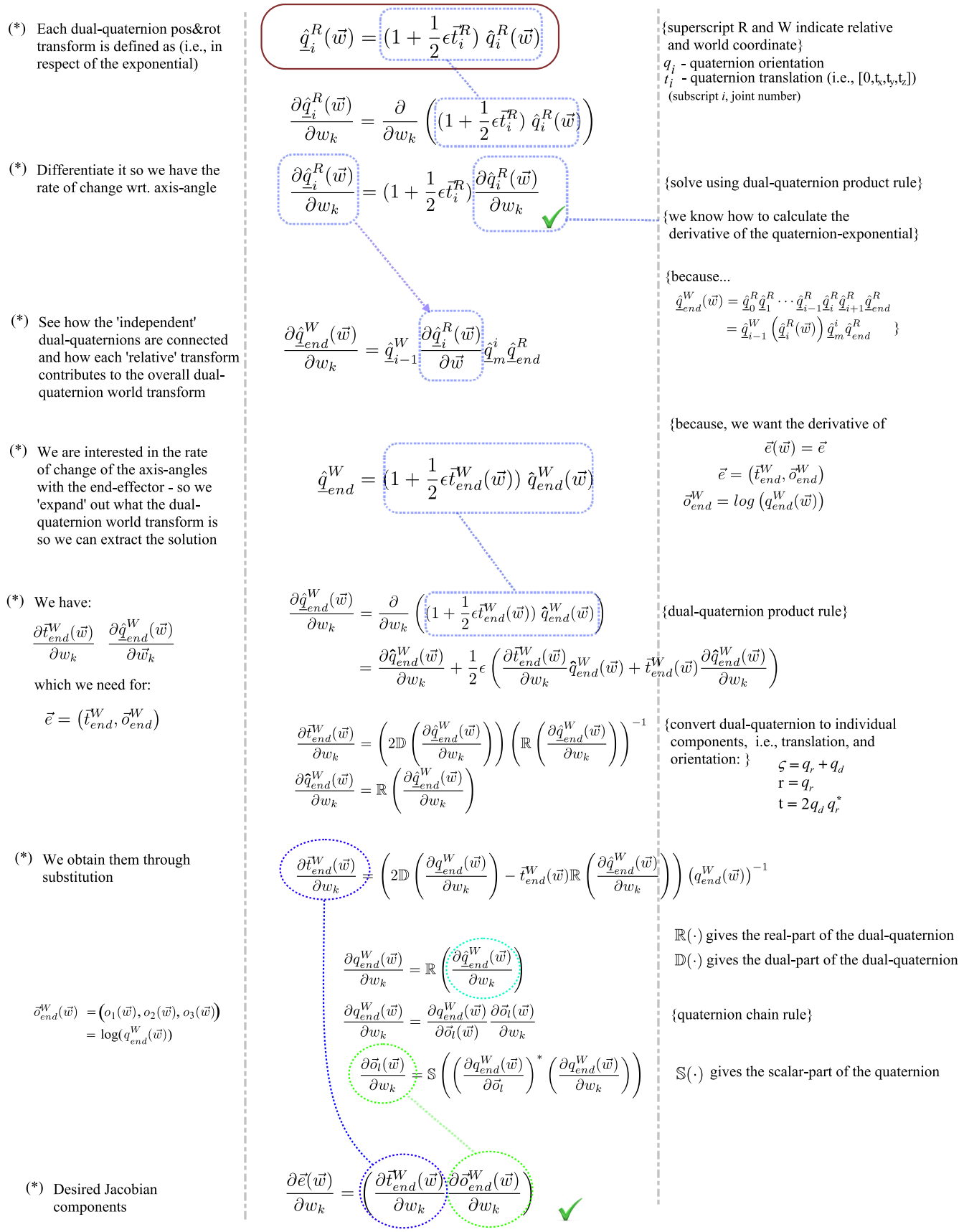

Figure 8. Step-by-Step Formulation of Dual-Quaternion and Quaternion Exponential Jacobian.

Dynamics and Control of Modular and Self-Reconfigurable Robotic Systems

Eugen Meister, Alexander Gutenkunst, and Paul Levi
Institute of Parallel and Distributed Systems
University of Stuttgart, Germany
Email: {Eugen.Meister, Alexander.Gutenkunst, Paul.Levi}@ipvs.uni-stuttgart.de

***Abstract*—In this paper, we introduce a framework for automatic generation of dynamic equations for modular self-reconfigurable robots and investigate a few adaptive control strategies. This framework enables to analyse the kinematics, dynamics and control for both, serial and branched multi-body robot topologies with different dyad structures. The equations for kinematics and dynamics are automatically generated using geometrical formulation methods and recursive Newton-Euler method. Different benchmarks examples are used to evaluate serial and branched robot configurations. As control strategies, computed torque method linearisation method together with Extended Kalman Filter estimator are used. A graphical tool has been developed, that enables easy to use interface and functionalities such as graphically selecting of robot topologies, visual feedback of trajectories and parameters editing.**

***Keywords*—multi-body kinematics and dynamics, self-adaptive systems, automatic model generator, adaptive control.**

I. INTRODUCTION

Modular robotics has its origin in the late eighties with the robotic platforms such as CEBOT developed by Fukuda. Most of the existing modular robotic platforms can only be assembled into different configurations manually, however, a few novel platform designes are able to locomote and therefore to assemble into various configurations autonomously. The framework introduced in this paper is primarily developped to be applied on two modular robots Scout and Backbone [1], which have been developped in projects Symbrion [2] and Replicator [3], but can also be used for diverse other modular systems. The state of the art of modular robot system can be reviewed for example in [4] or in [5]. Autonomy is one of the key challanges for such systems and opens a new spectrum of possible application scenarios especially in dangerous and hazardous environments [6], where robots are able to operate without human intervention.

Modular robotic systems are advantageous in comparison to specialised robots because they can help to reduce the developmental and production costs and can also easily be adapted to different situations and applications. However, the complexity for modelling and control also grows rapidly with each additional degree of freedom (DOF). The dynamics of such systems differ from those systems, which are operating in a fixed environment and without the capability to reconfigure and move. Consequently, new methods are required, which can reduce the modelling complexity of kinematics and dynamics as well as for control design.

In classical mechanics, dynamical systems are usually described by setting up the equations of motion. The most common methods in the robotics are Newton-Euler [7], Lagrange [8], and Hamilton [9] formulations, all ending up with equivalent sets of equations. Different formulations may better suit for analysis, teaching purposes or efficient computation on robot.

Lagrange's equations, for example, rely on energy properties of mechanical systems considering the multi-body system as a whole. This method is often used for study of dynamics properties and analysis in control design.

More applicable on real robots are the Newton-Euler formulation of dynamics. In this method, the dynamic equations are written separately for each body. This formation consists of two parts describing linear (Newton) and angular (Euler) motion [7].

In case of modular reconfigurable multi-body systems, obtaining of equations of motions can be a challenging and time consuming task. In this paper, we use a method using geometric formulation of motion equation, which was originally introduced by Park and Bobrow [10]. This method is based on recursive formulation of robot dynamics using recursive Newton-Euler combined with mathematical calculus of Lie groups and Lie algebras [11]. The description of motion is based on **twist** and **wrenches** summarizing angular and linear velocities as well as applied forces and moments in six-dimensional vectors [12]. This theory is also known as a Screw Theory [13] and was first published by Sir Robert Stawell Ball in the year 1900.

In the framework presented in this paper, the Newton's second law ($F = ma$) and Euler's equations are applied in two recursions: the forward (outward) and the backward (inward) recursion. Therefore, this approach is also called as a two-step approach. In the forward recursion, the velocities and accelerations of each link are iteratively propagated from a chosen base module to the end-links of multi-body system. During the backward recursion the forces and moments are propagated vice versa from the end-link to the base forming the equations of motions step-by-step. Recursive derivation of the equations makes it applicable to different types of robot geometries and moreover allows automatizing the process. There exist several publications generalising this method for variety of applications [14][15][16]. Most of efficient results use Newton-Euler algorithms, for example Luh, Walker, and Paul [17] expressed the equations of motion in local link

reference frames and by doing this reduced the complexity from $O(n^3)$ to $O(n)$. This approach was lately improved by Walker and Orin [18] providing more efficient recursive algorithm. Featherstone [19] proposed the recursive Newton-Euler equations in terms of spatial notation by combining the linear and angular velocities and wrenches into six dimensional vectors (Plücker notation). His 'Articulated Body Inertia' (ABI) approach becomes widely accepted in current research and is also of complexity $O(n)$.

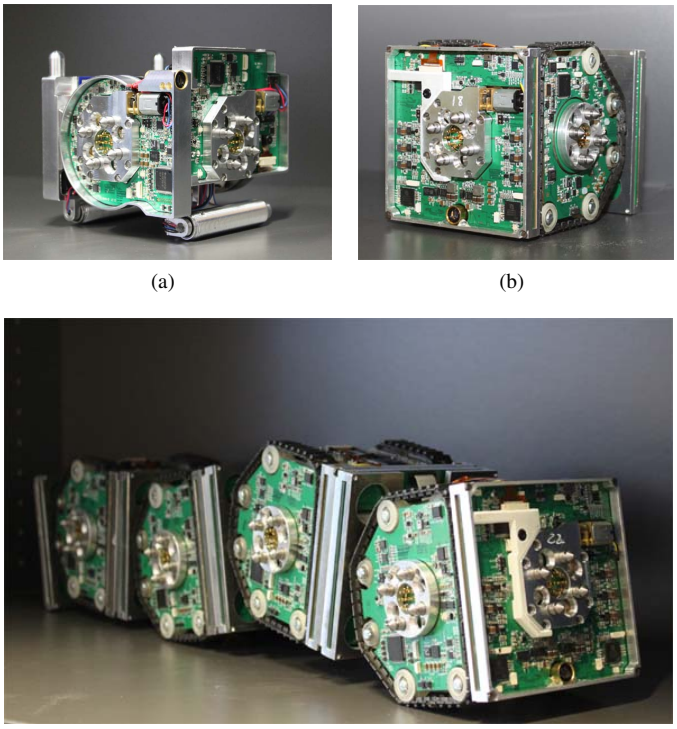

(a) (b) (c)

Figure 1: Modular robots developed in projects Symbrion and Replicator [20]. (a) Backbone, (b) Scout, (c) Robots docked.

In the projects Symbrion and Replicator two autonomous modular self-reconfigurable robots have been developped, which are capable of building multi-robot organisms (Figure 1(c)) by aggregating or disaggregating into various different configurations [6]. In this paper, we orientate our approach on the method proposed by Chen and Yang [21], which allows generating the motion equations in closed form based on Assembly Incidence Matrix (AIM) representation for serial as well as for tree-structured modular robot assemblies. The approach has been adapted to modular robots Backbone and Scout, because the geometry of modules differs from those proposed by Chen and Yang. Autonomous deriving of the motion equations enables studying model based control strategies for modular and self-reconfigurable multi-robot asseblies. In this paper, the second focus is set to investigate the robustness and scalability of classical control strategies for non-linear systems. There are different possibilities how to deal with non-linearities in complex systems either using standard linearisation approach such as Jacobi linearisation or try to compenstate the non-linear terms through feedback linearisation techniques. In this paper, we use the second method, additionally combining it with Extended Kalman Filter (EKF), which allows to simulate the behaviour of real robots with limited sensor capabilities.

The paper is organized in the following way. In Section II, we give basic theoretical background about geometrical formulations for rigid body transformations. In Section III, we describe how the robot kinematics can be formulated for modular robots. Section IV describes representation techniques for self-reconfigurable robot assemblies. Section V contains the recursive approach for calculation of dynamics equations. In order to evaluate the approach a graphical user interface called MODUROB is built and is explained in Section VI. Section VII describes the evaluation of a branched robot organism. Section VIII contains the control strategies for self-reconfigurable robotic systems and present the results based on computed torque method and Extended Kalman Filter. Finally, Sections IX concludes the work and gives a short outlook.

II. Theoretical Background

For kinematics analysis two Lie groups play an important role, the Special Euclidean Group $SE(3)$ and the Special Orthogonal Group $SO(3)$. $SE(3)$ group of rigid body motions consists of matrices of the form

$$\begin{bmatrix} R & p \\ 0 & 1 \end{bmatrix}, \tag{1}$$

where $R \in SO(3)$ is the group of 3×3 rotation matrices and $p \in \mathbb{R}^{3\times 1}$ is a vector.

Lie algebra is also an important concept associated with the Lie groups. Lie algebra of $SE(3)$, denoted as $se(3)$, is a tangent space at the identity element of G. It can be shown that the Lie algebra of SE(3) consists of matrices of the form

$$\begin{bmatrix} \hat{\omega} & v \\ 0 & 0 \end{bmatrix} \in \mathbb{R}^{4\times 4}, \tag{2}$$

where

$$\hat{\omega} = \begin{bmatrix} 0 & -\omega_z & \omega_y \\ \omega_z & 0 & -\omega_x \\ -\omega_y & \omega_x & 0 \end{bmatrix}. \tag{3}$$

Lie algebra is defined together with the bilinear map called Lie bracket, which satisfy following conditions:

- Skew-symmetry: $[a, b] = -[b, a]$.
- Jacobi identity: $[a, [b, c]] + [c, [a, b]] + [b, [c, a]] = 0$

If elements are square matrices, the Lie bracket is a matrix commutator $[A, B] = AB - BA$.

The connection between Lie Group $SE(3)$ and Lie algebra $se(3)$ is the exponential mapping [22], which maps $se(3)$ onto $SE(3)$. Exponential mapping allows an elegant way to formulate rigid body motions.

The exponential mapping $e^{\hat{s}q}$ can be interpreted as an operator that transforms a rigid body from their initial pose

to new pose combining rotations and translations at the same time [15]:

$$g_{ab}(q) = e^{\hat{s}q} g_{ab}(0), \tag{4}$$

where $g_{ab}(0) \in SE(3)$ is an initial pose and $g_{ab}(q)$ is the final pose. A twist associated with a screw motion is formulated as

$$s_i = \begin{bmatrix} -\omega_i \times p_i \\ \omega_i \end{bmatrix} = \begin{bmatrix} v_i \\ \omega_i \end{bmatrix}, \tag{5}$$

where $\omega \in \mathbb{R}^{3\times1}$ is a unit vector denoting the direction of the twist axis, $v_i \in \mathbb{R}^{3\times1}$ is a unit vector facing in the direction of translation and $q_i \in \mathbb{R}^{3\times1}$ is an arbitrary point on the axis. Revolute joints perform only pure rotations about an axis. Therefore the twist has the form:

$$s_i = \begin{bmatrix} 0 \\ \omega_i \end{bmatrix}. \tag{6}$$

Analogous, the pure translation is much simpler,

$$s_i = \begin{bmatrix} v_i \\ 0 \end{bmatrix}. \tag{7}$$

Linear mapping between an element of a Lie group and its Lie algebra can be performed by the adjoint representation. When X is given by $X = (R, p) \in SE(3)$, then the adjoint map $Ad_X : se(3) \mapsto se(3)$ acting on $y \in se(3)$ is defined by $Ad_X(y) = XyX^{-1}$. In [15] is also shown that $Ad_X(y)$ admits the 6×6 matrix representation

$$Ad_X(y) = \begin{bmatrix} R & \hat{p}R \\ 0 & R \end{bmatrix} \begin{bmatrix} v \\ \omega \end{bmatrix}, \tag{8}$$

where $\hat{p}$ is the skew-symmetric matrix representation of $p \in \mathbb{R}^3$. Linear mapping between an element of Lie algebra and its Lie algebra can be performed via the Lie bracket

$$ad_x(y) = [x, y]. \tag{9}$$

Given $x = (v_1, \omega_1) \in se(3)$, and $y = (v_2, \omega_2) \in se(3)$, the adjoint map admits corresponding 6×6 matrix representation

$$ad_x(y) = \begin{bmatrix} \hat{\omega}_1 & \hat{v}_1 \\ 0_{3\times3} & \hat{\omega}_1 \end{bmatrix} \begin{bmatrix} v_2 \\ \omega_2 \end{bmatrix}. \tag{10}$$

Similar to twists that contain angular and linear velocities in one vector, wrenches or general forces are described in a similar way. Wrenches are vector pairs containing forces and moments acting on a rigid body.

$$F = \begin{pmatrix} f \\ \tau \end{pmatrix}, \tag{11}$$

where $f \in \mathbb{R}^3$ is a linear force component and $\tau \in \mathbb{R}^3$ represents a rotational component. In contrast to general velocities as elements of $se(3)$, wrenches are acting on $se(3)^*$, the dual space and therefore behaves as covectors. For this reason wrenches transform differently under a change of coordinates by using so called adjoint transformation,

$$F_a = Ad^T_{g_{ba}} F_b, \tag{12}$$

where forces acting on the body coordinate frame B are written with respect to coordinate frame A. In spatial representation, this is equivalent as if the coordinate frame A were attached to the object.

III. Robot Kinematics

In modular reconfigurable systems the robot kinematics varies according to modules that are connected to each other. In homogeneous systems with the same physical parameters the kinematics depends only on the orientations of modules relative to each other. Such modular design is advantageous for autonomous systems. Using heterogeneous modules the modelling complexity grows with the number of different modules that are used. Therefore, in most cases we assume identical or similar structure of the modules with similar physical properties. Both robots have been designed with similar geometry, same docking units and differ mostly in several insignificant properties such as number of sensors, different sensors or actuators. Nevertheless, even if the differences are not crucial, we speak about heterogeneous modules because of the additional Degree of Freedom (DOF) in Scout robot that is able to rotate the docking element even if only in limited way. Table I summarizes the mechanical properties of Backbone and Scout modular robots.

TABLE I: Major differences between mechanical properties of Scout/Backbone robots.

	Cubic Modules (I. M. Chen)	Backbone / Scout
Module types	homogeneous	heterogeneous
Joint types	revolute, prismatic	revolute
# ports	6	4
DOFs	rot.: $\pm180^\circ$	Backbone: bend.:$\pm90^\circ$; Scout: bend.:$\pm90^\circ$, rot.: $\pm180^\circ$

Using only revolute joints without any prismatic joints simplify additionally the autonomous and recursive model generator for kinematics and finally for the dynamics model.

A. Dyad Kinematics

Dyad dependencies are common in recursive formulations because the calculation proceeds from one module to the next comprising only two modules. The calculation is done from the base module to all pendant links. In the approach proposed by Chen and Yang [21], a dyad is defined as two adjacent modules (v_i,v_j) connected by a joint e_j (Figure 2(a)). A link assembly is defined by taking one of those modules (link) together with one joint. The relative position and orientation of one frame attached to one module with respect to next frame in the second module can be described under joint displacement by a homogeneous 4×4 matrix $H_{i,j}(q) \in SE(3)$:

$$H_{i,j}(q_j) = H_{i,j}(0) e^{\hat{s}_j q_j}, \tag{13}$$

where $\hat{s}_j \in se(3)$ is the twist of joint e_j and q_j is the angle of rotation. The relative position and orientation between the modules can be recognized by the robot through different kind of on-board sensors such as accelerometers, compass or by vision system. In project Symbrion and Replicator the geometry of the Backbone (Figure 1(a)) and Scout (Figure 1(b)) robots differ from modules proposed by Chen and Yang. Backbone and Scout modules consist of two moving parts and one main hinge motor placed inside of each module and for this reason already implies a complete dyad as defined by Chen and Yang in each robot. In order to adapt the recursive kinematics approach to Backbone and Scout robot we need to extend the system boundaries of a dyad (Figure 2(b)). Since the most weight is concentrated in the middle of the modules where the main motors are placed, the attached coordinate frames for each module coincide with the centre of mass. Because of two robots and hence two revolute joints in a dyad only one joint is involved into calculation in each recursive step.

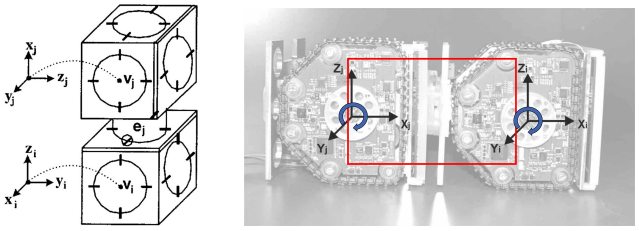

Figure 2: (a) A dyad defined by Chen and Yang [21], (b) Dyad for two Scout robots.

The orientation of axes of rotations depends on how robots are docked to each other. The relative pose can be described by 4×4 homogeneous matrix like in Equation (13).

B. Forward Kinematics

Forward kinematics for modular reconfigurable robotic systems determines the poses of the end-links providing joint angles as an input. In this section, we introduce the modelling technique for forward kinematics based on local frame representation of the Product-of-Exponential (POE) formula originally proposed in [23] or in [15]. This technique can be easily applied to tree-structured robots with many branches (e.g., multi-legged robots). Based on recursive dyad kinematics, the calculation can be done simultaneously for all branches. In this paper, all robots are considered to be cube shaped robots based on Backbone or Scout geometries consisting of one major DOF. In general case, the forward kinematics for serial connected robots can be obtained for an arbitrary number of links by simply multiplying the exponential maps as follows:

$$g_{st}(q) = e^{\hat{s}_1 q_1} e^{\hat{s}_2 q_2} e^{\hat{s}_3 q_3} \dots e^{\hat{s}_n q_n} g_{st}(0), \qquad (14)$$

where $\hat{s}_1$ to $\hat{s}_n$ have to be numbered sequentially starting with the chosen base module (Figure 3).

For a tree or branch structured robot configurations, the forward kinematics can be obtained in parallel way starting

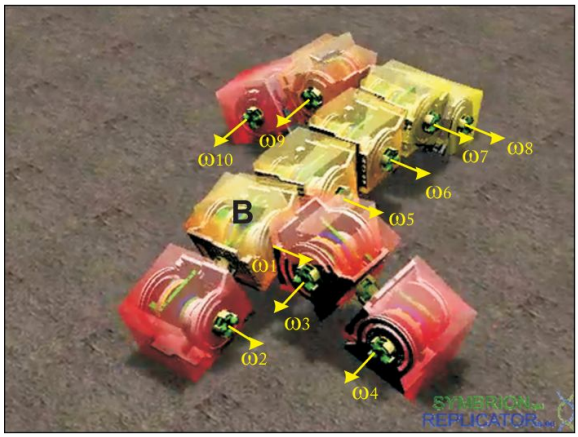

Figure 3: Multi-robot organism [24].

the calculation from a chosen base module to each pendant end-link in all branches. One possibility how the connecting order can be obtained is to use the AIM proposed by Chen and Yang [21]. For branched type of robots, two traversing algorithms are common to find the shortest paths: the Breadth-first search (BFS), and the Depth-first search (DFS) algorithms. The forward kinematic transformations for the branched robot configuration starting from base to each of the pendant links a_n of path k with m branches can be formulated as follows:

$$H(q_1, \dots, q_n) = \begin{bmatrix} H_1 \\ H_2 \\ \vdots \\ H_k \\ \vdots \\ H_m \end{bmatrix} = \begin{bmatrix} \dots \\ \dots \\ \vdots \\ \prod_{i-1}^{n} (H_{a_{i-1}a_i}(0) e^{\hat{s}_{a_i} q_{a_i}}) \\ \vdots \\ \dots \end{bmatrix}, \qquad (15)$$

where $H(q_1, \dots, q_n)$ represent all poses of all pendant end-links by using homogeneous 4×4 matrix representation.

IV. Robot Assembly Representations

Matrix notation is a powerful method to represent modular robots kinematic dependencies. The most common matrices used in robotics are the Adjacency and the Incidence matrix. Both matrices represent the connections between the neighbouring nodes. In [21], Chen proposes a method based on AIM that allows to represent the whole robot assembly consisting from links and joints additionally carrying the information about the type of robot and about used joints. A dynamic model for modular robot assembly is created autonomously from the AIM. This method was developed for a homogeneous kind of robots varying only in size with different joint possibilities including revolute or prismatic joints. Scout and Backbone robots contain only revolute joints however the number is not limited to one DOF. Therefore, the approach proposed in [21] cannot be directly used for this kind of modules and need to be adapted.

A. Adapted Assembly Incidence Matrix

The Backbone and the Scout robots are both cubic shaped robots, however provide only four sides that are equipped with docking units. Therefore, using the notation of gaming dice only ports $2-5$ are able to set a connection. A difference between modular robots proposed in [21] and the Scout/Backbone modules is that joints are not considered as a separate mechanical parts (joint modules), which are required to connect two modules, but rather are placed inside each of the modules. For these reasons each robot builds a full dyad already.

For simplicity, we allow docking only in horizontal plane and we also use the principle of gaming dice for side notations. Robot organisms have to go into initial configuration when additional robots decide to dock. Using this assumption, we distinguish between three major dyad configuration classes: the serial DS, the parallel DP and the orthogonal DO dyad class, where the second letter determines the axes of rotation of module j with respect to module i. A serial coupled dyad (DS) is given when the axes of rotation are in one line. When the rotational axes are parallel than the dyad becomes a member of a parallel class (DP). Finally, when the axes are orthogonal to each other, the robots are classified as the orthogonal to each other connected robot assembly (DO). This information can be easily extracted from the matrix and used for direct computation. Additionally, the symmetry of the platform allows neglecting the sign of the orientation because it does not affect the calculation. Table II summarizes all possible configurations considering that top and bottom side of the robots and hence the sides 1 and 6 of a gaming dice do not contain docking units.

TABLE II: Connections table between Scout and Backbone robots.

Set DS: Dyad: Serial Axes		**Set** DP: Dyad: Parallel Axes		**Set** DO: Dyad: Orthogonal Axes	
1^{st} Mod.	2^{nd} Mod.	1^{st} Mod.	2^{nd} Mod.	1^{st} Mod.	2^{nd} Mod.
2	2	3	3	2	3
2	5	3	4	2	4
5	2	4	3	3	2
5	5	4	4	3	5
				4	2
				4	5
				5	3
				5	4

The autonomous docking procedure is based either on IR sensor communication [25] or also can be fulfilled by using vision system [26][27]. Backbone and the Scout robots have one revolute joint as a major actuator, therefore, the information about the kind of actuators in the last row of the AIM is unnecessary. Instead, we use the last row for the three types of docking orientations for serial, parallel or orthogonal case. The last column in the AIM contains the information about the kind of robot, which is used. We denote the modified AIM as AIM_{SB}, where index 'SB' denotes the first letters of both robots: the Scout and the Backbone robot. In Figure 4, a small example of an organism and the corresponding graph is shown. The AIM_{SB} for this organism is shown in Figure 5.

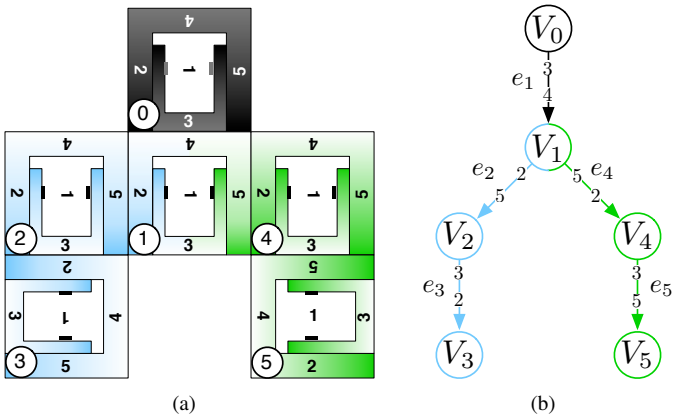

Figure 4: (a) Multi-robot organism example, (b) Directed graph representation.

$$AIM = \begin{array}{c|ccccc|c} & e_1 & e_2 & e_3 & e_4 & e_5 & \text{Links} \\ v_0 & 3 & 0 & 0 & 0 & 0 & S \\ v_1 & 4 & 2 & 0 & 5 & 0 & S \\ v_2 & 0 & 5 & 3 & 0 & 0 & S \\ v_3 & 0 & 0 & 2 & 0 & 0 & S \\ v_4 & 0 & 0 & 0 & 2 & 3 & S \\ v_5 & 0 & 0 & 0 & 0 & 5 & S \\ \hline \text{Joints} & DP & DS & DO & DS & DO & \end{array}$$

Figure 5: AIM of robot assembly from Figure 4(a).

B. Direct/Indirect Recursive Transformations

Structuring the kinematics dependencies into an AIM_{SB}, we are able to apply the transformations T_{ij} between the modules directly once the AIM is determined. By reusing the already calculated dependencies that are stored into lists it is fast and efficient to calculate the kinematics for big robot organisms. We use two lists: one list containing transformation results between consecutive joints, we call it a Direct-Transformation-List (DTL) and another list called Indirect-Transformation-List (IDTL) for non-consecutive transformations between joints however still in the same kinematics path.

In DTL as shown in Table III, each line represents one direct transformation. The first two columns indicate the connected modules and the last two columns hold the information, which sides are connected. IDTL contains the indirect transformations, which are calculated by two successive transformations ($T_{ij} = T_{ix} \cdot T_{xj}$). The first two columns denote the desired transformation. Next four columns hold two multiplied transformations that are stored in DTL or in IDTL. Both tables refer to the example shown in Figure 4.

A short example demonstrates the first traversing calcula-

TABLE III: Direct and indirect transformation list referred of example in Figure 4(a).

DTL			
T_{ij}		Sides	
i	j	from	to
0	1	3	4
1	2	2	5
2	3	3	2
1	4	5	2
4	5	3	5

IDTL					
T_{ij}		$=$	T_{ix}	$\cdot$	T_{xj}
i	j	i	x	x	j
0	2	0	1	1	2
0	3	0	2	2	3
0	4	0	1	1	4
0	5	0	4	4	5

tions using both lists:

$$\begin{aligned} T_{01} &= T_{01}(0)e^{\hat{s}_1 q_1} && \text{direct} \\ T_{12} &= T_{12}(0)e^{\hat{s}_2 q_2} && \text{direct} \\ T_{02} &= T_{01} \cdot T_{12} && \text{indirect} \\ T_{23} &= T_{23}(0)e^{\hat{s}_3 q_3} && \text{direct} \\ T_{03} &= T_{02} \cdot T_{23} && \text{indirect} \\ T_{14} &= T_{14}(0)e^{\hat{s}_4 q_4} && \text{direct} \\ T_{04} &= T_{01} \cdot T_{14} && \text{indirect} \\ T_{45} &= T_{45}(0)e^{\hat{s}_5 q_5} && \text{direct} \\ T_{05} &= T_{04} \cdot T_{45} && \text{indirect} \end{aligned} \tag{16}$$

This algorithm can be compared with DFS algorithm, providing a flexible way to calculate the order all possible transformations can be calculated during run-time.

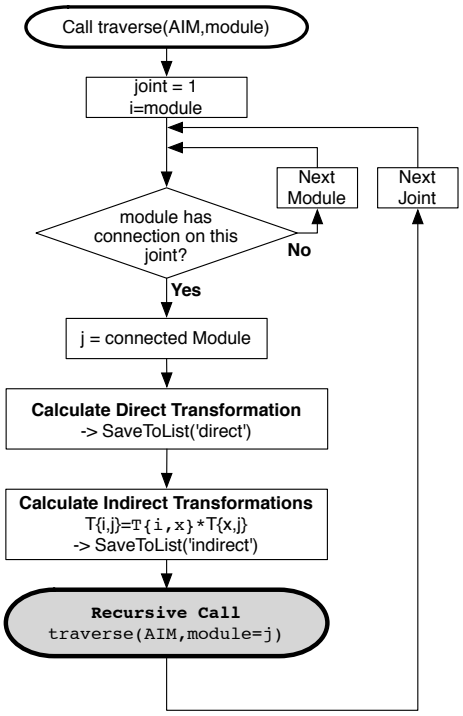

Figure 6: Traversing algorithm.

The flowchart of the algorithm is illustrated in Figure 6.

V. Modular Robot Dynamics

In general, two main branches of robot dynamics problems are mostly considered, namely the forward and the inverse dynamics problems. Forward dynamics play an important role in simulation of multi-body systems, also called as direct dynamics. Forward dynamics problem determines accelerations and external reaction forces of the system giving initial values for positions, velocities and applied internal/external forces, whereas the inverse dynamics problem determines the applied forces required to produce a desired motion. The first problem that appears in modular self-reconfigurable robotics is that the model of the robot assembly cannot be known a priori. Therefore, the robot should be able to generate its own model autonomously without human intervention.

A. Recursive Two-Step Approach

The original idea for recursive formulation and computation of the closed form equation of motion was introduced by Park and Bobrow [10]. The idea was extended by Chen and Yang by introducing the AIM. Starting with the AIM, that contains the information about how robots are assembled, the formulation of equations of motion is done in two steps: first applying forward transformation from base to the end-link, followed by the second recursion backwards from the end-link to the base module. Finally, we get the equation of motion in a closed-form. Before starting the recursion, some assumption and initializations should be done. In the first step, the system has to choose the starting module denoted as the *base* module. Starting from this module, the AIM is filled based on path search algorithms such as BFS or DFS. After the AIM is built and all paths are determined the recursive approach can be started.

- **Initialization:** Given V_0, $\dot{V}_0$, F^e_{n+1}

$$V_b = V_0 = (0 \;\; 0 \;\; 0 \;\; 0 \;\; 0 \;\; 0)^T \tag{17}$$
$$\dot{V}_b = \dot{V}_0 = (0 \;\; 0 \;\; g \;\; 0 \;\; 0 \;\; 0)^T, \tag{18}$$

where V_b and V_0 denote generalized velocities expressed in the starting frame 0 and all other quantities are expressed in link frame i.

- **Forward recursion: for** $i = 1$ **to** n **do**

$$V_i = Ad_{H^{-1}_{i-1,i}}(V_{i-1}) + S_i\dot{q}_i, \tag{19}$$
$$\dot{V}_i = Ad_{H^{-1}_{i-1,i}}(\dot{V}_{i-1}) - ad_{Ad_{H^{-1}_{i-1,i}}(V_{i-1})}(S_i\dot{q}_i) + S_i\ddot{q}_i. \tag{20}$$

- **Backward recursion:** for $i = n$ to 1 do

$$F_i = Ad^*_{H^{-1}_{i-1,i}}(F_{i-1}) - F^e_i + \mathcal{M}_i\dot{V}_i - ad^*_{V_i}(\mathcal{M}_i V_i), \tag{21}$$
$$\tau_i = s_i^T F_i. \tag{22}$$

Here, $\mathcal{M}_i$ is the generalized mass matrix of the form

$$\mathcal{M}_i = \begin{bmatrix} \mathbf{I} & 0 \\ 0 & mI_3 \end{bmatrix}, \tag{23}$$

where $\mathbf{I}$ is 3×3 inertia matrix and I is the identity matrix. The non-diagonal terms are zero because in our case the center

of mass coincides with the origin. F^e_{i+1} are the forces acting on the end-links of chained robots. This values can either be estimated or read from force or tactile sensors such as [28][29], which can be attached to the robots. F_i is the total generalized force traversed from link $i-1$ to i consisting of internal and external wrenches and τ_i is the applied torque by the corresponding actuator.

B. Equations of Motion

By expanding the recursive equations (19)-(22) in body coordinates, it can be shown that the equations for generalized velocities, generalized accelerations and forces can be obtained in matrix form:

$$V = TS\dot{q} \tag{24}$$
$$\dot{V} = T_{H_0}\dot{V}_0 + TS\ddot{q} + Tad_{S\dot{q}}V \tag{25}$$
$$F = T^T F^e + T^T M\dot{V} + T^T ad^*_V MV \tag{26}$$
$$\tau = S^T F \tag{27}$$

where

$$\begin{array}{lcl}
\dot{q} & = & column[\dot{q}_1, \dot{q}_2, \ldots, \dot{q}_n] \in R^{n\times 1} \\
\ddot{q} & = & column[\ddot{q}_1, \ddot{q}_2, \ldots, \ddot{q}_n] \in R^{n\times 1} \\
V & = & column[V_1, V_2, \ldots, V_n] \in R^{6n\times 1} \\
\dot{V} & = & column[\dot{V}_1, \dot{V}_2, \ldots, \dot{V}_n] \in R^{6n\times 1} \\
F & = & column[F_1, F_2, \ldots, F_n] \in R^{6n\times 1} \\
F^e & = & column[F^e_1, F^e_2, \ldots, F^e_n] \in R^{6n\times 1} \\
\tau & = & column[\tau_1, \tau_2, \ldots, \tau_n] \in R^{n\times 1} \\
S & = & diag[S_1, S_2, \ldots, S_n] \in R^{6n\times n} \\
M & = & diag[\mathcal{M}_1, \mathcal{M}_2, \ldots, \mathcal{M}_n] \in R^{6n\times 6n} \\
ad_{S\dot{q}} & = & diag[-ad_{S_1\dot{q}_1}, -ad_{S_2\dot{q}_2}, \ldots, -ad_{S_n\dot{q}_n}] \in R^{6n\times 6n} \\
ad^*_V & = & diag[-ad^*_{V_1}, -ad^*_{V_2}, \ldots, -ad^*_{V_n}] \in R^{6n\times 6n}
\end{array}$$

The n index represents the number of elements containing also virtual joints that are required to move the robot in space [30].

$$T_{H_0} = \begin{bmatrix} Ad_{H^{-1}_{0,1}} \\ Ad_{H^{-1}_{0,2}} \\ \vdots \\ Ad_{H^{-1}_{0,n}} \end{bmatrix} \in R^{6n\times 6} \tag{28}$$

$$T = \begin{bmatrix} I_{6\times 6} & 0_{6\times 6} & 0_{6\times 6} & \cdots & 0_{6\times 6} \\ Ad_{H^{-1}_{1,2}} & I_{6\times 6} & 0_{6\times 6} & \cdots & 0_{6\times 6} \\ Ad_{H^{-1}_{1,3}} & Ad_{H^{-1}_{2,3}} & I_{6\times 6} & \cdots & 0_{6\times 6} \\ \vdots & \vdots & \vdots & \vdots & \vdots \\ Ad_{H^{-1}_{1,n}} & Ad_{H^{-1}_{2,n}} & Ad_{H^{-1}_{3,n}} & \cdots & I_{6\times 6} \end{bmatrix} \in R^{6n\times 6n}, \tag{29}$$

where T is the transmission matrix for the whole robot assembly. The elements $H_{i,j}$ in T_{H_0} and in T can be read out directly from the DTL and IDTL lists.

The closed-form equation of motion of the classical form

$$M(q)\ddot{q} + C(q,\dot{q})\dot{q} + N(q) = \tau \tag{30}$$

is obtained by substituting the equations 24-27, where $M(q)$ is the mass matrix; $C(q,\dot{q})$ describes the Coriolis and centrifugal accelerations and $N(q)$ represents the gravitational forces as well as the external forces.

$$M(q) = S^T T^T MTS \tag{31}$$
$$C(q,\dot{q}) = S^T T^T (MTad_{S\dot{q}} + ad^*_V M)TS \tag{32}$$
$$N(q) = S^T T^T MT_{H_0}\dot{V} + S^T T^T F^e \tag{33}$$

VI. MODUROB - Modular Robotics Software Tool

MODUROB is a tool built in MATLAB® that contains a possibility to build robot topologies by simply clicking on topology matrix grid (Figure 7). Currently, two types of robots are provided: the Backbone (Figure 1(a)) and the Scout robot (Figure 1(b)). For simplification, robots are only allowed to assemble or disassemble in planar configurations on the ground. The automatic model can be built in two ways: analytically or numerically. The symbolic formulation in MATLAB is done by using the symbolic toolbox. For solving of differential equations the user can choose between the numerical integrators that are provided by MATLAB. In order to move the robot in a joint space, different gait generators are provided either using rhythmic generators based on rhythmic functions [30] or gait generators that use chaotic map. We use an approach proposed in [31], that allows to generate periodic gaits that result from synchronization effects of coupled maps. Such approach can help to control complex multi-body structures by mapping the active joints to an individual chaotic driver [32].

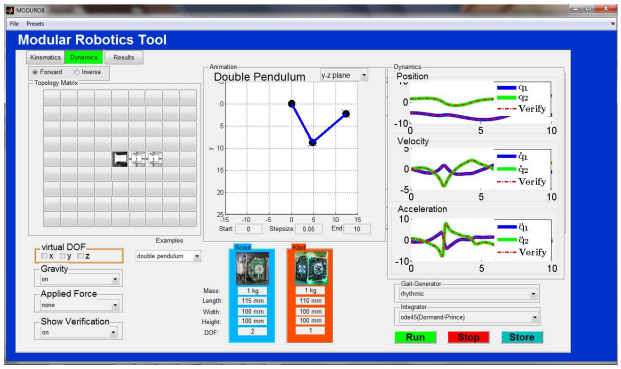

(a)

Figure 7: Benchmark example of Double pendulum.

For evaluation or benchmarking of the framework two examples are implemented based on Lagrangian equations and can be compared with the geometrical approach. One example is a double pendulum example (Figure 7(a)) for example derived in [33] and the second is an extended pendulum that is movable on a shaft like a crane presented in [1].

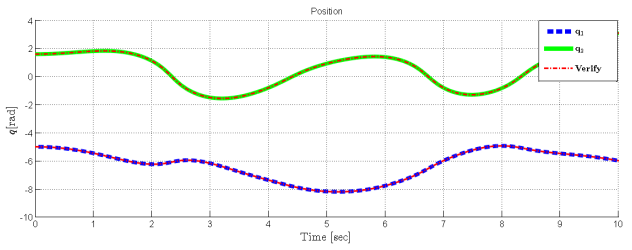

(a)

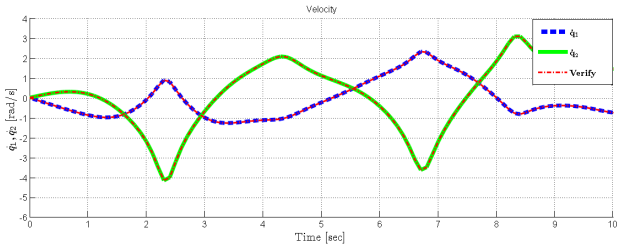

(b)

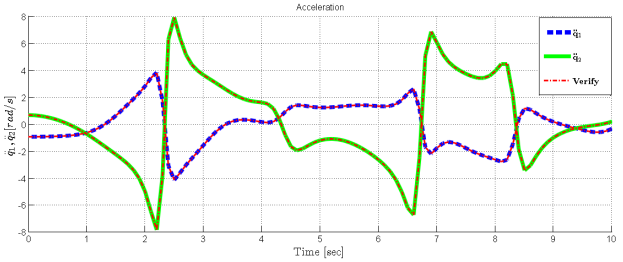

(c)

Figure 8: Verification (dashed line) of geometrical POE approach with Lagrangian method using double pendulum model. (a) Position; (b) Velocity; (c) Accelerations.

The example (Figure 8) shows absolutely identical behaviour between implementation based on Lagrangian equations and with the geometrical approach based on twist and wrenches.

VII. Evaluation of Branched Multi-body Systems

In the previous section, two basic examples, a pendulum and a crane example are used to evaluate the correct functionality of the geometrical approach proposed in this thesis. However, pundulum-like structures are the simplest form of robot assemblies, therefore, another benchmark with branched robot configuration (Figure 9) has been generated to make deeper evaluation of the framework.

While single or double pendulum example code can be easily found and downloaded from many sources, e.g. from [33], the code for more complex structures of multi-body systems are hardly available. For this reason, in order to evaluate other robot configurations, a new branched modular robot has been

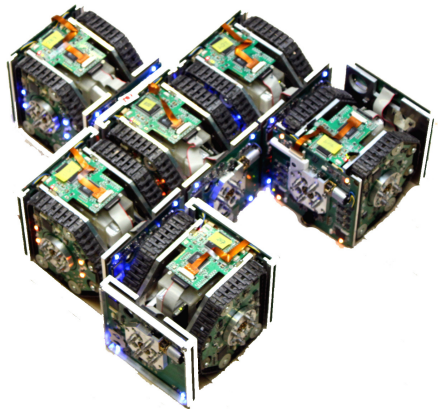

Figure 9: Crab-like multi-robot structure assembled with Scout robots.

modelled within the MATLAB SimMechanics toolbox [34]. This tool allows to simulate physical properties and dynamics of multi-body systems by use of Euler-Lagrangian modelling technique [35].

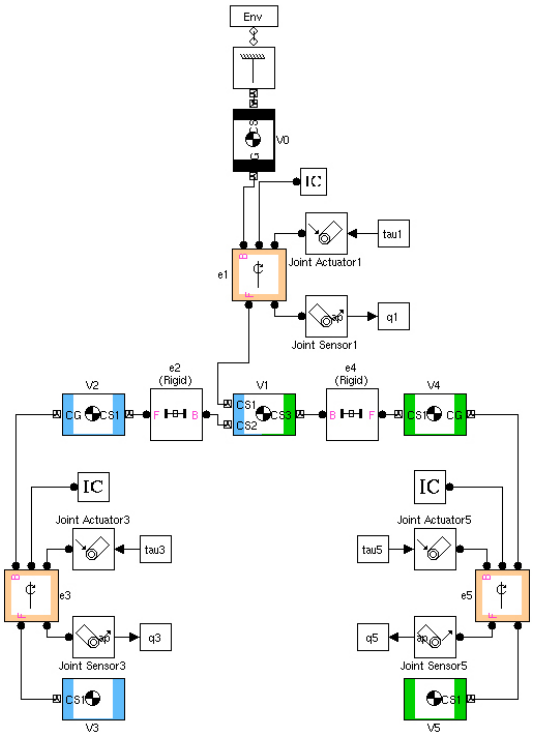

Figure 10: Simulink SimMechanics model of crab-like robot.

Figure 10 present a SimMechanics model of a crab-like robot organism, which is shown in Figure 9. The corresponding AIM and the graph representation of this organism structure can be reviewed in Figures 4-5. This structure has been chosen because it contains all three types of dyad structures (serial,

parallel and orthogonal), which are also listened in Table II. This structure implies also the case, where due to mechanical limitations, robots are not able to move with respect to each other and in this case the state space of dynamic model needs to be reduced. For this reason the framework should detect such cases and adapt the framework accordingly.

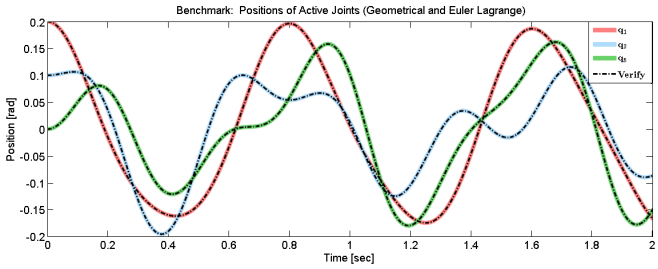

Figure 11: Position, velocity and acceleration of links based on crab-like robot structure.

In order to evaluate the proposed geometrical framework, identical robot structure, which is used in SimMechanics simulation (Figure 10) is also modelled with our model generator. The behavaiour of dynamics of both models can be examined in Figure 11. In this plot, it can be observed that both models produce identical set of results that similar like in the previous section, also proves the correctness of the framework.

VIII. Control of Multi-body Systems

Classical control theory provides a huge spectrum of controller design strategies for linear and non-linear systems including for example methods such as sliding mode control [36], optimal control [37], robust control [38], backstepping control [39] and different adaptive control mechanisms [40][41][42]. In the previous sections, an automatic model generator is presented, that enables to generate the dynamics model of the multi-robot organism based on geometrical formulation of motion equations. The generated model is a non-linear model, and to design a controller for a robot that is able to reconfigure and hence requires a new model representation is a huge challenge. One of the most used methods to deal with non-linear models is to linearise the model at a certain operation point by use of Jacobian linearisation techniques [43]. These methods are most common used in control theory, because it distinctly reduces modelling and computational complexity. During the last decades, the technological progress in microprocessor technologies opens new opportunities to apply methods for nonlinear control design techniques direct on embedded systems. Feedback linearisation also known as exact linearisation is an approach of nonlinear control design, that has attracted lots of research in recent years and is probably the first choice for mechanical systems containing only active joints.

In this section, a non-linear control design for a multi-body reconfigurable robots is presented based on computed torque method and EKF.

A. Inverse Dynamics

Most of robotic systems has a non-linear character. One of the concepts that currently becomes popular is the **feedback linearisation** [44] control strategy. This technique is a generalized concept and a special branch of it in robotics is also known as **inverse dynamics** or **computed torque** [45] control.

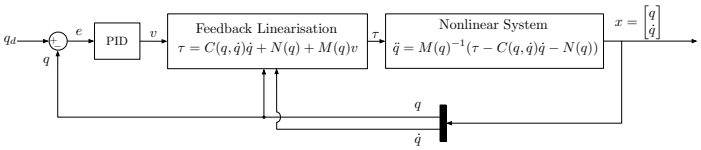

Figure 12: Structure of Computed Torque Method.

The block diagram of this approach is depicted in Figure 12. The inverse dynamics problem can be formulated in a joint space as follows:

$$\tau = M(q)\ddot{q} + C(q,\dot{q})\dot{q} + N(q), \tag{34}$$

which applied to Equation (30) yields to $\ddot{q} = v$. The new control input v needs to be designed and is typically chosen as:

$$v = \ddot{q}_d - \underbrace{K_0(q - q_d)}_{e_q} - \underbrace{K_1(\dot{q} - \dot{q}_d)}_{\dot{e}_q}, \tag{35}$$

where K_0 and K_1 are positive definite matrices. The error dynamics for the closed loop system can be formulated as:

$$\ddot{e}_q + K_1\dot{e} + K_0 e_q = 0, \tag{36}$$

where matrices K_0 and K_1 are the gain matrices. The error dynamics can be achieved to be exponentially stable by the proper choice of K_0 and K_1. In the framework presented in this paper, the torque can be computed for every selected robot configuration. The limitations are not given by the framework itself, but rather by the computation time for very big robot structures. Figure 13 shows step responses of the active joints in a crab-like robot structure from the Figure 9. Due to selected

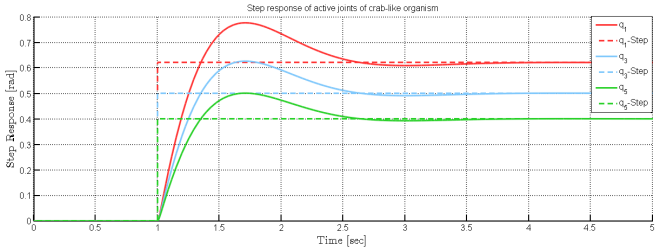

Figure 13: Step response of active joints of simulated crab-like robot configuration with applied computed torque linearisation.

robot configuration and its mechanical restrictions the number of active joints is reduced to three DOFs. As a conclusion we can summarise that with computed torque method and PID control we are able to stabilise the non-linear system in an acceptable short time.

B. States Estimation with EKF

Mutli-robot organisms, which are introduced in this paper are built of modular robot with one rotational degree of freedom. The electronics of the modular robots [46] Backbone or Scout allows to detect the absolute hinge angle of rotation by the use of hall sensors, which are placed inside the hinge motor. However, measuring only the hinge position is not enough to get the full set of states for a nonlinear system model. One of the promising approaches to estimate the missing or noisy states of a dynamical system is the Kalman filter. The EKF [47] is the nonlinear version of the classical Kalman filter. This recursive predictive filter runs in two steps: the prediction and the correction step. In this section, we give a short introduction of theoretical background of EKF and present the achieved results.

The structure of the model containing computed torque linearisation from previous section and the EKF are illustrated in the Figure 14.

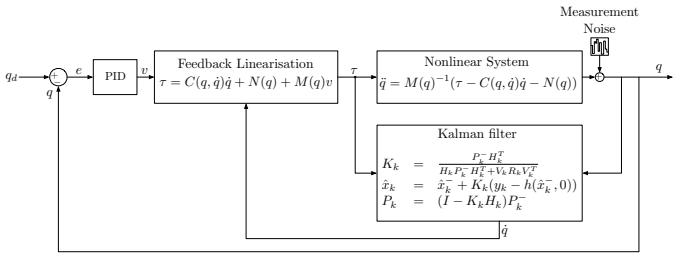

Figure 14: Schematic of system structure with computed torque, EKF and PID control.

Consider the nonlinear discrete-time model written in the standard state-space representation:

$$\begin{aligned} x_k &= f(x_{k-1}, w_{k-1}) \in \mathbb{R}^n, \\ y_k &= h(x_k, v_k), \end{aligned} \tag{37}$$

where k describes the time step; x_k is a vector of actual states; y_k is the actual output vector; w_k and v_k the system and the output noise.

The actual state and measurement vector can be approximated as

$$\begin{aligned} \hat{x}_k^- &= f(\hat{x}_{k-1}, 0), \\ \hat{y}_k &= h(\hat{k}_k^-, 0). \end{aligned} \tag{38}$$

The linear approximation of the Equation (37) can be formulated as:

$$\begin{aligned} x_k &\approx \hat{x}_k^- + A(x_{k-1} - \hat{x}_{k-1}^-) + W w_{k-1}, \\ y_k &\approx y\hat{x}_k^- + H(x_k - \hat{x}_k^-) + V v_k, \end{aligned} \tag{39}$$

where A_k is the Jacobian matrix defined as

$$A_{ij} = \frac{\partial f_i}{\partial x_j}(\hat{x}_{k-1}, 0). \tag{40}$$

W_{ij} is the Jacobian matrix of partial derivatives of f with respect to w:

$$W_{ij} = \frac{\partial f_i}{\partial w_j}(\hat{x}_{k-1}, 0). \tag{41}$$

H_{ij} is the Jacobian matrix of partial derivatives of h with respect to x:

$$H_{ij} = \frac{\partial h_i}{\partial x_j}(\hat{x}_k, 0). \tag{42}$$

V_{ij} is the Jacobian matrix of partial derivatives of h with respect to v:

$$V_{ij} = \frac{\partial h_i}{\partial x_j}(\hat{x}_k, 0). \tag{43}$$

The a priory prediction error can be defined as:

$$\hat{e}_{x_k}^- = x_k - \hat{x}_k^-. \tag{44}$$

The a priory measurement residual is:

$$\hat{e}_{y_k}^- = y_k - \hat{y}_k^-. \tag{45}$$

Using both equations (44) and (45), the prediction and measurement error can be approximated:

$$\begin{aligned} \hat{e}_{x_k}^- &\approx A(x_{k-1} - \hat{x}_{k-1}) + \epsilon_k, \\ \hat{e}_{y_k}^- &\approx H\epsilon_{x_k} + \eta_k, \end{aligned} \tag{46}$$

where ϵ_k and η_k are independent random variable with zero mean and covariance matrices WQW^T and VRV^T.

The second Kalman process that models the error estimates over time can be obtained by

$$\hat{x}_k = \hat{x}_k^- + \hat{e}_{x_k}. \tag{47}$$

The Kalman filter equation used to estimate $\hat{e}_k$ becomes:

$$\hat{e}_{x_k} = K_k \hat{e}_{y_k}^-. \tag{48}$$

Substituting the Equation (48) back into (47) leads to:

$$\hat{x}_k = \hat{x}_k^- + K_k \hat{e}_{y_k}^-. \tag{49}$$

The prediction step can be computed as:

$$\begin{aligned} \hat{x}_k^- &= f(x_{k-1}, 0), \\ P_k^- &= A_k P_{k-1} A_k^T + W_k Q_{k-1} W_k^T. \end{aligned} \tag{50}$$

Finally, the correction step becomes:

$$\begin{aligned} K_k &= \frac{P_k^- H_k^T}{H_k P_k^- H_k^T + V_k R_k V_k^T}, \\ \hat{x}_k &= \hat{x}_k^- + K_k(y_k - h(\hat{x}_k^-, 0)), \\ P_k &= (I - K_k H_k) P_k^-. \end{aligned} \tag{51}$$

The correction step corrects the state and covariance estimates with the measurement y_k.

C. Example

In the previous section, computed torque method (Figure 12) is applied to linearise the non-linear system 34. However, on a real robot not all states can be measured and therefore the EKF as an estimator has been included into the system. The structure of the system together with EKF is illustrated in Figure 14. In this example, the crab-like robot configuration is used again to investigate the system behaviour. Figures 15(a)-15(d) show the smulated output, states, estimate states and the error, which is the substraction between the real and estimated states.

For this example the matrices Q, W, R, V have been selected as:

$$Q = \begin{bmatrix} 0.1 & 0 & 0 & 0 & 0 & 0 \\ 0 & 0.1 & 0 & 0 & 0 & 0 \\ 0 & 0 & 0.1 & 0 & 0 & 0 \\ 0 & 0 & 0 & 0.0001 & 0 & 0 \\ 0 & 0 & 0 & 0 & 0.0001 & 0 \\ 0 & 0 & 0 & 0 & 0 & 0.0001 \end{bmatrix}, \quad (52)$$

$$W = \begin{bmatrix} 1 & 0 & 0 & 0 & 0 & 0 \\ 0 & 1 & 0 & 0 & 0 & 0 \\ 0 & 0 & 1 & 0 & 0 & 0 \\ 0 & 0 & 0 & 1 & 0 & 0 \\ 0 & 0 & 0 & 0 & 1 & 0 \\ 0 & 0 & 0 & 0 & 0 & 1 \end{bmatrix}, \quad (53)$$

$$R = \begin{bmatrix} 1 & 0 & 0 \\ 0 & 1 & 0 \\ 0 & 0 & 1 \end{bmatrix}, \quad (54)$$

$$V = \begin{bmatrix} 1 & 0 & 0 \\ 0 & 1 & 0 \\ 0 & 0 & 1 \end{bmatrix}. \quad (55)$$

Looking the results produced by the system that uses the EKF, we can assume that the framework enables correct estimations of missing or noisy states and therefore coclude that this control strategy can be used in modular multi-body robot configurations.

IX. Conclusion and Future Work

In this paper, we demonstrate a MATLAB framework that enables to analyse the kinematics, dynamics and control of modular self-reconfigurable robots. The autonomous calculation of self-adaptive model is based on a recursive geometrical approach. The proposed two-step approach for autonomous generation of motion equations was inspired by the work from Chen and Yang and has been modified and adapted to the needs of robot modules developed in projects Symbrion and Replicator. This paper is an extended version of the work presented in [1] and has been extended with non-linear control methods and with a state estimator for values that cannot be measured on a real mashine. The analysis and evaluation of the model and control strategies are inalienable before porting the software to the robots. A corresponding ongoing C++ framework, which will run on robots is currently in development and will be presented in a future publications.

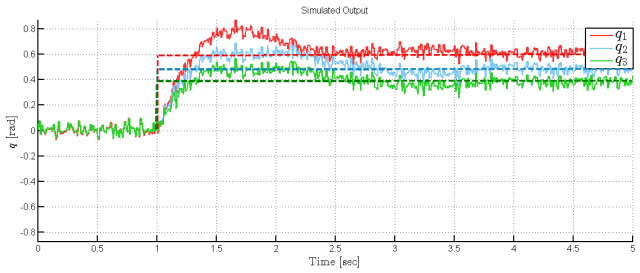

(a)

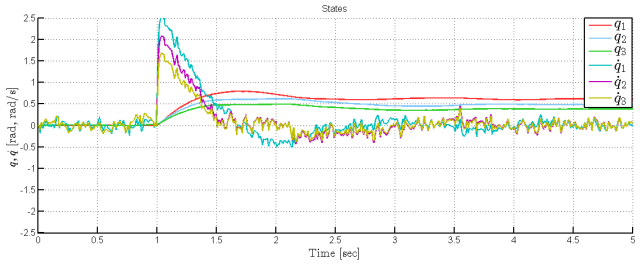

(b)

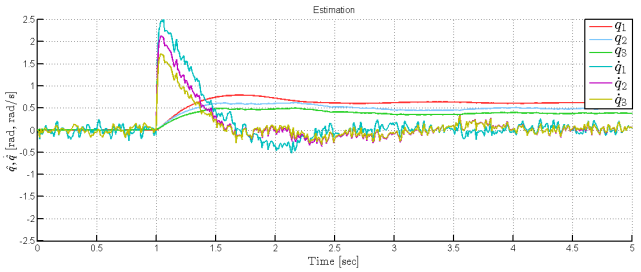

(c)

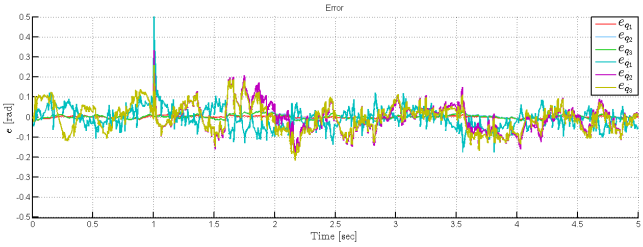

(d)

Figure 15: Simulation results for crab-like robot configuration. (a) Step response of active joints with simulated sensor noise; (b) system states; (c) estimated states; (d) error.

Acknowledgment

The "SYMBRION" project is funded by the European Commission within the work programme "Future and Emergent Technologies Proactive" under the grant agreement no. 216342. The "REPLICATOR" project is funded within the work programme "Cognitive Systems, Interaction, Robotics" under the grant agreement no. 216240.

REFERENCES

[1] E. Meister and A. Gutenkunst. Self-adaptive framework for modular and self-reconfigurable robotic systems. In *Proc. of the Fourth International Conference on Adaptive and Self-Adaptive Systems and Applications (ADAPTIVE 2012)*, Nice, France, 2012.

[2] SYMBRION. *SYMBRION: Symbiotic Evolutionary Robot Organisms, 7th Framework Programme Project No FP7-ICT-2007.8.2*. European Communities, 2008-2012.

[3] REPLICATOR. *REPLICATOR: Robotic Evolutionary Self-Programming and Self-Assembling Organisms, 7th Framework Programme Project No FP7-ICT-2007.2.1*. European Communities, 2008-2012.

[4] M. Yim, W.-M. Shen, B. Salemi, D. Rus, M. Moll, H. Lipson, E. Klavins, and G.S. Chirikjian. Modular self-reconfigurable robot systems. *IEEE Robotics & Automation Magazine, Magazine*, pages 43–52, 2007.

[5] S. Kernbach, O. Scholz, K. Harada, S. Popesku, J. Liedke, H. Raja, W. Liu, F. Caparrelli, J. Jemai, J. Havlik, E. Meister, and P. Levi. workshop on "modular robots: State of the art". In J. Guerrero, editor, *In Proc. of the IEEE International Conference on Robotics and Automation (ICRA-2010)*, pages 1–10, Anchorage, Alaska, 2010.

[6] P. Levi and S. Kernbach, editors. *Symbiotic Multi-Robot Organisms: Reliability, Adaptability, Evolution*. Springer-Verlag, 2010.

[7] M. D. Ardema. *Newton-Euler dynamics*. Springer, 2005.

[8] R. A. Howland. *Intermediate dynamics: a linear algebraic approach*. Mechanical engineering series. Springer, 2006.

[9] W. Greiner. *Classical Mechanics: Systems of Particles and Hamiltonian Dynamics*. Springer, 2010.

[10] F. C. Park and J. E. Bobrow. A recursive algorithm for robot dynamics using lie groups. In *Proc. of IEEE Conference on Robotics and Automation*, pages 1535–1540, 1994.

[11] W. Pfeifer. *Lie Algebra Su(N):*. Birkhuser, 2003.

[12] J. M. Selig. *Geometric Fundamentals of Robotics (Monographs in Computer Science)*. Springer-Verlag, 2004.

[13] R. Ball. *A Treatise on the Theory of Screws*. Cambridge University Press, 1900.

[14] I.-M. Chen. *Theory and Applications of Modular Reconfigurable Robotics Systems*. PhD thesis, Calfornia Institute of Technology, CA, 1994.

[15] R. M. Murray, Z. Li., and S. S. Sastry. *A Mathematical Introduction to Robotic Manipulation*. Boca Raton, FL: CRC Press, 1994.

[16] S. R. Ploen. *Geometric Algorithms for the Dynamics and Control of Multibody Systems*. PhD thesis, 1997.

[17] J. Y. S. Luh, M. W. Walker, and R. P. C. Paul. On-line computational scheme for mechanical manipulators. *Journal of Dynamic Systems, Measurement, and Control*, 102(2):69–76, 1980.

[18] M. W. Walker and D. E. Orin. Efficient dynamic computer simulation of robotic mechanisms. *Journal of Dynamic Systems, Measurement, and Control*, 104(3):205–211, 1982.

[19] R. Featherstone. *Rigid Body Dynamics Algorithms*. Springer-Verlag, 2008.

[20] S. Kernbach, F. Schlachter, R. Humza, J. Liedke, S. Popesku, S. Russo, R. Matthias, C. Schwarzer, B. Girault, and ... P. Alschbach. Heterogeneity for increasing performance and reliability of self-reconfigurable multi-robot organisms. In *In Proc. IROS-11*, 2011.

[21] I.-M. Chen and G. Yang. Automatic model generation for modular reconfigurable robot dynamics. *ASME Journal of Dynamic Systems, Measurement, and Control*, 120:346–352, 1999.

[22] J. M. Selig. *Geometric Fundamentals of Robotics*. Monographs in Computer Science. Springer, 2005.

[23] R. Brockett. *Mathematical theory of net-works and systems*, chapter Robotic manipulators and the product of exponential formula, pages 120–129. Springer, New York, 1984.

[24] L. Winkler and H Wörn. Symbricator3d a distributed simulation environment for modular robots. In Ming Xie, editor, *Intelligent Robotics and Applications, Lecture Notes in Computer Science*, pages 1266–1277, 2009.

[25] W. Liu and A. F. T. Winfield. Autonomous morphogenesis in self-assembling robots using ir-based sensing and local communications. In *Proceedings of the 7th international conference on Swarm intelligence*, ANTS'10, pages 107–118, Berlin, Heidelberg, 2010. Springer-Verlag.

[26] T. Krajník, J. Faigl, V. Vonásek, K. Košnar, M. Kulich, and L. Přeučil. Simple, yet Stable Bearing-only Navigation. *Journal of Field Robotics*, October 2010.

[27] R. Saatchi M. S. Ahmed and F. Caparrelli. Support for robot docking and energy foraging - a computer vision approach. In *Proc. of 2nd International Conference on Pervasive and Embedded Computing and Communication Systems*, 2012.

[28] E. Meister and D. Kryvoukhov. An artificial tactile sensor skin for modular robots. In P. Fisette J.C. Samin, editor, *Proc. of Multibody Dynamics 2011, ECCOMAS Thematic Conference*, Brussels, Belgium, 2011.

[29] E. Meister and I. Zilberman. Fuzzy logic based sensor skin for robotic applications. In *Proc. of the The 14th International Conference on Artificial Intelligence (ICAI 2012)*, Las Vegas, USA, 2012. IEEE Computer Society Press.

[30] E. Meister, S. Stepanenko, and S. Kernbach. Adaptive locomotion of multibody snake-like robot. In P. Fisette J.C. Samin, editor, *Proc. of Multibody Dynamics 2011, ECCOMAS Thematic Conference*, Brussels, Belgium, 2011.

[31] S. Kernbach, E. Meister, F. Schlachter, and O. Kernbach. Adaptation and self-adaptation of developmental multi-robot systems. *International Journal On Advances in Intelligent Systems*, 3:121–140, 2010.

[32] S. Kernbach, P. Levi, E. Meister, F. Schlachter, and O. Kernbach. Towards self-adaptation of robot organisms with a high developmental plasticity. In J. Guerrero, editor, *Proc. of the First IEEE International Conference on Adaptive and Self-adaptive Systems and Applications (IEEE ADAPTIVE 2009)*, pages 180–187, Athens/Glyfada, Greece, 2009. IEEE Computer Society Press.

[33] J. E. Hasbun. *Classical Mechanics With MATLAB Applications*. Jones & Bartlett Publishers, 1 edition, March 2008.

[34] W. D. Pietruszka. *MATLAB Und Simulink in Der Ingenieurpraxis: Modellbildung, Berechnung Und Simulation*. Lehrbuch : Maschinenbau. Vieweg+teubner Verlag, 2006.

[35] G. D. Wood and D. C. Kennedy. *Simulating Mechanical Systems in Simulink with SimMechanics.* Mathworks, The MathWorks, Inc.,, 2003. http://www.mathworks.com.

[36] S. V. Emel'janov. *Automatische Regelsysteme mit veränderlicher Struktur.* Akademie-Verl, 1971.

[37] D. E. Kirk. *Optimal Control Theory: An Introduction*. Dover books on engineering. Dover Publications, 2004.

[38] J. Ackermann and P. Blue. *Robust Control: The Parameter Space Approach*. Communications and Control Engineering. Springer, 2002.

[39] J. Zhou and C. Wen. *Adaptive Backstepping Control of Uncertain Systems: Nonsmooth Nonlinearities, Interactions Or Time-Variations*. Lecture Notes in Control and Information Sciences. Springer, 2008.

[40] A. S. I. Zinober and D. H. Owens. *Nonlinear and Adaptive Control: Ncn4 2001*. Lecture Notes in Control and Information Sciences. Springer, 2002.

[41] M. Krstić, I. Kanellakopoulos, and P.V. Kokotović. *Nonlinear and adaptive control design*. Adaptive and learning systems for signal processing, communications, and control. Wiley, 1995.

[42] R. Freeman. Nonlinear and adaptive control with applications. *Control Systems, IEEE*, 31(2):90–92, 2008.

[43] H. P. Geering. *Regelungstechnik: Mathematische Grundlagen, Entwurfsmethoden, Beispiele*. Springer-Lehrbuch. Springer-Verlag GmbH, 2003.

[44] I. Alberto. *Nonlinear Control Systems: An Introduction (Communications and Control Engineering)*. Springer, 1994.

[45] B. Siciliano and O. Khatib. *Springer Handbook of Robotics*. Gale virtual reference library. Springer, 2008.

[46] E. Meister, O. Scholz, J. Jemai, J. Havlik, W. Liu, S. Karout, G. Fu, and S. Kernbach. *Computation, Distributed Sensing and Communication.* Springer-Verlag, 2010.

[47] G. Welch and G. Bishop. An introduction to the Kalman filter. 1995.

Horizon Line Detection in Marine Images: Which Method to Choose?

Evgeny Gershikov, Tzvika Libe, and Samuel Kosolapov
Department of Electrical Engineering
Braude Academic College of Engineering
Karmiel 21982, Israel
e-mail: eugeny11@braude.ac.il, tzvika_libe1@walla.com, and ksamuel@braude.ac.il

Abstract— **Five algorithms designed to find a horizontal line separating sea and sky in marine images in real-life conditions were implemented in this work and compared by their performance: accuracy and relative speed. One of the selected algorithms was based on regional covariances in luminance images, the second one was based on edge detection and the Hough transform, the third one used maximal local edge detection and the least-squares method, the fourth one employed median filtering in small neighborhoods and linear regression and the fifth one was based on regional edge magnitudes and the least-squares method. Real-life images were used for comparison. The most accurate line with respect to the angular error was obtained by using the edge detection and Hough transform based algorithm. The highest accuracy with respect to the position of the line was achieved by the regional covariance method. However, the highest speed was achieved by using the regional edge magnitude algorithm.**

Keywords-horizon detection; marine images; edge detection; median filtering; image analysis; local edge magnitudes; regional edge magnitudes; regional covariances

I. INTRODUCTION

The horizon line is used for different purposes, such as navigation in airborne and marine vehicles and military surveillance. In an airborne vehicle, the horizon line can be used to determine, for example, its roll, pitch and yaw angles. In the case of military surveillance the horizon line is helpful in detecting the distance to targets.

Many horizon line detection methods are known today, for example, the methods in [1-8]. Some of these algorithms are based on edge detection [9], while others employ statistical methods [4]. Due to the variety of techniques, a comparison of the detection performance that they can achieve can be very helpful [1]. The goal of this research is to implement and compare the accuracy of a number of well-known as well as new or modified horizon-line detection approaches. Considering that in the later stages of this research the selected algorithm is to be implemented on a stand-alone hardware unit, algorithms complexity and their relative speed is also evaluated.

The structure of this paper is as follows. In the next section we present the algorithms discussed in this work for horizon line detection in marine images. Then, in Section III we describe possible improvements of the detection techniques. Section IV discusses the methods and criteria used in the comparison of the algorithms and Section V presents horizon detection results: quantitative and visual. Finally, Section VI provides a summary of this work and our conclusions.

II. ALGORITHMS COMPARED

Five algorithms are compared in this work, as described below. The motivation for their choice is comparison of local feature based algorithms, such as those based on edges (for example, H-HC or H-LSC), with global feature based methods, such as H-COV-LUM or H-REM, that use regional covariances and regional edge magnitudes, respectively. The H-MED algorithm extends the meaning of a local feature (edge) at a pixel to its small neighborhood and then looks for the maximal edge in the vertical direction. Thus, it introduces a compromise between local and global features. No algorithms that require a training stage, such as neural networks and support vector machines were chosen for the comparison, but only simple low complexity methods were taken. Considering future DSP implementations training was found to be impractical.

The compared methods are:

"H-COV-LUM" – an algorithm that uses regional covariances, as introduced in [4], but modified to calculate these covariances using luminance images. Although there are cases where the color information is important [10], in this case, using achromatic image data only improves the algorithm speed significantly with minimal loss in accuracy. COV-LUM stands here for Covariance of Luminance.

"H-HC" – uses pre-processing, Canny edge detector [11] and Hough transform [12]. HC stands for Hough and Canny.

"H-LSC" – uses pre-processing, maximal local edge detection and calibration by the least-squares method approach. LSC stands here for Least Squares Calibration.

"H-MED" – searches for the maximal edge in the vertical direction based on an extended neighborhood of a pixel, followed by median filtration in order to reject outlying points and linear regression. MED stands here for median.

"H-REM" – divides the image into vertical stripes and searches for the maximal regional edge magnitude in each stripe, followed by the least-squares technique to estimate the best line passing through the maximal edge coordinates. REM stands here for Regional Edge Magnitudes.

The algorithms are described in more detail in the next subsections.

A. Regional covariance based algorithm (H-COV-LUM)

An algorithm for horizon detection for remotely piloted Micro Air Vehicles was introduced in [4]. The algorithm

receives an image taken from the air as input and searches for an optimal partition of the image into two regions: sky and ground (or in our work sky and sea) using a line, which is the detected horizon. The optimization criterion is based on the determinants and traces of the covariance matrices of the two regions. More specifically, if we denote a sky pixel by $\boldsymbol{x}_{i,j}^{s} = [R_{i,j}^{s}\ G_{i,j}^{s}\ B_{i,j}^{s}]^{T}$, where $R_{i,j}^{s}, G_{i,j}^{s}, B_{i,j}^{s}$ are the primary red, green and blue values at the pixel (i,j), and we denote a ground pixel by $\boldsymbol{x}_{i,j}^{g} = [R_{i,j}^{g}\ G_{i,j}^{g}\ B_{i,j}^{g}]^{T}$, then the covariance matrices of the regions are given by $\Lambda^{s} = E\left(\left(\boldsymbol{x}_{i,j}^{s} - \mu^{s}\right)\left(\boldsymbol{x}_{i,j}^{s} - \mu^{s}\right)^{T}\right)$, $\Lambda^{g} = E\left(\left(\boldsymbol{x}_{i,j}^{g} - \mu^{g}\right)\left(\boldsymbol{x}_{i,j}^{g} - \mu^{g}\right)^{T}\right)$, where $\mu^{s} = E\left(\boldsymbol{x}_{i,j}^{s}\right)$ and $\mu^{g} = E\left(\boldsymbol{x}_{i,j}^{g}\right)$. $E()$ denotes here statistical mean. The optimization criterion, considered for the possible horizon line orientations and positions and maximized is given by [4]:

$$J = \frac{1}{\det(\Lambda^{s}) + \det(\Lambda^{g}) + trace^{2}(\Lambda^{s}) + trace^{2}(\Lambda^{g})}, \quad (1)$$

where det() denotes the determinant and trace() denotes the trace of the covariance matrices Λ^{s} and Λ^{g}.

We consider a similar criterion to the one in (1) for the luminance image, thus the optimization term J becomes

$$J = \frac{1}{\mathrm{var}(Y^{s}) + \mathrm{var}(Y^{g}) + \mathrm{var}^{2}(Y^{s}) + \mathrm{var}^{2}(Y^{g})}, \quad (2)$$

where var() stands for variance and Y^{s}, Y^{g} are the luminance values of the sky and ground regions, respectively. A simplified optimization criteria

$$J = \frac{1}{\mathrm{var}(Y^{s}) + \mathrm{var}(Y^{g})} \quad (3)$$

can be used instead of the one in (2) with similar results. Thus, we search for the line maximizing (3) among all considered horizon line orientations and positions. Also, defining a region of interest (ROI) in the image and searching the horizon line only in this area speeds up the algorithm significantly. Alternatively, the input image can be down-sampled prior to the application of the algorithm to reduce its runtime, but this will decrease the accuracy as well.

B. Edge detection and Hough transform based algorithm (H-HC)

The stages of this method can be summarized as follows.

1. Pre-process the image using morphological erosion to reduce the probability of the detection of weak edges in the later stages. A small circular structuring element can be used here. Alternatively, the image can be smoothed using a low pass filter, but we found morphological operations to provide better performance in terms of preserving the edges [13].
2. Apply Canny [11] edge detector to the pre-processed image.
3. Apply the Hough transform [12] to the edges map.
4. Choose the horizon line to be the longest line found in the previous step.

C. Edge detection and least-squares calibration based algorithm (H-LSC)

This algorithm is based on edge detection as well, but uses a simple algorithm to detect the maximal local edge in the vertical direction in each column of the image. Its stages are described below.

1. Pre-process the image using morphological erosion.
2. Find the maximal vertical local edge in each column of the image. The simplest way to measure the local edge magnitude is using an approximation of the vertical derivative, e.g., $\left|Y_{i+1,j} - Y_{i,j}\right|$. Store the *(i,j)* coordinates of the maximal edges.
3. Use the least-squares method to find the optimal line passing through the maximal edges' coordinates. Edges with very small values as well as very big ones can be discarded here since they are most likely caused by noise. This increases the algorithm robustness in the presence of varying lighting effects.
4. An optional step of median filtering can be added to remove outliers. This step can be applied to the vertical coordinates of the maximal edges (prior to Step 3) or to the regression errors (following Step 3). We define the regression error as the error at coordinates (*i*,*j*) of a maximal edge, i.e.,

$$err_{i,j} = \left|i - a_{1}j - a_{0}\right|, \quad (5)$$

where a_{0}, a_{1} are the optimal line coefficients found in Step 3. We define the median filtered error $err_{i,j}^{med}$ as $err_{i,j}$ after applying a median filter. Now the outliers are *(i,j)*, where $\left|err_{i,j} - err_{i,j}^{med}\right| > Th$, and can be removed. *Th* here is the threshold (e.g., a value of 1).

D. Median filtering and linear regression based algorithm (H-MED)

This algorithm employs median filters in several stages providing high performance in the presence of noise. The stages of the algorithm are:

1. Pre-process the image using morphological erosion.
2. Find the maximal vertical edge in each column of the image using the extended neighborhood of each pixel. Here the edge at pixel *(i,j)* is measured as the absolute difference between two median values of the 5 pixels above and including pixel *(i,j)* and the 5 pixels below it, i.e., $edge_{i,j} = \left|med_{i,j}^{1} - med_{i,j}^{2}\right|$, where

$$med_{i,j}^{1} = median\left\{Y_{k,j}\right\}_{k=i-4}^{i},$$
$$med_{i,j}^{2} = median\left\{Y_{k,j}\right\}_{k=i+1}^{i+5}. \quad (6)$$

The *(i,j)* coordinates of the maximal edges are stored.

3. Use linear regression to find the optimal line passing through the maximal edge coordinates.
4. An optional step of median filtering can be added to remove outliers. This step can be the same as Step 3 in H-LSC.

E. Regional edge magnitudes and least-squares calibration based algorithm (H-REM)

This algorithm extends the idea of local edge magnitudes used in the H-HC and H-LSC methods, for example, beyond the concept of extended neighborhoods used by H-MED to regional edge magnitudes. The steps of this method are:

1. Pre-process the image using morphological erosion.
2. Divide the image into vertical stripes each consisting of a number of columns. Run on each stripe separately and calculate the edge magnitude at each pixel in it in the vertical direction using a simple, but robust equation for the edge:

$$edge_{i,j} = \frac{1}{L}\left|\sum_{k=i-L}^{i-1} Y_{k,j} - \sum_{k=i+1}^{i+L} Y_{k,j}\right|, \quad (7)$$

where L is the number of pixels used in the calculation above and below the current pixel.
3. Sum the edge magnitudes of each row in the current stripe to get regional edge magnitudes.
4. Find the row of the maximal regional edge in each stripe. Associate it with the column number corresponding to the center of the stripe to get the maximal edge coordinates.
5. Use the least-squares method to find the optimal line passing through the edge coordinates. Edges with very small values as well as very big ones can be discarded here as in the H-LSC algorithm. This is optional since the algorithm employs a greater neighborhood for edge magnitude calculation making it more robust.
6. An optional step of median filtering can be added as in the H-LSC algorithm.

Next we discuss several possible improvements of the algorithms.

III. PROPOSED IMPROVEMENTS TO THE ALGORITHMS

Most of the proposed algorithms rely on a certain measurement of edge magnitudes (H-COV-LUM is an exception). To make these measurements more reliable we propose the following ideas.

A. Filtering out very dark or very bright pixels

The idea is to filter out the dark areas of the image as well as areas with sun light effects by calculating the image color energy everywhere and discarding the pixels where this energy is too high or too low [14]. A simple measure of the image color energy at pixel *(i,j)* is

$$energy_{i,j} = R_{i,j}^2 + G_{i,j}^2 + B_{i,j}^2 \quad (8)$$

or, alternatively,

$$energy_{i,j} = R_{i,j} + G_{i,j} + B_{i,j}. \quad (9)$$

A pixel is discarded if $energy_{i,j} < Th_{Min}$ (dark pixels) or $energy_{i,j} > Th_{Max}$ (pixels saturated with light) and it then cannot be chosen as the pixel with maximal edge magnitude in relevant algorithms (such as H-LSC). Note that Th_{Min} and Th_{Max} are the two thresholds determining which pixels are to be discarded: the low one and the high one, respectively. The effect of filtering out of pixels from the image is shown in Fig. 1 for the rotated Horizon_3 image. Note that the horizon appears jagged due to the marking of the line in the image itself subject to pixel resolution.

B. Adding weights to the neighboring pixels used in edge magnitude calculation

When an extended neighborhood is used for the edge magnitude calculation as, for example, in the H-REM method, we propose giving a decreasing weight to the pixels in the neighborhood based on their distance to the current pixel: a closer pixel will get a higher weight. Thus, the edge calculation of Equation (7), for example, can be replaced by

$$edge_{i,j} = \frac{1}{L}\left|\sum_{k=i-L}^{i-1} \alpha^{|i-k|} Y_{k,j} - \sum_{k=i+1}^{i+L} \alpha^{|i-k|} Y_{k,j}\right|, \quad (10)$$

H-REM result for rotated Horizon_3 w.o. filtering out pixels

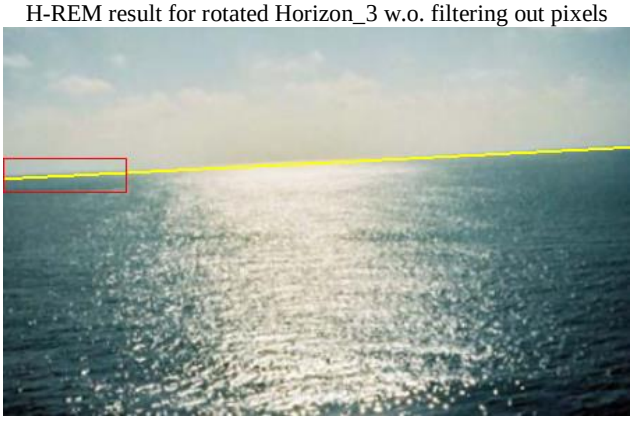

H-REM result for rotated Horizon_3 with filtering out pixels

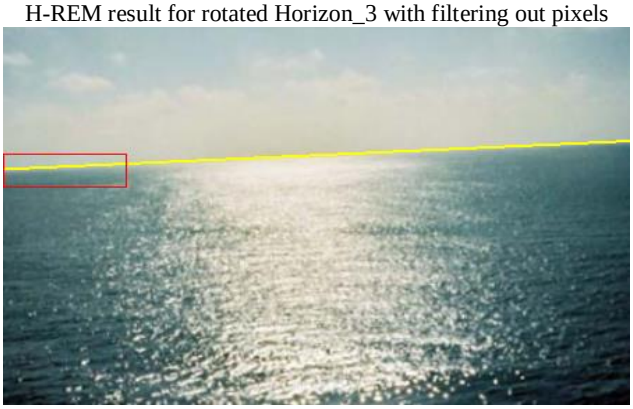

Figure 1. H-REM detection results for the rotated Horizon_3 image with and without (w.o.) filtering out of pixels. The horizon line is marked (in yellow). Note the error introduced in the top figure, especially in the area marked with the rectangular frame.

H-REM result for Horizon_4 without weighting

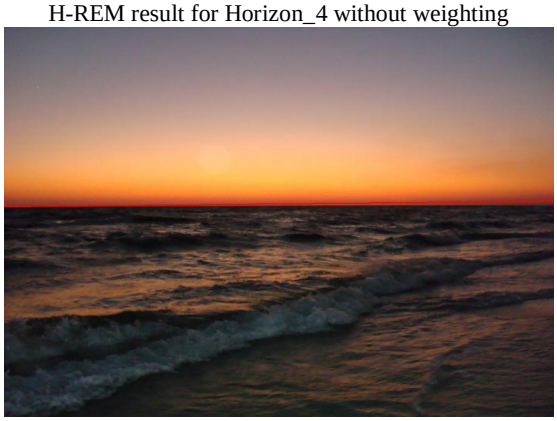

H-REM result for Horizon_4 with weighting

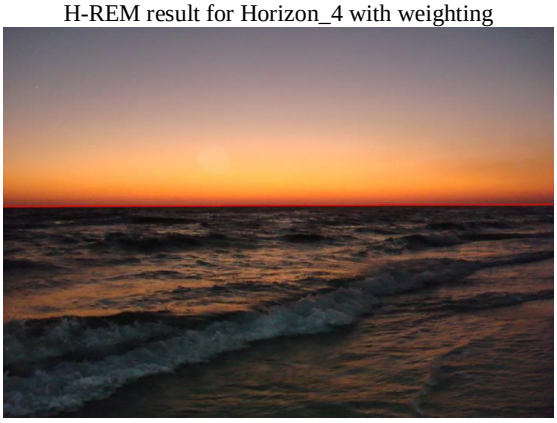

Figure 2. H-REM detection results for the Horizon_4 image with and without weighting. The horizon line is marked (in red). Note the error introduced in the top figure on the right side of the line.

H-REM result for Horizon_3 without hist. eq.

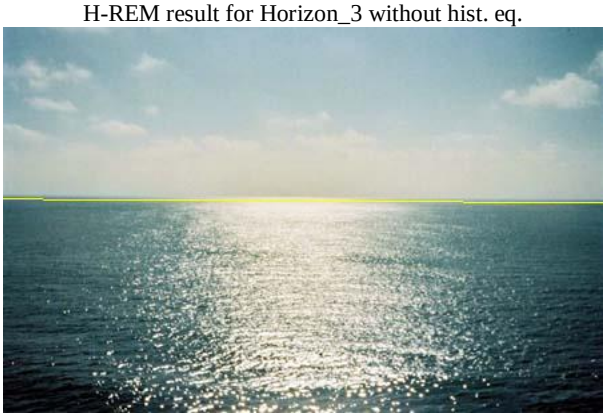

H-REM result for Horizon_3 with hist. eq.

Figure 3. H-REM detection results for the Horizon_3 image with and without histogram equalization (hist. eq.). The horizon line is marked (in yellow). Note the error introduced in the top figure.

where $0 < \alpha < 1$ is a real number. The expression given in (10) results in better edge magnitude estimation and better algorithm performance compared to using equal weights for all pixels in the neighborhood. This is shown in Fig. 2 for the Horizon_4 image. Note the error in the detected horizon line position when no weighting is used, i.e., the edge magnitude is calculated based on Equation (7).

C. *Introducing safety intervals in edge magnitude calculation*

Sometimes it makes sense to calculate the edge at pixel (i, j) using the pixels not directly above and below it, but starting from a certain distance (e.g., 1, 2 or 5 pixels) away. The reason may be blurring of the edges, which occurred, for example, due to errors introduced by compression of the processed image, especially when a simple digital camera is used.

Using this idea, Equation (7) of H-REM will turn into

$$edge_{i,j} = \frac{1}{L}\left| \sum_{k=i-D-L}^{i-D} Y_{k,j} - \sum_{k=i+D+1}^{i+D+L} Y_{k,j} \right|. \qquad (11)$$

Here D is a positive integer parameter denoting the safety interval, i.e., the distance of the closest pixel used in the calculation of the current pixel (i,j).

D. *Histogram operations prior to executing the algorithms*

A histogram operation prior to horizon detection may improve the detection performance if it increases the difference between sea and sky pixels and/or improves the similarity between pixels in the same region (sea or sky). Then the performance of algorithms based on regional covariances, such as H-COV-LUM, as well as local or regional edge magnitudes, such as H-LSC or H-REM, is expected to improve.

In this work we examine the use of histogram equalization of the luminance component of the image. This operation attempts to make the luminance levels more uniformly distributed while at the same time producing an image with a smaller total number of luminance levels. The result of applying histogram equalization (yielding 64 levels of luminance) to the Horizon_3 image and using the H-REM algorithm is shown in Fig. 3. Note the better precision of the detection in the bottom part of the figure.

All the proposed ideas are generally "safe to use", meaning the algorithms' performance is either improved or is not affected. For the images presented in Figs. 1-3 a visual improvement in the accuracy can be observed.

IV. COMPARISON METHODS AND CRITERIA

Next, we describe the images and criteria used for the comparison of the algorithms in this work.

A. Images used to compare the algorithms

The results of horizon detection for a group of 9 real-life marine images are presented in this work. Image input format is true color (24 bit per pixel) non-compressed BMP. Resolutions used vary from 249x169 to 900x675 pixels. Most images contain a horizon line separating the sea and the sky, clearly distinguished by the human eye. However, sometimes the horizon line is slightly distorted by camera optics and sea waves or concealed by marine vessels. It is clear that camera lens distortion may affect the accuracy of the horizon detection, however, for the methods and the images considered here this effect was found to be insignificant. To further challenge the selected algorithms, several images contained clouds or sun light effects near the surface of the sea water.

B. Comparison criteria

The algorithms were compared with respect to accuracy and speed. The accuracy was measured for the detected horizon angle relative to a horizontal line (in degrees) as well as the position of the line relative to the bottom left corner of the image (in pixels, sub-pixel resolution was not considered). The errors provided in the next section for these two horizon line parameters are measured relative to the line height and angle as determined visually. This means that the horizon line, as determined by the eye, was marked in the image manually and was considered the ground truth. Then the absolute difference of the determined line position and the one found visually was calculated and averaged on the group of test images. The same procedure was done for the determined line orientation relative to the one considered as ground truth. In addition, the algorithms' speed was measured in terms of run time (in seconds).

V. RESULTS

The accuracy comparison for the algorithms described above (height and angle deviations) is given in Table 1 in terms of the mean errors for the 9 test images. In some of these images the horizon is not horizontally aligned (e.g., see Fig. 4). As it can be seen, the angular deviation is very small on average for the H-HC, H-REM and H-LSC algorithms. We can speculate that the accuracy of H-HC results from the accuracy of the edge detection method by Canny [11] and of the employed Hough transform [12]. The height deviation is smallest for the H-COV-LUM method, based on regional covariances in luminance images. However, the fastest algorithm is H-REM, based on maximal edges and least-squares optimization, as seen from the run time comparison in Table 2. The H-LSC and H-HC methods are slower than H-REM, but the H-COV-LUM and H-MED algorithms are much slower than all of these three methods due to the required computations of regional covariances or local medians in the process of the horizon detection. The run-time was measured in a MATLAB environment.

A. Visual results

Visual results are provided in Figs. 4-7. As it can be seen, all the algorithms provide good results for the Horizon_1 image (Fig. 4), although the H-COV-LUM method slightly misses the horizon line. This is due to the effect of the clouds and the sunlight reflection in the sea water. A similar effect can be seen for the Horizon_5 image (Fig. 5), where the H-COV-LUM method provides a slightly less accurate estimate of the horizon line than the other algorithms. H-REM is influenced here by the strong regional edges in the area of the waves, but produces a line with a slight deviation from the horizon. The other three methods achieve visually similar performance with very good detection of the horizon.

Figs. 4 and 5 show that H-COV-LUM (denoted H-COV in the figures) is an efficient algorithm for locating the position of the center of the horizon line, but sometimes the line is slightly rotated compared to the optimal one introducing an angular error. The algorithm copes well with images where the sky and the sea are uniform in appearance even when marine vessels are present, but it may be confused by clouds, sun reflection effects (Fig. 4) and strong waves (Fig. 5). The solution to this may be a pre-processing stage which removes some of the clouds, light reflection effects and waves from the image resulting in more uniform sky and sea areas. This is currently under research.

In Fig. 6, all of H-COV-LUM, H-HC and H-REM methods provide good estimates of the horizon line, while H-LSC is less accurate. As for H-MED, its performance is inferior to the others due to a bigger angular error. This method is more affected by the closer ship concealing the horizon line. The reason for the performance decrease for H-LSC and H-MED is that both detect maximal edges at pixels of the larger marine vessel instead of the horizon that is partly hidden. Than the least-squares technique or the linear regression employed to find the optimal line passing through the maximal edge locations produce a line that is shifted downwards relative to the optimal horizon line. The solution to this problem can be calculating the optimal line many times using partial data and then choosing the one passing through or close to the maximal number of edge pixels. This idea is the subject of future research.

The H-HC algorithm, on the other hand, is robust to the hindrances introduced by the sea vessels in the image of Fig. 6 due to the use of the Hough transform that detects the line passing through the maximal number of pixels in the edge map. Thus, even though some of the ship pixels are detected as edges, this does not confuse the method as long as more pixels are marked as edges on the real horizon line.

In Fig. 7 the detection results for one more image are shown. Despite the fact that the sky in the image is very cloudy, good detection results can be observed for H-MED,

H-HC and H-LSC algorithms while in H-REM a small angular error is introduced. The worst performance here is that of H-COV since it is confused by the presence of the clouds resulting in a line located a noticeable distance above the horizon.

TABLE 1. MEAN HEIGHT DEVIATION (PIXELS) AND ANGLE DEVIATION (DEGREES) FOR THE FIVE ALGORITHMS

Algorithm	Mean height deviation	Mean angle deviation
H-LSC	1.92	0.23 °
H-COV-LUM	1.11	0.47 °
H-HC	1.67	0.13 °
H-MED	1.83	0.44 °
H-REM	2.28	0.19 °

TABLE 2. MEAN RUN TIMES (SECONDS) FOR THE FIVE HORIZON DETECTION ALGORITHMS

Algorithm	Mean Time (sec.)
H-LSC	0.33
H-COV-LUM	2.24
H-HC	0.45
H-MED	1.46
H-REM	0.14

VI. CONCLUSIONS

Five different algorithms for horizon detection in marine images were examined in this work. The techniques employed by these algorithms vary from using regional covariances of sky and sea regions (H-COV-LUM) to using edge detection and Hough transform (H-HC), using maximal edge detection and the least-squares method (H-LSC), using median filtering and linear regression (H-MED) and using regional edge magnitudes and the least-squares method (H-REM). The algorithms were implemented and compared for a group of test images with respect to accuracy as well as run time or speed. The most accurate method with respect to the angular error was found to be H-HC, while the other algorithms do not lag far behind. The H-COV-LUM algorithm provided the highest accuracy when estimating the height of the horizon line above the bottom left corner of the image. Also when comparing the algorithms' speed, the fastest method was H-REM. We conclude that all the algorithms examined in this work can be used for horizon detection in still marine images. They successfully deal with the biggest challenges of horizon line detection, such as varying illumination effects as well as the presence of the sun, waves, ships and clouds in the image. In addition to that, the algorithms can be used in images taken by infrared cameras, an idea that is currently being researched.

ACKNOWLEDGMENT

We would like to thank the administration of Ort Braude Academic College of Engineering and the Department of Electrical Engineering for providing the opportunity and financial means to conduct this research.

REFERENCES

[1] T. Libe, E. Gershikov, and S. Kosolapov, "Comparison of methods for horizon line detection in sea images", Proc. CONTENT 2012, Nice, France, 2012, pp 79-85.

[2] G. Bao, Z. Zhou, S. Xiong, X. Lin, and X. Ye, "Towards micro air vehicle flight autonomy research on the method of horizon extraction", Proc. IEEE Conf. on Instrumentation and Measurement Technology, 2003, pp. 1387-1390.

[3] G.-Q. Bao, S.-S. Xiong, and Z.-Y. Zhou, "Vision-based horizon extraction for micro air vehicle flight control", IEEE Trans. on Instrumentation and Measurement, vol. 54, 2005, pp. 1067-1072.

[4] S. M. Ettinger, M. C. Nechyba, P. G. Ifju, and M. Waszak, "Vision-guided flight stability and control for micro air vehicles", Proc. IEEE Conf. on Intelligent Robots and Systems, Lausanne, Switzerland, 2002, pp. 2134 – 2140.

[5] S. Fefilatyev, V. Smarodzinava, L.O. Hall, and D.B. Goldgof, "Horizon detection using machine learning techniques". Proc. International Conference on Machine Learning and Applications, 2006, pp. 17-21.

[6] S. Fefilatyev, D.B. Goldgof, and L. Langebrake. "Towards detection of marine vehicles on horizon from buoy camera". Proc. SPIE, 2007, pp. 6736:67360O.

[7] K. Nonami, F. Kendoul, S. Suzuki, W. Wang, and D. Nakazawa, Autonomous flying robots, Tokyo, Dordrecht, Heidelberg, London, New York: Springer, 2010.

[8] Y. Wang, Z. Liao, H. Guo, T. Liu, and Y. Yang, "An approach for horizon extraction in ocean observation", Proc. IEEE Congress on Image and Signal Processing, 2009, Tianjin, China, pp. 1-5.

[9] S. Kosolapov, "Robust algorithms sequence for structured light 3D scanner adapted for human foot 3D imaging", Journal of Comm. and Computer, vol. 8, 2011, pp. 595-598.

[10] E. Gershikov and M. Porat, "On color transforms and bit allocation for optimal subband image compression", Signal Proc.: Image Communication, vol. 22, Jan. 2007, pp. 1-18.

[11] J. Canny, "A computational approach to edge detection", IEEE Transactions on PAMI, vol. 8, 1986, pp. 679-697.

[12] R. O. Duda and P. E. Hart, "Use of the Hough transformation to detect lines and curves in pictures", Comm. ACM, vol. 15, 1972, pp. 11–15.

[13] D. Dusha, W. Boles, and R. Walker, "Fixed-Wing Attitude Estimation Using Computer Vision Based Horizon Detection", Proc. AIAC, 2007, Melbourne, Australia, pp. 1-19.

[14] S. Kosolapov, "Evaluation of robust algorithms sequence designed to eliminate outliners from cloud of 3D points", Proc. SMTDA, 2010, Chania, Crete, pp. 383-389.

Original Horizon_1 image

H-REM result for Horizon_1

H-COV result for Horizon_1

H-LSC result for Horizon_1

H-MED result for Horizon_1

H-HC result for Horizon_1

Figure 4. Horizon detection results for image Horizon_1. The (yellow) line marks the detected horizon. Note the clouds and reflected light effects in this image. H-COV stands here for H-COV-LUM.

Original Horizon_5 image

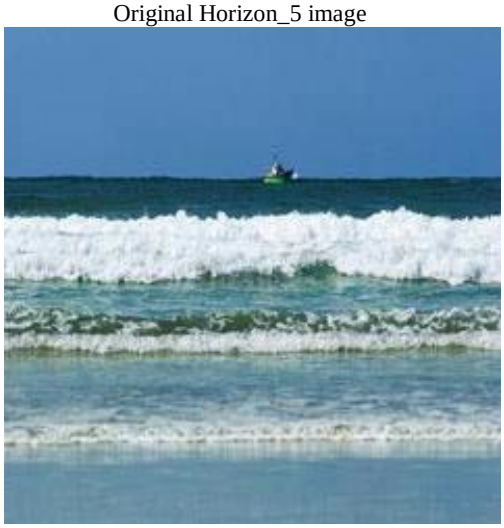

H-REM result for Horizon_5

H-COV result for Horizon_5

H-LSC result for Horizon_5

H-MED result for Horizon_5

H-HC result for Horizon_5

Figure 5. Horizon detection results for image Horizon_5. The (yellow) line marks the detected horizon. Despite the waves and the ship present, all the algorithms detect the horizon correctly.

Original Horizon_6 image

H-REM result for Horizon_6

H-COV result for Horizon_6

H-LSC result for Horizon_6

H-MED result for Horizon_6

H-HC result for Horizon_6

Figure 6. Horizon detection results for image Horizon_6. The (yellow) line marks the detected horizon. Note the waves and the sea vessels present in this image, especially the closer one blocking the horizon.

Original Horizon_7 image

H-REM result for Horizon_7

H-COV result for Horizon_7

H-LSC result for Horizon_7

H-MED result for Horizon_7

H-HC result for Horizon_7

Figure 7. Horizon detection results for image Horizon_7. The (yellow) line marks the detected horizon. Note that a significant area of the image is covered by clouds introducing a challenge for correct horizon detection.

More on MCS Ontology for Cognition: Revising Selected Concepts, Including Cognition and Time, Considering Cognition Links with Philosophy and Implementing Automated Cognition in the Real World

Jean-Daniel Dessimoz and Pierre-François Gauthey
HEIG-VD, School of Business and Engineering
HES-SO, Western Switzerland University of Applied Sciences
CH-1400 Yverdon-les-Bains, Switzerland
e-mail: {jean-daniel.dessimoz, pierre-francois.gauthey}@heig-vd.ch

***Abstract*—Designing advanced cognitive technologies and applications requires a formal ontology, such as the Model for Cognitive Sciences (MCS), the theoretical foundations now proposed for automated cognition, cognitics. Cognition has the ability to create and deliver pertinent information. Discussion is made in the current paper of a number of cognitive notions including those of reality, time and revisited "speed", change and discontinuity, innate and learned behaviors, as well as the human-inspired basics of communication in a group. These newly defined notions conveniently complement the existing MCS ontology. Notions are delineated in conceptual frameworks and can moreover be made operational, deployed in the real world, for validation purpose and for the benefit of users. All these elements confirm the rightness of our current approaches in solving concrete Artificial Intelligence problems and this is illustrated below by some concrete examples taken in domestic context, including robots capable of learning. Cognition would not make much sense per se, and the paper also shows how it can be implemented in the real world, notably using our Piaget proprietary environment for development and programming of smart robotized systems. Experiments prove that the resulting smart systems can indeed successfully operate in the real-world, and in particular interact with humans, performing with large quantities of cognitive components: knowledge, expertise, learning, etc. The quantitative approach of MCS and the operationalization of its cognitive concepts in real-world systems allow as well for a fruitful dialogue about core issues in philosophy as an effective design and realization of smart systems for the benefit of humans.**

Keywords - cognitive robotics; MCS ontology for cognition; cognitics; cognition; time; cognitive speed; discontinuity; reality; innate behavior; communication basics

I. INTRODUCTION

The current publication extends some of our past published works, and in particular largely revisits the recent paper [1], adds a new presentation of the concepts of cognition and time, discusses significant links between cognition and philosophy, as well as addresses the challenge of implementing cognition in the real-world.

In the past century, a major step in evolution has been made when information has been formally defined [2], and infrastructure has been provided for communication and processing of information in a massive scale.

In the early days of signal processing, in technical terms, information was neatly provided by some transmitters, typically originating from some other electronic devices, control panels, microphones or sensors. Machine-based sources of information were limited to signal generators, such as for sine waves or pseudo-random sequences.

Things have now become much more complex and cognition is the new domain to domesticate, where pertinent information is autonomously created by expert agents (e.g., [3]). It is with this very relevant goal that the MCS theory for cognitive sciences has been created (Model for Cognitive Sciences [4] [5]. See also the cognitive engine of Figure 1, the cognitive concept pyramid of Figure 2, and the metric system of Figure 3). The material published so far has already brought interesting benefits in terms of understanding the core cognitive properties, assessing quantitatively their values, and allowing for convincing implementation of cognitive robots in selected areas [6].

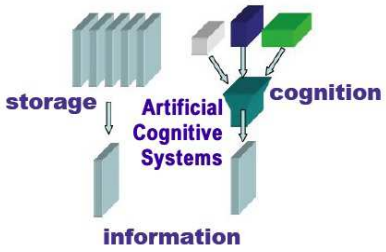

Figure 1. Cognition and, effectively, cognitive systems, allow for generating relevant information, exactly similar to pre-stored information - when the latter is available. Some kind of cognitive engine is necessary (e.g. human-based or artificial, implemented on machines).

Traditionally, people have developed context-dependent cognitive indicators (e.g., for expertise, Elo points for chess-players, Association of Tennis Professionals points for tennis-players, grading systems in schools, or IQ scores), but unfortunately, beyond the case of information, no other work, in our knowledge, has addressed the formal, technically-prone definitions of cognitive entities with associated units.

Figure 2 schematically presents the main cognitive entities in MCS theory context, and Figure 3 presents the equations for their quantitative assessments. Let us briefly review their definitions.

The top group is green, referring to MCS essentials. Knowledge is, for an agent (human or possibly machine-based) the property to deliver the right information; fluency, the cognition speed; expertise, the property to deliver information right and fast, the product of knowledge and fluency; learning, the ability to increase expertise levels; intelligence, the capability to learn, and quantitatively, the ratio of learning to experience; experience, the amount of information witnessed in terms of input and output associations ("examples", "experiments"); complexity, the amount of information necessary to exhaustively describe an object; abstraction, the property of delivering less information than it is incoming; concretization is the inverse of abstraction.

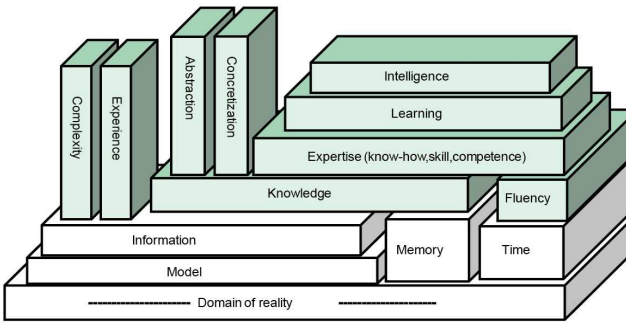

Figure 2. Main cognitive entities in MCS theory. Important cognitive concepts, defined in MCS theory, are colored in green (left). They are based on a few classic entities, including reality and time, which, though classic, also need a discussion from a cognitive perspective

The lower group is white. Even though in principle the corresponding concepts are classical, experience shows that their limits are not well understood, and this is especially disturbing as the new, green concepts are built on them. Thus information is very much time-dependent, the delivery of it essentially making its repetition useless; information is essentially subjective, which means that the same message may convey different quantities to different users; memory is considered here as a support for the permanence of messages, such as an engraved stone, i.e., without the typically associated writing and reading processes; the last 3 quoted concepts, reality, model and time, are further discussed in the sequel of this paper.

In cognitive systems, scale and time are dimensions that are typically much more important than usually perceived. In particular, individuals can collectively yield groups, systems can often be analyzed as a network of subsystems; and in all control loops, occurring in single agents or multi-agent systems, strict dynamic constraints allow – or not – for stable outcomes. Partial autonomy may have to be granted to ancillary subsystems/agents (re. Figure 4).

In general, commonsense, classical concepts, and corresponding MCS concepts are quite synonymous and can be described by the same words; nevertheless, there remain often subtle differences, and in the sequel of this article, when the respective distinctions should be made, the "c-" prefix will be added for the terms defined in MCS Ontology; for example c-speed (1/s unit) is not the usual displacement, motion speed (m/s unit).

Information:	$n = \sum p_i \log_2(1/p_i)$ [bit]
Knowledge:	$K = \log_2(n_{out}\, 2^{n_{in}}+1)$ [lin]
Fluency:	$F = 1/\Delta t$ [s^{-1}]
Expertise:	$E = K \cdot F$ [lin/s]
Learning:	$\Delta E = E(t_1)-E(t_0)$; >0 [lin/s]
Experience:	$R = r(n_{in}+n_{out})$ [bit]
Intelligence:	$I = \Delta E/\Delta R$ [lin/s/bit]
relative Agility:	$A_r = \tau/T$

T: $Fluency^{-1}$ and communication delays
τ: Reaction time of target system, to be controlled

Figure 3. Equations for assessing quantitatively the core properties in cognition. Information keeps its classical definition though (re. Shannon 1948 [2]).

Today another step is considered, whereby artificial cognitive agents should effectively approach human cognitive capabilities for three complementary reasons: better functional services (including those involving human-machine cooperation), better understanding of human nature, and implementation possibility of theories in order to make them operational, and thereby possibly validate them. Proceeding should now be done in incremental steps along two complementary ways: the understanding of concepts, and the operationalized implementation of cognition in machines.

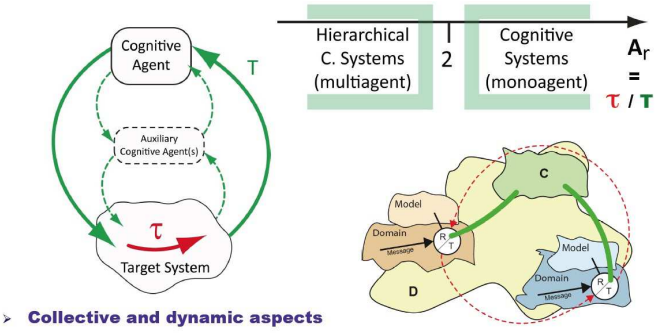

Figure 4. Time and scale matter. Cognitive agents may have to be organized in a hierarchy, for large scope, and dynamically stable control. They can aggregate to form groups or be analyzed at a lower scale as a nerwork of sub-systems.

In this endeavors, a first surprise had been to experience that the prerequisites, the basis on which the MCS theory was built, were not at all as widely understood as expected (re. general surveys [7] [8] and focused discussions below). A complement had to be progressively brought in MCS, re-discussing classical topics, namely those relating to the notions of information, models and memory.

Now, at the moment of addressing in its "generality" the cognitive faculty of humans, another necessary pre-condition for implementing it in machine-based agents appears. A

further analysis, of deeper foundations yet on which the MCS theory is grounded, cannot be escaped. What is reality? What is time? How to cope with the infinite complexity of reality? How much innate or wired can be the cognitive capability we are considering?

The paper addresses these questions in successive sections: Section II for reality; Section III for time; Section IV for ways to cope with the infinite complexity of reality, in particular including the innate versus learning paradigms for producing new cognitive agents. The general presentation made so far will be illustrated in Section V with detailed concrete examples, taken from the field of cooperative robotics; they will address cooperation both for human and machine-based cases, relating to cognitive aspects and operations. The final 4 sections will additionally discuss cognition in three different contexts: conventional AI and aspects of implementation in the real-world (VI), Piaget as a key example of environment allowing to automate and implement cognition in the real-world (VII), illustrating applications (VIII), and considerations relating cognition and philosophy (IX).

II. WHAT IS REALITY?

In MCS theory, reality is in principle viewed as everything, including not only physical objects but also immaterial ones, including information repositories, models, assumptions, novels and if-worlds. It corresponds to the universal definition of Parmenides: What is, is. As illustrated in Figure 5, reality is infinitely complex (re. the definition of complexity in MCS ontology: an infinite amount of bits or megabytes of information would be required for the exhaustive description of reality), so much so that even any tiny part of it, in practical terms, is infinitely complex as well. Reality, including self, is also always the ultimate reference. All subjects facing reality are bound to adopt a constructivist approach [9], relying on means initially self-provided, as innate or "wired", and later on, hopefully improving those means, in particular by proceeding with exploration and learning by experience (Concretely, a human starts in particular with DNA; a typical robot of ours is given in particular a computer and an executable program; then they explore and learn and ultimately successfully achieve many new, unforeseen operations).

This position is similar to the one of Kant [7], for whom innate, pre-existing "categories" are initially required, allowing cognitive agents to perceive. And simultaneously, by careful axiomatic contributions, complex cognitive structures including possible collective, shared models (culture) can be elaborated.

In summary, in a first stage where a single individual is considered, we do not need to know what is reality, as we benefit from the beginning, of an innate (or "wired" in machines) capability to cope with it (models). Moreover, in parallel, rational processes can also develop, and, with automated cognition, with possible exploration tasks, and on the basis of acquired experience, this can usually yield significant improvements.

At the next stage, where the creation of a new capacity to cope with reality is considered, ingenuity is the key, as defined in MCS ontology [5].

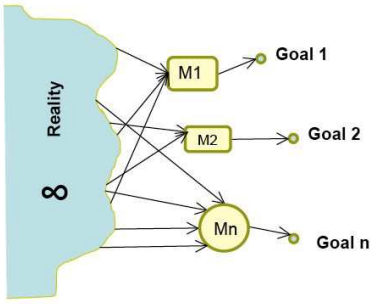

Figure 5. Experience strongly suggests that reality is infinitely complex. Models may be simple and validly serve singular goals, but they should always be considered as very specific for those goals and infinitely lacunary with respect to reality

III. WHAT IS TIME?

Strangely, time is far from well defined in classical terms. The proposal of Kant is interesting with his complementary attitudes, leaning on one hand towards intuition, whereby everyone has a spontaneous understanding of the time concept; and leaning on the other hand towards rationality (Weltweisheit, philosophy), by which a rigorous, "mathematical", definition could be elaborated – with no guarantee but chance however to have this latter construct coincide with the former one. Similarly, St-Augustine claims to know very well what is time - as long as nobody asks for a formal definition of it! Even in the contemporary time where philosophy and science have both well developed, Rosenberg apologizes for simply defining time as follows: "time is duration" and "duration is the passage of time" [8].

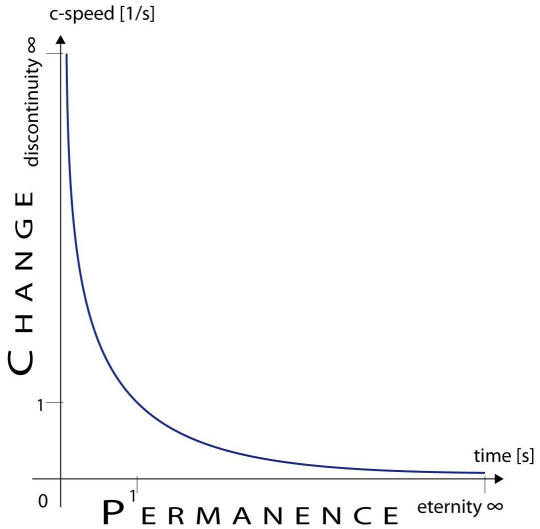

Figure 6. Time characterizes permanence, and speed as defined in MCS ontology, i.e., "c-speed", does it for change.

It is well known that dictionaries tend to have circular definitions. This should be accepted for at least two reasons: as clearly stated by Kant, reality and cognitive world are disconnected; in this sense, a "first" definition, i.e., relating directly to reality is impossible (convenient complements to circumvent this definition obstacle include gaining experience by direct confrontation to reality, visits to museums, science parks, touring and lab experiments). Now, with circular definitions, the cognitive world appears as a maze with multiple entry points. In a chain of 10 so-related concepts, the reader has ten chances to hop with his/her/its intuition from reality to the cognitive world (which includes libraries, languages, dictionaries and Wikipedia).

Time has already been addressed in MCS ontology, as well as two other closely related concepts fluency and agility. Here, however, things improve: a clearer articulation is made between time and change; speed is defined in a universal way, which then helps, with appropriate, specific complements, better handle changes in a variety of domains. Fluency, thus, becomes the speed of expert information delivery and agility the speed of action.

We propose here to define time as a distributed axiom, in a cloud of 6 interconnected concepts: time, permanence, eternity, change, speed, and discontinuity (re. Figure 6):

- Time is a measure of permanence, and is quantified by the "second" as a unit.
- Permanence is the property of things that do not change.
- A permanence that is persistent for an infinite amount of time is eternity.
- Speed is a measure of change, and is quantified, in MCS ontology ("c-speed"), by the inverse of a second (notice that this is more general than the usual motion speed, assessed in meter per second; it can also apply to all dimensions other than linear in distance, e.g., speed of rotation, heating, speech, sedimentation, or general cognitive operations).
- Change is the property of things that do not remain same, stable, permanent over a certain time.
- A change that occurs at an infinite speed is a discontinuity.

If any single one of the six previous statements is intuitively understood, this evidence can be rationally propagated to all the other 5 associated concepts.

Changes can be of different orders: the speed of change may be permanent, constant over a certain time (1st order change); or the speed itself may change at constant speed, yielding the notion of permanent acceleration (2nd order change), etc. (re. "jerk" for 3rd order change).

In summary, even though time has somehow been defined in various ways in the fields of philosophy and physics, in MCS ontology it gains in clarity and compatibility with other entities crucial for natural cognition and automated cognition.

IV. HOW TO COPE WITH THE INFINITE COMPLEXITY OF REALITY?

Section II has shown that reality should be considered as infinitely complex. Yet, it appears that much can often be achieved in practice. So, what paradigms allow for such positive outcomes? The current section presents 5 of them, including the selection of (prioritized) goals, the pragmatic exploration of local circumstances, the generation of agents with some innate or wired initial capabilities, an iterative process improving performance, and the accelerated progress resulting from setting multiple, coordinated actions in parallel.

A. Necessity of selecting a goal

As illustrated in Figure 5, experience shows that numerous goals can be reached while ignoring most aspects of reality. Numerous simple ad hoc models prove effective. To the point where even bacteria not only survive in our often-hostile world, but even usually live well and multiply.

A basic paradigm consists in focusing attention on selected contexts, successively considering them with as many constraints as possible. A good example of this approach is notably the famous "hic et nunc – here and now" framework in Jesuits' case studies. Here, are some other typical cases: "under assumption", "with abstract and holistic views", "with more detailed analytical representations", etc.

Critical for success is the proper selection of a goal. A goal in practice always has a number of peculiarities that open possibilities for effective and simple modeling (re. also Figure 5). In AI, it is often said in substance that experts know what to ignore in a given situation.

For example, we have stated above what is the main goal of the research we refer to in this paper: to make possible the design of artificial cognitive agents effectively approaching human cognitive capabilities, with further possible positive impacts in three areas (see Introduction section). Toward this goal, an effective model implies in particular the proposed extensions of MCS ontology.

Some other, more intuitive arguments for selecting a goal include the following two:

- It may be useful to map in cognitive context the well established A* algorithm for navigation in space [10] crucial elements are the location of goal-site and the one of current position.
- As reality is infinitely complex, non-oriented efforts would get as diluted and ineffective as curry powder thrown in a river (re. Thai motto recommending humans to focus on selected goals).

B. Pragmatic approach adapted to circumstances

Careful attention must be given to "current" status, as the latter typically evolves. In a pragmatic way, we propose to start with the world as is, modeled as simply as necessary for reaching the considered goals. In cognition, backtracking is the rule. From the selected goal, specifications are derived, which then lead the cognitive process, and in particular an active perception ("exploration") faculty capable of acquiring useful information and the possible experience elements eventually allowing for improvements (re. Figure 7).

C. Innate goal and capabilities

A prominent place is initially given to innate and current capabilities (re. Figure 8).

In practice, it is precious to be aware that even humans do not start, individually, from scratch. At birth time, they already know for example how to grasp, crawl, find their food; these tasks are not necessarily obvious for a robot.

Some chicken for example have such an elaborate pre-design that they can be industrially grown without any social assistance; they can get out of their egg and develop without the help of previous generations.

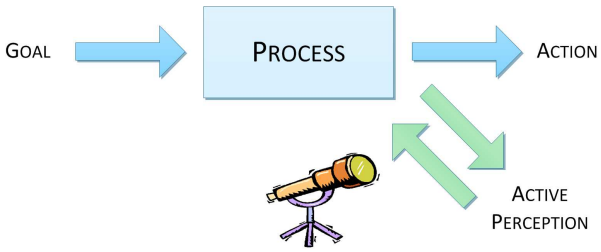

Figure 7. In cognition, backtracking is the rule. From the selected goal, specifications are derived, which then lead the cognitive process, and in particular an active perception ("exploration") faculty capable of acquiring the experience necessary for improvements.

Therefore, it is legitimate also for machine-based agents under study to start from some predefined (let us say "wired", or pre-programmed) initial state. And humans have created robots.

D. Improved goal and capabilities

In the paragraph about reality, care had been taken to keep things as simple as possible. Nevertheless, multiple cognitive processes, including some innate capabilities, and possibly newly acquired experience elements could already been mentioned, opening the way for improvements and learning.

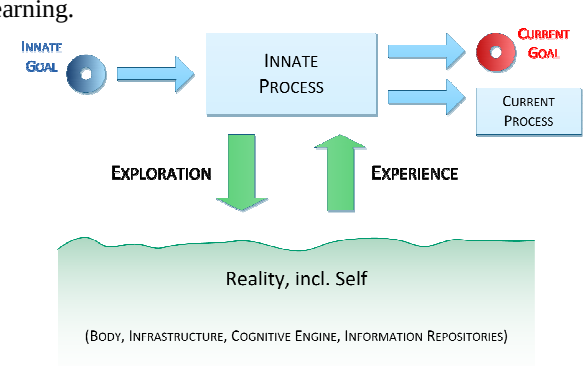

Figure 8. Current goals and processes may result from exploration performed and/or experience acquired by an agent running a given cognitive process in a certain domain of reality. Initial goals and processes are innate (or "wired").

The next interesting stage occurs when the design and creation of a new capacity to cope with reality is considered (Figure 9). For connecting directly to reality, chance (as in Darwin's theory,) or ingenuity (as defined in MCS ontology [5]) are the main keys.

E. Collective approach; elements of communication, credibility, reputation, and trust

Experience shows that the coordinated forces of multiple agents – groups- increase the possibilities of successful actions in the world.

This paradigm can be exploited in a multiplicity of ways. Of particular interest for our context, we find groups of humans, of robots, and of hybrid resources – robots cooperating with humans.

Groups have already been defined in MCS ontology. In this context a critical ingredient has been identified as the culture of the group, and, in reference to it, the communication channel and some kind of formalism, protocol or language.

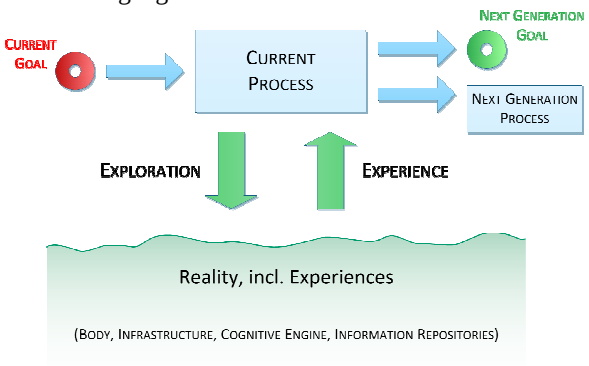

Figure 9. Current goals and processes may lead to improvements in next generation system (in particular for humans or machines).

Two new elements come now under scrutiny. The first one is, for inspiration, the case of baby communication, a case reasonably simple for the purpose of progressive transfer of approach to machine-based systems. The second one is the sharing of error probability of a source, among humans, which expands at group-level a feature already taken into account for individual cognitive agents.

In their early months of existence, babies appear to have at least 4 types of communication capabilities. In some circumstances, babies can express strongly (high arousal) their emotions [11], their states of happiness and unhappiness (positive or negative valence); they cry, or smile, which typically leads to corresponding correcting or sustaining actions from their parents. They also test the good understanding and adequacy of key behaviors and gestures by imitating, and mimicking; they also sometimes just synchronize with others in their attitudes and actions (they join in or trigger yawning, and laughing).

The MCS theory has introduced a value, in terms of probability of error, for cognitive agents delivering information. This affects the quantitative estimation of knowledge characterizing these sources. Now we can add a similar, interesting property at group level, which allows for appropriate propagation of the expected error-rate. In this framework, agents would take into consideration the credibility of sources and in particular of other group members; if shared at group level, this credibility could form the basis for, collectively, building up a reputation. Thus when receiving a message, such agents could associate to it a

trust value, based on reputation. Improvements would result in terms of modulation of risk-taking and in the respective weighting of multiple conflicting sources being integrated (fused).

V. DETAILED EXAMPLES IN COOPERATIVE ROBOTICS

Let us consider a typical test task of Robocup@Home (RaH) competitions, "Fetch and Carry" (F&C). In substance, team members can in particular talk to their robots, giving a hint about what to fetch (e.g., "a grey box"), and where it stands (e.g., "near the front door"); the robot should by then know enough about topology and navigation to be able to autonomously reach there, locate the object accurately enough to get it in the "hand", grasp it, lift it up, and transport it back to the starting location (re. Figure 10).

The results of Sections II and IV, including §A to E in the latter case can be illustrated here, both in human and in machined contexts.

A. *Illustration in human context*

In a first stage, a group of international experts have elaborated a rulebook where the general goal of designing systems useful for humans (re. to Section II, in short SII) is focused towards a domestic goal (re. to Section IV.A, in short SIV.A), and then backtracked into the specification of even more focused subgoals: elementary capabilities to be devised. One of them is the task called "Fetch and Carry", addressing a "natural" way for a robot to find, grasp and transport an object (SIV.A). This intermediary goal is then searched in parallel by multiple teams (SIV.E). This task adapts to local infrastructure (SIV.B) and is iteratively considered, year after year (SIV.C-D).

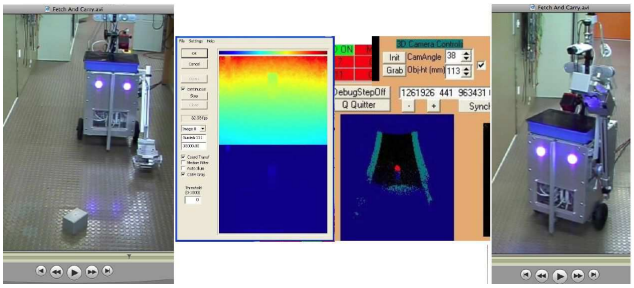

Figure 10. In the F&C task, our proprietary robot RH-Y uses in particular a vocal dialogue, a navigation capability typically using a ranger for navigation purpose, a time-of-flight camera for recognising and locating objects (*center*) and position and force controlled arm and gripper (*left and right*).

B. *Illustration in robotic context*

The demonstration system is real and thus very complex. An overview of the task can be seen on a video available online (e.g., [12]) and multiple aspects are presented elsewhere. Here we shall discuss a minimum of aspects for purpose of example.

Consider first as an analogy, the problem for a human to jump over a wall. This can be easily achieved, or may remain totally impossible, depending on how high is the wall; the metric height is critical. Similarly, in the cognitive world, properties must be precisely defined and metrically quantified in order to allow for meaningful descriptions and effective requirement estimation.

For the F&C test task, referees typically retain about 20 objects, which may be randomly put in 20 possible locations. Robots may more or less be wired with initial expertise, e.g., in terms of topologies and functions; a common culture is also defined ("names" of standard objects and locations are published on a wall one day or more before the test). Let us practice a quantitative estimation of requirements in terms of cognitive entities (re. concepts of Figure 2). Ignoring here many processes, such as e.g., word perception and recognition, or navigation and handling, let us focus on the cognitive task of understanding which object is where. The input space would consist in about 10 bits of information for each object and rough location specified. On this basis, at the most abstract level, one out of 20x20=400 possibilities should be resolved (i.e., about 9 bits) to know which object is to be fetched, and where it is roughly located. In this very minimal form, the necessary knowledge for correctly understanding the vocal dialogue amounts to approximately K=14 lin. With a dialogue lasting for 5 s, the amount of expertise for this cognitive task amounts to E=14/5=2.8 lin/s. Learning is demonstrated and can be quantitatively estimated on this domain: without dialogue the task cannot be achieved in the 5 min allotted to the task (roughly, K=0 lin, and therefore, E=0 lin/s), while with a successful dialogue, lasting for, say 5 s, E increases to about 3 lin/s. The MCS intelligence index is thereby of $i=3/5=0.6$ lin/s^2.

In the specified location (e.g., "near the door") the object is manually moved by referees by +/- 20cm just before the test, making it impossible for robots to have it fully (pre-) wired. Therefore exploration as in SIV.B is performed, using Time-of-Flight (TOF, distance) perception. Notice that here, as in most usual cases, the perception process features (or requires) a lot more knowledge and expertise than the above cognitive operation: in particular the input space includes here 176x144 samples, each with 1cm accuracy in a 500cm range, i.e., about 150'000 bits of information; similarly, the output stage is relatively large for successful trajectory specification (about 10'000 bits of output information), and the processing time is short (say, 0.1s).

Time is a very important feature for success, in many contexts of these applications (motor control, parallel agent management, sensor-based exploration process, etc.). In our proprietary "Piaget" environment [13], agents run in parallel, with very short, individually granted, time slots, lasting for about 100 nanoseconds each in average. Therefore, at low level, Piaget defines its own fine-grained time basis ("TicksPerSecond"); permanence quantities are estimated as numbers of scheduler cycles ("Ticks"), which individually last for about 1 microsecond in average. At higher level and for longer time increments (>10 ms) time is managed on the basis of the system clock, and is thereby compatible with the general culture, common to multiple robots and humans, that makes effective cooperation possible.

VI. CONVENTIONAL AI, COGNITION AND IMPLEMENTATION OF COGNITION IN THE REAL-WORLD

(Artificial) Intelligence is but one concept in a broader field, which is (Artificial) cognition.

AI has been addressed for half a century and longer (Turing 1950 [14]), yet no formal theory about it has been widely accepted today. Worse than that, experience shows that most people intuitively feel that, ultimately, intelligence is a property to be exclusively found in humans, implicitly thereby making AI, i.e., machine-based intelligence an empty set. As a stronger line of defense, the limits for this latter case are sometimes restricted to the frontiers of the so-called general intelligence.

The situation is really hard for conventional AI. Consider even some researchers who address explicitly the goal of designing intelligent machines (e.g., [15] Konidaris et al., 2012). They state their aim at bringing together intelligence and machines, implicitly stating once more that machines have no intelligence. A better concept and wording would be to develop the intelligent capabilities of machines.

In science and engineering, there have always been some researchers looking for integrated solutions, systemic answers. For this kind of people, in the case of AI in particular, beside the core aspects of world representation and information processing at a cognitive level, complementary aspects of autonomous implementation and immersion in the real world have also been part of the target. Some have even gone further to consider that cognition could only emerge from an autonomous, real-word, structure (e.g., discussion in [16]).

Traditional difficulties in providing a formal theory, or even simply in delineating an appropriate ontology for cognition may in particular have come from two major facts: first attention has traditionally been deviated from "what is it?" to "how to let it operate?"; and the second is that connection has not been sufficiently made to the well-defined information theory (consider e.g., [17]).

Now as developed above, with MCS theory, reality appears as infinitely complex and yet for selected goals, much simpler models can be effective.

VII. PIAGET FOR IMPLEMENTING COGNITION IN THE REAL-WORLD

Cognition has some interest per se, nevertheless, its main value relates to the ability to change the world. In this section, four aspects of this topic will be treated: the necessity of implementing automated cognition in the real-world, the strategy for ensuring the best possible design, the requirements for a new environment supporting development and control in this regard, and finally an overview of Piaget, which provides solutions in this context.

A. Necessity of implementation of cognition in the real-world

As discussed above, implementing cognition in the real world is a crucial requirement for smart machines. In our view input information for subsequent reasoning must be acquired – perception. And cognitive operations are useless if they do not yield results, information to be somehow converted into world changes – action.

Again, let us insist and remind the reader that if he/she dogmatically defines intelligence to be exclusively human, intelligent machines are obviously impossible. By this token, to *try* to merge intelligence and robots is the most that can be done, and do not hope for success. On the contrary, by the definitions we advocate above, experience shows that AI is not only feasible, but also in fact already largely deployed. So the merge has already been done, yet of course significant improvements are still clearly expected.

Notice first that cognition does not only imply information and knowledge, but also critically requires an engine – step 1 into the real world. In practice we have cognitive systems, in particular humans, or artificial cognitive systems (ACS).

And adding the perception and action capabilities to cognition is a second step into the real world. This already defines a robot; to be possibly augmented with some locomotion and communication capabilities.

Moving along this road, we have searched for the best possible design.

B. Strategy for the best possible design

The goal just stated in previous paragraph calls for a very complex system, embedded in the real world, and in particular operational in real-time, capable to address the most advanced applications in terms of automation and cognitive, human-related tasks.

To be tractable, the proposed system must be organized as a hierarchy of coordinated, specialized resources (e. g. Figure 11), contexts, and points of view, each being individually much simpler

Another element of strategy is, at all levels of the hierarchy, starting from the very top, to rely in as much as possible on existing elementary solutions – subsystems.

Here where lots of integration must be done, the first priority in selecting potential components, strangely, is less on the top functional capabilities of these elements than on their safe availability and operational robustness.

Possible candidates in terms of possible components may be found, from case to case, on the market, in scientific and technological publications, or other sources yet, including new proprietary developments.

C. Requirements for a new set: architecture and language

On day one, back in 1998, like today still, the system we aimed at could not be found, ready-made, on the market or in other labs. Nevertheless, more and more powerful components were being developed. At the hinge between these two realities, the first component to appear as necessary for our goal has been the design of a novel set, architecture and language, which we have called "Piaget" in reference to the famous psychologist of same name, recognized scientist of human cognition, who had made major contributions especially in the context of young children development. It is in fact a computer-based

environment, favorable for developing and intelligently controlling mobile cooperative agents and industrial robots.

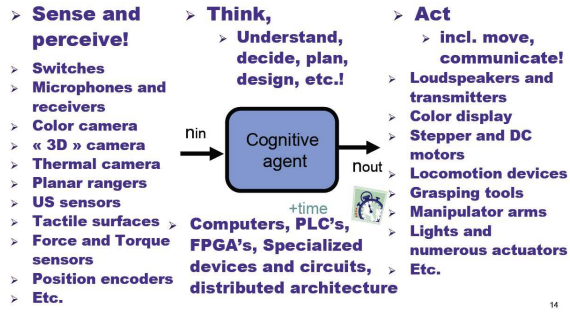

Figure 11. Smart systems sense, perceive, think and act. The table names some of the underlying physical resources we have been using in Piaget context.

D. Overview of Piaget

The "Piaget" concept for architecture and language has evolved in two or three major stages, and is described in detail in Dessimoz, Gauthey and Omori 2012 [13]. For convenience, a few elements about this concept are also provided in this paragraph.

Computers have been around for some time, as well as standard products in electronics, precision engineering and microtechnologies. Some of such major real-world components integrated in our intelligent robots with Piaget are shown in Figures 11 and 12.

The cognitive components of the processes involving the real-world resources of Figures 11 and 12 typically relate to large amounts of information (>> 1 Mb), and operate at high speed (up to 10^7 [1/s] and more).

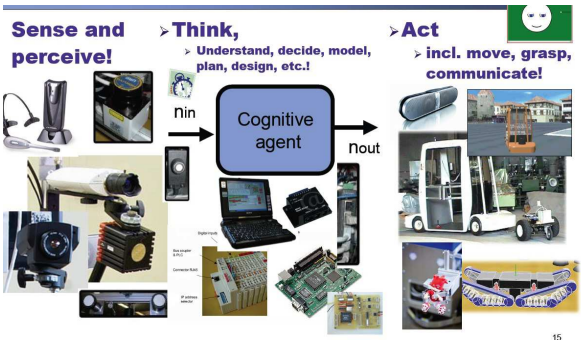

Figure 12. Smart cognitive systems sense, perceive, think and act. While the previous figure includes general names, the current one illustrates by pictures the corresponding elements. Other elements not shown here include Kinect sensor, Katana arm, Aldebaran NAO humanoid, and Kuka / Stäubli industrial robots for example.

The cognitive components of the processes involving the real-world resources of Figures 11 and 12 typically relate to large amounts of information (>> 1 Mb), and operate at high speed (up to 10^7 [1/s] and more).

The first crucial component that appeared to be missing though, was an application-oriented environment, with parallelism and real-time capabilities, and very open possibilities for integration of numerous, heterogeneous, products and services.

```
…..
11: SleepAGN(0.05);                                  break; case
12: if(!SignalIn(NSIStart))
      GoState(6);
    else
      GoState(20);                                   break; case
20: DemarrerMatchAGN();              // start 90 s timer etc.
                                                     break; case
21: SignalOutAGN(NSOAspirateur, true) ;  // start motor vacuum
                                                     break; case
22: SignalOutAGN(NSORouleauIN, true) ; // start motor brush
                                                     break; case
23 : ApproAGN(HoleNb1, 15);                          break; case
24: MoveAGN(HoleNb1);                                break; case
25: MoveAGN(Trans(173,90,-90));                      break; case
26: ObserverLigneAGN(NL, NCStart, NCStop)  //  Visual analysis of a row
    if (N2Jaune>0)                  // totems are yellow; balls are white
        {PositionTotemOuBalle[1].TypePosition=Totem;
        nbTotem = nbTotem+1;}
        else
        PositionTotemOuBalle[1].TypePosition=Balle;
                                                     break;  case
27: …
```

Figure 13. Example of instructions in Piaget language.

In Piaget instructions are numbered (re. Figure 13). A meta-level program counter is defined for each task and is typically realized in the implementation, lower level language as a switch paradigm. A possible "AGN" suffix explicitly indicates, when present, that, for the next allocated time slot, the program proceeds at the next numbered Piaget instruction.

Our applications make typically use, on the supervisory computer, of about 20 parallel agents. And experience shows that common, current computers can in average visit (enter, do the work, and step out) each task in a single 100 nanosecond long time slot.

The Piaget language includes in principle very specific, application-oriented instructions, such as for example the "ChooseTheBridgeVisually" instruction. It has been found useful also to integrate in it a kind of subset of the excellent VAL language for robotics, derived from AL [18]. This decision brings two main advantages: 1. VAL keeps a relatively general view at robotic and automation level (e.g., "Signal i" instruction to turn on the digital output number i), useful for the early phase of a new application. And 2. this paves the way to a common standard for novel, mobile agents and classical, industrial robots. Val can be traced back to the beginning of industrial robotics, or even further to the above-mentioned AL language, and keeps evolving.

Piaget supports direct and inverse kinematics as well as extensive support for transformation and frame ancillary computations, in matrix form and homogeneous coordinates. Motion control is typically hierarchized in three levels: programming, coordination and joint control, with elementary cycle speed respectively situated at about 500, 15, and 0.5 milliseconds.

Now Piaget is typically running on a heterogeneous system including powerful components in principle interconnected with Ethernet and TCP-IP capabilities; due to lack of availability in this standard, quite a few resources are similarly connected in a complementary, USB mode. At supervisory level, a PC in Windows context is the rule, still for reasons of compatibility with complementary existing resources (e.g., Figure 14 for interactive "cockpit"). Closer to physical action, we can see specialized components such as servo-controllers, PLC, cameras, rangers; and the latter typically provide their own information processing resources, with power and robustness, in their own environment (re. Figure 15).

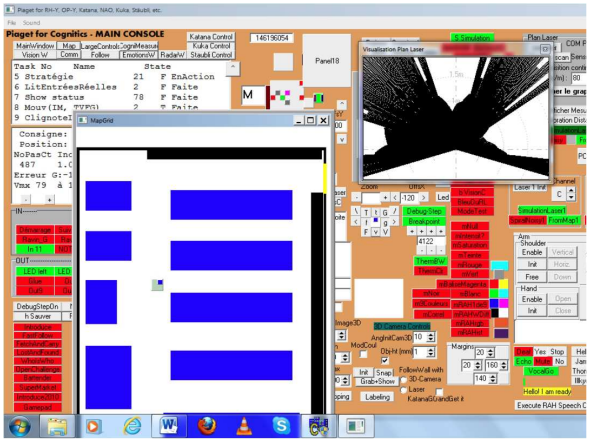

Figure 14. Example of main screen in interactive Piaget context, along with more specialized forms (map of environment and polar ranger data).

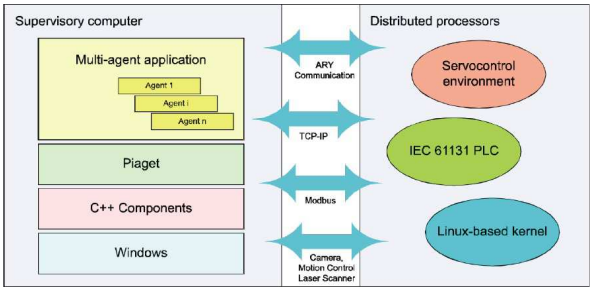

Figure 15. The high cognitive and action requirements of our complex applications in the real world require a great sophistication of structures, and a contingent heterogeneity of resources, communication channels, and protocols.

Piaget has a number of interesting, original features, and some of them are the following: extensive simulation capabilities, easy interactive actions (interpreted language elements), progressive levels of programming techniques, and various degrees of inter-cooperation performance.

The various levels of programming makes it very easy for less expert users to define new strategies, as is regularly required in matter of hours (and sometimes minutes!) in world-level competitions (for more demanding development work though, such as, typically, implementing Piaget on a new platform, OS, language, the effort is similar to usual software engineering). The open architecture allows quite effortless to reuse specialized subsystems and software packages.

VIII. Examples and Proven Results – Cognitics and Piaget

This section provides 3 sets of exemplary applications developed and driven by Piaget, of examples in automated cognition, in cognitics (or AI, in classical terms, deployed in the real-world). The first ones reflect two of the main successive application areas of Piaget: Robocup@Home [19] [20], and industrial robotics; the last one highlights the ease of estimation in quantitative cognitics (re. Dessimoz 2011 [5]) as supported in Piaget. Some prominent concepts of MCS are illustrated below, but of course not all of them can be illustrated here; they have also been validated though.

A. Piaget and cognitics for intelligent robots in Robocup@Home competitions

Piaget had concretely first been created for Eurobot competitions. On the other hand, industrial robotics, computer vision and classical AI techniques had been practiced in R&D initiatives, projects and ad hoc curricula (e.g.. Figure 16). Then those fields somehow converged in a project adopting the common goal of the Robocup@Home league.

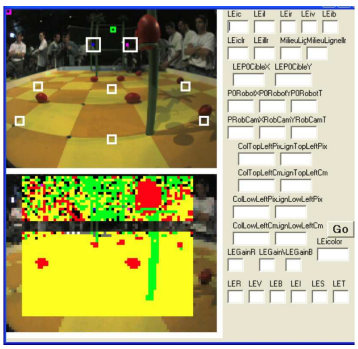

Figure 16. Early skilled competences in Piaget environment included the fast visual perception of colors and recognition of objects, as well as coordinate transforms from picture onto field, as illustrated here, as well as, not shown here, the 300 times per second localization of opponent robot.

Moving to Robocup@Home called for more complexity, in particular as a result of merging into less structured environment (home), and because of the necessity of cooperation, moreover in a "natural" way, with humans.

Figure 17 illustrates vocal and dialogue management as typically supported in Piaget environment and language, as well as vision-based face recognition. At the moment the screen is frozen, we are between recognized sentences; a recognized vocal sentence could be for example "Go to door". If "echo" is selected, the robot will typically confirm:

"I have heard: go to door", and if this is critical, the dialogue manager will ask for a confirmation ("is this correct?").

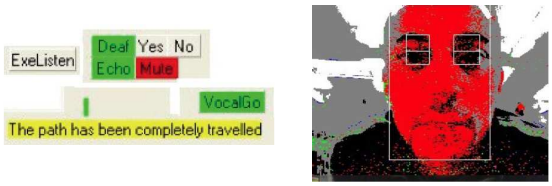

Figure 17. On the left, Piaget panels and text-typed fields illustrate typical vocal dialogues: e.g., recognized commands are shown in green (here " ") and synthetized text in yellow; yes/now buttons can at will simulate microphone inputs. On the right a face is recognized for "Who is Who" test.

Advanced tests in terms of cognitive capabilities and human robot interaction capabilities have been demonstrated in Robocup@Home world competitions, e.g., "CopyCat": programming by showing – the robot learns what to do; (Figure 18) and "FastFollow": leading and training a robot in new homes just by walking –the robot learns a path, and can for example guide the human back to the starting point; "OpenChallenge": in Singapore our robotic group included three coordinated robots, and in particular a humanoid for the purpose of mediation between human and machines (Figure 19).

Figure 18. On the left, RH-Y robot visually analyzes and immediately replicates each of the object displacements manually performed by President Asada. On the right, RH-Y moves fast, following its guide, crossing another team, and completing first the imposed visit of a home.

Figure 19. "Open Challenge" (Robocup@Home world competition, Singapore). Nono, a NAO-typed robot, discusses with "Daniel", moves on OP-Y platform and then calls RH-Y, which brings drinks and snacks. Application developed and programmed in Piaget

Like for Eurobot competitions, in Robocup-at-Home contests, results have always been reasonably good, in both cases reaching the 4th place in rank for the best year. Many videos of past competitions are available, on our server and/or on YouTube.

B. Piaget and cognitics for intelligent robots in industrial applications

Industrial applications can also been driven by Piaget. Figures 20 and 21 illustrate two cases, the former one involving a Staubli robot and the latter one a Kuka.

Figure 20. "Chip count and accuracy test": Application mostly developed and programmed in Piaget, including the industrial robot arm visible on the picture and other resources: optical fiber, PLC, camera, motorized rotating table, servocontroller, Ethernet switch, PC and other components yet.

In both cases, the robot arms are driven, at elementary, lowest level, by manufacturers' controllers (incl. KRL for Kuka; Val3 for Stäubli) and, at higher levels, by a program developed in Piaget environment and expressed in Piaget language.

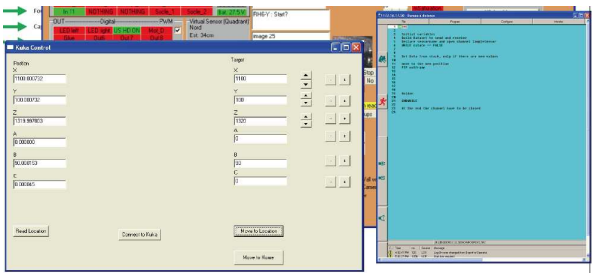

Figure 21. Three windows relating to an industrial application involving a Kuka robot (The first two belong to Piaget environment; the third one is a remote desktop linked to Kuka controller).

Piaget supports fast and robust vision, in many modes (infrared/BW, color, thermal, 3D-time of flight sensors; various processes).

C. Integrated capabilities in Piaget for quantitative estimation of cognitive properties

A particular interest of Piaget environment is to provide a tool for convenient, quantitative estimation of core cognitive properties: knowledge, expertise, experience, speed/fluency, intelligence, as well as low-level ingredients: probability

calculus, quantization, sampling rate, input and output information signals and quantities, all this along with an interactive example (Figure 22).

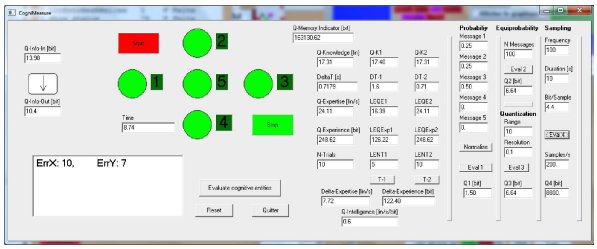

Figure 22. Piaget environment includes a form for the quantitative estimation of cognitive properties in general, along with a specific example: learning how to accurately click in the center of 4 targets.

IX. COGNITION AND PHILOSOPHY

Cognition was given ontology above, including notably definitions for time, reality and wisdom. This overlaps to a large extent with domains of interest in classical philosophy though. Nevertheless, each fields retains important distinctive properties. This section suggests that a cross feeding of results achieved in the respective fields mutually helps and it shows some concrete examples in this regard.

Philosophy literally means "love of wisdom" and was used in Ancient Greek to refer to any pursuit of knowledge [21-24]. In that era, the field was very broad, including not only core cognitive elements, such as formal logic and syllogisms but also domains considered today on their own, such as physics, sciences and politics. In fact even today philosophy keeps the universal view, and in this sense keeps including the latter domains, though in their most abstract forms only.

On the other side advances in tools and techniques have progressively led to automation and, more recently, out of necessity, to a formal and quantitative theory of cognition. In this evolution, the scientific approach has led to epistemic observation and a theory including axiomatic definitions of core concepts and the proposal of related metrics [5] [25-27]. Cognition is essentially the faculty to deliver correct information, ensured by specific internal structures and operative flows, typically processing information rationally, with high performance levels, for example in terms of complexity, knowledge, abstraction, learning, or expertise. While historically rather exclusively considered in human context, cognition is also, today, and increasingly, concerning man-made artifacts (re. artificial cognition, traditionally commonly described as AI).

In philosophy, cognition is central, and yet as the etymology of the former word can doubly prove it, philosophy is much more than that. Interestingly, Thomas Aquinas has formally distinguished behavior in two main categories. While indeed the cognitive category is one of them, there is also a decisive other one, which encompasses the affective components, feelings and emotions [28]. Precisely with the notions of « love » and « wisdom », philosophy strongly refers to non-cognitive components: the former case is evident, love is a feeling; the latter case requires more explanations. Wisdom is a specific property of cognitive agents, referring to their ability to take good decisions (to be expert in delivering the messages that make agents reach a given goal); here at least two problems remain out of cognitive reach: which goal is appropriate? And are the required non-cognitive components, necessary to reach the goal, also ready for action (e.g., availability of energy, affects, physical elements or social partnerships)?

In consequence, philosophy is necessary for addressing problems at both ends of the reasoning chain, typical of cognitive processes: 1. the intuitive, experimental process extracting initial, axiomatic data and model features from reality; 2. the selection of relevant goals (re. ethics and, ultimately for humans, the choice of individual roles in universe).

Reciprocally, as is shown below in five points, the formal framework initially developed for advances in machine-based cognition, with means for quantitative assessments, suggests that other distinctions can be beneficial and allow for a novel clarity of many philosophical issues.

Rational, cognitive processes, for humans as for machines, can only develop in formal, well-defined structures that finally remain necessarily extremely simple with respect to reality; they develop in the scope of ad hoc models. Figure 5 above has qualitatively illustrated the fact that the simplicity of models has a huge cost: a similarly extreme restriction in terms of respective goals that any model can help to reach. The mentioned framework for cognitive sciences quantitatively defines complexity (and in an analog way, simplicity) as a direct function of the quantity of information (for which quantitative assessment is well-founded). Everyone knows that models are never complete with respect to reality, but going quantitative shows that the ratio in their complexities with respect to reality tends to zero (“zero–plus”?). This has tremendous consequences in philosophy: in particular what debate with respect to truth can be meaningful? How not to underestimate the importance of goal setting? The fact is that faith cannot, ultimately, be the defense of any truth, but in priority should represent adherence to a certain freely chosen goal.

Research in cognition has brought other, new results in terms of system granularity and group nature. A similar scheme can repeatedly be observed at very different scales, whereby apparently “individual”, autonomous systems can appropriately be merged thereby yielding the emergence of a new holonic entity (a “group”), or on the contrary those same structures can be observed as coherent, collective entities (i.e., as ”groups” as well), and consequently be analyzed in finer cooperating substructures. In particular, from a cognitive perspective, much of the paradigm is similar 1. as neural networks cooperate at brain/body level (re. “thinking”), and 2. as individual agents cooperate at a collective, higher level, yielding a group behavior (re. “society”).

Experience shows that the effective, integral capability of groups is not always guaranteed, at any level, and the challenge gets more serious when, as is most of the time the case, a same resource may simultaneously be part of multiple groups, of different “cultures” and boundaries. Consider for example the risk of schizophrenia and possibilities of

membership conflicts for a human involved in several allied families, an employing company, various friendship circles, one or multiple religious entities, political parties cooperating in broader, secular frameworks, spaceship Earth, etc.

A particular advantage of automated cognition is that it allows theory in cognition to be operationalized. Coherence between a theory and the corresponding praxis has probably never been so close to guarantee. The very equations and structures that describe a cognitive phenomenon can now be computed in real-time and used to guide actions accordingly in the real world, as embedded computers and cooperating robots start routinely to do so.

Research in automated cognition has brought further, crucial results in terms of system dynamics. Careful, quantitative estimations and specific structural aspects can for example detect instability conditions and may call for changes in organization, such as granting autonomy to selected subsystems. Consequences can be drawn with benefits in the context of social philosophy. Reciprocally, it is also true that classical models in philosophy can help design novel automated systems featuring machine cognition (including AI).

X. CONCLUSION

Designing advanced cognitive technologies and applications requires a formal ontology, such as the MCS Model for Cognitive Sciences, the theoretical foundations now proposed for automated cognition, cognitics. Cognition has the ability to create and deliver pertinent information, both for the case when it is embedded in humans, and also for the case when it is machine-based, automated (re. « cognitics » in this latter case).

Starting in a pragmatic way from where we stand, in particular with humans creating robots, progressing with distributed axioms, navigating through small contexts in direction of selected goals (the design of high performance machines, of robots cooperating with humans, and a better understanding of cognition in humans), we adopt a constructivist approach in conceptual framework and validate them gradually by making them operational in test tasks.

Past works had taken for granted that reality and time were notions evident for everyone. Now, at the moment of attempting a practical implementation of those notions in robots, the situation is quite different. Early results in the context of MCS theory had made it clear that reality is infinitely complex, practically out of reach for cognition, under condition of exhaustivity.

Discussion has been made above of a number of cognitive notions including those of reality, time and revisited “speed”, change and discontinuity, innate and learned behaviors, as well as the human-inspired basics of communication in a group. These newly defined notions conveniently complement the existing MCS ontology. Notions are delineated in conceptual frameworks and can moreover be made operational, deployed in the real world, for validation purpose and for the benefit of users. All these elements confirm the rightness of our current approaches in solving concrete Artificial Intelligence problems and this is illustrated below by some concrete examples taken in domestic context, including robots capable of learning.

Further research has been performed and the current paper could sketch ways to cope with the infinite complexity of reality. Several other cognitive notions could also be newly discussed, including those of time and revisited “speed”; change and discontinuity; innate and learned behaviors; as well as the human-inspired basics of communication in a group. On the basis of the proposed MCS ontology, and taking often advantage of innate/wired expertise, it can be concluded that robots can be effectively deployed in quantitatively bound domains, as illustrated in several concrete examples.

Cognition would not make much sense per se, and the paper has also shown how it can be implemented in the real world, notably using Piaget, our proprietary environment for development and programming of smart robotized systems. Experiments prove that the resulting smart systems can indeed successfully operate in the real-world, and in particular interact with humans, performing with large quantities of cognitive components: knowledge, expertise, learning, etc.

The quantitative approach of MCS and the operationalization of its cognitive concepts in real-world systems allow as well for an effective design and realization of smart systems for the benefit of humans as a fruitful dialogue about core issues in philosophy.

ACKNOWLEDGMENTS

The authors acknowledge the contributions of numerous engineers, interns and students, as well as the support of various research funds, private companies and technical services in our university HEIG-VD, who have more or less directly contributed to the reported project. In particular, this year, Neenarut "Nann" Ratchatanantakit, and Panuwat “Jarr” Janwattanapong can be mentioned.

REFERENCES

[1] Jean-Daniel Dessimoz, Pierre-François Gauthey, and Hayato Omori, "Some New Concepts in MCS Ontology for Cognitics; Permanence, Change, Speed, Discontinuity, Innate versus Learned Behavior, and More", Cognitive-12, The 4th International Conference on Advanced Cognitive Technologies and Applic., Nice, France, July 22-27, 2012.

[2] Shannon, C. E. , A mathematical theory of communication. in: Bell System Technical Journal, Vol. 27, 1948, pp.379-423, 623-656.

[3] Bernard Claverie, “Cognitique - Science et pratique des relations à la machine à penser”, Editions L'Harmattan, 2005, pp. 141.

[4] Jean-Daniel Dessimoz, "Cognition Dynamics; Time and Change Aspects in Quantitative Cognitics", Second International Conference on Intelligent Robotics and Applications. Singapore, 16 - 18 December, 2009; also in Springer Lecture Notes in Computer Science, ISBN 978-3-642-10816-7, pp. 976-993.

[5] Jean-Daniel Dessimoz, "Cognitics - Definitions and metrics for cognitive sciences and thinking machines", Roboptics Editions, Cheseaux-Noréaz, Switzerland, ISBN 978-2-9700629-1-2, pp. 169, January 2011, also, http://cognitics.populus.ch.

[6] Wisspeintner, T., T. van der Zant, L. Iocchi, and S. Schiffer, "RoboCup@Home: Scientific Competition and Benchmarking for Domestic Service Robots", Interaction Studies, vol. 10, issue Special Issue: Robots in the Wild, no. 3: John Benjamin Publishing, pp. 392--426, 2009.

[7] Frederick Charles Copleston, “A history of philosophy”, Volume 6, Continuum International Publishing Group Ltd.; Édition : New edition, June 5, 2003, pp. 528.

[8] Alexander Rosenberg, “Philosophy of science: a contemporary introduction”, Routledge comtemporary introductions to philosophy, 2005

[9] George E. Hein, “Constructivist Learning Theory”, The Museum and the Needs of People CECA (International Committee of Museum Educators) Conference, Jerusalem Israel, 15-22 October, Lesley College. Massach., USA, 1991.

[10] Hart, P. E.; Nilsson, N. J.; and Raphael, B., "A Formal Basis for the Heuristic Determination of Minimum Cost Paths", IEEE Transactions on Systems Science and Cybernetics SSC4 4 (2), pp. 100–107, 1968.

[11] Julie A. Jacko (Ed.), “Human-Computer Interaction. Novel Interaction Methods and Techniques” 13th Internat. Conf., HCI Internat. 2009, Proc. Part II, San Diego, CA, USA, Springer.

[12] http://rahe.populus.ch/rub/4 , last downloaded on June 3rd, 2012.

[13] Jean-Daniel Dessimoz, Pierre-François Gauthey, and Hayato Omori, "Piaget Environment for the Development and Intelligent Control of Mobile, Cooperative Agents and Industrial Robots", accepted for publication, ISR 2012, International Symposium for Robotics, Internat. Federation of Robotics, Taipei, Taiwan, Aug.27-30, 2012.

[14] Turing, A. M. “Computing Machinery and Intelligence”, in: Mind, New Series, Vol. 59, No. 236, 1950, pp. 433-460.

[15] Konidaris, George, Byron Boots, Stephen Hart, Todd Hester, Sarah Osentoski, and David Wingate, Org., Designing Intelligent Robots: Reintegrating AI, AAAI Spring Symposium 2012, March 26th-28th, Stanford University

[16] D. Vernon, G. Metta, and G. Sandini. A survey of artificial cognitive systems: Implications for the autonomous development of mental cap- abilities in computational agents. IEEE Transaction on Evolutionary Computation, 11(2):151–180, 2007.

[17] Z. W. Pylyshyn. Computation and Cognition (2nd edition). Bradford Books, MIT Press, Cambridge, MA, 1984.

[18] Goldman, R. “Recent work with the AL system”. Proceedings: Fifth Annual Conference on Artificial Intelligence. M.I.T., 1977.

[19] Kitano, H., M Asada, Y Kuniyoshi, I Noda, and E. Osawa, “Robocup: The robot world cup initiative”, AGENTS '97 Proceedings of the first international conference on Autonomous agents, ACM New York, NY, USA ©1997

[20] van der Zant, T. and Thomas Wisspeintner, « RoboCup@Home: Creating and Benchmarking », Tomorrows Service Robot Applications , Robotic Soccer, Book edited by:Pedro Lima, ISBN978-3-902613-21-9, Itech Educationand Publishing, Vienna, Austria, pp.598, December 2007

[21] Philosophy - Wikipedia, the free encyclopedia, http://en.wikipedia.org/wiki/Philosophy,Retrieved2011-08-06.

[22] "Philosophia, Henry George Liddell, Robert Scott, "A Greek-English Lexicon", at Perseus" (http://www.perseus.tufts.edu/hopper/text?doc=Perseus%3Atext%3A1999.04.0057%3Aentry%3D%23111487&redirect=true). Retrieved 15.05.2013.

[23] "Online Etymology Dictionary". Etymonline.com. http://www.etymonline.com/index.php?search=philosophy&searchmode=none. Retrieved 15.05.2013.

[24] The definition of philosophy is: "1.orig., love of, or the search for, wisdom or knowledge 2.theory or logical analysis of the principles underlying conduct, thought, knowledge, and the nature of the universe". Webster's NewWorld Dictionary (Second College ed.). Retrieved 15.05.2013.

[25] John McCarthy, What is Artificial Intelligence?, rev. 12 Nov. 2007, http://www-formal.stanford.edu/jmc/whatisai/whatisai.html , Retrieved 15 May (2013).

[26] T. Fong, I. Nourbakhsh, and Kerstin Dautenhahn, “A survey of socially interactive robots”, Robotics and autonomous systems, 2003, Elsevier

[27] John Child “Organizational structure, environment and performance: the role of strategic choice”, Sociology, 1972

[28] Cognition - Wikipedia, the free encyclopedia, http://en.wikipedia.org/wiki/Cognition, Retrieved 15.05.2013.

Reducing Requirements Defect Density by Using Mentoring to Supplement Training

John Terzakis
Intel Corporation, USA
john.terzakis@intel.com

***Abstract*—In a previous short paper [1], data demonstrating that using mentoring to supplement training had a significant impact on reducing requirement defect density levels from initial to final versions of requirements specifications for a software product was presented. This paper provides additional details of the initial training, mentoring and review methods delivered by the requirements Subject Matter Expert (SME). In addition, data from a third generation of the requirements specification is now available, which supplements the existing defect data from the earlier two generations. Requirements authors typically receive little formal university training in writing requirements. Yet, they are expected to write requirements that will become the foundation for most future product development. Defects introduced during the requirements phase of a project impact multiple downstream work products and, ultimately, product defect and quality levels. Many companies, including Intel Corporation, have recognized this skills gap and have created requirements training classes to address this issue. While effective in providing the fundamentals of good requirements writing, much of this knowledge can be misapplied or lost without proper mentoring from an experienced requirements SME. Our experience over the last decade at Intel has found that adding SME peer mentoring improves both the rate and depth of proper application of the training, and improves requirements defect density more than training alone. The data from case studies across three generations of a software product will expose the issues with training alone and the benefits of combining training with SME mentoring in order to reduce requirements defect density levels. All three generations of requirements specifications achieved at least a 90% reduction in requirements defect density from initial to final releases.**

Keywords-requirements specification; requirements defects; requirements defect density; training; mentoring; multi-generational software products.

I. INTRODUCTION

This paper is an extension of a previous short paper [1] that presented data demonstrating the benefits of using mentoring by an experienced requirements SME to supplement requirements training. Details of the training materials, additional mentoring and review examples and additional defect density data from a third generation of the software requirements specification will be presented.

While bachelor's degrees exist for a variety of Engineering disciplines, degrees and even undergraduate courses in Requirements Engineering are scarce. Primary requirements authors (those whose primary role is to elicit and write requirements) may have some training. However, secondary authors (those whose primary role is architecture, development, testing, etc.) may have little or no requirements training. As Berenbach, et al, state "Requirements analysts typically need significant training, both classroom and on the job, before they can create high-quality specifications." [2] To close this skills gap, many companies have created in-house requirements courses or contracted third-party trainers to teach the basics of well-written requirements. Many are based on the IEEE 830 standard, [3], or the good, practical books published in the field over the past fifteen years [4][5]. At Intel, in-house requirements courses have been taught to over 15,000 employees since 1999. While useful for providing an initial understanding of the issues and challenges of requirements authoring, the knowledge gained through these courses can be misapplied or lost due to the inexperience of authors in writing effective requirements. By pairing them with an experienced requirements SME, the authors can be provided with early feedback on the deficiencies of their requirements.

This paper is organized into six sections. Section I is the introduction. Section II reviews the requirements training materials in detail. Section III discusses the backgrounds of the authors and the review process for the requirements. Section IV provides information on trust, early requirements samples and mentoring. Section V presents the requirements defect densities for all three requirements specifications. Section VI analyzes the data and derives conclusions based on the data.

II. REQUIREMENTS TRAINING MATERIALS

The requirements authors attended a training session on requirements writing (some details of which are available publicly [6]) prior to beginning work on the Software Requirements Specification (SRS) for their generation of the software. These training sessions focused on the issues with natural language, attributes of well-written requirements, a consistent syntax for requirements and an

introduction to Planguage ("Planning Language") [7]. This training class was a full day in length.

The training begins with the purpose of requirements. Specifically, requirements help establish a clear, common, and coherent understanding of what the system must accomplish. Clear means that all statements are unambiguous, complete, and concise. Common indicates that all stakeholders share the same understanding. Coherent ensures all statements are consistent and form a logical whole. Given the number of people that consume requirements and their differing experiences and backgrounds (SW, HW, testing, etc.), it is essential to project success to create a set of requirements that produces this clear, common and coherent understanding of what is being architected and designed. Without this, assumptions will be made and differences of interpretation will form leading to defects, rework, and schedule slips. A defect is defined as a mistake in a work product (SRS, code, etc.). Defects can be caused from lack of knowledge, lack of attention or both. Minimizing defects improves product quality.

A good analogy is building a house. If a house is built with improper specifications and with shoddy workmanship (i.e., a poor foundation), it will likely be unstable and require "propping up" (rework) to improve its stability. Similarly, a software product built with a poorly written set of requirements (i.e., high defect rate) will also be unstable and require "propping up" (defect fixes) to stabilize it. An unhappy customer is the likely result in both cases.

The class continues with a discussion of natural language, the language used in everyday conversations and writing (e.g., emails and other correspondences). It is typically the easiest form of language to learn and usually requires no formal training. Infants learn natural language by listening and repeating the words spoken by their parents or siblings. While this is true for any language, the training (and this paper) focuses on the natural language of American English.

While easy to learn, natural language presents a plethora of issues for requirements. These issues include ambiguity, weak words, unbounded lists and grammatical errors. Ambiguity occurs when a requirement can have multiple interpretations. Weak words lack a precise or common meaning (i.e., they are subjective). Unbounded lists have no beginning, no end or lack both. Grammatical errors include improper verb selection, using a slash (e.g., does read/write mean "read and write" or "read or write"), compound statements and passive voice.

Here are few examples that demonstrate the issues with natural language:

The software should log invalid access attempts.
Issue: "should" implies that this is optional

The software shall be easy to install.
Issue: "easy to install" is subjective

An error report shall be generated.
Issue: passive voice—who or what is generating the error report?

The software shall support 25 or more users.
Issues:
- "support" is a weak word, i.e., it lacks a precise meaning
- 25 or more is an unbounded list (there is no upper limit)

In order to reduce the issues with natural language, the class next presents the ten attributes of well-written requirements. They are listed in Table I below.

TABLE I: 10 ATTRIBUTES OF WELL-WRITTEN REQUIREMENTS

Attribute	Attribute
Complete	Prioritized
Correct	Unambiguous
Concise	Verifiable
Feasible	Consistent
Necessary	Traceable

A requirement is **complete** when development can proceed with minimal risk of rework or wasted effort. If a requirement is not complete enough, the development team will have to make assumptions about its meaning. These assumptions can lead to differences of interpretation among architects, coders and testers, which will result in a higher number of defects being filed by the testing team, and ultimately to inefficiency and unnecessary work.

Not Complete: *The software shall allow some number of incorrect login attempts.*

Complete: *When more than 3 incorrect login attempts occur for a single user ID within a 5 minute period, the software shall lock the account associated with that user ID until reset by the administrator.*

A requirement is **correct** when it has been reviewed by stakeholders and SMEs (both technical and requirements) and any errors have been fixed. These reviewers should ensure that the requirement is accurate and does not contain invalid assumptions, logic errors, typos, or conflicts with internal documents or industry specifications.

Not Correct: *The software shall calculate the area of a triangle as the base multiplied by the height.*

Correct: *The software shall calculate the area of a triangle as one-half of the base multiplied by the height.*

A requirement is **concise** when it conveys its intent as succinctly as possible. A requirement is not concise if it contains more words than necessary, multiple requirements

("ands" or multiple sentences), or superfluous information (opinions, rationale, etc.). A concise requirement is written using the least number of words needed to express its intent.

Not Concise: *We've had a lot of negative feedback about the format of the current local time. It is now displayed only in 24 hour format. We should have a configuration menu option to select 12/24 hour format.*

Concise: *The configuration menu shall display an option to display the current local time in either 12 hour or 24 hour format.*

A requirement is **feasible** if it can be shown to be implementable. Feasibility can be demonstrated through implementation in previous products, simulations, analysis and prototyping. Evolutionary requirements, those based on pre-existing, verified requirements, are typically easier to prove feasible. Revolutionary requirements, those that have no current basis for development, will require a much more thorough analysis by experienced architects and developers.

Not Feasible: *The software shall allow an unlimited number of concurrent users.*

Feasible: *The software shall allow a maximum of two thousand concurrent users.*

A requirement is **necessary** when it is needed from a customer, stakeholder, business or competitive perspective. These requirements may have been gathered during an elicitation process (internal or external), included as part of a strategic roadmap or business plan, required as the result of a competitive analysis or created to provide a product differentiator. Requirements that are not necessary create wasted effort and bloat project budgets.

Not Necessary: *The software shall be distributed on magnetic tape, 5.25 inch floppy disks, 3.5 inch floppy disks, CD-ROM and DVD media.*

Necessary: *The software shall be distributed on DVD media.*
Rationale: DVD media listed as the top choice for distribution based on feedback from our top 50 OEMs.

A requirement is **prioritized** when it is assigned a rank or order level relative to other requirements. Priority can be determined by a number of factors including value, risk, development time, project cost, and resources required. Priority levels are typically on a three point (High, Medium and Low) or five point scale (1 = Highest and 5 = Lowest). An alternative is to rank each from 1 to n, where n is the total number of requirements. However, this method is usually eschewed by most development teams if there are more than fifty requirements due to the time required to assess and assign a unique value to each.

Not Prioritized: *All requirements are critical and must be implemented.*

Prioritized: *80% of requirements High, 15% Medium and 5% Low.*

Priority is an important attribute for requirements to possess. Too often, all requirements are deemed "critical". If the schedule slips, the team has no basis for determining which requirements can be postponed to a future release since all are of equal priority.

A requirement is **unambiguous** when it has the same meaning for everyone. Since requirements will be read and utilized by many different stakeholders, writing them unambiguously is critical to achieving a common understanding. Each stakeholder has a different background and experience level, so the requirements must be written with precise language that is not open to different interpretation. All subjectivity must be removed.

Ambiguous: *The software must install quickly*

Unambiguous: *Where using unattended installation with standard options, the software shall install in under 3 minutes 80% of the time and under 4 minutes 100% of the time.*

A requirement is **verifiable** if it can be determined that the requirement will be or has been implemented properly. This can be accomplished in a number of ways including prototyping, analysis or testing. A requirement is not verifiable if it is incomplete, incorrect, not feasible or ambiguous, so there is a dependency on some of the other attributes.

Not Verifiable: *The user manual shall be easy to find on the DVD.*

Verifiable: *The user manual shall be located in a folder named "User Manual" in the root directory of the DVD.*

A requirement is **consistent** when it does not contradict any other requirements or documents. This is an attribute that must be evaluated for against the entire set of requirements, not just an individual requirement. The consistency test must be applied to other requirements, roadmaps, internal specifications and industry standards. Of all the attributes of a well-written requirement, this one is the most difficult to determine because of all the interrelationships that must be examined.

Not Consistent:
#1: The user shall only be allowed to enter whole numbers.
#2: The user shall be allowed to enter the time interval in seconds and tenths of a second.

Consistent:
#1: The user shall only be allowed to enter whole numbers except if the time interval is selected.
#2: The user shall be allowed to enter the time interval in seconds and tenths of a second.

A requirement is **traceable** if it has a unique and persistent identifier. Unique means that each requirement has its own identifier and there are no duplicate names. Persistent indicates that an identifier, once associated with a requirement, can never be used for another requirement. Traceability allows requirements to be linked to other design artifacts like use cases, test cases and even source code. Many requirements management tools automatically assign these identifiers.

Not Traceable: *The software shall prompt the user for the PIN.*

Traceable: *Prompt_PIN: The software shall prompt the user for the PIN.*

Many of these ten attributes are interrelated. For example, a requirement cannot be complete if it is ambiguous. Likewise, a requirement cannot be correct if it is not verifiable. With the exception of consistent, each requirement can be evaluated individually relative to the nine other attributes.

In order to provide consistency, the Intel requirements training introduces a requirements syntax of the form:

[Trigger][Precondition] Actor Action [Object]

Note that the objects in square brackets are optional. The actor is the part of the software or system that implements the requirement. The action is the act taken by or event done by the actor. Finally, the object is what the actor takes the action on. When present, a trigger is some event or state that causes the requirement to occur. When present, the precondition must be satisfied for the requirement to be executed.

Intel has adopted the convention of using the imperative "shall" for functional requirements and "must" for non-functional requirements, which aligns with the common usage in industry. The words "should" and "may" imply optionality and thus are not used for requirements. Developers should not be given the option as to whether to implement the requirement or not. Any requirement assigned to a developer must be implemented.

While the words "shall" and "must" are generally recognized as imperatives in the U.S., it is not the case in some other countries. In fact, sometimes the exact opposite is true. The word "should" carries a stronger meaning than the word "shall". This discrepancy can be resolved by adding a note at the beginning of any requirements specification indicating that "shall" is the imperative.

Here is an example of a requirement written using the syntax above:

When the high temperature threshold limit is exceeded and event logging is enabled, the event monitoring software shall record the date and time of the high temperature event in the system log.

Trigger: the high temperature limit is exceeded
Precondition: event logging is enabled
Actor: event monitoring software
Action: record
Object: date and time of the high temperature event

To complement this syntax, the Intel requirements program has adopted EARS (Easy Approach to Requirements Syntax) that was developed by Alistair Mavin et al [8] at Rolls-Royce. This group applied EARS to requirements for the aviation industry. It establishes a small number of specific constrained natural language patterns for various types of requirements. They are summarized in Table II.

TABLE II: EARS PATTERNS

Pattern Name	Keyword(s)	Description
Ubiquitous	N/A	Always occurring or a fundamental property
Event-Driven	When	Occurring as the result of an event or trigger
Unwanted Behavior	If…then	Occurring as the result of an unwanted behavior or error condition
State-Driven	While	Only occurring while in a particular state
Optional Feature	Where	Only occurring where an optional feature is present
Complex	Combinations of the patterns when, if/then, while, and where	Occurring as the result of multiple patterns

Ubiquitous requirements are universal. They exist at all times and state a fundamental system property. They do not require any stimulus in order to execute. For most products, ubiquitous requirements are usually in the minority. Here is an example:

The software shall be available for purchase on the company web site and in retail stores.

Requirements that are **event-driven** occur as the result of an event or a trigger. In other words, there must be some stimulus that causes the requirement to execute. The keyword "when" denotes this pattern. Here is an example:

***When** a DVD is inserted into the DVD player, the software shall illuminate the "DVD Present" LED.*

The **unwanted behavior** pattern applies to requirements that handle unwanted behaviors including error conditions, failures, faults, alarm conditions, disturbances and other undesired events. The keywords "If" and "then" designate this pattern. Here is an example

***If** there are not sufficient funds in the account, **then** the software shall reject the withdrawal request.*

A **state-driven** requirement occurs if and only if the system is in a particular state. States can be conditions like operating on battery power, using cruise control and holding down a key. The keyword "while" indicates this pattern. Here is an example:

***While** the AC power is off, the software shall illuminate the yellow LED.*

The **optional feature** pattern applies to requirements that only occur if an optional feature is present. These features may be software or hardware related. Here is an example:

***Where** a HDMI port is present, the software shall allow the user to select HD content for viewing.*

A **complex** requirement occurs when multiple patterns are needed to describe the action or actions. It uses combinations of the four previous keywords (when, if/then, while, and where). Here is an example:

***While** in startup mode, **when** the software detects an external flash card, the software shall store video on the flash card.*

The last part of the class teaches an overview of Tom Gilb's Planguage [7], along with exercises to reinforce the concepts. Planguage utilizes a series of keywords to help define a more complete requirement by using a standard format. The result is that requirements have fewer omissions or missing information, reduced ambiguity and increased reuse. Examples of essential keywords for functional requirements appear in Table III.

TABLE III: KEYWORDS FOR FUNCTIONAL REQUIREMENTS

Keyword	Description
Name	a short, descriptive name for the requirement
Requirement	text defining the requirement
Rationale	justification for the requirement
Priority	importance of this requirement relative other requirements
Status	current state of the requirement
Contact	who to contact with questions
Author	who originally created the requirement
Revision	revision number for the requirement
Date	date of the latest revision
Defined	an acronym or term definition

Additional essential keywords for non-functional requirements appear in Table IV that follows. These keywords help bound the testing space for quality and performance requirements. The Scale and Meter define what the measure is and how it will be measured. Intel uses Minimum, Target and Outstanding (referred to in *Competitive Engineering* [7] as Must, Goal and Stretch) to define success for the non-functional requirement. Note that Planguage is flexible in allowing keyword names to be changed and other keywords to be added.

TABLE IV: KEYWORDS FOR NON-FUNCTIONAL REQUIREMENTS

Keyword	Description
Scale	scale of measure used to quantify the requirement
Meter	process or device used to establish location on a Scale
Minimum	minimum level required to avoid political, financial, or other type of failure
Target	level at which good success can be claimed
Outstanding	feasible stretch goal if everything goes perfectly

The requirements previously presented would be entered into the "Requirement" keyword field. The other fields would be entered by the original author or added by others as more details about the requirement become available. The essential keywords should be entered for all requirements. Additional, optional keywords can be added as needed by team responsible for the requirements. If a Requirements Management Tool (RMT) is used, it may populate many fields automatically (e.g., persistent ID, author, revision, and date).

An example of a functional requirement written using Planguage is shown in Table V. The name is short and succinct. The text is written for an optional feature using the EARS pattern ("where") and the proper requirements syntax. All other keyword fields are populated. Any missing information is quickly identifiable.

TABLE V: EXAMPLE FUNCTIONAL REQUIREMENT

Keyword	Description
Name	Display_Optional_Thesarus_Icon
Requirement	Where a thesaurus is present, the software shall display a thesaurus icon on the toolbar.
Rationale	Only display the icon if the thesaurus has been purchased.
Priority	High
Status	Implemented
Contact	John Jones
Author	Sue Morris
Revision	1.1
Date	January 18, 2013

An example of a non-functional requirement written using Planguage is presented in Table VI. The word "minimize" in the requirement is ambiguous. However, since this is a non-functional requirement, the additional keywords Scale, Meter, Minimum, Target and Outstanding define what "minimize" means (between 2 and 5 seconds). The requirement describes what will be measured in the Scale (time) and how it will be measured in the Meter (from order submit to order complete displayed). Optional keywords could include Past (a list of previous order processing times), Record (the fastest processing time recorded) and Current (current order processing time).

TABLE VI: EXAMPLE FUNCTIONAL REQUIREMENT

Keyword	Description
Name	Order_Processing_Time
Requirement	The software must minimize order processing time.
Rationale	Improvement request from top 5 customers
Priority	High
Status	Committed
Contact	Nick Terry, Director of Marketing
Author	Kristina Smith
Revision	0.7
Date	November 19, 2012
Scale	Time
Meter	Measured from the user clicking on the "Submit Order" icon to the display of the "Order Complete" message on the order entry menu.
Minimum	5 seconds
Target	4 seconds
Outstanding	2 seconds

III. AUTHOR BACKGROUNDS & REVIEW PROCESS

The three lead requirements authors (denoted as Author1, Author2 and Author3) attended the requirements writing training described in the previous section. None had any prior experience writing requirements. All were senior software developers with extensive product experience and were located in the United States.

Author1 created the first SRS for the software (SRS1). Prior to this SRS, the "requirements" that existed were scattered across a variety of locations (documents, presentation slides, spreadsheets, emails and web sites) and lacked a consistent syntax. This author captured a combination of important legacy and new requirements that were stored in a RMT. No other authors wrote requirements for SRS1.

Author2 started with the final set of requirements from the first author's SRS (SRS1, revision 1.0). Due to the increasing complexity of the product, Author2 was assisted by four other authors starting with revision 0.4. They contributed to about 25% of the new requirements. None of these authors received the requirements writing training and they were all located in different countries. Their impact on requirements defect density will become apparent when the data is presented in a subsequent section.

Author3 began with the final set of requirements from the second author's SRS (SRS2, revision 1.0). This author was assisted by over a dozen other authors starting at revision 0.5. They wrote approximately two thirds of the new requirements. About half of these authors were in the United States and attended the requirements writing class. Those outside the U.S. did not. Only the composite data for all authors will be reported. No defect statistics by geographic location were collected.

Each of the requirements authors followed a similar process. After completing the requirements writing training, the authors began work on their SRS and submitted early samples for review. The same requirements SME provided feedback to each of them to provide consistency. Since requirements were reused across SRS generations, Author2 and Author3 were able to benefit and begin their work from a stable, well-reviewed set of requirements from their predecessors, although some defects did remain. There was approximately one year between the start of each SRS.

The early review samples (part of the revision 0.3 release for each SRS) showed requirements defect densities of about 10, 5 and 4 defects per page for Author1, Author 2 and Author3 respectively. These figures represent the baseline for this paper. While some of the key concepts taught in the requirement writing training were applied (e.g., a consistent syntax and use of Planguage), other key concepts were not (including the authors' continued use of weak words, failure to check requirements for the ten attributes, and logic issues). With this baseline in place, the requirements SME began mentoring each of the authors.

Each SRS followed a similar path to a mature document. Revision 0.5 documents captured feedback from peer (other software developers) reviews of previous revisions. Revision 0.7 documents incorporated stakeholder (testers and other cross functional team members) feedback. Formal change control was started at revision 0.8. At that point, any changes to the requirements had to be formally submitted to and approved by a change control board. Revision 1.0 was the "official" release. All SRS revisions were managed from the RMT.

Note that the examples that follow have been slightly modified from their original form to maintain author and product confidentiality. Also, only the requirement itself is presented, not the full complement of Planguage keywords.

IV. Early Requirements Samples & Mentoring

To be most effective, requirements mentoring needs to occur early in the requirements lifecycle. In this way, writing style mistakes and tendencies can be corrected before they are copied and repeated on the hundreds of requirements that will follow. This is known as *defect prevention* (versus the *defect detection* that occurs as part of the testing process). However, many authors are reluctant to release requirements before they are "ready" from their perspective. At this point, many bad habits may have already been developed. To avoid this situation, the requirements SME must establish a trust relationship with the author.

How is this trust relationship established? First, the requirements SME must demonstrate a level of understanding of the product domain. The SME does not have to be a content expert but should know about the key functionality of the software. Second, the SME has to offer constructive feedback. The requirements should be reviewed against a checklist of criteria and the specific deficiencies clearly identified using objective feedback ("this word is ambiguous" vs. "this wording is bad"). Third, confidentiality has to be maintained. The author must feel comfortable that the feedback on the early requirements samples provided will not be provided to management or used in any way as part of a performance review. Fourth, the requirements SME has to provide the feedback in a timely manner. Otherwise, writing issues will propagate to other requirements.

Outside of an initial introductory face-to-face meeting, all interactions between the requirements SME and the primary authors were conducted over the telephone since they worked at different locations. In the case of the international authors, all meetings were held via telephone. As the data will demonstrate, geographic dispersion was not a detriment to the mentoring and learning process.

After establishing the trust relationship with Author1, the requirements SME reviewed early requirements samples, identified quality issues, documented those issues and then worked with the author to rewrite the requirements to remove the defects. Here is an initial sample requirement from Author1:

The software should have radio style buttons to enable/disable graphics cards.

Issues with this requirement include its optionality, the design constraint, use of a slash and over generalization. Specifically, the word "should" implies optionality. In other words, it is not mandatory. The word "shall" is the preferred choice for functional requirements. The term "radio style buttons" is a design constraint. Requirements should focus on the "what", not the "how". Why is this style of button specifically called out? Requirements should not constrain designs unnecessarily--leave the implementation details to the software developers. The slash ("/") can cause confusion as it can mean "and" or "or". In this case, the meaning is clear ("or") but in other cases, it may create confusion (e.g., administrators/users. Does this mean "administrators and users" or "administrators or user"?). Finally, the term "graphics cards" is an over generalization. Which type of graphics cards? All graphics cards? Specific graphics cards?

Having identified and documented the issues, the mentoring sessions focused on answering the questions about the missing pieces of information, discussing how to correct the defects and then rewriting the requirements. Some of this information could only be obtained through direct interaction with the author. In the previous example, the updated requirement became:

The software shall display an option to enable or disable graphics cards installed in the PCIe bus.

The requirement now has an imperative ("shall") and clearly identifies the action to be taken without ambiguity or unnecessary implementation details. Other requirements in this initial sample had similar types of defects. Additional mentoring sessions were conducted to discover and correct these requirements.

For later revisions of the SRS, the requirements SME reviewed all requirements and provided detailed feedback on the defects identified. Each requirement was then updated in a mentoring session. By the latter revisions of the SRS, this author was self-reviewing requirements using the checklists provided in the requirements training class. These SRS revisions required only minor rewrites and contained far fewer defects.

Author2 had the advantage of starting with the well-reviewed set of requirements from Author1. This author had to determine what changes were needed from the baseline of existing requirements and then started writing requirements for new features. Despite the strong foundation, initial samples from Author2 demonstrated similar issues as Author1. Here is a sample:

The software needs to provide the ability to wake on a wireless LAN event.

An analysis of this requirement reveals that it is written as a ubiquitous requirement when it really is not ubiquitous, lacks an imperative, uses weak words and is ambiguous with respect to the wireless LAN event. First, this is not a requirement that is universal. It does require a stimulus. What causes the software to wake? Second, the word "needs" should be replaced with "shall". Third, the action

"provide the ability" uses a weak set of words. How is it provided? What ability? Finally, there are many different types of wireless LAN events. Which specific one is being referenced here?

During a mentoring session with Author2, the requirements SME was able to elicit the missing information. The key pieces of information were that this requirement should only occur in a certain OS state (sleep) and that there needs to be a trigger (detection of a "Magic Packet" on the wireless network). Once all the pieces of the requirement were identified, the rewrite became:

While the operating system (OS) is in a sleep state, when the software detects a Magic Packet on the wireless network, the software shall wake the OS.

Defined: Magic Packet: A broadcast frame containing anywhere within its payload 6 bytes of 1's (0xFFFF FFFF FFFF) followed by 16 repetitions of the system MAC address.

The requirements SME reviewed all new requirements from revision 0.3 through revision 1.0. Starting with revision 0.4, four additional international authors contributed to the SRS. Unfortunately, the requirements training was not available at their work sites. This made the mentoring more difficult as they were not familiar with the rules and concepts from the course. It also resulted in a noticeable increase in requirements defect density. However, the one-on-one mentoring sessions to discuss feedback and rewrite their requirements were eventually effective in counteracting that original trend. The SME was assisted by Author2, as this particular author embraced the training to the extent that he would help others to correct their requirements during review meetings.

Author3 benefited from the requirements work done by the previous two authors. This author inherited a document of slightly over 100 pages and feature requests from software developers and testers that added another 200 pages to the initial SRS release. The requirements SME did not get the opportunity to review any early samples of requirements. The first review of SRS3 was done at revision 0.3. Here is an example of a requirement from it:

In the past, we didn't handle image errors well. Need the ability to recover from a corrupt image.

This requirement has multiple issues. The first sentence is additional information and should not be part of the requirement text. The second sentence is written in the passive voice. There is no actor identified to do this "recover". In addition, "ability to recover" is vague and ambiguous. It needs to be defined more clearly. Finally, what is a corrupt image? How is that determined? With mentoring, this requirement became:

If the calculated and stored software image checksums do not match, then the software shall:

- *Display an error message indicating that the image is corrupt*
- *Prompt the user to select loading a new image from a USB port or to exit the update process*

Rationale: Customer feedback from our top OEM has indicated that error handling for corrupt software images needs to be improved.

V. RESULTS

The data in the tables that follow documents the requirements defect densities (measured in defects per page or DPP) for each revision of the SRS documents. A single requirement could have multiple defects (e.g., not feasible, weak words, ambiguity, etc.). Note that these formatted revisions were generated from requirements that were stored and maintained in the RMT. The elapsed time from initial to final release was approximately one year in each case. The same requirements SME mentored all contributing authors and reviewed all SRS revisions.

Table VII presents the requirements defect density for SRS1, which was written by Author1. From revision 0.3 to 1.0, the defect density dropped from 10.06 DPP to 0.22 DPP, a reduction of about 98%! Without mentoring, this author would have continued to inject about 10 defects per page of requirements. At revision 1.0, there would have been approximately 450 defects in the SRS. As a result of SME mentoring, the actual document had only 10 defects, a difference of 440 defects. The vast majority of these defects would have eventually propagated into the code, requiring rework to remove them.

TABLE VII: REQUIREMENTS DEFECT DENSITY SRS1

Revision	# of Defects	# of Pages	Defects/ Page (DPP)	% Change in DPP
0.3	312	31	10.06	
0.5	209	44	4.75	-53%
0.6	247	60	4.12	-13%
0.7	114	33	3.45	-16%
0.8	45	38	1.18	-66%
1.0	10	45	0.22	-81%
Overall % change in DPP revision 0.3 to 1.0: ***-98%***				

The data in Table VIII shows the requirements defect density for SRS2. This document was written primarily by Author2, who was assisted by four additional authors starting at revision 0.4. Their impact is immediately evident from the table. While the defect rate dropped slightly from revision 0.3 to 0.4, it rose by 20% from revision 0.4 to 0.5 with the contributions from the untrained authors. However, with mentoring from the requirements SME, the downward trend in defect density resumed with

revision 0.7 and subsequent revisions. Overall, this SRS went from an initial 4.58 DPP to a final 0.94 DPP, an overall decrease of 79%. Again, the importance of mentoring is quite apparent. At the 5.40 DPP rate present at revision 0.5 (due to the injection of requirements from untrained authors), the final revision of the SRS would have had about 659 defects versus the 115 defects present in revision 1.0. The result is 544 fewer defects introduced into the software development process.

As mentioned previously, the four additional requirement authors that contributed to SRS2 were located outside of the United States. The key challenges for the requirements SME were to provide mentoring without these authors having taken the training and to establish trust relationships without meeting these authors in person. The first challenge was addressed by reviewing the training materials with the authors on a one-on-one basis. While not as effective as full classroom training, the key concepts were conveyed. The second challenge was a bit more difficult due to the distance and language barriers. However, by providing previous testimonials on the advantage of mentoring and the data on the importance of minimizing requirements defects, the trust relationships were built. All requirements mentoring sessions were conducted via email and phone.

TABLE VIII: REQUIREMENT DEFECT DENSITY SRS2

Revision	# of Defects	# of Pages	Defects/ Page (DPP)	% Change in DPP
0.3	275	60	4.58	
0.4	350	78	4.49	-2%
0.5	675	125	5.40	+20%
0.7	421	116	3.63	-33%
0.75	357	119	3.00	-17%
1.0	115	122	0.94	-69%
Overall % change in DPP revision 0.3 to 1.0: ***-79%***				

The requirements defect density for SRS3 appears in Table IX. It was initially composed by Author3. Due to a significant increase in functionality and requirements requests from members of the cross functional team, the first release of SRS3 had almost triple the number of pages as the final release of SRS2. The initial defect density for Author3 was 3.67 DPP, which reflected the good foundation of requirements that the first two requirements authors had provided. With mentoring, this rate went down to 2.54 DPP at revision 0.5 (about a 31% decline).

Starting at revision 0.5, over a dozen other authors started contributing requirements to the SRS. Those authors located in the U.S. received the requirement writing training prior to entering requirements into the database. Those authors located elsewhere in the world were not trained. Again, the consequence of having untrained authors writing requirements is apparent. While the defect density dropped by 31% from revision 0.3 to revision 0.5 (as the requirements SME mentored Author3), it rose by 9% when the new authors contributed requirements for revision 0.6.

An intensive mentoring period ensued that focused on the large number of open defects (830 in total). The requirements SME scheduled phone meetings with the domestic authors. Due to the time zone differences, most of the mentoring with the international authors was done primarily via email. Requirements defects were identified and an explanation was provided as to the nature of the problem. Any defects that could not be resolved via email were eventually addressed with a phone meeting. While perhaps not as effective as one-on-one calls, the email mentoring was successful in reducing the number of defects from 830 to 212 from revision 0.6 to 0.68 (an almost 75% decrease). Overall, the requirements defect density for SRS3 dropped from 3.67 DPP at revision 0.3 to 0.40 DPP at revision 1.0 (an 89% decrease), despite the large influx of authors. At the original 3.57 DPP rate, the final 425 page document would have had over 1500 defects versus the actual number of 172. Mentoring continued to be very effective in reducing requirements defects.

TABLE IX: REQUIREMENT DEFECT DENSITY SRS3

Revision	# of Defects	# of Pages	Defects/ Page (DPP)	% Change in DPP
0.3	1126	307	3.67	
0.5	750	295	2.54	-31%
0.6	830	300	2.77	+9%
0.65	335	298	1.12	-60%
0.67	212	377	0.56	-50%
0.80	177	404	0.44	-21%
1.0	172	425	0.40	-9%
Overall % change in DPP revision 0.3 to 1.0: ***-89%***				

VI. CONCLUSIONS

This multi-year study yielded three key results. First, limited training alone is not sufficient to take untrained requirements authors and turn them into authors capable of writing high quality software requirements specifications. There is simply too much information for them to absorb and apply in a one or two day course. Second, mentoring, when combined with training, is effective in quickly correcting bad writing habits. The focus on requirements defect prevention yields dramatic reductions in overall defect density rates within several document revisions. Third, distance is not a barrier to mentoring. Excellent results can be achieved even with thousands of miles and double digit time zone differences separating the mentor from the mentee.

To the inexperienced requirements author, training on best requirements writing practices can be like “trying to drink from a fire hose”. There are so many new concepts presented, rules to follow and syntaxes to adhere to that the student may be overwhelmed and unable to fully apply all

the concepts. In this study, the defect rates for the three lead requirements authors at their initial SRS release were 10.06, 4.58 and 3.67 DPP (the defects rates for Author2 and Author3 are actually higher if the number of defects and pages that existed in the prior revision 1.0 documents are removed). Without mentoring, these authors would have produced final versions of their software requirements specifications with hundreds to thousands of defects. A significant percentage of these requirements defects would have appeared as code defects.

The impact of mentoring to supplement training is immediately evident in the defect density data. Author1 demonstrated a 50% defect density reduction in the first revision following the start of mentoring and a 98% drop by revision 1.0. Author2 and Author3 showed decreases of 2% and 31% respectively in their first revisions with mentoring. The defect density rate for the four new requirements authors on the second SRS declined by a collective 33% following mentoring. Similarly, there were reductions of 60% and 50% in the DPP rates for the requirements authors on the third SRS after engaging with the requirements SME. The benefits of this defect prevention focus were exemplified by the final defect density rates of less than 1 DPP at revision 1.0 for all three documents.

As noted, all requirements mentoring sessions were conducted remotely. Requirements authors were scattered across the United States and several other countries. Most of the lead authors were located several thousand miles and three time zones away from the requirements SME, so frequent in-person meetings were not economically feasible. When the international sites were added, travel was not an option. Hence, the majority of the mentoring time was conducted via the telephone. Despite the lack of direct contact, dramatic decreases in SRS defect density rates (>79% in each case) were made in all three documents.

This paper has provided data demonstrating the benefits of combining requirements SME mentoring to supplement classroom requirements training in order to produce higher quality software requirements specifications. Even with classroom training, inexperienced authors will continue to inject defects into their requirements. In a SRS with several hundred pages, a requirements defect rate of between 5-10 DPP will result in thousands of defects. Ultimately, these defects will need to be corrected in the software at a much higher cost than correcting them in the requirements phase. Requirements mentoring, which focuses on defect prevention through early reviews, is a cost effective way of improving SRS quality. This is a process requiring human interaction and evaluation. While word processors can be used to detect some defects (e.g., weak words or unbounded lists), the majority of the defect detection must be done by a requirements SME using established criteria. The benefits of fewer requirements defects will lead to less project rework and ultimately to improved overall software quality.

ACKNOWLEDGEMENTS

The author would like to acknowledge Erik Simmons, who authored the Intel requirements training course materials referenced in this paper (sections available from several conference proceedings including the 2011 Pacific Northwest Software Quality Conference [6]) and Bob Bogowitz and Sarah Gregory for their contributions to the review of this paper.

REFERENCES

[1] J. Terzakis, "Requirements defect density reduction using mentoring to supplement training," Proceedings of the Seventh International Multi-Conference on Computing in the Global Information Technology (ICCGI 2012), 2012, pp. 113-114.

[2] B. Berenbach, J. Kazmeier, D. Paulish, and A. Rudorfer, Software & System Requirements Engineering in Practice, McGraw Hill, March 26, 2009.

[3] IEEE Std 830-1998, "IEEE recommended practice for software requirements specifications," the Institute of Electrical and Electronics Engineers, Inc., June 25, 1998 .

[4] K. Wiegers, Software Requirements, 2nd Edition, Microsoft Press, March 26, 2003.

[5] G. Kotonya and I. Sommerville, Requirements Engineering: Processes and Techniques, John Wiley & Sons Ltd., August 25, 1998.

[6] E. Simmons, "21st century requirements engineering: a pragmatic guide to best practices," Proceedings of the 2011 Pacific Northwest Software Quality Conference (PNSPC), 2011, pp. 21-40.

[7] T. Gilb, Competitive Engineering: A Handbook For Systems Engineering, Requirements Engineering, and Software Engineering Using Planguage, Butterworth-Heinemann, June 25, 2005.

[8] A. Mavin, P. Wilkinson, A. Harwood, and M. Novak, "EARS (Easy approach to requirements syntax)," Proceedings of 17th International Requirements Engineering Conference (RE '09), 2009, pp. 317-322.

Provenance Framework for the Cloud Infrastructure: Why and How?

Muhammad Imran and Helmut Hlavacs
Research Group Entertainment Computing, University of Vienna, Austria
email: {muhammad.imran,helmut.hlavacs}@univie.ac.at

***Abstract*—Provenance is an important aspect in the verification, audit trails, reproducibility, privacy and security, trust, and reliability in distributed computing, in-silico experiment and generally in e-science. On the other hand, Cloud computing is the business model of distributed computing and is considered the next generation of computing and storage platforms. Cloud computing requires an extension of the architecture of distributed and parallel systems by using virtualization techniques. Key to this extensible architecture is to support properties such as compute on-demand and pay-as-you-go model. Many research domains have already adopted Cloud paradigm into their existing computational and storage platforms and, thus, a shift of technology is in progress. In this paper, we give an overview of Cloud architecture and the importance of provenance in Cloud computing. We provide the mechanism for the collection of the provenance data while addressing the challenges offered by this new paradigm. These challenges include mainly the abstraction, high scalability and the inability to modify or extend the Cloud services. We provide a framework that requires minimal knowledge and understanding of underlying services and architecture of a Cloud. We assure trust by augmenting a Cloud infrastructure with provenance collection in a structured way. Then, we present the architectural overview of the provenance framework and the performance results of the extended architecture. The experimental results show that our provenance framework has a very low computation overhead (less than milliseconds), which makes it a good fit for the Cloud infrastructure.**

Keywords*—*provenance, middleware, cloud.

I. INTRODUCTION

This paper is the extension of our previous article [1], where we proposed a framework that addressed the challenges posed by Cloud paradigm. Here we extend that work and present the more detailed framework and results by adding some contents from our article [2].

Oxford dictionary [3] defines provenance as the place of origin or earliest known history of something. In distributed computing, provenance is defined by a set of different properties about the process, time, and input and manipulated data. Provenance is considered an important ingredient for tracing an object to its origin. Provenance is used to answer a few basic questions such as when the object was created, the purpose of creation, and where the object originated from (e.g., the creator of the object). In computing science, a provenance system is used to collect, parse, and store related metadata. Such data is used for verification and tracking, assurance of reproducibility, trust, and security, fault detection, and audit trials. These metadata include functional data required to trace back the creation process of objects and results, but also nonfunctional data such as the performance of each step including, e.g., energy consumption.

Cloud is an evolving paradigm which is based on virtualization and offers on-demand computing and pay-as-you-go model. Furthermore the architecture of a Cloud enforces high scalability and abstraction. The vision of this new paradigm is to address large scale computation and distributed storage management, e.g., a complex engineering, medical or social problem. Cloud enables the end user to run complex applications and satisfy his needs for mass computational power via resource virtualization. Many experiments are performed on Cloud on a large scale and shift towards Cloud is already in progress [4], [5]. Infrastructure as a Service (IaaS) is one of the service models of Cloud that is utilized by researchers to deploy complex applications [6]. This is different than grid [7] and distributed environments, where a user had to adopt their application to the grid infrastructure and policies. IaaS scheme provides a raw resource which is hired and updated according to the requirement of the application by a user without knowing the complexity and details of the underlying architecture.

The execution of complex applications in Cloud means, to request various resources and updating them accordingly. In this case, provenance can be broadly categorized into categories of: user data (applications installed on a virtual machine), instance type (memory, disk size), number of instances, resource type (image ID, location) and information about the users and Cloud provider. Such information is of high importance to utilize the Cloud resources, e.g., a resource already built and updated by one user can be used by others with minimum or no change of the installed applications and components. Furthermore, mining provenance data can be used to forecast a future request, e.g., Eddy Caron [8] used string matching algorithm on recent history data to forecast a next request. Similarly, networks in general and Clouds in particular are prone to errors, and the history data can be utilized in Clouds to resolve the errors with minimum effort [9].

Cloud infrastructure (IaaS) is composed of various services and components that cannot be modify and therefore, existing techniques are not suitable for Cloud environment and to address Cloud specific challenges. A possible approach is to follow an independent and modular provenance scheme as described in [10]. Such a scheme is possible by extending the middleware of Cloud infrastructure where various components and services are deployed (extension of third party tools and libraries). This scheme is loosely coupled (domain and

application independent) and hence works independently of Cloud infrastructure, client tools and is of high importance to support future e-science. There is a strong need to propose a provenance scheme for this dynamic, abstract and distributed environment. In addition to challenges for distributed computing, the abstraction and highly flexible usage pose new demands, i.e., a provenance framework for Clouds has to support these issues.

In this paper, we provide a discussion of provenance with a particular focus on open or research Clouds infrastructure. We present underlying architecture of open Cloud, discuss the possible schemes to incorporate provenance, and propose a framework for provenance data collection in the Cloud. Hereby, we address the most important properties of the proposed framework, that is, independence of the Cloud architecture, low storage and computational overhead of provenance data, and usability. Following are the major contribution of this article:

- giving reasons of the importance of provenance data and highlighting the challenges for provenance collection in Clouds;
- a brief overview of research Clouds IaaS and a detailed discussion of possible schemes to incorporate provenance into Cloud environment.
- a framework that can be deployed to the Cloud environment while addressing different vendors and architectures;
- a use case of provenance usage and example metadata from IaaS Cloud.
- the detailed architecture of our provenance framework for Cloud IaaS and the evaluation of collecting and storing provenance data.

The rest of the paper is organized as follows. Section II provides the related work in field of distributed computing and gives an overview of the Cloud architecture. Section III highlights the importance and the implication of a provenance enabled Cloud. Section IV discusses the possible schemes to incorporate provenance in Cloud, an overview of the related provenance data while addressing the challenges offered by Cloud infrastructure. Section V gives the details of the provenance framework by extending the underlying architecture (middleware) used by the research Clouds in a seamless and modular fashion. Section VI presents the results for the collection and storage of provenance data in Eucalyptus Cloud. Section VII gives a brief overview to use the provenance data and utilize Cloud resources, where Section VIII concludes our work and presents the directions for the future work.

II. Related Work and Background

Provenance has been addressed in distributed and workflow computing, e.g., Rajendra Bose et al. [11] present a detailed survey of computational models and provenance systems in these environments. However, none of the approaches support provenance in the Cloud environment. These existing schemes rely on the support of native services from distributed or workflow computing, e.g., process schedulers. Generally, provenance systems in grid, workflow, and distributed computing are either strongly part of the enactment engine or they use Application Programming Interfaces (APIs), which are enactment engine specific [12].

Numerous techniques and projects have been proposed during the last few years for provenance in computational sciences for validation, reproduction, trust, audit trials and fault tolerance. These techniques range from tightly coupled provenance system to loosely coupled systems [13]–[16]. Provenance Aware Service Oriented Architecture (PASOA) [17], [18] uses Service Oriented Architecture (SOA) [19] for provenance collection and its usage in distributed computing for workflow management systems. myGrid [20] and Kepler [21] are examples of projects for executing in-silico experiments developed as workflows and they use Taverna [22] and Chimera [23] schemes respectively for provenance data management in these computational systems. However, none of these approaches were designed specifically for Cloud computing architecture.

Recently, Muniswamy-Reddy et al. [24] discussed the importance of provenance for Cloud computing services offered by AMAZON EC2 [25] using Provenance-Aware Storage Systems (PASS) [26]. PASS collects the provenance data on file system level and records the various calls made to different objects. These calls are recorded on kernel level and therefore, virtual images with only PASS installed will collect and produce provenance data. A similar approach to PASS is proposed in [27] which gathers data provenance by recording system calls but without modifying the kernel. This scheme [27] uses a plug-in interface called dtrace for file system and browser, etc., and requires the knowledge of all valid entry points where provenance should be recorded in the corresponding application or domain. Since Clouds are categorized into different categories, e.g., application, infrastructure, platforms and storage, etc. Therefore, mostly research work is focus on one or more particular component. For example, there are research works that consider provenance at the layers like a web browser [28] and virtual machine [29]. Similarly, a short survey about various techniques from grid and distributed computing is provided that discuss the tracking of data in Cloud by following the layered architecture of Cloud and the provenance data for various layers [30]. In the e-science domain, experiments are performed in dry labs (in-silico), which requires hiring various resources from Cloud infrastructure and updating them accordingly. In this case, a provenance system has to address the data collection and availability in the Cloud environment and, therefore, our focus in this paper is to collect the provenance data for Cloud infrastructure.

A. Cloud Architecture

Cloud computing is the ability to increase capacity or add capability such as storage, computation and/or networking on the fly. It relies on sharing computational and storage resources over the network. Cloud computing is not a single entity and the architecture is divided into various components. These components depends on the deployment model of services, the deployment model of infrastructure and the characteristics

provided by a Cloud environment [31]. Clouds are generally categorized as business Cloud, research or private Cloud and hybrid Cloud. Infrastructure as a Service (IaaS), Platform as a Service (PaaS) and Software as a Service (SaaS) are the terms heavily used in a Cloud computing paradigm and is mostly broken into these three segments.

- IaaS: a service provided for the infrastructure (hardware and software) over the internet. Such an architecture provides servers, virtualized operating systems and data storage units. Elastic Cloud is a commonly used term for IaaS and users pay for required resources as they go. Amazon Elastic Compute Cloud (Amazon EC2), Nimbus[1], OpenNebula[2] and Eucalyptus[3] are the leading examples of IaaS.
- PaaS: a platform which is build on top of IaaS. PaaS provides an interface for software developers to build new or extend existing applications, e.g., Google App Engine and Microsoft Azure.
- SaaS: is an application service provided to the end user by a vendor, e.g., google mail. This application is executed on the Cloud infrastructure and the data is stored in Cloud database but, this is not visible to the end user.

Private Cloud IaaS schemes are mostly used in a research environment and small businesses by using open source technologies. They are rapidly growing in the size and magnitude and expanding in different domains. With the new technologies and advancements, a private Cloud can be part of other public or private Clouds thus, providing the functionality of a hybrid Cloud.

B. *Eucalyptus*

Eucalyptus is an open source implementation of Cloud computing IaaS scheme using JAVA and C/C++ for various components. Users can control an entire Virtual Machine (VM) instance deployed on a physical or virtual resource [32]. It supports modularized approach and is compatible with industry standard in Cloud, i.e., Amazon EC2 and its storage service S3. It is one of the most used platforms to create scientific and hybrid Clouds. Eucalyptus gives researchers the opportunity to modify and instrument the software which is been lacking in the business offerings, e.g., Amazon EC2. Figure 1 presents the extended architecture of Eucalyptus Cloud. The main components of IaaS Cloud are summarized below:

- Application tools: Application Programming Interface (API) available to communicate with Cloud services, e.g., resource hiring, starting, stopping, saving and/or describing the state of a particular resource. This works as a client side application to communicate with Cloud infrastructure.
- Cloud, Cluster and Node Controller (CLC, CC and NC): CLC (middleware), CC and NC communicates with each other and outside applications using Mule [33] and Apache Axis2/C framework. CLC is the entry point to the Cloud when requests are made by users via application tools. CLC interacts and routes the incoming request to a particular CC. CC is the part of Cloud used to manage clusters in the network. CC interacts and controls different NCs by associating and differentiating them using unique addresses and also balancing load in the cluster. NC assign a VM for the job execution submitted by a user.
- Storage: Cloud offers a distributed storage unit (object based storage) to save user data and raw disk images. These raw images (virtual machines) are later run as resources. Communication with a storage unit is controlled by a service, e.g., Walrus in Eucalyptus. Walrus can be used directly by users with REST protocol to stream data in/out of Cloud, e.g., files. Walrus can also be used indirectly by using SOAP protocol while communicating with CLC services to upload, modify and delete virtual images.

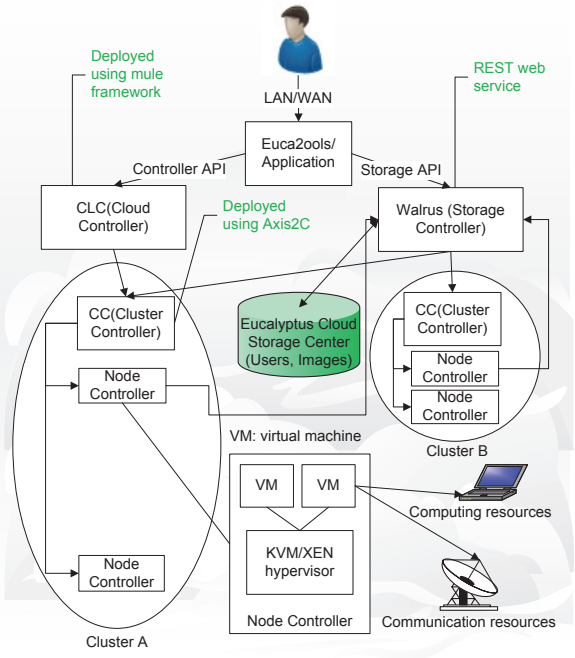

Fig. 1: Extended architecture of Eucalyptus Cloud.

All the communications between different components of Eucalyptus Cloud are achieved by using SOAP, XML, WSDL, and HTTP communication protocols via Axis2/C and Mule framework.

III. PROVENANCE IN CLOUD: *Why*

There are various alternative terms of Cloud computing, e.g., utility computing, autonomic computing and virtualization along with various definitions [34] because it is used as per the understanding, knowledge and requirements by different organizations, research communities and users. Indeed, there

[1]http://www.nimbusproject.org/
[2]http://opennebula.org/
[3]http://open.eucalyptus.com/

are some differences from previous computing paradigms, for instance virtualization, on-demand computing and storage, pay-as-you-go model, extremely flexible and more abstract architecture. Ian Foster et al. [35] present an overview of the major differences between Cloud and grid and mentions the most important feature of Cloud technology is the total dependence on services (SOA architecture). There is underlying architecture for networking of software and hardware but, to the end user it is completely abstract and hidden. The abstraction allows the end user to send data to Cloud and get data back, without bothering about the underlying details. This behavior is fine for a normal user but, in research environment, scientists are more interested in the overall process of execution and a step by step information to keep a log of sub-data and sub-processes to make their experiments believable, trust able, reproducible and to get inside knowledge. With improvements of in-silico experiments, most of the computation and processing is done by using computing resources and not in a real lab.

The execution and deployment of application on Cloud requires various resources from the Cloud infrastructure and updating them accordingly as per application requirements. This process involves the communication between the client and Cloud infrastructure. Cloud infrastructure is divided into various components as described in previous section that handles the incoming request and routes them accordingly. Each component in the process contributes some specific metadata (provenance) from Cloud, Cluster, Node, Storage, Provider and User perspective. This provenance data is not only important for the verification of the application execution but it plays an important role in the behavior analysis of Cloud. This behavior is further utilized for the efficient allocation of the resources and predicting future request.

Users of Cloud environment may not be interested in the physical resources, e.g., brand of computer but, surely they are interested in the invoked service, input and output parameters, time stamps of invocation and completion, overall time used by a process, methods invoked inside a service and the overall process from start to finish. For the Cloud infrastructure this also includes the details about the provider, users, provided resources and the details of each particular resource hired by a user. This metadata that provides the user an ability to see a process from start to finish or simply track back to find the origin of a final result and the details information about the processes and resources taking part in the final output is called provenance. Generally, provenance is used in different domains by scientists and researchers to trust, track back, verify individual input and output parameters to services, sub process information, reproducibility, compare results and change preferences (parameters) for another simulation run. Provenance is still missing in Cloud environment and needs to be explored in detail as mentioned in [24], [36].

A. Implication of a Provenance Enabled Cloud

Introducing the provenance data into Cloud infrastructure would result in following advantages:

- Patterns: The use of provenance data to find patterns in the Cloud resources usage. These patterns can be further utilized to forecast a future request.
- Trust, reliability, and data quality: The final data output can be verified based on the source data and transformation applied.
- Resources utilization: In Cloud, provenance data can be used to utilize the existing running resources by allocating a copy of a running resource. This will be achieved by comparing a new request to the already running resources and this information is available in provenance data.
- Reduced cost and energy consumption: Provenance data results in a cost and energy efficiency by using patterns to forecast a future request and by utilizing existing running resources.
- Fault detection: Provenance data can pinpoint the exact time, service, method and related data in case of a fault.

IV. Provenance Scheme and Discussion

In this section, we focus on the challenges offered by Cloud technology for the collection of provenance data. Thereby, we present the important provenance data and how the Cloud architecture can be extended to incorporate provenance collection.

A. Provenance Challenges in Cloud

Usual provenance challenges include: collecting provenance data in a seamless way with a modularized design and approach, with minimal overhead to object identification, provenance confidentiality and reliability, storing provenance data in a way so it can be used more efficiently (energy consumption) and presenting such information to the end user (query, visualization). Cloud brings more challenging to these existing challenges because we have to address the scalable, abstract and on-demand model and architecture of a Cloud. A provenance framework in Cloud should address the following challenges:

- Domain, Platform, and Application independence: How the provenance system works with different domain (scientific, business, database), platforms (windows, linux) and applications.
- Computation overhead: How much extra computation overhead is required for a provenance system in a particular domain.
- Storage overhead: How and where is the provenance data stored. It depends on the type, i.e., copy of original data or a link reference to original data, granularity (coarse-grained or fine-grained) and storage unit (SQLServer, MySQL, file system) of provenance data.
- Usability: It determines the ease of use of a provenance framework from a user and Cloud resources provider perspective. How to activate, deactivate and embed a provenance framework into existing Cloud infrastructure and services, e.g., is it completely independent or modification is required on Cloud services layer.
- Object identification: Identify an object in the Cloud and link the provenance data to source by keeping a reference or by making a copy of the source object.

- Automaticity: With the huge amount of data and process computation within Cloud, collecting and storing provenance data should be automatic and consistent.
- Cloud architecture: Addressing the on-demand, abstract and scalable structure of Cloud environment with availability and extensibility of different components.
- Interaction with Cloud services: Cloud services cannot be modified or extended. Business Clouds are propriety of organizations and open source Clouds needs understanding of every service if change is required. The better approach is to provide an independent provenance scheme, which requires no change in the existing services architecture.

B. Provenance Data

A provenance framework should address two different perspectives in collecting metadata for Cloud architecture. Applications running on Cloud as SaaS or PaaS and provenance of Cloud infrastructure (IaaS). Users of Cloud are more interested in their application provenance where, providers are interested in IaaS services provenance to observe resource usage and find patterns in applications submitted by users to provide with a more sophisticated model for resources usage. Following is the list of mandatory metadata in a Cloud environment:

1) Cloud process data: Cloud code execution and control flow between different processes (web services), e.g., in EUCALYPTUS are CLC, CC, Walrus and NC services. Web service and method name in particular.
2) Cloud data provenance: Data flow, input and output datasets which are consumed and produced and parameters passing between different services.
3) System provenance: System information or physical resources details, e.g., compiler version, operating system and the location of virtualized resources.
4) Timestamps: Invocation and completion time of Cloud services and methods.
5) Provider and user: Details about Cloud users and services provider, e.g., location of clusters and nodes. Different providers have different trust level and there could be laws against usage of resources for a particular geographical area.
6) Instance data: Instance is a running resource and the provenance data includes information about disk size, memory, resource type, number of instances for a particular operation, and number of cores (CPU), etc.
7) Cloud user data: This data is part of the Cloud infrastructure. When users hires various resources, they populate them according to the application requirement before the resource is in running state. This usually includes the initial script and the basic architecture required to deploy the application such as Java Development Kit (JDK), Java Runtime Environment (JRE), database system and web services engine for example.

C. Provenance as a Part of Cloud Services

In this scheme, the Cloud provider needs to provide a service which will communicate with other Cloud services including cluster, node and storage to collect provenance data. This scheme proposes the application of provenance as a part of overall Cloud Infrastructure as presented in Figure 2. The following list the advantages of provenance inside the Cloud IaaS.

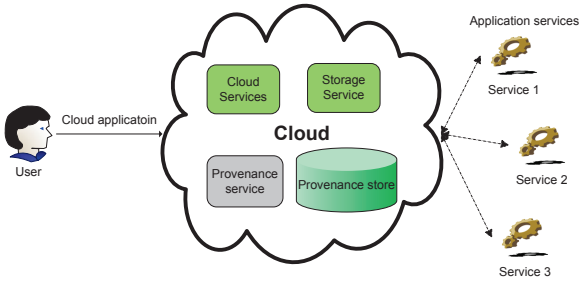

Fig. 2: Provenance service as part of Cloud services.

- Easy to use as provenance is already a part of Cloud infrastructure and a user can decide to turn it on/off just like other Cloud services.
- Users will prefer this scheme as they do not need to understand the structure of provenance framework and is the responsibility of the Cloud provider to embed such a framework.

The following list the disadvantages of such a provenance scheme.

- Cloud providers cannot charge users for such a scheme unless it has some benefits of resource utilization and initialization for users.
- In case of Cloud services failure, provenance system will also fail and there is no way to trace the reason for the failure.
- There will be extra burden on the Cloud provider because the usage of Cloud resources must increase due to incorporating the provenance framework as a part of Cloud infrastructure.
- Such a scheme can only work with a particular version of Cloud IaaS. Any change in Cloud model or services signature needs an appropriate change in the provenance framework.

In distributed, grid and workflow computing, there are many examples of provenance data management and schemes [12]–[15]. Each of these schemes is designed for a particular environment and they rely on the underlying services model. Therefore, these existing techniques cannot be applied to Cloud environment as Cloud services are not extensible to third party applications.

D. Provenance is Independent of Cloud Services

A provenance scheme that adopts a modular and an agent like approach to address cross platform, applications and different Cloud providers is independent of Cloud infrastructure. Such a scheme must address on-demand, pay-as-you-go and extremely flexible Cloud architecture. Advantages of an independent provenance scheme are:

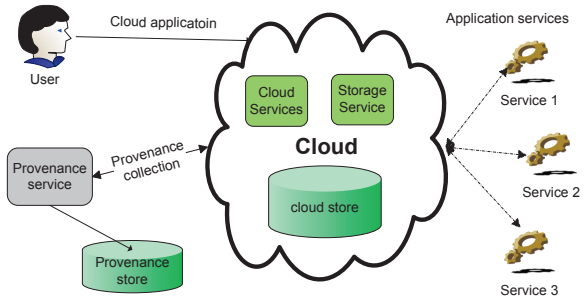

Fig. 3: Provenance as an independent module.

- Independent of Cloud services and various applications domain.
- Failure of Cloud will not affect provenance scheme as it is not a part of a Cloud.
- The users and Cloud providers will be able to track faults and errors if some Cloud services failed to work properly.
- Usability and simplicity of such a scheme is very high because a user has a complete control of the provenance system.

Disadvantages of such a scheme are as follows:

- Complete understanding of Cloud services is required to make any changes and communicate with the Cloud infrastructure.
- Trust is required on behalf of the Cloud provider because of request, permission and response from the Cloud services to the provenance module.
- Any change in Cloud services, their signature, or communication mechanism will need an appropriate change in provenance scheme.

In workflow computing, Karma [37] is using a notification broker where all the activities are published to and stored in a provenance store. The technique proposed by the Karma service is not part of a workflow enactment engine and it works as a bridge between the provenance store and the enactment engine. Figure 3 gives a brief overview of an independent provenance scheme in Cloud.

E. Discussion

Both of these approaches have their pros and cons. While considering provenance for Cloud IaaS, the major challenge is to address the Cloud extensibility. Clouds are not extensible by nature and in case of open Clouds, a developer needs a deep understanding of the source code in order to make any changes. Keeping this point in view, we propose a provenance framework that is independent of Cloud IaaS and requires minimal or no changes in the Cloud architecture and services model.

V. Provenance Framework: *How*

A Cloud infrastructure is deployed and it relies on the open source third party tools, libraries and applications. Eucalyptus Cloud in particular depends on the Apache Axis, Axis2/C, and Mule framework. These third party libraries are used for the communication mechanism between various components of Cloud infrastructure. Cloud infrastructure is the orchestration of different services and the third party libraries works as a middleware to connect these services. The purpose of Cloud computing is to bring more abstraction than previous technologies like grid and workflow computing and therefore, Cloud services cannot be modified.

One method to implement provenance into the Cloud infrastructure is by changing the source code. This could be very cumbersome as deep understanding of the code is required. This will also restrict the change to the particular version of the Cloud. This method is not feasible to address the provenance challenge for various Cloud providers, domains and applications. The second method is to capture the provenance data on the middleware of a Cloud. This is possible by extending the third party libraries used by a Cloud infrastructure and add custom methods to collect provenance data at various different levels. Such a scheme will lead to the minimum efforts and can be deployed across any Cloud scheme. Further, there will be no change required in Cloud services architecture or signature. To understand this techniques and hence the proposed provenance framework, we give a brief overview of the most important Mule and Axis2/C architecture.

A. Mule Enterprise Service Bus

Mule is a lightweight Enterprise Service Bus (ESB) written in JAVA and is based on Service Oriented Architecture (SOA). Mule enables the integration of different application regardless of the communication protocol used by those applications. Eucalyptus CLC services are deployed using Mule framework. CLC services are divided into different components including core, cloud, cluster manager, msgs, etc. These different components are built and deployed as *.jar* files and they use Mule framework messaging protocols (HTTP, SOAP, XML, etc.) to communicate with each other and with other Eucalyptus services (NC and CC).

Extending Mule: Mule framework is based on layered architecture and modular design. Mule offers different kind of interceptors (EnvelopeInterceptor, TimeInterceptor and Interceptor) to intercept and edit the message flow. Since, provenance is metadata information flowing between different components (services) and we do not need to edit the message structure; therefore, we use EnvelopeInterceptor. Envelop interceptors carry the message and are executed before and after a service is invoked.

Configuring Mule Interceptor: There are two steps involved for configuring a Mule interceptors to Cloud services. First step is to built a provenance package (JAVA class files) and copying to the Cloud services directory. Second step requires editing Mule configuration files used by different CLC components. Interceptors can be configured globally to a particular service or locally to a particular method of a service. Listing 1 is a sample *"eucalyptus-userdata.xml"* Mule configuration file used to verify user credentials and groups.

Listing 1: Configuration of provenance into Mule.

```
<?xml version="1.0" encoding="UTF-8"?>
<mule xmlns="http://www.mulesource.org
    /..." >
  <interceptor-stack name="CLCProvenance">
    <custom-interceptor class="eucalyptus.
        CLCprovenance"/>
!.. indicating path of the package and
    class name for CLC services provenance
     data
  </interceptor-stack>
  <model name="eucalyptus-userdata">
    <service name="KeyPair">
      <inbound>
        <inbound-endpoint ref="KeyPairWS
            "/>
      </inbound>
      <component>
        <interceptor-stack ref="
            CLCProvenance"/>
!.. configuring "keypair service" to
    provenance module
        <class="com.eucalyptus.keys.
            KeyPairManager"/>
      </component>
      <outbound>
        <outbound-pass-through-router>
          <outbound-endpoint ref="
              ReplyQueueEndpoint"/>
        </outbound-pass-through-router>
      </outbound>
    </service>
  </model>
</mule>
```

B. Axis2/C Architecture

Eucalyptus NC and CC services are exposed to other components by using Apache Axis2/C framework. Axis2/C is extensible by using handlers and modules [38]. Handlers are the smallest execution unit in Apache engine and are used for different purposes, e.g., web services addressing [39] and security [40]. A message flow between different components of CC and NC go through Axis2/C engine and we deploy custom handlers for provenance data collection inside Axis2/C. Similar concept is used in [41] for workflow services deployed in a tomcat container. This framework is not extensible to Cloud services and architecture. We differ from that work in many factors including interceptors for Mule, Apache Axis and Apache Axis2/C. There is no tomcat container available for Cloud services to deploy the provenance framework and Cloud services use HTTP, XML, SOAP and REST based protocols. Further, the proposed framework is developed for Cloud services provenance data collection and therefore, parsing, storing, and accessing provenance data is different than their architecture.

Configuration: Axis2/C modules and handlers can be configured globally to all services by editing *axis2.xml* file, or to a particular service and method by modifying *services.xml* file. Listing 2 describes the configuration of provenance module to Eucalyptus NC service.

Listing 2: Configuration of provenance into Axis2/C.

```
<?xml version="1.0" encoding="UTF-8"?>
<service name = "EucalyptusNC">
  <module ref="NCprovenance"/>
!..this will configure provenance to all
    methods in NC
  <Operation name="ncRunInstance">
    <Parameter name = "wsmapping">
      EucalyptusNCncRunInstance
    </Parameter>
  </Operation>
  <Operation name="ncAttachVolume">
    <module ref="NCprovenance"/>
!..this will configure provenance to this
    particular method
    <Parameter name = "wsmapping">
      EucalyptusNCncAttachVolume
    </Parameter>
  </Operation>
</Service>
```

C. Framework Components

Proposed framework is divided into the following components to address the modularity and layered architecture of Cloud:

1) Provenance Collection: When a message enters Apache engine, it goes through InFlow and invokes all the handlers inside. InFaultFlow is similar and handles a faulty incoming request, e.g., sending wrong arguments to the web service method or any other unexpected condition that prevents the request to succeed. OutFlow is invoked when a message is moving out of Apache engine (invoking all handlers in OutFlow) and the OutFaultFlow is invoked when something goes wrong in the out path, e.g., a host is shut down unexpectedly. Various Flows within Apache engine and the execution of a service with input and output messages is described in Figure 4. The left side of Figure 4 details the different flows and the right side gives an overview of one single flow with phases and handlers concepts (both built in and user defined). Custom handlers, using C/C++ for provenance collection are deployed in four different Flows of the Apache execution chain. When a component inside Cloud IaaS is invoked, provenance collection module intercepts the flow, collects and parses the message for provenance data in the corresponding execution flow.

2) Provenance Parsing and Storing into XML File: SOAP message inside Apache engine is intercepted by the collector module which passes this message to the parser. The parser reads the SOAP message, parse it accordingly and store the data in a well defined XML file. We used XML schema for the collected provenance data because it is widely used model for data representation. The XML can be used to maximize the advantages of custom algorithms and third party applications. To query the provenance data, it is better to

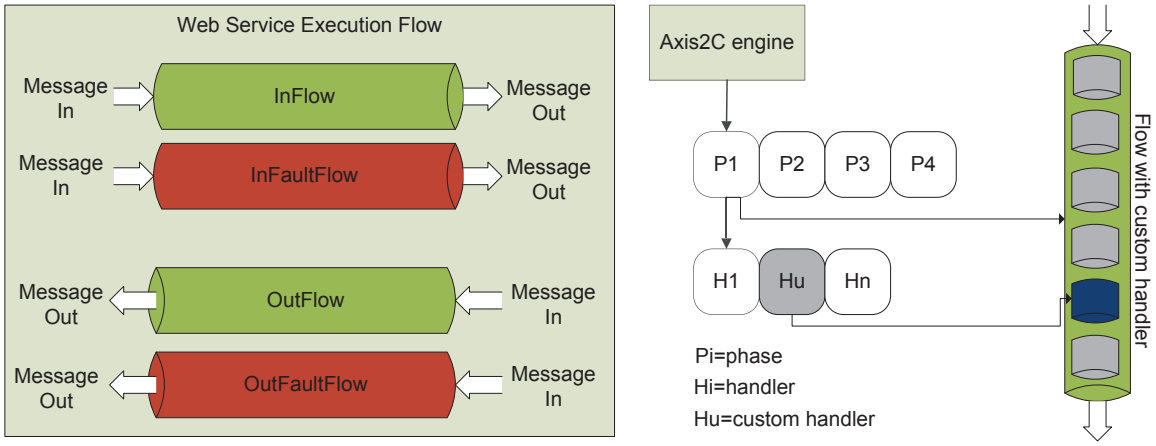

Fig. 4: Apache Axis2/C architecture.

provide a standard schema and hence the usage according to individual preferences.

Table I presents a sample of collected, parsed and stored provenance data by our provenance framework. This data represents a user activity for methods of Eucalyptus cluster service and detail the timestamps, resource type and instance specific information. <UserData> is the list of applications specified by user to populate the resource and <TimeStamp> are corresponding start and finish time of a web service method.

3) Provenance Query: Custom applications can query provenance data based on the user requirements. We find the activity pattern in Cloud IaaS based on a resource type, instance type, time used or user ID in our example query. This information can be used to monitor Cloud IaaS and the frequently used resources can be moved to a faster CPU/disk unit for better performance. Algorithm 1 is used to find activity patterns based on the the resource-ID.

Algorithm 1 Solve Query Q: Q = Return Resource Types (emi-IDs) in XML Store.

Require: XMLStore, ClusterName
Ensure: XMLStore is not Empty
Begin
Array ResouceType[] T
OpenXMLFile(XMLStoreLocation)
FindCluster(ClusterName)
while ParentNode<MethodName> == RunInstance) **do**
$T \leftarrow$ ChildNode(<ImageID>)
end while
End

4) Provenance Visualization: The visualization component takes the query as input parameter. This query is further analyzed to find the various components and their relationship. For example, a sample query:
Visualize the instances types for user1 from last 48 hours.
This query is analyzed to find the relationship between the user1, various instances requested by user1 over the last 48 hours. The result is visualized in chart form that can be changed on run time with different types of chart, e.g., line, graphs and pie, etc.

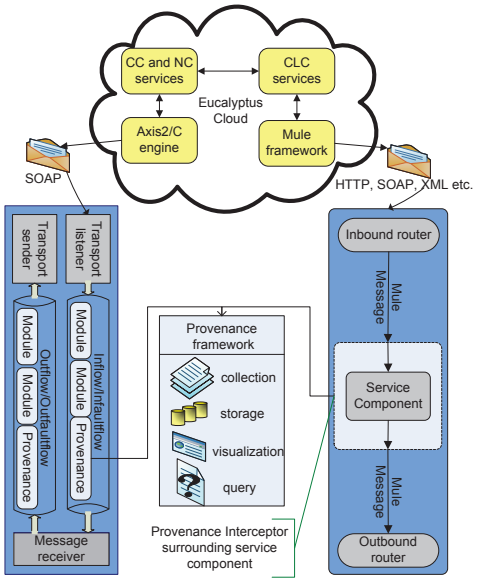

Fig. 5: Framework components.

Figure 5 presents the framework components and the interaction between Cloud services using various communication protocols.

VI. Evaluation

Different approaches are proposed in literature for collecting and storing provenance data to reduce the computation and storage overhead [42]. Mainly, there are two methods. The first method proposes to collect provenance data and store a copy of the parent object. The disadvantage of this method is a

<EucalyptusServiceName> ClusterController</EucalyptusServiceName>		
<MethodName>StartNetwork</MethodName>	<TimeStamp> Start and End Time of Method</TimeStamp> <ClusterAddress> 131.130.32.12</ClusterAddress> <UserID>admin</UserID>	
<MethodName>RunInstance</MethodName>	<ImageID>emi-392B15F8</ImageID> <KernelID>eki-AE1D17D7</KernelID> <RamdiskID>eri-16981920</RamdiskID> <ImageURL>emi-URL</ImageURL> <RamDiskURL>eri-URL</RamDiskURL> <KernelURL>eki-URL</KernelURL>	Instance Type <Name>m1.small</Name> <Memory>512</Memory> <Cores>1</Cores> <Disk>6</Disk> <UserData>DataFile</UserData>
<MethodName>StopNetwork</MethodName>	<TimeStamp> Start and End Time of Method</TimeStamp> <UserID>admin</UserID>	

TABLE I: Sample metadata of Cloud IaaS.

huge storage overheard. This method is not feasible for Cloud infrastructure because the size of objects (virtual machines and raw resources) is in gigabytes. Similarly, persistent data stored in Walrus can vary in size but storing a copy of this huge amount of data is not practical. The second method proposes to store links of the parent object. This method is faster and storage overhead is very low. The disadvantage of this method is to handle the consistency problem in case a parent object is deleted or moved.

To store provenance data we followed the second approach and the proposed framework stores only the link information about the activity of users and Cloud components. The provenance data consists of information like: Cloud images, snapshots, volumes, instance types, provider and user data, etc. Real data is already stored in the Cloud storage unit and we do not make a copy of this data. Since links are lightweight, therefore computation and storage overhead for the provenance data is very low. To get the evidence, we performed two kind of test cases.

A. Independent Testing of Middleware

First, we evaluate the Mule and Axis2/C framework independently. In this case, we calculated the increase in time for provenance collection, parsing and logging to text file. Echo service that takes an input parameter (string) and log the message to the output container was invoked 100 times in row. Five multiple runs are performed for the calculation of best time, worst time and average time of execution. The process is executed by considering overall (Inflow and Outflow), only Inflow and only Outflow provenance. The underlying architecture and system details for this test case are following:

Operating system: Ubuntu 10.04, Processor: Intel Core 2 (2 GHz), RAM: 2 GB, Axis2/C version: 1.6.0, Web service: Echo

Figure 6 presents the performance of these different execution runs on Axis2/C engine. Left side of the Figure 6 details multiple runs of Echo service without provenance, with provenance (Inflow and Outflow), only Inflow and only Outflow provenance. Y-axis represents the time required for execution. Right side of the Figure 6 shows the increase in time by comparison to without provenance. This increase in time is calculated for overall provenance, only Inflow provenance and only outflow provenance. The comparison is done for average values by using formula 1, where T_2 is time including provenance and T_1 is time excluding provenance.

$$Time\,increase = T_2 - T_1 \quad (1)$$

The average increase in time for 100 simulation runs of Echo service for collecting and logging overall provenance data is only 0.017 ms when compared to the execution without provenance. The average increase in time for only Inflow provenance is 0.009 ms and for only Outflow provenance is 0.013 ms when compared to without provenance. The individual Inflow and Outflow provenance were collected for experimental purposes to observe the respective overhead. In a real lab experiment, the overall provenance of process is essential. The increase in time for provenance collection and logging is too less and negligible when considering the advantages like fault tracking, resource utilization, patterns finding and energy consumption of a provenance enabled Cloud. Furthermore, the successful deployment of provenance collection to Axis2/C and Mule frameworks support our theory of a generalized and independent provenance framework.

B. Testing of Cloud Services

In this test case, we evaluated the cluster and node controller services of the Eucalyptus Cloud. The results were surprising for collection and storage module of the provenance framework. To get physical evidence, timestamps were calculated at the beginning of provenance module invocation and later on when the data is parsed and saved into XML file. Time overhead including the provenance module for Inflow and Outflow phases of Apache were very low (milliseconds). To find the storage overhead we calculated file size of provenance data for individual methods. We chose a worst case scenario where all the incoming and outgoing data was stored. This process was performed for every method in Eucalyptus cluster and node service and, the average file size of stored provenance data is about 5 KB for each method. Evaluation was performed by using the underlying architecture detailed in Table II. Physical machine details for running IaaS Cloud are following: Number of PCs: 2 (PC1 with Cloud, Cluster and Storage Service, PC2 with Node service), Processor: Intel Core (TM) 2: CPU 2.13 GHz, Memory: 2GB, Disk Space: 250 GB.

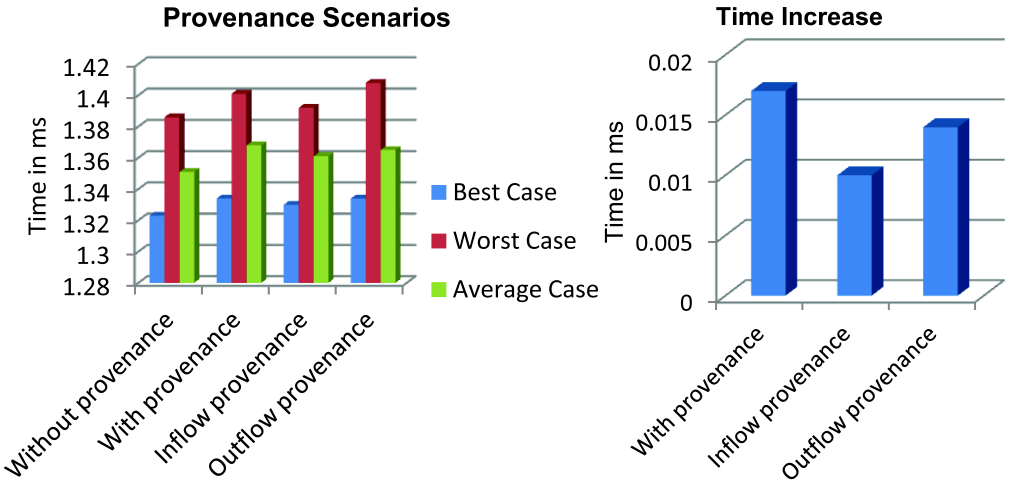

Fig. 6: Test results of Echo service.

TABLE II: Underlying architectural components.

Cloud provider	Operating system	Cloud services engine	Languages	Storage unit	Virtualization	Service tested
Eucalyptus 1.6.2	Linux Ubuntu 10.04 Server	Axis2/C 1.6.0	C,C++	File system (XML)	KVM/XEN	Cluster and Node controller

Table III presents the performance overhead of provenance for CC and NC components. The maximum times are the exceptional cases and, therefore, we calculated the average time from multiple runs (50). The average time presents the overhead for collection, parsing and storing of the provenance data into properly defined XML files. Formula 2 is used to calculate the overall overhead by summation of individual overhead of Cloud, Cluster, Storage and Node components for the Cloud infrastructure.

$$Total\,Overhead = \sum_{i=0}^{n}(\mathbf{CLC})i + \sum_{i=0}^{n}(\mathbf{SC})i + \sum_{i=0}^{n}(\mathbf{NC})i + \sum_{i=0}^{n}(\mathbf{CC})i \quad (2)$$

It is essential to note that the low computation and storage overhead of the provenance frameworks is because of two reasons. First, we used an approach where the extension of the middleware is achieved by built in features. This approach does not add any extra burden except the collection of provenance data. Second, we collect and store the provenance data by using a link based approach. This approach saves the space and time required to make a copy of the original object. Furthermore, these objects already exists in Cloud database and therefore we do not need to make a copy of the existing items and objects.

C. Framework Experience

The extension of middleware (Apache, Axis2/C, Mule) by exploiting the handler and module features facilitated in the provenance collection that is independent of any Cloud provider and various IaaS schemes. We followed a modular approach and divided our framework into different components. We believe that the future of provenance in Cloud lies in a lightweight and independent provenance scheme to address cross platform, different Clouds IaaS and application domains. The proposed framework can be deployed without making any changes to the Cloud services or architecture. Following are the **advantages** of such a scheme:

- It is independent of Cloud services and platform and it works with any Cloud IaaS which use the Apache, Mule or similar frameworks.
- The proposed framework follows a soft deployment approach and therefore, no installation is required.
- Some of the challenges offered by Cloud infrastructure are virtualization, "on-demand" computing, "pay-as-you-go" model, encapsulation and abstraction, extremely flexible and the inability to modify Cloud services and architecture by nature. The proposed framework address these challenges in automatic fashion as being part of the Cloud middleware.

Major **disadvantage** of the proposed framework is to rely completely on the extension of the middleware and cannot work on any other Cloud IaaS where middleware is not extensible.

TABLE III: Calculation overhead (in time) for provenance.

Cloud Component	Max time(ms)	Min time(ms)	Avg time(ms)
Infrastructure (NC)	15	2	4
Infrastructure (CC)	20	7	12
Combined			16 ms

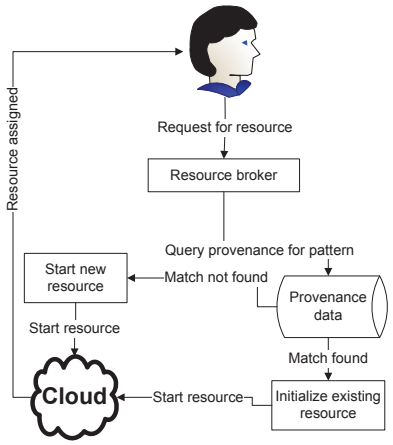

Fig. 7: Resource initialization by using provenance.

VII. Application Scenario

Description: Resource utilization is critically important both from the resource provider and Cloud performance perspective. In the Cloud resource allocation process, a user may request a resource with the input file of required applications that is the same as a previously initialized resource. If the information regarding the previously populated resources is not available, that would require to build the new resource from scratch. The utilization of Cloud resources can be maximized if one is able to provide automatic discovery of already running instances, saved volumes and snapshots. The volume and snapshot contains information of the user activity such as installing a particular software. The automatic discovery will not only help in resource utilization but will also provide means to reduce the time and energy consumed. Our proposed framework collects the metadata information regarding time, user, cluster and location of newly created volumes or snapshots and stores it in a provenance database. To make the process of resource allocation efficient and automatic, the broker (which takes input from user) compares the user input file with existing provenance data. If the comparison of input file results in an exact match then instead of starting a new resource from scratch, the existing resource, volume, and/or snapshot is deployed.

Actors: End-user and Cloud provider. A user benefits from this scheme by saving his time and effort to build a resource from scratch. On the other hand, the Cloud provider utilizes existing deployed resources and saves energy.

Advantages:

- the faster initialization of a resource in case a match is found
- the utilization of existing deployed resource (volumes, snapshots) to save energy, cost and time
- the increase in performance for the overall Cloud architecture

Figure 7 describes the process of using provenance data and making Clouds more efficient and proactive.

VIII. Conclusion

In this paper, we explored the Cloud architecture (IaaS), its dependencies and reasoned about the importance of provenance for this evolving paradigm. With the technology shift and changes, open Clouds such as Eucalyptus, Nimbus and OpenNebula are becoming the target domain for large scale computation and storage, e.g., deploying complex applications. We proposed a framework which collects and stores the important provenance data for these environments. This framework can be deployed with minimum knowledge of the underlying architecture and without modifying the basic architecture or source code of the services. Further, we present the major challenges for the collection of provenance data in a Cloud and the proposed framework address those challenges in a structured way. While addressing the challenges, proposed framework has the properties, e.g., independent of basic architecture, simple to use, easy to deploy and works with open Cloud providers. The framework is modular and divided into different components which address various parts of Cloud infrastructure. The calculated overhead for the collection and storage of the provenance data is very low and hence does not affect the performance of the Cloud architecture and its services.

References

[1] M. Imran and H. Hlavacs, "Provenance in the cloud: Why and how?" in *Third International Conference on Cloud Computing, GRIDs, and Virtualization (CLOUD COMPUTING 2012)*, USA, July 2012.

[2] M. Imran and H. Hlavacs, "Provenance framework for the cloud environment (iaas)," in *Cloud Computing 2012*. IARIA, 2012, pp. 152–158.

[3] "Oxford dictionary," Website http://oxforddictionaries.com/ definition/english/provenance, [retrieved: May, 2013].

[4] C. N. Hoefer and G. Karagiannis, "Taxonomy of cloud computing services." USA: IEEE Communications Society, December 2010, pp. 1345–1350.

[5] C. Hoffa, G. Mehta, T. Freeman, E. Deelman, K. Keahey, B. Berriman, and J. Good, "On the use of cloud computing for scientific workflows," in *Proceedings of the 2008 Fourth IEEE International Conference on eScience*. IEEE Computer Society, 2008, pp. 640–645.

[6] A. Lenk, M. Klems, J. Nimis, S. Tai, and T. Sandholm, "What's inside the cloud? an architectural map of the cloud landscape," in *Proceedings of the 2009 ICSE Workshop on Software Engineering Challenges of Cloud Computing*, ser. CLOUD '09. Washington, DC, USA: IEEE Computer Society, 2009, pp. 23–31. [Online]. Available: http://dx.doi.org/10.1109/CLOUD.2009.5071529

[7] I. Foster, C. Kesselman, and S. Tuecke, "The anatomy of the grid: Enabling scalable virtual organizations," *Int. J. High Perform. Comput. Appl.*, vol. 15, no. 3, pp. 200–222, Aug. 2001.

[8] E. Caron, F. Desprez, and A. Muresan, "Forecasting for grid and cloud computing on-demand resources based on pattern matching," ser. CLOUDCOM '10. IEEE Computer Society, pp. 456–463.

[9] M. Imran and H. Hlavacs, "Applications of provenance data for cloud infrastructure," in *The 8th International Conference on Semantics, Knowledge & Grids (SKG2012)*, Beijing, China, October 2012. [Online]. Available: http://eprints.cs.univie.ac.at/3555/

[10] A. Marinho, L. Murta, C. Werner, V. Braganholo, S. M. S. da Cruz, E. S. Ogasawara, and M. Mattoso, "Provmanager: a provenance management system for scientific workflows," *Concurrency and Computation: Practice and Experience*, vol. 24, no. 13, pp. 1513–1530, 2012.

[11] R. Bose and J. Frew, "Lineage retrieval for scientific data processing: a survey," *ACM Comput. Surv.*, vol. 37, no. 1, pp. 1–28, Mar. 2005.

[12] Y. L. Simmhan, B. Plale, and D. Gannon, "A Survey of Data Provenance Techniques," Computer Science Department, Indiana University, Bloomington IN, Tech. Rep., 2005.

[13] M. Szomszor and L. Moreau, "Recording and reasoning over data provenance in web and grid services." ser. LNCS, R. Meersman, Z. Tari, and D. C. Schmidt, Eds., vol. 2888. Springer, 2003, pp. 603–620.

[14] Y. Cui and J. Widom, "Lineage tracing for general data warehouse transformations," in *Proceedings of the 27th International Conference on Very Large Data Bases*, San Francisco, USA, 2001, pp. 471–480.

[15] P. Buneman, S. Khanna, and W. chiew Tan, "Why and where: A characterization of data provenance," in *ICDT '01: Proceedings of the 8th International Conference on Database Theory*, 2001, pp. 316–330.

[16] M. Imran and K. A. Hummel, "On using provenance data to increase the reliability of ubiquitous computing environments," in *iiWAS*, 2008.

[17] S. Miles, P. Groth, M. Branco, and L. Moreau, "The requirements of recording and using provenance in e-Science experiments," University of Southampton, Tech. Rep., 2005.

[18] pasoa. [retrieved: May, 2013]. [Online]. Available: http://www.pasoa.org/

[19] oasis. [retrieved: May, 2013]. [Online]. Available: http://www.oasis-open.org/

[20] mygrid project. [retrieved: May, 2013]. [Online]. Available: http://www.mygrid.org.uk/

[21] I. Altintas, C. Berkley, E. Jaeger, M. Jones, B. Ludscher, and S. Mock, "Kepler: An extensible system for design and execution of scientific workflows," in *IN SSDBM*, 2004, pp. 21–23.

[22] Taverna workflow management system. [retrieved: May, 2013]. [Online]. Available: http://www.taverna.org.uk/

[23] W. System, I. Altintas, O. Barney, and E. Jaeger-frank, "Provenance collection support in the kepler scientific workflow system," in *IPAW*. Springer-Verlag, 2006, pp. 118–132.

[24] K.-K. Muniswamy-Reddy, P. Macko, and M. Seltzer, "Making a cloud provenance-aware," in *1st Workshop on the Theory and Practice of Provenance*, February 2009 2009.

[25] Amazon elastic compute cloud. [retrieved: May, 2013]. [Online]. Available: http://aws.amazon.com/ec2/

[26] K.-K. Muniswamy-Reddy, D. A. Holland, U. Braun, and M. I. Seltzer, "Provenance-aware storage systems." in *USENIX Annual Technical Conference, General Track*. USENIX, 2006, pp. 43–56.

[27] E. Gessiou, V. Pappas, E. Athanasopoulos, A. D. Keromytis, and S. Ioannidis, "Towards a universal data provenance framework using dynamic instrumentation." in *SEC*, ser. IFIP Advances in Information and Communication Technology, D. Gritzalis, S. Furnell, and M. Theoharidou, Eds., vol. 376. Springer, 2012, pp. 103–114.

[28] D. W. Margo and M. I. Seltzer, "The case for browser provenance," in *Workshop on the Theory and Practice of Provenance*, 2009.

[29] P. Macko, M. Chiarini, and M. Seltzer, "Collecting provenance via the xen hypervisor," in *Workshop on the Theory and Practice of Provenance*, 2011.

[30] O. Q. Zhang, M. Kirchberg, R. K. L. Ko, and B.-S. Lee, "How to track your data: The case for cloud computing provenance," in *CloudCom'11*, 2011, pp. 446–453.

[31] P. Mell and T. Grance, "The NIST Definition of Cloud Computing," Tech. Rep., Jul. 2009. [Online]. Available: http://www.csrc.nist.gov/groups/SNS/cloud-computing/

[32] S. Wardley, E. Goyer, and N. Barcet, "Ubuntu Enterprise Cloud Architecture," *Technical White Paper*, Aug. 2009.

[33] Mule esb. [retrieved: May, 2013]. [Online]. Available: http://www.mulesoft.org/what-mule-esb

[34] L. M. Vaquero, L. Rodero-Merino, J. Caceres, and M. Lindner, "A break in the clouds: towards a cloud definition," *SIGCOMM Comput. Commun. Rev.*, vol. 39, no. 1, pp. 50–55, Dec. 2008. [Online]. Available: http://doi.acm.org/10.1145/1496091.1496100

[35] I. Foster, Y. Zhao, I. Raicu, and S. Lu, "Cloud Computing and Grid Computing 360-Degree Compared," in *2008 Grid Computing Environments Workshop*. IEEE, 2008, pp. 1–10.

[36] M. A. Sakka, B. Defude, and J. Tellez, "Document provenance in the cloud: constraints and challenges," in *Proceedings of the 16th EUNICE/IFIP*. Springer-Verlag, 2010.

[37] Y. L. Simmhan, B. Plale, D. Gannon, and S. Marru, "Performance evaluation of the karma provenance framework for scientific workflows," in *IPAW*. Springer, 2006, pp. 222–236.

[38] A. S. Foundation, "Apache axis2/java - next generation web services," Website http://ws.apache.org/axis2/, Jul. 2009.

[39] Axis2- ws-addressing implementation. [retrieved: May, 2013]. [Online]. Available: http://axis.apache.org/axis2/java/core /modules/addressing/index.html

[40] Apache axis2/c manual. [retrieved: May, 2013]. [Online]. Available: http://axis.apache.org/axis2/c/rampart/docs/rampartc_manual.html

[41] F. A. Khan, S. Hussain, I. Janciak, and P. Brezany, "Enactment engine independent provenance recording for e-science infrastructures." in *Proceedings of the Fourth IEEE International Conference on Research Challenges in Information Science RCIS'10*, 2010, pp. 619–630.

[42] D. Koop, E. Santos, B. Bauer, M. Troyer, J. Freire, and C. T. Silva, "Bridging workflow and data provenance using strong links," ser. SSDBM'10. Berlin, Heidelberg: Springer-Verlag, pp. 397–415.

Multidimensional Adaptiveness in Multi-Agent Systems

Nadia Abchiche-Mimouni, *Member, IBISC Laboratory,* abchiche@ibisc.fr
Antonio Andriatrimoson, *Partner member, IBISC Laboratory,* tsiory.andriatrimoson@ibisc.univ-evry.fr
Etienne Colle, *Member, IBISC Laboratory,* etienne.colle@ibisc.univ-evry.fr
Simon Galerne, *Member, IBISC Laboratory* simongalerne@gmail.com

***Abstract*—The work presented in this paper is focused on the design and the implementation of an adaptive framework for ambient assisted living applications. The challenge is to design an approach to deal with a dynamic environment in order to provide an adequate service to an elderly or a sick person at home. It is necessary to take into account constraints such as, the degree of urgency of the service and the degree of intrusion of the system. The evolution of the degree of intrusion based on the degree of urgency and the availability of the different communication devices that constitute the ambient environment are particularly targeted. Through an adaptive approach based on coalitions of agents, our multi-agents system ensures answers to various and/or unforeseen situations. Our coalitions protocol formation has been implemented in a real scenario. A more sophisticated version of our system has been designed allowing an intelligent and a declarative method for modeling the coalitions formation process. Indeed, the system includes a rule-based system so that the reasoning implementing the coalitions formation process can be tuned in a declarative way. This new version of our system is characterized by a multi-dimensional adaptiveness because four levels of adaptiveness are observed. The computational dimension is observed during the coalition formation process. The functional and methodological dimension concerns the service modeling. The ethical level deals with the intrusion level of the system. At last, the control level allows the behaviors triggering and criteria management. *Application objective:* A mobile robot interacts and cooperates with a set of communicating objects in order to provide a set of services and teleservices to an elderly or a sick person at home. *Research objective:* Providing a multi-a gent system that could be used for evaluating the relevance of the rules that are used during the coalitions formation process. *Results:* The proposed solutions have been implemented on a real system and evaluated in real situations. Several protocols for coalitions formation are being compared.**

***Keywords*—Adaptive control, adaptiveness, rule-based system, multi-agent system, ambient assistance.**

I. INTRODUCTION

ADAPTIVITY is widely studied as a capability that makes a system able to exhibit a cooperative and intelligent behavior. Moreover, software increasingly has to deal with ubiquity, so that it can apply a certain degree of intelligence. Ambient assistive robotics can be defined as an extension of ambient intelligence which integrates a robot and its embedded sensors. The interaction among the components in such systems is fundamental. In a previous [1] work, we presented Coalaa (Coalitions for ambient assistance), which concerns the design and the implementation of an ambient assistive living framework that takes advantage of an ambient environment: a robot cooperating with a network of communicating objects present in the person's home. The aim was to provide a service to an elderly or a sick person. A multi-agent system (MAS) reifies the sensors and the mobile and autonomous robot, allowing the cooperation among the agents by means of adaptation features. The agents form coalitions by adapting the cardinality of the coalitions according to the availability of data sensors so that the whole system can answer to a user request (obtain a particular effect). In the present work, adaptiveness of Coalaa has been improved by integrating a rule-based system able to determine, in a dynamic way, a priority for the criteria to consider during the coalition formation process. On the other hand, new experimental results show the validity of the approach implemented in Coalaa. Multiple dimensions of the adaptiveness have been identified allowing Coalaa being extendable with a meta model of the adaptiveness.

The next section details the context application and describes a particular usage scenario. Section III includes a brief overview of existing ambient assistive living systems and argues for a new one based on adaptive coalition-based MAS. The designed system Coalaa is described in details in Section IV. The Section V describes the rule-based module and the adaptation behaviors of the agents. Evaluations and analysis of Coalaa in the context of robotic localization are presented in Section VI. Finally, Section VII draws some conclusions and introduce future works.

II. THE PROBLEM DESCRIPTION

Ambient Assisted Living (AAL) constitutes a fundamental research domain. It refers to intelligent systems of assistance for a better, healthier and safer life in the preferred living environment and covers concepts, products and services that interlink and improve new technologies and the social environment, with a focus on older people. A panorama of European projects can be found in [2]. Our specific context is to assist a person in loss of autonomy at home. It concerns either the elderly or people with specific disabilities. Maintaining such people at home is not only beneficial to their psychological conditions, but helps reduce the costs of hospitalizations. House is equipped with a network of communicating objects (CO) such as sensors or actuators for home automation. A complete telecare application for remote monitoring of patients at home, including a wireless monitoring portable device held

by the patient, is added for detecting alarming situations. A mobile robot with embedded CO is also present in the house. The context application is essential in this work. So, a usage scenario is described in details so as to illustrate the different application challenges and the scientific issues addressed in this paper, which is implementing multidimensional adaptiveness.

A. A scenario description

The scenario consists of a variety of situations where an alarm has occurred. The scenario and robot configuration have been determined in cooperation with the remote monitoring center SAMU-92, which is attached to Public Paris Hospital [3]. An alarm can be triggered by a device worn by the person or the sensor network of the ambient environment. Thanks to its capability to move, the robot helps to confirm and evaluate the severity of the alarm by cooperating with the CO. The robot begins by searching the person and then provides an audiovisual contact with a distant caregiver. That way, the distant caregiver is able to remove the doubt of a false alarm, to make clear the diagnosis and to choose the best answer to the alarming situation. It is important to note that the embedded device monitors the physiological parameters and the activity of the person. The originality of the proposed approach is that the robot tries to take advantage of ubiquity. The autonomy of the robot is obtained by a close interaction between the robot and the ambient environment (AE). So, the services the robot can bring to the user are directly related to the effectiveness of the robot mobility in the environment. Even if the AE is installed in a static way for a period of time, the robot takes advantage of ubiquity and it does not perceive always the same data according to the degree of intrusion that is allowed. For example, off camera inhibits the robot to use images. So, the robot has to adapt its perception in order to locate itself and try to help the person. Indeed, before providing a service to the person, the robot has to locate itself by interacting with the AE. In such scenarios, an ethical dimension, named level intrusion of the system, has been introduced to preserve the privacy of the person. The level of intrusion of the system is defined according to the degree of freedom of the CO regarding to the actions. For instance: maximal distance allowed between the robot and the person, activating a camera, switching on a light and so on. The level of intrusion of the system is supposed to be minimal except in a case of emergency.

B. Robot localization task

Using a robotic assistant for the task rather than a simple set of fix cameras in all rooms is an advantage in two cases: i) the assistance is only needed for a limited period such as convalescence period or ii) the residence has many rooms, e.g., nursing homes. Moreover, the general quality of video and audio sensors increases. The goal of the robot is reaching the person and setting up an audiovisual communication with the distant surveillance center.

Figure 1 shows a robot in the person's home; the patient has fallen. To move towards her/him and to guide its camera to the remote caregiver, the robot has to be located first. A visual contact will help the remote caregiver to perform a correct diagnosis of the situation.

If the robot is located at P1 position, then its mobile camera can identify the visual marker Y. With further information from a fixed camera environment, the robot manages to locate itself by a mean of an adequate localization algorithm. The direction taken by its mobile camera that detected a visual marker also allows the robot to know its orientation relative to a fixed reference in the environment. This information can also be inferred from previous values using odometry on the one hand and its linear and angular speeds on the other hand. It is thus easy and straightforward to identify and understand that the more information you have the better the accuracy of the location of the robot is. If the robot is in P2 position, it has no marker on its visual field and has no element enabling it to locate itself. It then uses two different strategies to find a visual marker. Either its moves randomly or turns its pan-tilt camera. In two cases, it is necessary that the intrusion level of the system permits it. It can also query the detectors of presence to learn about the place in which it has been seen lately. In the case of several conflicting reports, it will be decided according to the data freshness criteria, or according to the consistency with the data criteria already available thanks to the sensors of the robot. This simple scenario shows that robot localization is a complex task and there is no evidence for an approach that could be able to choose the relevant interactions between the robot and the AE. The difficulty lies in choosing the most relevant criterion to be considered first: is it the closest CO, the most accurate and or the least intrusive? The problem analysis suggests that depending on the context, the criterion to consider is different. As the context itself is dynamic and difficult to predict, a centralized algorithmic solution is to be excluded. What is required is an approach that can adapt the selection and the use of criteria based on the context and the choice of a level of intrusion aligned with the level of urgency.

III. State of the art

Adaptive systems [4] are known to meet the requirements of the addressed scenario in our work. More precisely, adaptation features are inherent to MAS. So, the designed and implemented approach exploits the MAS adaptiveness [5] potential to design a distributed system to deal, in a dynamic way, with scenarios such as the one described above. The adaptiveness is also needed to deal with dynamic addition and suppression of sensors. Furthermore, MAS are relevant to our applications domain because they allow easy deployment in new and temporary environments. While the purpose of the paper is not to describe the localization algorithm but a selection mechanism of the agents participating to this task, it is not necessary to explain the robot localization. Before addressing a state of the art in the MAS domain, a brief overview of existing ambient assistive living approaches is given.

A. Ambient assistive living existing approaches

In the context of ambient intelligence, the communicating objects of the AE play a "facilitator" role in helping the

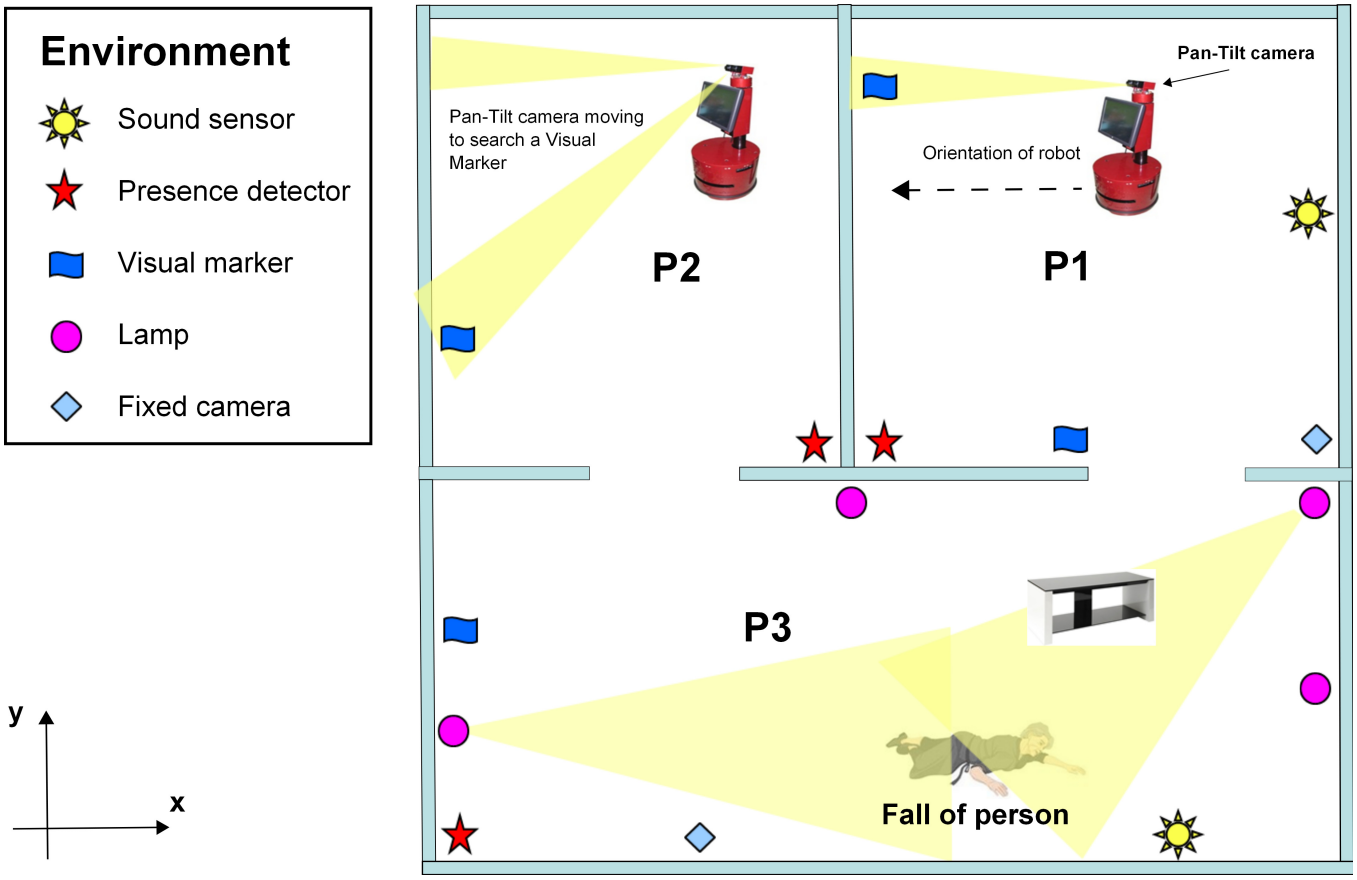

Fig. 1. A person falls scenario

robot in the Ambient assistive living. Conversely, sensors and robots can be seen as communicating objects which are used by services to the person in loss of autonomy. Several projects have been interested in combining home automation, pervasive sensors and robotics, for the safety of the patient at home. The IDorm project [6] is designed to assess an ambient environment composed of three categories of communicating objects: static objects associated with the building, a robot and mobile devices. IDorm architecture consists of a MAS that manages the operations of all the environment sensors and the robot. The sensors are controlled by an agent and the robot by another one. The sensor agent receives the different measures from sensors and controls actuators which are linked to sensors like a pan-tilt camera. The robot agent acts as a data server and coordinates exchanges of information between the user and the robot. It controls the navigation of the robot by combining different functions such as the obstacle avoidance or the search for targets. The CARE ([4]) project is a Research and Development activity running under the Ambient Assisted Living Joint Program, which is co-funded by several European countries. Its main objective is fall detection and person monitoring at home by Smart camera. As part of this project, algorithms essentially based on a biologically-inspired neuromorphic vision sensor for fall detection have been developed. The system aims to define a level of reliable supervision by avoiding as much as possible interactions with the person in her/his own home. ProAssist4Life ([5]) is a German project of situation of helplessness detection System for elderly. This project consists in developing an unobtrusive system that provides permanent companionship to elderly people living in single households or in retirement facilities. Multisensory nodes mounted on the ceiling of a room register an individual's movements. One multisensory node contains six motion sensors, one brightness sensor, and one oxygen sensor. According to data provided by various physiological sensors, the system is based on a predictive approach based on finite state automata modeling the previous activities of the patient. Another project developed at the University of Camerino is named ACTIVAge [7]. In order to keep people at home also, this project aims to provide services and teleservices based on the context. The system consists of an adaptive planning solver based on webservices orchestration and choreography with decision making algorithms. A knowledge base is used to model persistent data of the ambient environment. In each of these projects, the authors seek to design a system to avoid interfering with the patient at home. Ethical dimension is still much debated in the field of ambient assisted living, this constraint is managed by the projects mentioned above by

discrete sensor systems. Although the last described project pretends dealing with adaptiveness, this concept remains a major challenge in ambient assistive applications. The work presented in this paper is focused on implementing adaptiveness while designing several application aspects. The evolution of the inconvenience (intrusion level of the system) based on the degree of urgency and the availability of different communication devices that constitute the environment are particularly targeted. The coalition-based MAS presented in this paper reflects this constraint. The purpose of the paper is to describe a selection mechanism of the agents participating to the localization task, so localization algorithm is not presented in details.

B. Coalition-based protocols

Multi-agent systems involve agents interacting, with each other on one side and with their environment on the other side. The agents work to achieve individual and/or group goals. The achievement of group goals requires that agents work together within teams. As it is argued in [8], there exist several ways for the modeling the team behaviour. The principle of coalitions aims at temporarily putting together several agents for reaching a common goal. Several works have illustrated the relevance of coalition-based approaches for adaptiveness [9], [10], [11], [12]. The methods are various: either incremental or random or centralized. But, all of them proceed in two stages: (1) the formation of agent coalitions according to their ability to be involved in achieving a goal and (2) the negotiation stage between the coalitions in order to choose the one that provides the closest solution to the goal. The interests of the coalition-based formation protocols are the flexibility with which coalitions are formed and straightforwardness of the coalition formation process itself. The coalitions can get rid of dynamically reorganize with local and simple rules defined in the agents.

IV. Coalitions for Ambient Assisted living applications

Coalaa (Coalitions for Ambient Assisted living applications) is a MAS [13], [14], [15] based on coalitions formation protocol.

The particularity of our system reside in the fact that each agent encapsulates one CO. The CO include not only those which are installed in the home nor the ones which are embedded on the person or on the robot. So, the agents associated to the embedded CO act in the same way as the others (that are embedded). They participate to the coalition formation. Note that the robot is not agentified. The robot has a particular role; it is able to move, it should need some services (i.e. locate itself). Because the agents encapsulate CO, they are called ambient agents. Each ambient agent decides in a local and proactive way how to contribute to the required service to the person. In fact, we have introduced a more general notion than a service, which we have called an effect. An effect can be a particular lighting at a precise place of the residence or the localization of a robot. The MAS configures itself for providing a solution according to the availability of the CO and the respect of criteria. The adaptation to the context is inherent to the multi-agent modeling, strengthened by coalitions and negotiation mechanisms. Note that the goal is not to find the optimal solution but a solution close enough to the required effect. In our coalition formation protocol, the obligation to respect the result and an intrusion level depending on the urgency of the situation, are the most important considered criteria. These criteria are also used during the reorganization of the agents while trying to achieve a desired effect. The obligation result criteria is used in priority, while the level of intrusion is modified only if needed, i.e., to acquire new data and thus to activate the sensors (ex. tilt-camera) likely to cause discomfort to the person.

As shown in the Figure 2, several kinds of components are necessary to deal with the complexity of our ambient assistive application. These components are described hereafter.

A. Knowledge modeling

An effect is modeled in the form of a triple $\sigma = <t, c, f>$ where $t \in T$, $c \in C$ and $f \in F$ and:

- T is a set of tasks labels: localize a robot or a person, enlighten, cognitive stimulation.
- C is a set of criteria: accuracy, efficiency, time constraint, neighborhood.
- F is a list of influencing factors: intrusion level, urgency degree.

The criteria are assigned by the designer (programer) of the system in a static way, while the influencing factors are dynamically fine-tuned by the end-user. Since the criteria concern the capabilities of the CO, they are stored in the ontology in a static way for each CO. But the addition of CO allows new capabilities to be dynamical stored in the system. The influencing factors are directly related to the degree of freedom that the end-user (person at home or the caregiver) want to give to the system.

B. Agents environment

The ambient agents operate in an ambient environment consisting of habitat model within which the patient and the robot are together. They argue according to the different measures and relevant information that smart objects provide.

1) Ontology: Information handled by the system is classified into two types. This so-called persistent information, related to the application domain, puts together data about the structure of the residence and the features of the CO. The second type concerns volatile data mainly the measures provided by the sensors and the orders sent to actuators. The information types are handled differently. The volatile data are distributed in each agent, while persistent data are instances of an ontology named AA (Ambient Assistance) [16], [17]. The AA ontology contains four categories of information related to the application domain: The Home category for defining the structure of the environment, the CO category for knowing their characteristics and their operating mode, the User category for defining the user profile and the Task category that puts together the tasks and services that the system is able to achieve (see

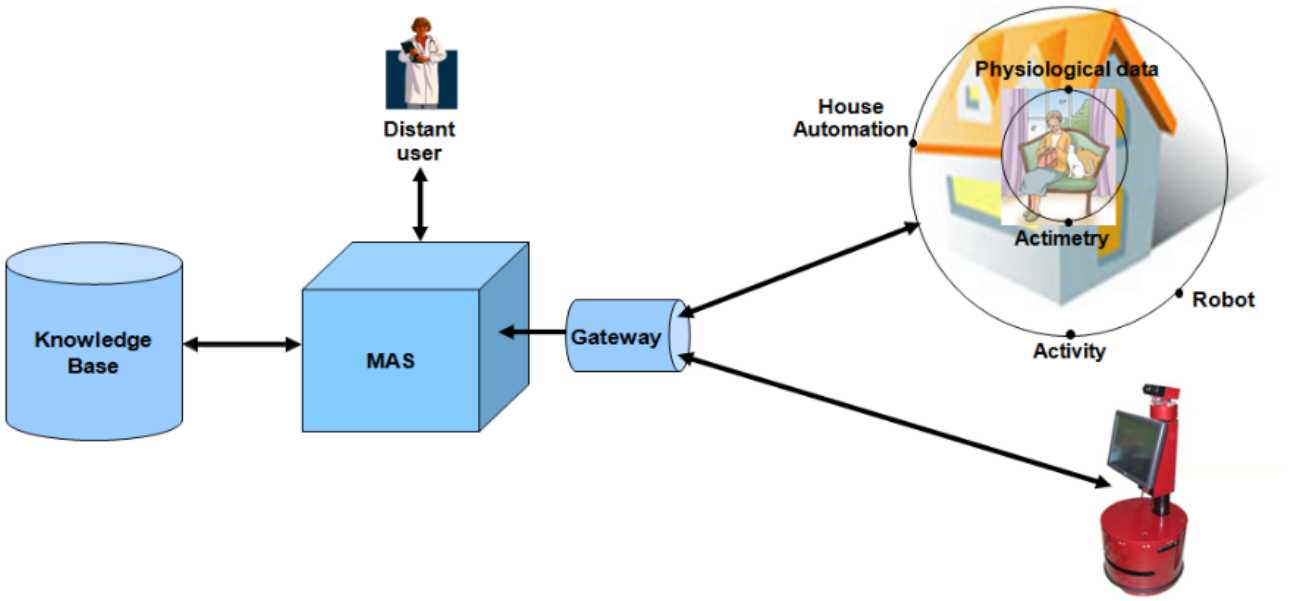

Fig. 2. Integral architecture of Coalaa

Figure 3). These categories define the four concepts of the ontology that are implemented for the studied usage scenario. But the ontology can easily be extended with new concepts if new CO were installed in the environment allowing new services to be offered. Our system needs to set up links between members of the same concept such as a topological relationship between two parts of the residence. Links are also needed between members of different concepts. For example, to process a measure provided by a sensor, the system has to locate the sensor in the residence. These links are referred to as ontological properties. We have defined three types of properties: relationship, use, and attribute. The ontological property relationship defines a logical relationship, generally of ownership, which links concept members between each other. The ontological property use defines the function of an object. The ontological property attribute refers to the features of a concept or a concept of an individual member of the ontology. It specifies the operating mode of the object, for example, a camera can be used to perform the localization task.

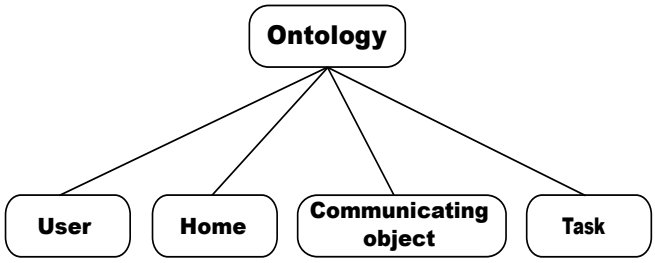

Fig. 3. Ambient Assistance Ontology

In this ontology, a property named topological distance is defined as the number of hops between two instances. The hops are relations as defined above in the ontology. If the structure of the ontology is defined by a graph, the topological distance is the number of nodes which separate two individuals minus one. This topological distance is used by agents of the MAS to determine their neighborhood during the coalition formation. This knowledge base is complemented by the dynamic information from the ambient environment through the gateway.

2) Gateway: The gateway is a module for the standardization of information exchanged between the ambient environment the MAS. Its role is to make the agents manipulating a common information format. This standardization is necessary because of the heterogeneity of the protocols from different manufacturers. Thus, the MAS receives and acts on the ambient environment through the gateway without worrying about the format of the collected data.

C. Agent internal architecture

Figure 4 represents the internal architecture of an ambient agent. The decision making module takes in charge the agent adaption and reactivity by using three main parameters that are neighborhood, history, and ability. The neighborhood sets the list of agents that are close to this agent at a given time, according to the topological distance. The history stores previous perceived information which comes from the sensors. This is a simple succession of perceived data which helps to consider the timescale during the process of coalitions formation. At last, the ability identifies the skills of the agent which are directly related to the encapsulated CO.

D. Agent behaviors

In the process of the coalition formation, an agent may be either initiator or candidate. Any agent whose ability can

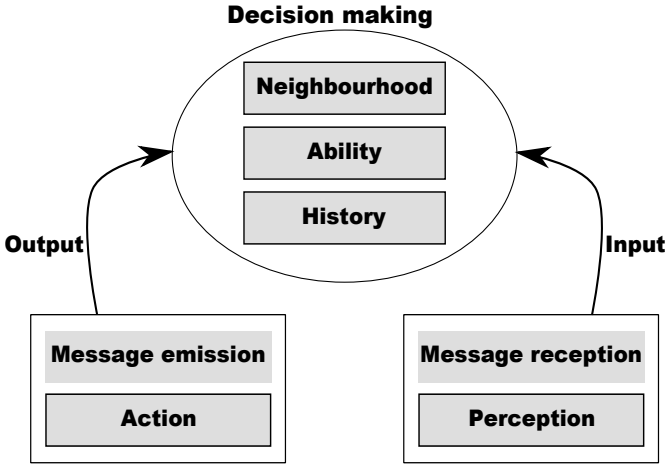

Fig. 4. Agent internal architecture

partially meet the desired effect can be a coalition initiator. The initiator exchanges messages with other agents, potential members of the coalition, called candidate agents. The Protocol is based on exchanges of messages between the initiator agent and candidate agents. As soon as the overall ability of the coalition is close to the desired effect, the initiator agent is pending the negotiation phase. The measure of closeness to the desired effect is performed according to an interval that is, in the case of a localization task, the precision of the task. At the end of the coalition formations, each initiator agent that is the referent of a coalition is negotiating with other initiators agents to choose the winning coalition. The coalition whose ability is the closest to the desired effect is the winning coalition.

The concept of ability is generic. In the localization application example, it is instantiated by the measures precision. The principle is simple. Each initiator agent sends a message that contains the ability obtained by its coalition. On receipt of this message, each initiator agent compares the ability of the coalition it received to its own one. If its ability is lower than that received, the coalition will be no more considered, otherwise, it is a winning coalition up to receiving a new message. Apart from the desired effect, the formation of coalitions uses other criteria such as the topological neighborhood to reduce the response time or the obsolescence of a measure when the desired effect depends on sensor data. Thus, the first step is the identification of candidate neighbors according to its own location in the environment (defined by the topological distance) and the desired effect. The aim of this strategy is to respond in the shortest time to the desired effect by forming coalitions. For that purpose, the first selection criteria considered is the topological distance. Once all candidate agents are known, each initiating agent continues the selection of candidates based on the recent measures criteria. When no coalition is able to meet the desired effect, a new search for a successful coalition is restarted after having relaxed the constraints on certain criteria. Indeed, it is possible to increase the level of intrusion of the system despite of the tranquility of the person at home. This authorization increases the level of intrusion allowing, for example, to operate a pan-tilt camera of the robot to acquire new measures. Then, the system is restarted hoping that the chances of finding a winning coalition is increased.

The MAS protocol is defined as a set of rules that ambient agents follow to find out a solution. The protocol of coalition formation is composed of two distinct steps. The first step consists in forming coalitions of agents according to their ability. The second step is a negotiation and refining phase so that the best coalition, in satisfying the desired effect, is chosen. In summary, after initialization, these exchanges follow three main actions:

1) Formation of all possible coalitions for each referent.
2) Selection of the best coalition according to the coalition precision.
3) Deployment of the winning coalition.

To make decisions and follow the protocol, each agent executes the appropriate behavior and starts in a state corresponding to the behavior adopted.

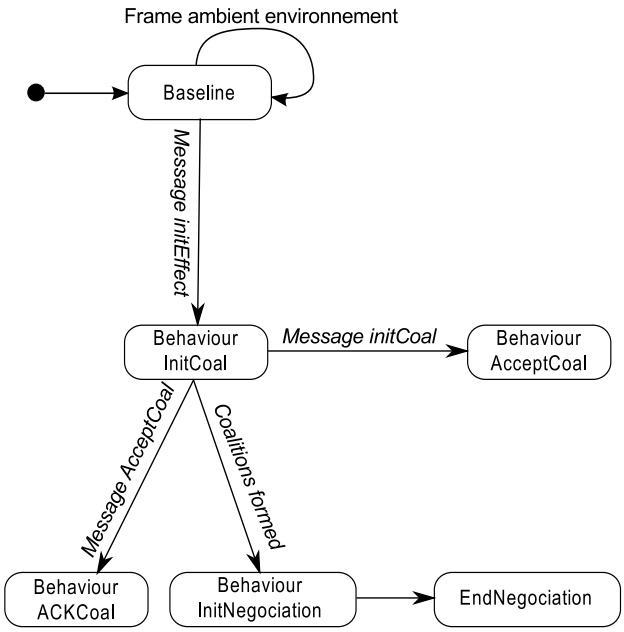

Fig. 5. Behaviors of an agent

Figure 5 shows the state transition diagram of the behaviors of an ambient agent. Each ambient agent includes six parallel and cyclic behaviors. The Baseline behavior represents the minimum treatment of an agent. Upon receipt of a frame from the environment (by the mean of the gateway), the agent must recover the sensor ID associated with it, therefore it can access the ontology and updates the ability attribute. InitCoal Behavior, AcceptCoal Behavior, ACKCoal Behavior and InitNegociation Behavior include the process of coalition formation and negotiation. For the formation of coalitions, the

first behavior to be executed is sending InitCoal following receipt of a InitEffect. Running an InitCoal behavior consists in sending a message, containing the ability of the agent, to the neighborhood agent. All agents that receive this message accept or refuse to be part of the coalition. Agents that accept must then execute the AcceptCoal Behavior and then send an acceptance message or refusal message. Initiators that receive an acceptance reply with a confirmation. Finally, the EndNegociation Behavior runs when a winning coalition has emerged. This is a behavior that allows the deployment of the coalition.

E. Interaction between agents

The interaction between the agents is performed by sending messages. For the formation of the coalitions, two types of messages are defined: Request message and Response messages. For the messages exchanging, we have defined a semantic that is based on speech act theory, introduced by John Searle [18]. Such a semantic allows the agents to define message subtype as outlined below.

Initialization: Initialization messages subtype is used in two situations: by the Interface Agent (AI) to send an effect to achieve (InitEffect) to the agents of the system and, the initiator agents after all coalitions have been formed so that it is possible to initiate the negotiation (InitNegociation).

Coalition: A Coalition message type is sent in response to the reception of a desired effect.

Acknowledgement: A confirmation message (ACKCoal) or a refuse message (RefuseCoal) is an Acknowledgement message subtype.

Reaction: This subtype includes two main messages that are AcceptCoal and ArgNeg. AcceptCoal is a message Reaction subtype that is sent by an agent when accepting an InitCoal proposal. The second message Reaction subtype is ArgNeg that is sent by an agent to respond to a request for negotiation. Each message type contains the ability of the sending agent while forming the coalitions, and the ability of the coalition during the negotiation step.

F. Agent genesis

The initialization step of the MAS is performed by a particular initialization module. It is to trigger a behavior that scans the environment of each agent and creates the agents. Each created agent is initialized by loading locally, a data set from the ontology and information from the physical environment (the gate).

G. Robot localization scenario

In this scenario, three sensors of the environment are used: a robot pan-tilt camera, a fixed camera and a presence detection sensor. These three communicating objects are encapsulated by three respective ambient agents: a Presence Detector Agent (APD), a Fixed Camera Agent (AFC) and a Pan-Tilt Camera Agent (APTC). Visual markers like Datamatrix are associated with each camera. Figure 4 shows a sequence diagram of the different agents that are involved in the scenario already described in Section II.A.

Following the fall of the patient, a request for a localization effect is generated in the form of a triple σ = <t, c, f> (cf. Section IV.A). t is the localization task which matches with the localization effect, c matches with a singleton containing the precision criterion needed for the localization task and f matches with a set containing two influencing factors that are: the intrusion level and level of urgency. In the considered scenario, we have considered a precision equal to 0.1, a level of urgency equals to 3 (three levels of urgency are considered: low=1, medium=2, high=3) and an intrusion level initialized to 0 (the lowest intrusion level). So, the triple becomes: <Locate; f0:1g; f3; 0g>. The Interface agent (AI) has received the desired effect and then broadcasts the request InitCoal (<Locate; f0:1g; f3; 0g>) to all the agents of the MAS. Each agent which received the desired effect checks its ability. As all sensors in the environment have a precision that is not better than the desired effect, each agent initiates a coalition with immediate neighborhood. In this figure, only interactions with APD agent are shown. Assuming that all agents are topologically close, APD broadcast a coalition formation request by sending an InitCoal message. Each agent receiving the initialization message checks if its ability is adequate with the request of coalition formation. If yes, it sends an acceptance message labelled AcceptCoal to be a candidate. Such a message contains the precision of the agent. APD adds progressively answer acceptance, and accumulates the abilities which are the precision in the considered localization task. By this way, it calculates the overall ability of the coalition until it reaches that of the desired effect. Then, it sends ACKCoal acceptance to confirm the membership of the candidate to the formed coalition.

The next step is to activate the coalition. The robot moves to the place designated by the coalition and guides its pan-tilt-camera to the remote caregiver. First of all, the distant user has to verify that the person is in his field of vision, so he can perform a correct diagnosis of the situation and adopt an adequate action.

Conversely, if the person is not well located the system restarts searching for a new result, after having increased the intrusion level. This allows the cameras to be moved randomly so that the chances of getting a visual marker are increased. The consequence will be improving the precision of result (coalition).

This simple scenario shows that the management of the criteria is critical. Indeed, the result (a successful coalition) depends on the order in which the criteria are considered. In the above scenario, if the level of intrusion was considered before the precision, the first result would have been the correct one. Then, the question could be the following: why can one not have a management criteria step integrated in the coalitions formation process?

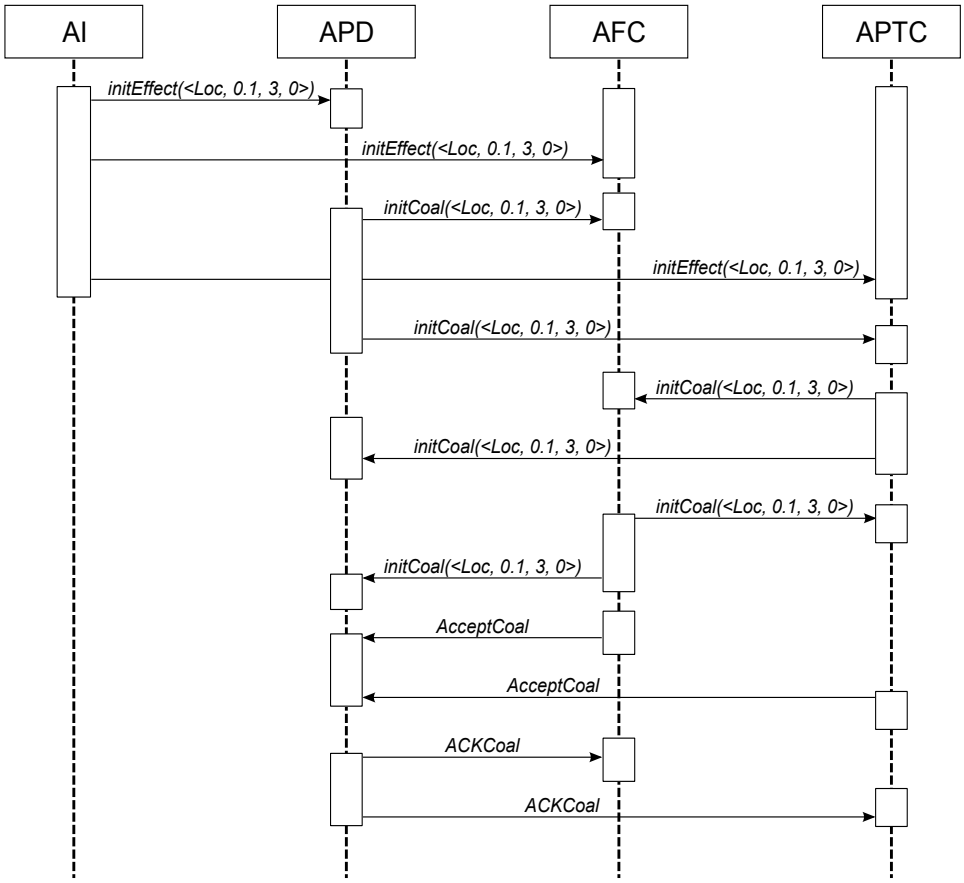

Fig. 6. Usage scenario example

V. AGENT RULE-BASED MODULE

In order to introduce some degree of intelligence in the coalitions formation process, the agent architecture has been provided with a rule-based system able to reason to fixe a priority for the criterion. On the other hand, such a rule-based system is used to interleave the execution of the behaviors of the agents in a dynamic way. A rule-based system is composed of a set of rules named knowledge rules, a set of facts named knowledge facts and an inference engine. The rules are given in the form of implications. The knowledge facts describe the state of the world and the inference engine is a special interpreter that controls when the rules are invoked according to the knowledge facts. The syntax of a rule is:

IF <antecedent> THEN <consequent>

The <antecedent> is the condition that must be satisfied to trigger the rule. The <consequent> is the action that is performed when the rule is triggered. The antecedent is satisfied if the condition matches the knowledge facts. Some examples are given below.

A. Dynamic behaviors triggering

Instead of having a procedural control (such as described in section IV D), each behavior is modeled in a production rule whose activation condition is precisely the context of the execution of the behavior. The behaviors of the agents are associated with trigger conditions. These conditions represent the context that makes behaviors possible to be executed. Explicit chaining between the behaviors is no more needed since the rules are performed by the inference engine embedded in the agents. For example, the AcceptCoal behavior is chained with the InitCoal behavior. So the InitCoal behavior is executed once the AcceptCoal behavior is terminated. Expressing this assertion in a production rule will give the rule below:

IF (Message InitCoal Locate) and (Ability Locate) THEN execute the core of the behavior AcceptCoal

This rule expresses the fact that if the agent has in its working memory (knowledge facts) a message with certain attributes and if the agent has the ability of locating an object or a person, so the rule can be triggered. In this case, the core of the behavior associated with the rule is executed.

Note that all behaviors are not controllable. Some of them, such as the message reception behaviors are supposed to be generic and are automatically executed to threat the reception

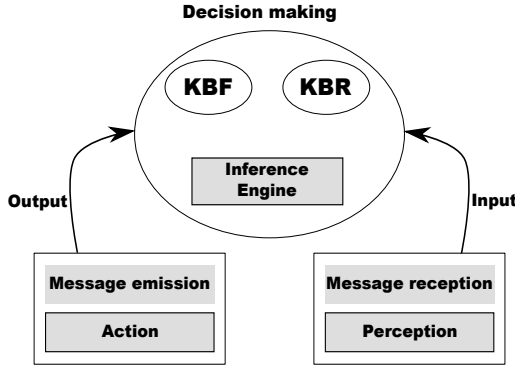

Fig. 7. Extended Agent Architecture

of the messages.

B. Flexible criteria management

In the first version of Coalaa, the priority of the criterion and the criterion themselves were fixed. Two main criteria were considered during the coalition formation process; the most prior is the topological distance and the second is the precision. When the result is not correct, a new search for a successful coalition is restarted after having relaxed the constraints on certain criteria. In the last case, the intrusion level is increased so that this increases the likelihood of finding a new satisfying coalition. In the version presented in this paper, the architecture of the agents has been modified with an embedded RBR (rule-based reasoning) module responsible of a declarative reasoning process.

In the new agent architecture, as it is is shown in the Figure 7, the inference engine replaces the procedural algorithm which implemented the decision module. The knowledge base facts (KBF) represents the knowledge extracted from the ontology, the perceived data and the exchanged messages between the agents.

For that purpose, a set of rules is defined to determine, depending on the context, the most relevant criteria to consider first at each step of the coalition formation process. On the other hand, when the coalition proposed by the system is not a correct one, the RBR is in charge of determining the most relevant criteria to relax. The rules involved in this case are some kinds of heuristics that guide the coalition process in managing the criterion. For example, if a CO involved in the coalition does not include a CO whose precision is sufficient (such as a camera), it is advisable to relax the intrusion level. This increases the degree of freedom of the system regarding to its actions allowing, for example, the cameras to be activated or lights to be switched on. Another use of the RBR for the management criteria concerns the addition of new criterion such as the time or more precisely data freshness. It is sometimes more relevant to consider not sufficiently precise data if they are very recent. For example, a presence detector can only inform that the person is situated in a particular room. Suppose that a particular presence detector says that the person is in the room R1 and a camera says that the person is in the right corner of the room R2. Of course, the information given by the camera is more accurate, but if it is too old it should be obsolete and will not help correctly locating the person. What is suggested here is to consider the date of perceived information while determining the priority of the criteria. So the system is able to deal with conflicting information. Providing such a reasoning to the system is done by adding a new rule to the set of criteria management rules, without any other change in the system.

VI. Contributions and results/outcomes

The results are obtained in a real environment composed of heterogeneous sensors and markers. The platform includes several sensors obtained of the market and dedicated sensors developed by the laboratory. The environment is composed of a room equipped with a set of sensors and the robot with its own sensors. The localization is based on goniometric measurements provided by robot on-board sensors and environment sensors. These can provide localization information to obtain the localization of the robot in its environment using real-time data either from the robot on-board sensors or from the sensors in the environment. Coalaa has been implemented using a multi-agents system platform: Jade ([16]). Jade provides generic behaviors, which facilitates controlling the execution of the agents. The RBR is implemented using a Java Expert System Shell: Jess (see [19].

Thanks to the RBR, the adaptiveness of our system has been broaden, so a fourth dimension is identified[1]:

1) Computational level: during the coalition formation process,
2) Functional and methodological level: while service modeling,
3) Ethical level: intrusion level of the system which is integrated in the behavior of the system,
4) Control level: for behaviors triggering and criteria management.

A. Computational adaptiveness

To validate the protocol used in Coalaa, a comparison to a well known protocol which is the Contract Net Protocol (CNP) has been performed. The CNP was the first approach used in MAS to solve the problem of tasks allocation. Proposed by Smith in 1980 [20], it is based on an organizational metaphor. The agents coordinate their work based on building contracts. There are two types of agents, a manager agent and contracting agents. The contractor agent must complete a task proposed by the manager. The manager breaks down each task into several subtasks, and then announces each subtask to a network of agents by sending a proposal. Agents contractors that have adequate resources respond by sending their submission. The manager agent analyses all received bids and based on the result of this analysis assigns the task to the best contractors. The contractors commit with the manager to perform the

[1]Indeed, in the previous version of this work, only three dimensions of the adaptiveness had been considered

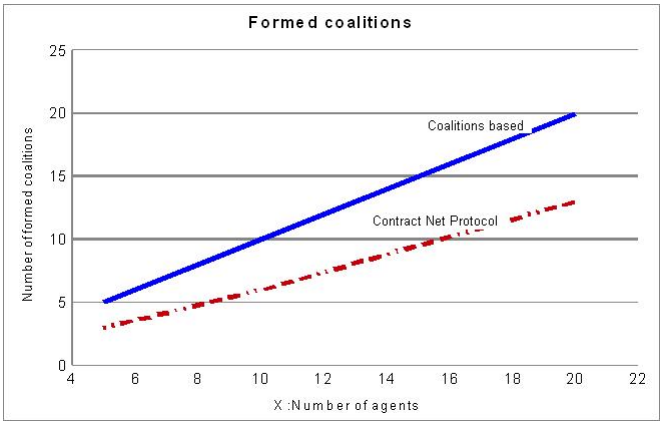

Fig. 8. Formed Coalitions

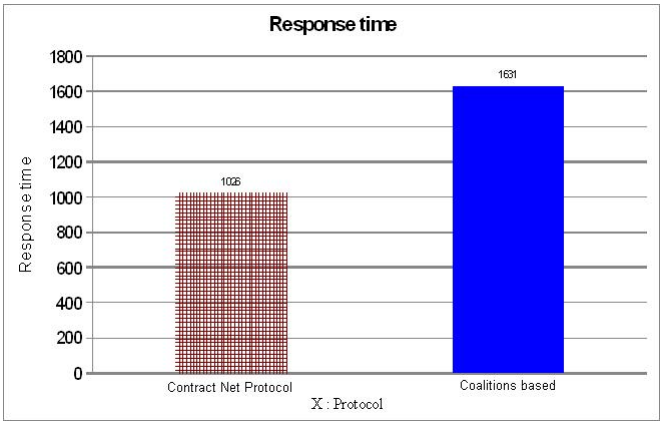

Fig. 9. Response time

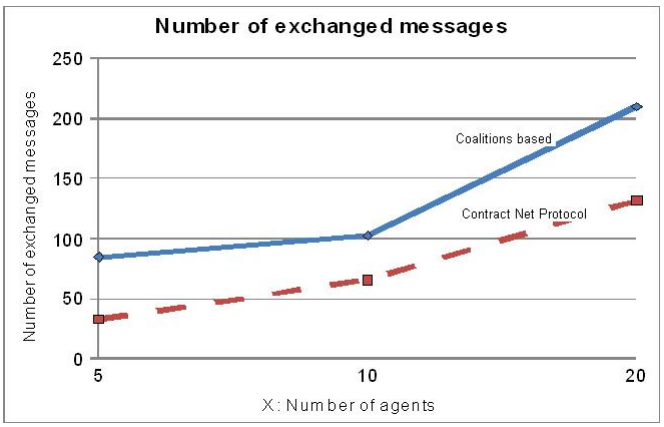

Fig. 10. Exchanged messages

assigned subtask. From the methodological point of view, there are two main differences between Coalaa the CNP. First, in Coalaa there are no commitments between the agents, they just do heir ”best” to achieve the desired effect. Second, an agent can leave the coalition during the coalition formation process. Second, there is no fitness function that the coalition must achieve.

The CNP and the Coalaa protocols have been tested with a dozen scenario using in each scenario, different values for the criteria. Each scenario has been executed with both protocols. The showed results represent an average of the results of the scenario. Evaluations have been performed on a MAS whose cardinality varies. The results are broken down into three categories:

1) The number of coalitions for an initiator with cardinality greater than or equal to 2,
2) Comparing the response time of each protocol,
3) The number of messages exchanged during the formation of coalitions.

Figure 8 shows the number of formed coalitions depending on the number of agents present in the MAS. The preferred strategy in our approach is to obtain a maximum number of coalitions that meet the selection criteria. The goal is to maximize the number of solutions to meet the request to increase the chances of securing a result. The number of coalitions is always equal to the number of initiators. In terms of the number of formed coalitions, the Contract Net protocol is less efficient than Coalaa protocol.

The response times are compared (see Figure 9). This time corresponds to the time spent in calculating the coalitions, including the message exchanges.

The fact that the number of coalitions that the CNP can form is lower than the number of initiators has a direct effect on the response time. It also impacts the number of exchanged messages represented by Figure 10. The curve representing the number of exchanged messages follows the same rate for the two protocols. However, Coalaa shows a higher number of exchanged messages. Unlike the CNP, Coalaa avoids system crashes, by a progressive coalition formation which in contrast increases the number of exchanged messages. In terms of performances (time response and number of exchanged messages) measures, Coalaa and CNP are almost similar, CNP is slightly better in terms of response time. But in terms of obtained results Coalaa is better. Indeed, a failure can be catastrophic and thus the few milliseconds delay in the response time may be insignificant, if success to complete the task is assured. This is explained by the fact that Coalaa continues to reorganize itself until finding a solution (even with deteriorated criteria), while with CNP, the system can fail and do not offer a solution.

B. Methodological and functional adaptiveness

The genesis of the MAS is done automatically. In spite of the fact that this has not been detailed in this paper, this is a very important feature of the system. In fact, modifying the ambient environment, by adding or suppressing CO, automatically updates the ontology Habitat and triggers automatic MAS reconfiguration. In case of such modifications, the user does not need to do any specification to make the system adapting its architecture to AE dynamic updating. This ability of the system is qualified by methodological adaptiveness. We refer to functional adaptiveness when dealing with services that the

system can offer to the user. The description of the ability of the CO used by the agents to construct services according to the "effect description" is included in the "ask" ontology part. This allows the agents to perform an automatic detection of their ability to perform an effect.

C. Ethical adaptiveness

An original specificity of our system is its dealing with an ethical dimension, which is the level of intrusion of the system. In fact, the system is able to adapt the intrusion of the robot, the CO and the embedded software according to the urgency of the situation and be allowed to cause discomfort for the person or its entourage only if needed.

D. Control adaptiveness

The fact that an inference engine has been employed instead of a procedural algorithm has a direct effect on the intelligence of the system. The behaviors of the agents are involved only when their associated rules are triggered, which are themselves triggered when some declarative conditions are met. Since the conditions of the rules can be modified without any procedural modification, the control of the execution of the behaviors is completely adaptive. The user can control and modify the execution of the behaviors even during the execution of the system itself. The system is also able to detect missing information which can lead to the execution of a particular behavior. So, if more generic rules are more the system intelligence can be improved. If it is easy to convince that adding new rules does not imply to modify the implementation of the system, suppression of rules is not trivial. The process of suppressing rules has to deal with consistency of the remaining data because of the possible inference which are related to the rule to be suppressed.

The convergence of the coalition formation process and the MAS itself have not been adressed from the conceptual point of view. A time out makes the system to stop if a coalition has not been emerged. This well be held in a future version of the system.

A last long term perspective concerns the construction of our AA ontology. While the utility of the ontologies is now well established, their construction, updating and using raise several scientific challenges, especially in new domain such as ambient intelligence.

VII. Conclusion and perspectives

An adaptive approach has been presented for an assistive ambient alarm detection by implementing the Coalaa system. Coalaa is a coalition-based multi-agent system in which the adaptiveness is considered from multiple dimension. The computational, the methodological, the ethical and control points of view of adaptation have been considered.

The advantages of Coalaa in comparison with a simple system in which: *a patient with alarm key and mounted on the ceiling movable video camera with a zoom lens that is controlled by a care provider*, are various. One can mention:

- Minimizing the number of zoom cameras that are more expensive and more intrusive than simple ones.
- Temporar or reversible installation of ambient environments.
- The robot is intended to be able to offer different kinds of services to the person.

The feasibility of this approach has been widely demonstrated on a usage scenario to remove the doubt of a false alarm. The first results illustrated with the robot localization application are promising. The validation of the system with a great data size has been performed by the generation of statistical distributions of data that provide more meaningful results. Moreover, comparing our protocol to the contract-net protocol has shown that even more time is spent with Coalaa, the number and the diversity of the solutions is greater.

In spite of conclusive results, several improvements of Coalaa are under consideration. The efficiency of Coalaa can be improved by making the initiator agents revising the way of choosing their partners during the coalitions formation process. This can be based on past obtained results. The agents can infer the capabilities of their potential partners through repeated interactions such as done in [21].

Another perspective is to implement more flexible way to calculate the cardinality of the coalitions. This could be done by the agents by evaluating their behavior and self-adapt for improving the overall model of criteria evaluation [22].

At a short-term perspective, we plan to apply our approach to other services such as cognitive stimulation and the detection of the person activity. The rule-based reasoning implemented in the second version of Coalaa can be used to infer information about the activity of the person. This can be done by making inferences based on the dating of information that are available during the activity of the agents. For example, if at t_i the person is in her/his bathroom and at $ti + n$ she/he is at the kitchen and now (at $ti + n + m$) she/he is in the dining room, one can infer that after having fixed herself, the person has prepared the meal and now she/he is feasting the meal she/he prepared. Indeed, a rule-based reasoning can be easily detect the rules that are linked and construct reasoning paths that lead to the description of the activity of the person.

At a long-term perspective, we will propose to wrap an agent in each communicating object, so that no time is spent to acquire information from the gate.

An original application of Coalaa could be to calculate an optimal deployment of the sensors in the houses so that to improve the services that the system can provide to the person. On the other hand, we are thinking about further development of our approach so that it can be extended for everyday life. An interesting challenge is to cope with large number of needed sensors if everyday applications are considered. Despite the inherent modularity of MAS, it will be necessary to improve the localization algorithm in such cases.

Another challenge would be comparing the solution not only with CNP but also with other coalition formation approaches (i.e., learning based ones). This can lead to a computational environment for experimenting coalition formation algorithms.

ACKNOWLEDGMENT

The authors would like to thank the ANR for accepting the implementation of the QuoVADis project that spread from 2008 to 2011.

REFERENCES

[1] A. Andriatrimoson, N. Abchiche-Mimouni, E. Colle, and S. Galerne, "An adaptive multi-agent system for ambient assisted living," in *ADAPTIVE 2012, The Fourth International Conference on Adaptive and Self-Adaptive Systems and Applications*. IARIA, ThinkMind, 2012, pp. 85–92.

[2] M. Biddle, "Catalogue of projects 2012: Ambient assisted living"," 2012.

[3] A. Andriatrimoson, T. Simonnet, P. Nadrag, P. Hoppenot, and E. Colle, "Quovadis project: Functionalities of the robot and data-processing architecture," *AAATE*, 2009.

[4] A. Eduardo, D. Kudenko, and D. Kazakov, *Adaptation and Multi-agent Learning*. Springer-Verlag Heidelberg, 2003.

[5] M. Sims, C. Goldman, and V. Lesser, "Self-Organization through Bottom-up Coalition Formation," in *Proceedings of Second International Joint Conference on Autonomous Agents and MultiAgent Systems*. Melbourne, AUS: ACM Press, July 2003, pp. 867–874. [Online]. Available: http://mas.cs.umass.edu/paper/238, accessed on June 26th 2013

[6] P. Remahnino, H. Hagras, N. Monekoss, and S. Velastin, *Ambient Intelligence a gentle introduction*. Paolo Remahnino, Gian Lucas Foresti, Tim Ellis (Eds.), 2005, ch. 1, pp. 1–14, book title: Ambient Intelligence: A Novel Paradigm.

[7] F. Corradin, E. Merelli, D. R. Cacciagrano, R. Culmone, L. Tesei, and L. Vito, "Activage: proactive and self-adaptive social sensor network for ageing people," *ERCIM News*, vol. 2011, no. 87, 2011.

[8] B. Jarvis, D. Jarvis, and L. Jain, *Teams in Multi-Agent Systems*. Springer US, 2007, vol. 228.

[9] M. Sims, C. Goldman, and V. Lesser, "Selforganization through bottom-up coalition formation," in *the 2nd AAMAS*, 2003.

[10] T. Scully, M. Madden, and G. Lyons, "Coalition calculation in a dynamic agent environment," in *the 21st ICML*, 2004.

[11] L.-K. Soh and C. Tsatsoulis, "Reflective negotiating agents for real-time multisensor target tracking," in *IJCAI'01*, 2001.

[12] L. Soh and C. Tsatsoulis, "Allocation algorithms in dynamic negotiation-based coalition formation," in *AAMAS02 Workshop 7 "Teamwork and coalition formation"*, 2002, pp. 16–23.

[13] M. N. Huhns, *Distributed Artificial Intelligence*. Pitman, 1987.

[14] M. N. Huhns and M. P. Singh, *Readings in Agents*. Morgan Kaufmann, 1997.

[15] M. Wooldridge and N. R. Jennings, "Agent theories, architectures, and languages: a survey," in *Intelligent Agents*, Wooldridge and J. Eds, Eds., Berlin: Springer-Verlag, 2009, pp. 1–22.

[16] A. Kivela and E. Hyvonen, "Ontological theories for the semantic web," in *Semantic Web Kick-Off in Finland*, May 2002, pp. 111–136.

[17] R. Arnand, E. M. Robert, H. C. Roy, and M. M. Dennis, "Use of ontologies in a pervasive computing environment," in *Knowledge Engineering Review*, vol. 18, 2003, pp. 209–220.

[18] J. Searle, *Speech acts. an essay in the philosophy of language*. Cambridge University Press, 1969.

[19] E. F. Hill. Manning Publications, 2003.

[20] R. Smith, "The contract net protocol: high-level communication and control in a distributed problem solver," in *IEEE Transactions on Computers*, 1980, pp. 1104–1113.

[21] G. Chalkiadakis and C. Boutilier, "Sequentially optimal repeated coalition formation under uncertainty," *Autonomous Agents and Multi-Agent Systems archive*, vol. 24, no. 3, pp. 441–484, May 2012.

[22] F. Klugl and C. Bernon, "Self-adaptive agents for debugging multi-agent simulations," in *ADAPTIVE 2011, The Third International Conference on Adaptive and Self-Adaptive Systems and Applications*. IARIA, ThinkMind, 2011, pp. 79–84.

Building a Cultural Intelligence Decision Support System with Soft-Computing

Zhao Xin Wu, Roger Nkambou
Computer Science Department, University of Quebec in Montreal, PO Box 8888, Downtown, Montreal, QC. H3C 3P8, Canada
zhao_xin_wu@hotmail.com
nkambou.roger@uqam.ca

Jacqueline Bourdeau
LICEF, Télé-Université, 100 Sherbrooke, O. Montreal, QC, H3C 3P8, Canada
Jacqueline.bourdeau@licef.ca

Abstract **- The international business and traditional business intelligence face challenges in successfully adapting to cultural diversity. This paper introduces cultural intelligence as a new perspective and a new way to alleviate these challenges. Furthermore, based on soft computing technology, this research aims to invent a cultural intelligence computational model and to implement the model in an expert system. In the cultural intelligence domain, this paper presents how this model deals with linguistic variables, soft data and human decision making with hybrid neuro-fuzzy technology, which also possesses parallel computation and the learning abilities.**

Keywords - Cultural Intelligence, Decision Making, Fuzzy Logic, Artificial Neural Network, Soft-Computing.

I. INTRODUCTION

Globalization has dramatically changed the way business is conducted. It has intensified worldwide social relations and connected workers in distant localities, making local concerns global and global concerns local. Individuals, companies and organizations have capitalized on this reality to establish centers in different countries in order to develop their international business activities. In this new reality, individuals, companies and organizations must form global strategic alliances to deal with worldwide competitors, suppliers and customers [1]. When confronted with cultural diversity, some are able to make appropriate decisions and adapt successfully to the new cultural business environment [2], while others are not. What is the decisive factor for these opposing responses? How can good decisions be made in culturally diverse business environments [3] ?

In recent years, researchers have shown a vast interest in globalization and intercultural management. Ang and Earley introduced the concept of cultural intelligence (CQ) to the social sciences and management disciplines in 2003 [4]. CQ has, therefore, been presented as a new phenomenon capable of answering the above-mentioned questions [5]. Organizational psychology and human resource management have paid a great deal of attention to CQ since its introduction. These fields of study have yielded valuable results that apply to the real business world.

However, since Earley and Ang put forward the concept of CQ in 2003, there has been no research on CQ with artificial intelligence (AI) technology with the purpose of assisting individuals, companies and organizations in making good decisions in order to function effectively in this culturally diverse environment. Indeed, most current studies pertaining to CQ do not integrate any AI technology. The current state of CQ research in AI leaves an important gap in our understanding of what individuals, companies and organizations need to function effectively in this global work environment. In addition, traditional business intelligence (BI) has encountered two challenges: the first involves determining the means of adapting to cultural diversity; the second pertains to treating cultural soft data for decision making [6]. Our claim is that when CQ is applied to individuals, companies and organizations in the fields of business, it should be computerized.

This research attempts to offer effective solutions to the aforementioned problems. It is the first attempt to invent a computational model of CQ implemented in an intelligent system to resolve cross-cultural business challenges. The main reason for inventing such a system is that, in the real business world, there are not enough qualified cultural experts to help users make better business decisions, and these experts may lose some of their effectiveness after long consecutive hours of work. Moreover, the sphere of application has been confined to cultural experts and researchers. From a user's point of view, this research offers an intelligent system that behaves like an efficient team of top cultural experts that works continuously with users. Furthermore, this system has the potential to achieve better performance results than human experts.

There are three goals behind such a system that aims to help individuals, companies and organizations cooperate more effectively with people from different cultural backgrounds: (1) to assist them in their business decision-making processes involving cultural affairs; (2) to assist them in improving their CQ capacity, which would be particularly well suited to overseas assignments [4]; and (3) to facilitate the work of researchers and to equip them with more effective tools in their studies on CQ.

This paper consists of eight sections, which is highly focused on the conceptual-theoretical background of CQ computational model and the general architecture of our system. In Section I, we state the research question and research objectives. In Section II, we briefly discuss the concepts that are applied to this research, in particular the concept of CQ and its dimensions. In this section, the relationship between business and CQ will be present. Also included is our CQ conceptual model; on the basis of this model, we create our CQ computational model. In Section III, we provide a detailed explanation of our AI technology choices applied to our computational model. Furthermore,

we introduce the theory of fuzzy and fuzzy rules that are applied to our system. In Section IV, we discuss the fundamental CQ computational model. In Section V, we demonstrate how our computational model is implemented into an expert system. We present the structure of our system and identify the main modules in the structure, and we explain how these modules work. In addition, we explain how we collect and analyze data and knowledge in the CQ domain for our system in order to make its design more explicit. In Section VI, we present an overview of the system's cognitive architecture and its cognitive processes. In Section VII, we explain the details of the evaluation of our computational model and the system. Finally, in Section VIII, we state the contributions of this research.

II. LITERATURE REVIEW AND RELATED WORK

This research draws from many different fields, each with its own richness, peculiarities and complexities. We attempt to bring the many concepts, points of views and propositions to work together. As such, the discovery of a global theory is an appropriate first step for our research and providing a clear view of what is generally understood is a necessity in this first step.

CQ is based on two basic concepts: one is *culture*, and the other is *intelligence*. In this section, we first define the concept of culture. We then explain the concept of intelligence. We present definitions of CQ and its dimensions from the different points of view of various researchers and explain the links between CQ and business.

A. Culture

According to a dictionary definition, culture is: *"the totality of socially transmitted behavior patterns, arts, beliefs, institutions, and all other products of human work and thought''* (The American Heritage Dictionary of the English language, Fourth Edition, 2000). Dictionary definitions of culture can incorporate multiple elements such as history, common traits, geographical location, language, religion, race, hunting practices, music, agriculture, art, etc.

Culture is not something that has an existence outside of the actions and experiences of the individuals who reproduce it. Culture is a context; it informs and shapes individual behavior only as it is simultaneously reproduced and reinforced by that very behavior. Cohen et al. propose a definition of culture [7]: *"Culture is an information pool that emerges when members of a community attempt to make sense of the world and each other as they struggle and collaborate with each other to get what they want and need (e.g., food, sex, power, acceptance, etc.). Because individuals construct their conceptions of the world from their own experiences and for their own motivations, their understandings vary from one another depending on the characteristics of the individuals, the nature of the domain learned, and the social situations in which learning takes place''.*

Hofstede [8] defines culture as subjective and considers national culture to be a part of a greater global culture. Hofstede [9] states that culture is a structure of collectively held values and collective mental programming, which separate or distinguish various groups of people from others. He believes that although there may be various subcultures, all nations share a national culture. Hofstede identifies the three levels in his model of collective mental programming as human nature, culture, and personality (see Fig. 1). All three levels of mental programming have an impact on how individuals react to their environment. Human nature plays a role in the development of culture over time, as well as in the development of people. An individual's culture, although it can be the same among a group of people, differs slightly with each individual, as an individual may act and behave slightly differently than others in his/her culture group due to the influence of human nature and personality. An individual's personality indirectly influences culture as it plays a role in how an individual accepts or rejects various parts of his/her culture.

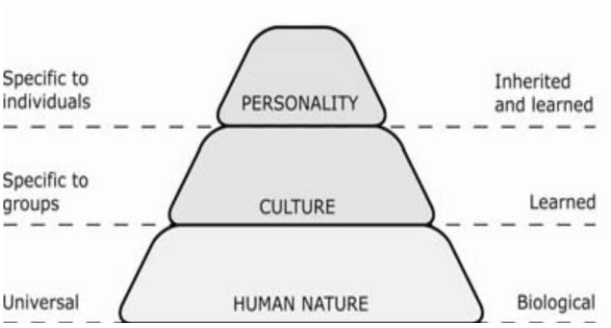

Figure 1. Three Levels of Mental Programming (Hofstede, 1980)

B. Intelligence

Early research in academic settings tended to view intelligence narrowly as *the ability to grasp concepts and reason correctly with abstractions and solve problems* [10]. Sternberg et al. [11] identified a new type of intelligence known as real-world intelligence. They declared that intelligence may be displayed in places other than the classroom and focuses on specific content domains. In our review of the literature, we found about twenty definitions of academic and 'real-world' intelligence. Although an extraordinary diversity is found within these definitions, there are striking commonalities as well. To better understand the conceptions of intelligence, we classify and summarize the domains referred to by Sternberg et al. [11] in Table 1, which covers the majority of definitions of intelligence. The framework does not capture the detail of any single definition; it shows, however, the degree to which there exists a consensus among theorists regarding the broad outlines of a definition of intelligence. Furthermore, it shows how quite diverse conceptions of intelligence all have a certain basic premise in common.

As we can see in the Table 1, theorists identify three main loci of intelligence: (1) intelligence within the individual; (2) intelligence within the environment; and (3) intelligence within the interaction between the individual and the environment. Within these three main loci, there are a number of more specific definitions of intelligence.

1) Intelligence within the Individual

Theorists identifying intelligence as existing within the individual define three main levels:

TABLE 1. OVERVIEW OF DEFINITIONS OF INTELLIGENCE (STERNBERG ET AL., 1986)

I: In individual					II: In Environment		III: Individual-environment interaction
A: Biological level	1.Across Organisms	a. Between species			A. Level of culture/society	1.Demands	
						2.values	
						3.Demands-values interaction	
		b. Within species			B. Level of niche within culture/society	1.Demands	
		c. Between-within interaction				2.Values	
	2.Within organisms	a. Structure				3.Demands-values interaction	
		b. Process					
		c. Structure-process interaction					
	3.Across-within interaction						
B: Molar level	1.Cognitive	a. Metacognitive	i. Processes		C. Level × sublevel interaction		
			ii. Knowledge				
			iii. Process-knowledge interaction				
		b. Cognition	i. Processes				
			ii. Knowledge	(a) Selective attention			
				(b) Learning			
				(c) Reasoning			
				(d) Problem solving			
				(e) Decision making			
			iii. Process-knowledge interaction				
		c. Metacognition-cognition interaction					
	2.Motiviational	a. Level (magnitude) of energy					
		b. Direction (disposition) of energy					
		c. Level-direction interaction					
C. Behavioral level	1. Academic	a. Domain General					
		b. Domain-specific					
		c. General-specific interaction					
	2. Social	a. Within- person					
		b. Between-person					
		c. Within-between person					
	3.Practical	a. Occupational					
		b. Everyday living					
		c. Occupational-everyday living interaction					

a) *Biological level*, which can be established either across or within organisms. Intelligence can be viewed within the context of the evolution of a single species and the genetics of that species, or within the interaction between the evolution of an interspecies and the genetics of that interspecies. Within organisms, intelligence can be viewed in terms of the structure of the organism, or in terms of process. Furthermore, it is possible to look at the interaction between structure and process.

b) *Molar level* emphasizes three principal aspects of mental functioning:

- *Cognitive Aspect*: This deals with three main kinds of cognition: (1) Metacognition; (2) Cognition; and (3) the interaction between Metacognition and Cognition. Metacognition refers to knowledge about and control of one's cognition. Cognition refers to what is known and controlled by metacognition. Cognitive theorists place a great deal of importance on the interaction between metacognition and cognition for individuals to function intelligently; metacognition must be modified to accommodate cognition and vice versa. Both aspects of functioning seem to be a necessity for cognitive theorists, regardless of what they are called or how they are classified.
- *Motivational Aspect*: Motivational theorists argue that there is more to intelligence than cognition and that motivation must also be taken into consideration. Three principal properties of motivation need to be considered: (1) the level of the motivation; (2) the direction of the motivation; and (3) the interaction between the level and direction of motivation. An individual may have the motivation to learn, but this motivation may not be equally directed to all kinds of learning; therefore, it is necessary to take direction into account. Intelligence is affected not only by the amount of learning, but also by the kinds of learning, and both the amount and kind of learning are affected by motivation.
- *Behavioral level*: This is an analysis of what one does rather than what one thinks about. Behavioral theorists argue that intelligence resides in one's behavior rather than in the mental functioning that gives rise to the behavior.

2) Intelligence within the Environment

Some theorists view intelligence as residing within the environment, either as a function of one's culture and society, or as a function of one's niche within the culture and society, or both. In essence, culture determines the very nature of intelligence. The culture, society or niche within the culture and society is generally a function of the demands of the environment in which people live, the values held by the people within that environment and the interaction between these demands and values.

3) Intelligence within the Interaction between the Individual and the Environment

Many theorists define intelligence as the interaction between the individual and the environment. Understanding intelligence may be facilitated by considering the interaction of people with one or more environments and by recognizing the possibility that people may be differentially intelligent in different environments, depending on the demands of these various environments.

C. Cultural Intelligence and its Dimensions

In the literature, researchers have different opinions regarding the concept of CQ. Earley and Ang [12] present CQ as a reflection of people's ability to collect and process information, to form judgments, and to implement effective measures in order to adapt to a new cultural context. They also indicate that CQ should predict performance and adjustment outcomes in multicultural situations when an individual is faced with diversity. Earley and Mosakowski [13] redefine CQ as the ability of managers to deal effectively with different cultures. They suggest that CQ is a complementary form of intelligence, which may explain the capacity to adapt to cultural diversity, as well as to operate in a new cultural setting. Peterson [14] interprets CQ in terms of its operation. He believes that the concept of CQ is compatible with the cultural values of Hofstede and their five main dimensions [15], i.e., individualism versus collectivism, masculinity versus femininity, power distance, uncertainty avoidance, and short- and long-term orientation. Brisling et al. [16] define CQ as the level of success people obtain when adapting to another culture. Thomas [17] [18] explains CQ as the ability to interact efficiently with people who are culturally diverse. Ng and Earley [19] present CQ as the ability to be effective in all cultures. Johnson et al. [20] define CQ as the ability of an individual to integrate a

set of knowledge, skills and personal qualities so as to work successfully with people from different cultures and countries, both at home and abroad.

Researchers in this field also use different dimensional structures to measure CQ. All of this research is associated with conceptual models. These structures seek first to explain the attributes that enable people to develop their abilities in various cultural contexts, and then to determine how people can improve these capabilities. Earley and Ang [21] present the first structure of CQ, which integrates the following three dimensions: Cognition, Motivation and Behavior. While Thomas [22] agrees with this tridimensional CQ, he does not share their point of view regarding what these three dimensions should be. Therefore, he advocates another tridimensional structure. His belief is founded on the theory of Ting-Toomey [23], which states that the structure of CQ should be based on the skills required for intercultural communication, that is to say, knowledge, vigilance and behavior. Vigilance acts as a bridge connecting knowledge and behavior, which is the key to CQ. Tan [2] believes that CQ has three main components: (1) strategic thinking about culture; (2) dynamics and persistence; and (3) specific behaviors. Tan stresses the importance of behavior as being essential to CQ. If the first two parts are not converted into action, CQ is meaningless. Ang et al. [6] subsequently suggest a multifactor construct based on Sternberg and Detterman's framework of general intelligence [11]. CQ similarly focuses on a specific domain-intercultural setting of intelligence, and is motivated by the practical reality of globalization in the business workplace [12]. They divide CQ into metacognitive CQ, cognitive CQ, motivational CQ and behavioral CQ. This structure has been widely used in the following cultural research and studies. Here, we give more details of the role of each of the four CQ dimensions from their work:

1) *Metacognitive CQ* is the critical dimension that enables users to move beyond cultural stereotypes and to know when and how to apply their cultural knowledge. Individuals with a high metacognitive CQ are aware of unique individual characteristics, such as diversity within cultures and the influence that context has on behavior. They know when to suspend judgment and when to look for additional cues. Consequently, they engage in more appropriate behaviors in different intercultural situations.

2) *Cognitive CQ* emphasizes the knowledge of cultural values and orientations, as well as the knowledge of cultural universals such as the legal, political, economic and social systems of different cultures. This knowledge provides a useful starting point for users in their interactions with others. Users with a high cognitive CQ understand key issues and differences in behaviors. This helps them to adapt their own behaviors appropriately according to the situation, and consequently, to interact more effectively with people from a culturally different society.

3) *Motivational CQ* provides the important drive for users to persist in intercultural interactions. Users with a high motivational CQ are likely to direct more energy toward learning and understanding cultural differences. They are likely to persist and practice new behaviors even when faced with challenges.

4) *Behavioral CQ* enables users to enact appropriate behaviors. Effective intercultural interactions require users to possess a high behavioral CQ and to enact the desired behaviors. Effective intercultural interactions require competences in both verbal language and nonverbal behaviors such as gestures and displays of emotion. Individuals with a high behavioral CQ are able to adapt to their situation and display the appropriate behaviors.

D. Cultural Intelligence and Business

Business is becoming increasingly globalized, and partnerships are a means to gain a competitive advantage. We believe that cultural differences have a greater impact on cross-cultural business efficiency than previously thought. Cultural backgrounds influence how people think, act and interpret information during business activities. Thus, the potential for success or failure depends on the ability of organizations and leaders to make appropriate decisions within a framework of cultural diversity. Businesses and leaders must understand and become proficient in intercultural communication. In this regard, CQ offers strategies to improve cultural perception and to make it possible to understand the culturally motivated behavior of individuals, companies and organizations. Many articles [24] [25] [26] address the importance of CQ and culture in the context of international business [27] [28] [29]. Huber [30] indicates that the performance of an international business, in terms of efficiency and effectiveness, is determined by the quality of its organizational intelligence. Ang and Andrew [31] specify that organizational intelligence is the CQ of businesses. CQ in business is based on the research on psychology concerning the CQ of individuals, as well as on the views of the organizations. CQ permits businesses to collect a set of resources and to develop their capabilities. Ang and Andrew suggest that, when organizations venture into foreign territories, CQ is a necessary predictor of organizational performance. The involvement in international trade offers significant advantages and challenges to the business development of a company. A business may be successful at home because of its cultural sensitivity. However, this does not guarantee that it will be able to attract international suppliers, partners and customers. If the business does not learn to adapt to cultural differences, it risks losing and missing business opportunities. A business approach that is culturally inappropriate may be detrimental when doing business abroad. Knowledge and sensitivity toward other cultures result in increased business success. Consequently, CQ is of the utmost importance when engaging in international business practices.

In sum, research on CQ has provided a new perspective and presented a new way to alleviate cross-cultural businesses challenges. This research aims to invent a CQ computational model in order to process cultural knowledge and to support international business decision-making processes.

E. Development of our Conceptual Model

Making a good cross-cultural business decision depends on many factors. In the past, cultural scholars used CQ only to evaluate an individual's ability to adapt to cultural diversity. In this study, we consider the cultural factor, which is the effect of CQ on business decision-making processes. Thus, the concept of CQ is for the first time extended in order to assess cross-cultural business decision making. Business decisions with a high CQ are expected to have a more effective performance in and adjustment to multicultural situations.

Sternberg et al. [11] state that general intelligence has four dimensions, i.e., Metacognition, Cognition, Motivation and Behavior. They consider the correlation between the four dimensions as an entity and take full account of their integrity because of their interdependence. Therefore, we assume CQ should also include and consider its four dimensions and their correlation. We agree that the four dimensions of CQ are critical factors that can help individuals, companies and organizations to overcome cross-cultural challenges. Thus, the result of the main theories we developed from this study is that the diverse structures of CQ should be considered collectively in order to integrate the elements required to respond to the cultural knowledge acquired and to respect the decision-making process in cross-cultural business activities. Therefore, we created a CQ conceptual model in order to complete the theories of CQ and the decision-making process required.

We present our model as a whole aggregate multidimensional construct by considering the following conditions: (1) the entire construct considers that the four CQ dimensions occupy the same important level in conceptualization; and (2) the four CQ dimensions form the construct. In sum, in our research we put forward the cognitive theory that the metacognitive CQ, cognitive CQ, motivational CQ and behavioral CQ are four interrelated components built into the CQ, and we integrate our theory into the model (see Fig. 2).

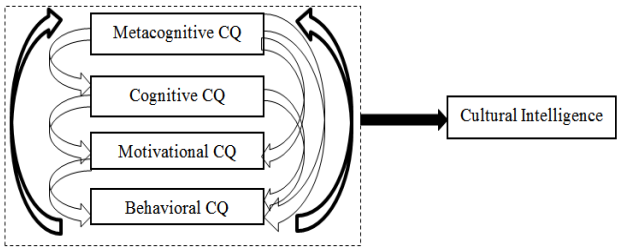

Figure 2. Cultural intelligence conceptual model

This conceptual model proposes a cyclical process of CQ decision making in four stages, while respecting the correlation and interdependence between the four dimensions: (1) It observes the behaviors, promotes active thinking and drives individuals to adapt and revise their strategies in different cultural settings; (2) It acquires and understands the knowledge that can influence individuals' thoughts and behaviors; (3) It considers the implications and emotions associated with cultural settings, and it drives efforts and energy toward effective functioning in a new culture; and (4) It transfers knowledge through verbal and nonverbal behaviors to the culturally diverse situations. This process enables us to identify the elements of the global CQ so we may apply it as a whole, regardless of whether these dimensions are decision variables or other measurable parameters. In this process, we adopt a holistic approach that does not aim to reduce the model to its individual components.

III. CHOICES OF AI TECHNOLOGIES

Individuals, companies and organizations need research combining CQ and AI to support them in decision making in international business. We have not yet found any research that attempts to combine AI and CQ in the context of using CQ knowledge to develop a business intelligent system. This is a gap in the present research. Below, we present how our work meets the challenge of filling the gap between AI and CQ studies for business decision-making support.

A. AI Technologies

We make use of technology solutions to invent a computational model based on our conceptual CQ model with many complex behaviors without degrading the conceptual model's overall quality of human-like thinking in business activities. Business intelligence generally involves two types of data: the first type consists of traditional crisp values, or numbers; the second type is uncertain, incomplete and imprecise. This information is presented in a manner that reflects human thinking and is called "soft data." When we introduce the cultural concept to cross-cultural business activities, we usually use soft information represented by words rather than traditional crisp numbers. The traditional computational technique, known as "hard" computing, is based on Boolean logic and cannot treat cross-cultural business soft data. In order to enable computers to emulate a way of thinking that resembles that of humans, and in order to improve CQ soft data interpretation, we first used fuzzy logic to design the computational model. This technology is capable of operating with uncertain, imprecise and incomplete information. It attempts to model a human-like understanding of words in decision-making processes. Fuzzy logic technology is used for three reasons: (1) The CQ concepts are described in natural language containing ambiguous and imprecise linguistic variables, such as "*this person has low motivation*" and "*that project is highly risky because of this religion*." (2) Fuzzy logic is well suited to modeling human decision-making processes when dealing with "soft criteria." These processes are based on common sense and may contain vague and ambiguous terms [32]. (3) Fuzzy logic provides a wide range of business cultural expressions that can be understood by computers.

Although fuzzy logic technology has the ability and means to understand natural language, it offers no mechanism for automatic rule acquisition and adjustment. To remedy this defect, the second technology that we

choose is the Artificial Neural Network (ANN). ANN presents a viable solution for processing incomplete and imprecise business cultural information. ANN can learn from historical business cultural cases and manage new data input and CQ generalization rules of acquired knowledge automatically. ANN technology is used for two reasons: first of all, it can be used to extract hidden CQ knowledge in large quantities of cultural data; second, ANN can also be used to correct CQ fuzzy rules. In other words, where acquired CQ knowledge is incomplete, ANN can refine the knowledge, and where CQ knowledge is inconsistent with some given cultural data, neural networks can revise the CQ rules. In our computational model, ANN technology avoids the tedious and expensive processes of CQ knowledge acquisition, validation, and revision.

Fuzzy logic and ANN are complementary paradigms in our computational model. This hybrid neuro-fuzzy technology makes use of the advantages and power of fuzzy logic and of ANN. The soft-computing technology infers the characteristics of the CQ in an environment of cultural diversity and invents an updated computational model taking into account the CQ knowledge. This soft-computing technology is able to reason and learn in an uncertain and imprecise cultural environment. Soft-computing technology represents the essence of our computational model.

Furthermore, because this hybrid technology is applied to our computational model, the model represents both a symbolic approach and a connectionist approach. CQ symbol representations are the product of human cultural work, which means that there is direct access to semantic CQ knowledge. CQ knowledge about the external cultural world is abstracted via perception and represented using a symbolic framework. We use CQ symbol manipulation processes to equip the model and logical rule-based approaches to apply to the model. The CQ symbols are interpreted and reasoned about by using fuzzy logic technology. This technology for CQ symbolic representation mechanisms allows the model to reason about the external cultural world. This method easily and efficiently adapts and interacts with the external world, predicts the future and uses reasoning capabilities.

The connectionist approach that we use in the model is ANN; it is the construction of skills through a self-organizational (behavioral) process in which the model interacts in real time with its environment. In the connectionist approach, the model depends on the parallel processing of non-symbolic distributed activation patterns. Contrary to the rule-based fuzzy logic that we used in the symbolic approach, statistical methods are applied in order to process information in this part.

B. Linguistic Variables and Fuzzy Rules

The concept of fuzzy logic is not only a technology but also a new philosophical concept in the cultural domain. At the heart of fuzzy logic lies the concept of a linguistic variable. The idea of linguistic variables is one basis of the fuzzy set theory. A linguistic variable is a fuzzy variable. The cultural values of linguistic variables are words rather than numbers. For example, when we say "*Cultural Intelligence is high*," it means that the linguistic variable of CQ takes the linguistic value *high*. We use IF-THEN fuzzy rules to incorporate the knowledge of human cultural experts. Thus, our linguistic variables are used in fuzzy rules. For example:

Rule 1:

IF	metacognition is high AND cognition is high AND motivation is high AND behavior is high
THEN	CQ is high

The fuzzy set operations used in our system are *Intersection* and *Union*. For example, the fuzzy operation used to create the *Intersection* of two fuzzy sets A and B is as follows:

$$\mu A \cap B(x) = min[\mu A(x), \mu B(x)] = \mu A(x) \cap \mu B(x), where\ \ x \in X \quad (1)$$

The operation to form the *Union* of two fuzzy sets A and B is as follows:

$$\mu A \cup B(x) = max[\mu A(x), \mu B(x)] = \mu A(x) \cup \mu B(x), where\ x \in X \quad (2)$$

The fuzzy sets are shown in Fig. 3. Each universe of discourse consists of three fuzzy sets: *Low*, *Medium* and *High*. As we can see in Fig. 3, a person who has a score of 6.8 in fuzzy logic has a membership in the '*High*' set with a degree of 0.2. At the same time, he/she has also a membership in the '*Medium*' set with a degree of 0.15 This means that a person with a score of 6.8 adheres partially to several sets.

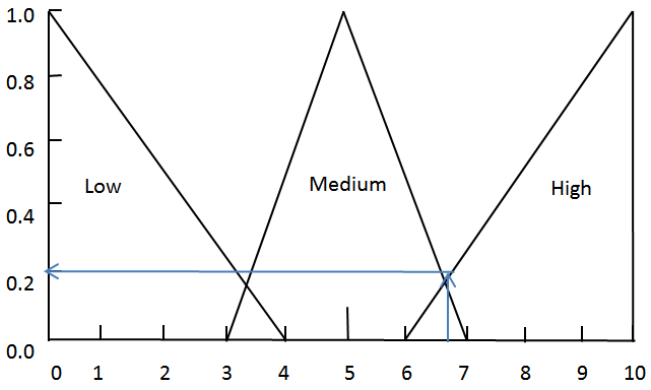

Figure 3. Three fuzzy sets: Low, Medium, and High fuzzy sets

As we explained above, our hybrid neuro-fuzzy computational model uses AI technologies and combines the advantages of fuzzy logic and ANN. It can be trained to develop IF-THEN fuzzy rules. CQ expert knowledge is easily incorporated into the structure of the neuro-fuzzy model. At the same time, the connectionist structure prevents fuzzy inference, which would entail a substantial computational burden.

CQ decision making is often based on the intuition, common sense and experience of experts. A large number of

fuzzy rules provide us with a means of modeling how experts make decisions in cross-cultural activities. Based on these rules, users' decisions can be evaluated and appropriate suggestions can be offered by the system.

IV. DESIGNING THE CULTURAL INTELLIGENCE COMPUTATIONAL MODEL

In this section, we explain how to extract cultural information from a business decision-making process and how to assess decisions through our CQ computational model. The purpose of creating our computational model is to help users make decisions in cross-cultural activities.

A. Computational Model

On the basis of our whole aggregate multidimensional CQ conceptual model (see Fig. 2), we computerize this CQ conceptual model into a CQ computational model.

The model is a multilayer neural network that is functionally equivalent to a fuzzy inference model. It uses a technique called the fuzzy inference method by Mamdani [33]. Fig. 4 illustrates an example of the application of this technique in the model through the use of triangular sets.

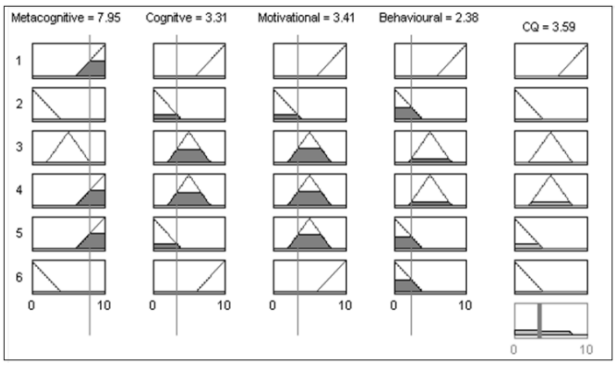

Figure 4. Example of Mamdani-Style fuzzy inference using triangular sets

We define the fuzzy inference model as having four crisp inputs: *Metacognitive CQ*, *Cognitive CQ*, *Motivational CQ* and *Behavioral CQ*, and as having one output: CQ. For example, input metacognition is represented by metacognitive fuzzy sets 1, 2, 3, 4, 5, and 6; output CQ is represented by fuzzy sets CQ 1, 2, 3, 4, 5, and 6. Each row represents a rule; each column represents a crisp input which determines the degree to which these inputs belong to each of the appropriate fuzzy sets.

Fig. 5 shows the neuro-fuzzy model that corresponds to this fuzzy inference model. It is represented with a neural network composed of five layers in the model. Each layer of the network is associated with a particular step in the fuzzy inference process by Mamdani [33]. We also have four inputs in our computational model: Metacognitive CQ, Cognitive CQ, Motivational CQ and Behavioral CQ, and one output: CQ.

We explain the network inference process of the computational model as follows:

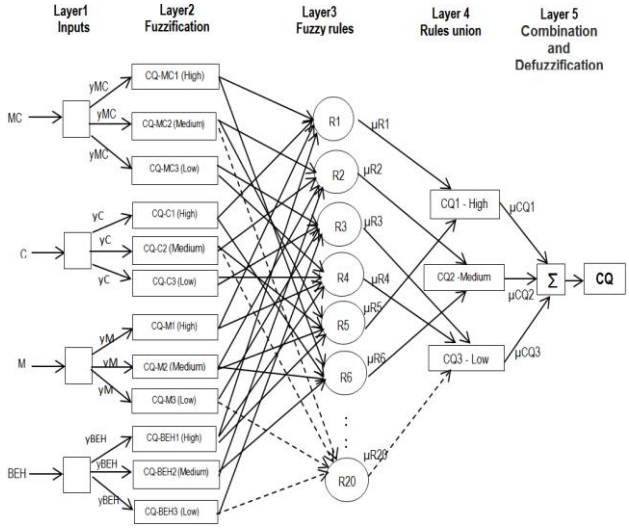

Figure 5. Computational model of cultural intelligence for decision making

Layer 1 - Inputs: No calculation is made at this layer. Each neuron corresponds to an input cultural variable. These input values are transmitted directly to the next layer.

Layer 2 - Fuzzification: Each neuron corresponds to a business CQ linguistic label (e.g., *High*, *Medium* and *Low*) associated with one of the input CQ variables in Layer 1. In other words, the connection of the output, which represents the membership value, specifies the degree to which the input CQ values belong to the neuron's fuzzy set. The connection is computed at this layer.

Layer 3 - Fuzzy Rules: The output of a neuron at this layer is the cultural fuzzy rules. Each neuron corresponds to one CQ fuzzy rule. The CQ fuzzy rule neurons receive inputs from Layer 2, which represent CQ fuzzy sets. For example, neuron R1 represents CQ rule 1 (Rule 1: *IF metacognition is high AND cognition is high AND motivation is high AND behavior is high THEN CQ is high).* Neuron R1 receives input from the neurons *CQ-MC1 High*, *CQ-C1 High*, *CQ-M1 High and CQ-BEH1 High*.

Layer 4 - Rules Union (or consequence): At this layer, neurons have two main tasks: (1) to combine the precedent of CQ rules; and (2) to determine the output level (*CQ1-High*, *CQ2-Medium* and *CQ3-Low*).

Layer 5 - Combination and Defuzzification: This layer combines all the consequential rules and computes the crisp output after defuzzification. The composition method "sum-product" [34] is used. It computes the outputs of the membership functions defined by the weighted average of their centroids. We apply, in this case, the triangle calculation in our computational model, which is the simplest calculation of the fuzzy set as shown in Fig. 6.

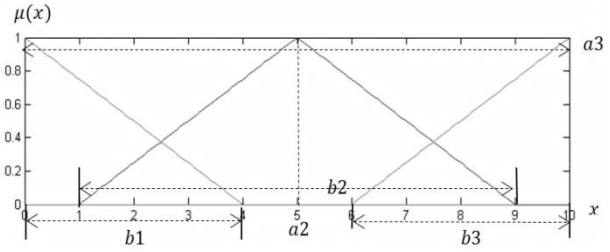

Figure 6. Calculation of cultural intelligence fuzzy sets

The calculation formula (see Equation (3)) of the weighted average of the centroids of the clipped fuzzy sets *CQ3 (Low)*, *CQ2 (Medium)* and *CQ1 (High)* is calculated.

$$y\,(Cultural\ Intelligence) = \frac{\frac{1}{3}b_1^2\mu 1 + a_2 b_2 \mu 2 + \left(a_3 - \frac{1}{3}b_3\right)b_3\mu 3}{b_1\mu 1 + b_2\mu 2 + b_3\mu 3} \quad (3)$$

where a_2 and a_3 are the respectively center of the medium and high triangles; b_1, b_2 and b_3 are the widths of fuzzy sets, which correspond to *CQ 3*, *2* and *1*.

In Fig. 7, we present the first input (MC) of Fig. 5 in order to explain the process of obtaining the value of the Metacognitive CQ dimension. The other three dimensions, i.e., Cognitive CQ, Motivational CQ, and Behavior CQ, follow the same process.

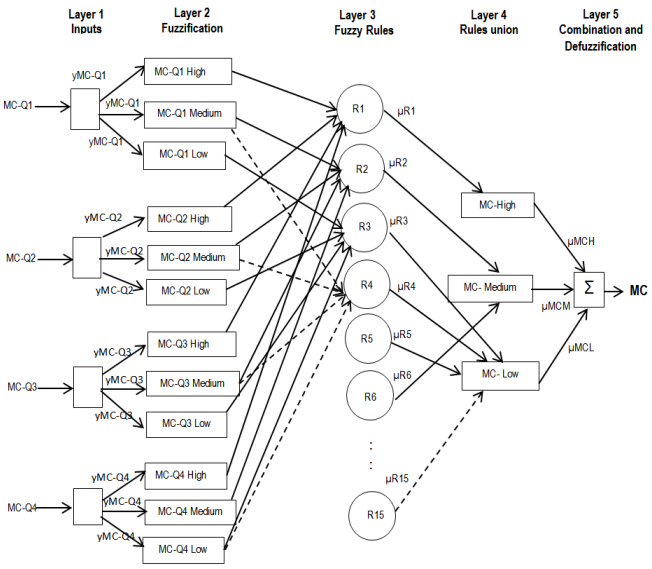

Figure 7. Example of inference to obtain the Metacognition value in the computational model

Fig. 7 shows the neuro-fuzzy model that also respects the fuzzy inference model, which has four inputs *MC-Q1*, *MC-Q2*, *MC-Q3* and *MC-Q4*. The model is composed of five layers. Each layer of the neural network is associated with the same steps in the fuzzy inference process by Mamdani [33].

In detail, a business decision in the metacognitive dimension can be devised using four aspects. The four aspects are expressed in natural language as follows: 1) This decision is conscious of the cultural adaptation it uses when interacting with people with different cultural backgrounds; 2) This decision adjusts its cultural adaptation as it interacts with people from a culture that is unfamiliar to it; 3) This decision is conscious of the cultural adaptation it applies to cross-cultural interactions; 4) This decision checks the accuracy of its cultural adaptation as it interacts with people from different cultures. Thus, we have four inputs to the model, which represent these four aspects in the metacognitive dimension, and one output: Metacognition (MC).

Layer 1 - Input: Four inputs represent the answers of four aspects of users in metacognitive dimension. For example, MC-Q1 is the aspect 1 of Metacognitive CQ**.** These four input variables correspond to four neurons (*MC-Q1*, *MC-Q2*, *MC-Q3* and *MC-Q4*), and are transmitted directly to the next layer, which is expressed as:

$$yi^{(1)} = xi^{(1)},\ i = MC-Q1; MC-Q2; MC-Q3; MC-Q4 \quad (4)$$

where, $xi^{(1)}$ are the four inputs; $yi^{(1)}$ is the output of the four input neurons.

Layer 2 - Fuzzification: For simplicity, each user answer is divided into three fuzzy sets. For example, for aspect 1, the input *MC-Q1* is represented by three fuzzy sets *MC-Q1 High*, *Medium* and *Low*. Three other inputs also respect this principle, which is represented by the same three fuzzy sets *High*, *Medium* and *Low*. We have 12 neurons in this layer. Each neuron receives a crisp input and determines the membership degree to which this input belongs to the neuron's triangular fuzzy set. A triangular membership function by two parameters {a, b} is specified as follows:

$$y_i^{(2)} = \begin{cases} 0 & if\ x_i^{(2)} \le a - \frac{b}{2} \\ 1 - \frac{2|x_i - a|}{b}, & if\ a - \frac{b}{2} < x_i^{(2)} < a + \frac{b}{2} \\ 0 & if\ x_i^{(2)} \le a + \frac{b}{2} \end{cases} \quad (5)$$

$$i = MC-Q1; MC-Q2; MC-Q3; MC-Q4$$

where *a* and *b* are parameters that control the center and the width of the triangle, $xi^{(2)}$ is the input, and $yi^{(2)}$ is the output.

Layer 3 - Fuzzy Rule: Every single neuron in this layer represents a metacognitive fuzzy rule. For example, *R1* corresponds to Rule 1. The value of *yR1* is the output of fuzzy rule 1; it also represents the strength of *R1*. The rule is calculated by the fuzzy operation *Intersection*; therefore, the output of neuron *yR1* is obtained as:

$$yR1^{(3)} = \mu MC\_Q1H \times \mu MC\_Q2H \times \mu MC\_Q3H \times \mu MC\_Q4H = \mu R1 \quad (6)$$

where $\mu MC\_Q1H, \mu MC\_Q2H, \mu MC\_Q3H, \mu MC\_Q4H$ are the inputs and $yR1^{(3)}$ is the output of metacognitive fuzzy rule neuron *R1*.

Layer 4 - Rules Union: The neurons in this layer receive inputs from the corresponding metacognitive fuzzy rule neurons from Layer 3 and combine them. The output of the *MC* is also expressed by fuzzy sets *MC High*, *Medium* and *Low*. The fuzzy operation we use is *Union*. For example, the *Medium* of *Metacognition (MCM)* is expressed as:

$$yMCM^{(4)} = MAX(\mu R2, \mu R6) = \mu MCM \qquad (7)$$

where $\mu R2, \mu R6$ are the inputs and $yMCM^{(4)}$ is the output in Layer 4.

Layer 5 - Combination and Defuzzification: Each neuron represents a single output of the network. We need to combine them into a single fuzzy set. The combined output fuzzy set must be defuzzified. Here, we use the same calculation and principle as for the CQ to calculate Metacognition; the formula is given as follows:

$$y\ MC = \frac{\frac{1}{3}b_1^2\mu MCH + a_2 b_2 \mu MCM + \left(a_3 - \frac{2}{3}b_3\right)b_3\mu MCL}{b_1\mu MCH + b_2\mu MCM + b_3\mu MCL} \qquad (8)$$

where *MCH* represents the metacognitive *High*, *MCM* represents the metacognitive *Medium*, and *MCL* represents the metacognitive *Low*.

The section above describes our basic concept computational model. Applying fuzzy set theory, many similar fuzzy inference styles have been built, such as Mamdani-style and Sugeno-style. However, in this real practical research, many computational bottlenecks are needed to break through when implementing fuzzy inference process in a neural network.

B. Supervised Learning

One of the main properties of the model is supervised learning, which has the ability to learn from CQ expert experiences and to improve performance by modifying the CQ rules through learning. Supervised learning involves cultural inputs and cultural outputs that are available to our multilayer neuro-fuzzy network. The task of the network is to predict or adjust inputs to the desired outputs.

This multilayer neuro-fuzzy network can apply standard learning algorithms, such as back-propagation, to train it. The network offers a mechanism for automatic IF-THEN rule acquisition and adjustment. This mechanism is very useful, especially in situations where cultural experts are unable to verbalize the knowledge or problem-solving strategy they use.

The principle of the back-propagation algorithm in supervised learning in our model is that we provide the model with the final external CQ data that supervised learning requires; these data represent the results of a user's decision. Each case contains the original input cultural data and the output data offered by CQ human experts to be produced by the model. The model compares actual output with the CQ experts' data during the training process. If the actual output differs from the data given by experts in the training case, the model weights are modified.

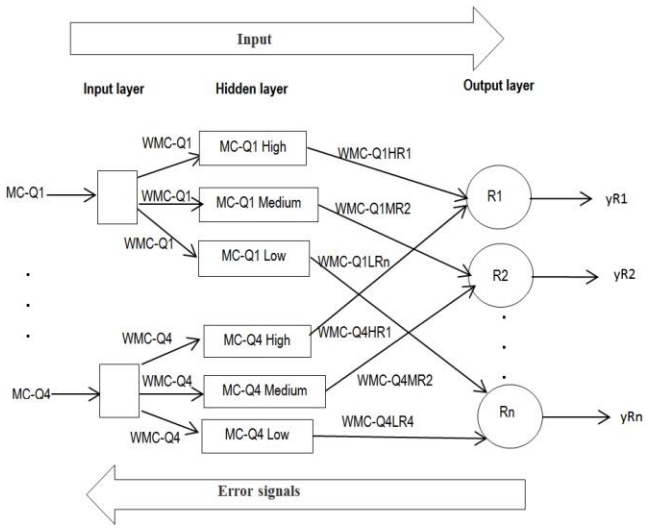

Figure 8. Back-propagation in CQ Neuro-Fuzzy network learning

Figs. 5 and 7 explain neuro-fuzzy inference structure. Fig. 8 shows how to train this neuro-fuzzy network. It is from one part of our Fig. 7 with three layers (Input layer, Hidden layer and Output layer), as an example to illustrate how the neuro-fuzzy network learns by applying the back-propagation algorithm. *MC-Q1* and *MC-Q4* refer to neurons in the input layer; *MC-Q1High*, *MC-Q2 Medium* and *MC-Q1Low* refer to neurons in the hidden layer; and *R1*, *R2* and *Rn* refer to neurons in the output layer. We explain our model's learning process theory in three steps as follows:

Step 1 - Input Signals: We input signals from *MC-Q1* to *MC-Qn* into the model; these signals are propagated through the neuro-fuzzy network from left to right, while the difference signals (or error signals) are propagated from right to left.

Step 2 - Weights Training: To propagate difference signals, we start at the output layer and work backward to the hidden layer. The difference signal at the output of neuron *R1* at sequence *s* is calculated as follows:

$$D_{R1}(s) = y_{e,R1}(s) - y_{R1}\ (s) \qquad (9)$$

where $y_{e,R1}(s)$ is the cultural experts' desired output data of neuron *R1* at iteration *s*. $D_{R1}(s)$ is the difference between the output $y_{R1}\ (s)$ and the experts' desired output data at iteration . For example, we use a forward procedure method to update the CQ rules' weight $W_{MC-Q1HR1}$. Rule *R1* for updating weight at the output layer at iteration *s* is defined as:

$$W_{MC-Q1HR1}(s+1) = W_{MC-Q1HR1}(s) + \Delta W_{MC-Q1HR1}(s) \qquad (10)$$

where $\Delta W_{MC-Q1HR1}(s)$ represents the weight correction of the *MC-QHR1* at iteration *s*.

Step 3 – Iteration: We increase iteration *s* by one and repeat the process until the preset difference criterion is satisfied.

Following the above three-step learning procedure, we give a concrete example to show how the model obtains the desired value after learning. Suppose we have collected five people's input data, and get five corresponding CQ results from the output of the model as: y = [5, 6, 7, 3, 2]. On the other hand, the cultural experts give five desired CQ output values as: yd = [7, 7, 6.5, 4.5, 7]. We now use these five pairs of input data and desired values to train the model.

We use this example with two different training algorithms to compare how the computational model learns. This approach facilitates the comparison of the results of two different algorithms that we used in our training process. The first algorithm considers the balance of the five-layer network and the generalization of the model. As shown in Fig. 9, after the training with 10 epochs (an epoch is the presentation of an entire training set to the model during training.) The vertical axis (Training-Blue) represents the difference (or error) between the system outputs and the targets.

```
>> net=mycreat(7);
t =
    7.0000    7.0000    6.5000    4.5000    7.0000
>> net=mytrain2(net,p2,t);
TRAINLM, Epoch 0/100, MSE 41.2922/0, Gradient 7.85865/1e-020
TRAINLM, Epoch 10/100, MSE 0.583818/0, Gradient 2.26785e-016/1e-020
TRAINLM, Maximum MU reached, performance goal was not met.
>> sim(net,p2)
ans =
    7.0620    5.5925    7.4443    4.3537    7.1457
>> t
t =
    7.0000    7.0000    6.5000    4.5000    7.0000
>> t-sim(net,p2)
ans =
   -0.0620    1.4075   -0.9443    0.1463   -0.1457
```

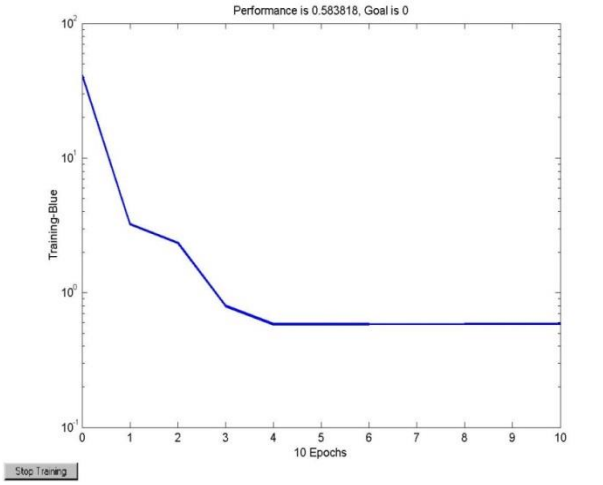

Figure 9. Learning algorithm 1 in computational model

However, the model learns very slowly. The computational model stops learning after 10 epochs, and the model reproduces five final results that still differ from the desired CQ output values. For example, the first desired data requires 7; after training, the model shows the training result 7.062, with a difference of -0.0620. Thus, as the message shows, our performance goal has not quite reached the desired value.

We use the second algorithm to train the model. This training method does not consider the balance of the neuro-fuzzy network and the generalization of the model. After 9 epochs training processes, we get the new output from the model as: y = [7, 7, 6.5, 4.5, 7], shown in Fig. 10.

```
>> net=mycreat(7);
>> net=mytrain3(net,p2,t);
TRAINLM, Epoch 0/9, MSE 45.2964/0, Gradient 13.567/1e-010
TRAINLM, Epoch 9/9, MSE 1.65969e-022/0, Gradient 4.16374e-012/1e-010
TRAINLM, Maximum epoch reached, performance goal was not met.
>> sim(net,p2)
ans =
    7.0000    7.0000    6.5000    4.5000    7.0000
>> t
t =
    7.0000    7.0000    6.5000    4.5000    7.0000
```

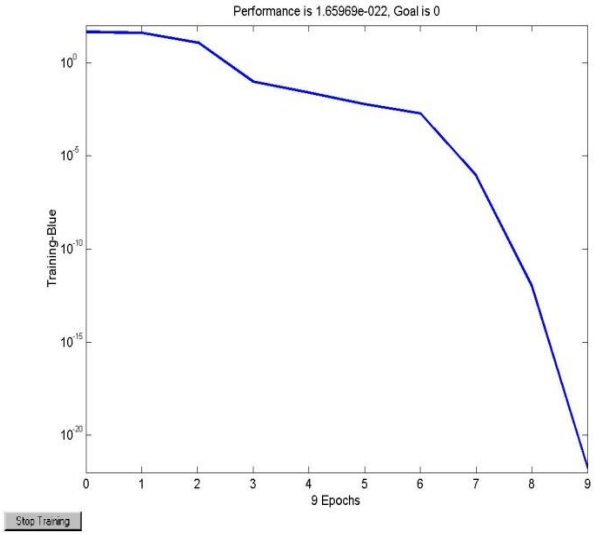

Figure 10. Learning algorithm 2 in computational model

The output of the model quite accurately resembles the desired CQ values yd = [7, 7, 6.5, 4.5, 7] from the cultural experts, and we believe our computational model has reached the training goal, that is to say, the model has the ability to learn new CQ knowledge.

In this model, we only change the weights following the fuzzy rules layer. In order to prevent an overfitting problem, we prefer the algorithm 1. However, a detailed description of learning algorithms is beyond the scope of this paper. The algorithm criterion is that it not only guarantees training speed but also considers balance and generalization in our neuro-fuzzy computation model. Fig. 11 shows another graphic in three dimensions that demonstrates how the neuro-fuzzy network converts bad rules weights into the desired CQ rules weights.

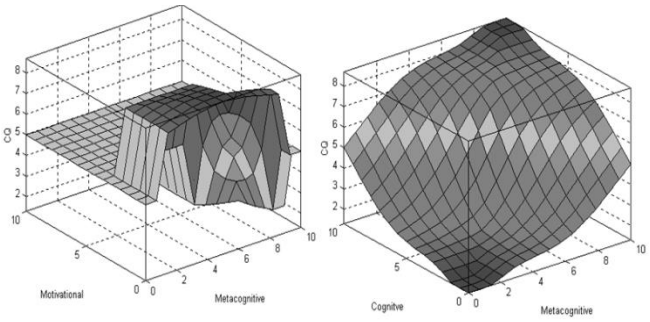

a) Bad rules b) Desired rules

Figure 11. Example of the result after supervised learning

V. IMPLEMENTING THE MODEL IN AN EXPERT SYSTEM

This section presents the general conceptual structure of our system, which includes three parts. First, we explain why we implemented our computational model in an expert system. Second, we describe the structure of the system. Third, we provide details of the CQ domain by collecting and analyzing both data and knowledge thus making key concepts of the system design more explicit.

A. Why an Expert System

In the preceding sections, we presented the two basic premises of our computational model through the application of soft computing: (1) to study the thought processes of human cultural experts; (2) to represent these thought processes for computer use; and (3) to be capable of acquiring, extracting and analyzing the new knowledge of cultural experts. In this section, we want the system should be able to express knowledge in a form that is easily understood by users and deal with simple requests in natural language rather than a programming language. Second, the system should act as would an efficient team of cultural experts capable of making decisions and providing explanations in the decision-making process in culturally diverse settings. Hence, we integrated the computational model into an expert system, which is designed to mimic the decision making of human experts [35] [36].

B. Cultural Intelligence Decision Support System

The system is called the Cultural Intelligence Decision Support System (CIDSS). The CIDSS represents CQ knowledge through the heuristic manipulation of a CQ database center. The CIDSS has three application domains: *Business Activities*, *Expatriate Assignments* and *Business Project Evaluation*. Fig. 12 illustrates the general structure of the CIDSS. The structure includes four main modules:

1) The CQ Computional Model contains CQ knowledge that is useful for solving business cultural problems. The *Cultural Intelligence Model* in this structure is represented by the trained neural-fuzzy network. This module supports all the cultural decision-making steps in the system. It connects with three different units: *New Data*, *Training Data* and the *Cultural Intelligence Database Center*. *New data* include users' requests for solving a given problem that involves cultural business affairs. *Training Data* are a set of training examples that are used for training the network during the learning phase. *The Cultural Intelligence Database Center* predominantly contributes to the knowledge gathered from the data about different cultural aspects, which have been collected from different countries.

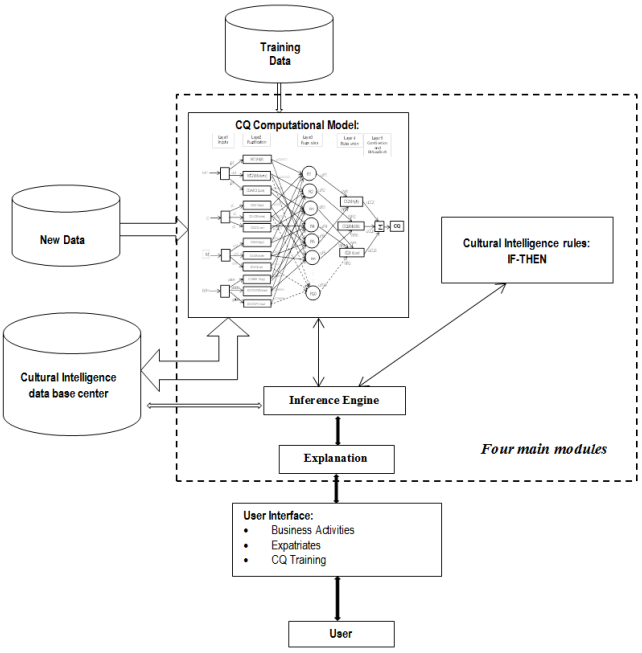

Figure 12. General deployment structure of CIDSS

2) The Cultural Intelligence IF-THEN Rules examine the CQ knowledge base, which is represented by the computational model, and produce rules which are implicitly "buried" in the neuro-fuzzy network.

3) The Inference Engine is the core of the CIDSS. It controls the flow of business cultural information in the system and initiates inference reasoning from the CQ knowledge base. It also concludes when the system has reached a decision.

4) The Explanation clarifies to the user why and how the CIDSS has achieved the specific business cultural decsions. These explanations include analyses, advice, conclusions and other facts required for deep reasoning.

As a hybrid intelligent system, it provides comprehensive and global solutions and forms a system of rules capable of adapting to a multicultural environment. This is the context in which the CIDSS was born. We combined two intelligent technologies: hybrid neural-fuzzy and expert system. The hybrid neural-fuzzy technology ensures that the CIDSS is capable of reasoning and learning in an uncertain and imprecise business cultural environment. The expert system, meanwhile, uses the knowledge of cultural experts and inference procedures in order to solve difficult problems normally requiring human expertise in the

CQ domain. This synergy improves adaptability, fault-tolerance robustness and speed of system.

The CIDSS possesses generic CQ and is not specific to a particular culture, such as that of the United States or China. The system shows big capabilities of cultural adaptation by modeling the human decision-making process in situations characterized by cultural diversity. Furthermore, due to its intricate cultural schemas and analytical abilities, the system can help users identify and understand key issues in cultural judgment and decision making. It also gives them the corresponding explanations. In this research, C/C++ is chosen as the programming language.

C. Data and Knowledge Acquisition

When more CQ knowledge has been collected, the system becomes stronger. CQ Data for the CIDSS are often collected from different sources, there are four different types of data in the CIDSS: (1) incompatible data, which is often the data we want to store in code and numbers in packed decimal format; (2) inconsistent data, which is often the same facts represented differently in CQ databases; (3) missing data, considered as actual cultural data records that often contain blank fields. We usually infer useful information from them and fill in the blank fields with average values; and (4) examples of previous CQ data that we use to train the neuro-fuzzy network. For example, we use a self-assessment questionnaire developed by Ang et al. [4] as the input data to CIDSS. This questionnaire has 20 items that measure CQ and was used to collect data for studies on the test subjects regarding their capacity for cultural adaptation.

In the process of knowledge acquisition in the CQ domain, we collect CQ knowledge by reading books and reviewing documents, manuals, papers, etc. We also collect additional information by interviewing cultural experts. During a number of interviews, cultural experts are asked to identify some typical cases, describe how they solve each case and explain the reasoning behind each solution. However, extracting knowledge from a human expert is a difficult process. Usually, cultural experts are unaware of the knowledge they have and the problem-solving strategy they use and they are often unable to verbalize these. Experts may also provide us with incomplete, inconsistent or irrelevant information. We then analyze the acquired knowledge and repeat the entire process. The example of CQ knowledge acquisition is given in Section III.

VI. CIDSS COGNITIVE ARCHITECTURE

As we mentioned in Section III, the CIDSS uses both the symbolic and the connectionist approaches of AI. The CIDSS respects the cognitive concepts regarding global CQ theories and details how the human mind works in decision-making processes. Noubel [37] considers that a decision-making process follows four major steps and describes how the path from idea to the action is organized in decision making. The sequence is used of the basis of the analysis in our cognitive cycle architecture:

1) *The reflection level:* Intelligence mobilizes and cross-fertilizes available knowledge via a refined synchronous or asynchronous dialogue, either through face-to-face contact or remotely. Dialogues draw on new horizons, allow the anticipation of conflicts, and prepare all decision makers for consensus.

2) *The options formulation level:* This level owes its quality to upstream thinking. This is a sensitive step that requires as much objectivizing of object-links (i.e., projects, threats, needs, etc.) as with elimination processes that require strong knowledge mobilization. It usually leads to a final option.

3) *Selection of the final option:* If steps 1 and 2 are managed with intelligence, then the selection of the final option is much easier. Candidate options are richer, more detailed, more flexible, and ultimately more representative.

4) *The action level:* This level engages new intelligence processes, knowledge interaction and operational coordination between decision makers. The cycle from steps 1 to 4 is permanent and self-inclusive. It functions like an endless spiral.

The CIDSS also relies on engineering concepts in its solutions for the design and implementation of software information. It offers better learning mechanisms, which emulate human intelligence. The CIDSS is a distributed and modular architecture. It relies on the functional "*cultural consciousness*" mechanism for much of its operations. Its modules communicate and offer information to each other.

By using its cognitive cycle, the CIDSS recognizes business-related information in natural language from its complex environment. The CIDSS influences its environment by offering a decision or recommendation to users. Fig. 13 describes the cognitive architecture of CIDSS.

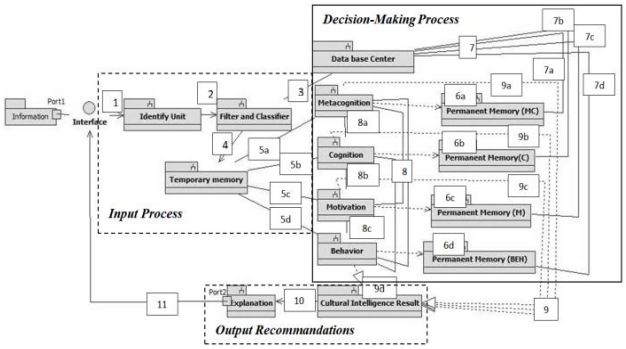

Figure 13. Cognitive architecture of CIDSS

The three main parts of the architecture are: (1) The *Input Process* presents information or a phrase in natural language, which expresses a user's demand via the input of the user interface. Through the *Identify Unit* to distinguish which domain the user wants to consult, the *Filter and Classifier module* takes the inputted information, classifies it, and filters what is not useful for analysis in the next steps; (2) The *Decision Making Process* is a neural network with fuzzy inference model capabilities. The system can be trained to develop IF-THEN CQ fuzzy rules and can

determine membership functions for input and output variables. This module has four sub-modules: *Metacognition (MC)*, *Cognition (C)*, *Motivation (M)* and *Behavior (BEH)*; (3) The *Recommendation* explains the results of decision making to users in natural language and provides suggestions.

The following describes these steps, which correspond to the numbers inside the rectangles in Fig. 13.

Step 1: The business information is in natural language and expresses a problem, a question or a requirement of the user. It is input through the user interface. The information enters the *Identify* module, which identifies the information used to determine what the user requires.

Step 2: The business information goes to the *Filter and Classifier* module. In this module, the information is classified. Useful information is filtered from non-useful information. The useful information is culturally analyzed in the following steps.

Step 3: To perform this classification, the module is associated with the *Cultural Intelligence Database Center*. This center has the necessary data required by the system, such as countries, religions, languages and laws.

Step 4: The classified business cultural data are ready to be sent to the *Temporary Memory* module. This module keeps the data temporarily and, at the same time, interacts with the other modules.

Step 5: Modules 5a-*Metacognitive*, 5b-*Congnitive* 5c-*Motiviational* and 5d-*Behavioral* collect the business cultural data belonging to them in the *Temporary Memory*.

Step 6: Each module depends on the consultation of its own *Permanent Memory*. These permanent memory modules are 6a for metacognition, 6b for cognition, 6c for motivation and 6d for behaviour. Each permanent memory represents a complete and specific cultural database that is used by its associated module to analyze the business cultural information stored in the *Temporary Memory*.

Step 7: 7a, 7b, 7c and 7d analyze the business cultural information. If data are missing, *Permanent Memory* modules go to the *Cultural Intelligence Database Center* to assist in the cultural analysis of the respective modules.

Step 8: After the analysis has been completed in each module, the four modules interact with each other to adjust their respective cultural decisions. This interaction enables each module to make a complete and effective decision before continuing to the next step.

Step 9: Following the interaction among the modules of the different dimensions of cultural intelligence, the four modules in steps 9a, 9b, 9c and 9d send their final cultural decisions to the *Cultural Intelligence Result* module. In this module, the decisions of these four modules are generalized and offer significant information to the user.

Step 10: The *Explanation* module justifies and explains in detail using natural language understandable to the user why these decisions were presented.

Step 11: The explanations are sent to the *User Interface*.

Figs. 14 and 15 present an example of two outputs of the *Expatriate Assignment* application domain that show how the CIDSS can help a user make decisions by taking into consideration his/her inputted request. The CIDSS prototype system follows the decision-making cycle process shown in Fig. 13. The input data are specific business questions in natural language provided by users. The system provides two outputs as answers to the question. Output 1 (Fig. 14) gives a general decision to answer the question put by the user.

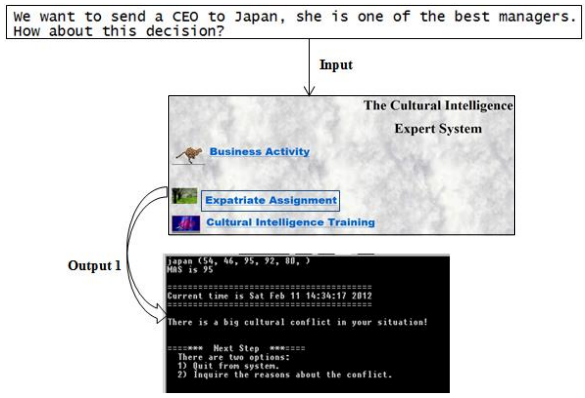

Figure 14. Example of CIDSS prototype system (Output 1)

Output 2 (Fig. 15) provides more detailed explanations, which clarify to the user why the system reached that decision.

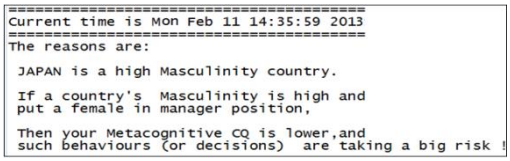

Figure 15. Example of CIDSS prototype system (Output 2)

VII. EVALUATION OF THE MODEL

Three cultural experts have validated our computational CQ model and the CIDSS prototype system. This validation ultimately reflects the consistency between the real world and the artificial CIDSS system. The CIDSS prototype system was also tested with two hundred people by measuring their CQ value. The effectiveness and robustness of the system is evaluated by carrying out a regression analysis on these data. Fig. 16 shows the results of the analysis.

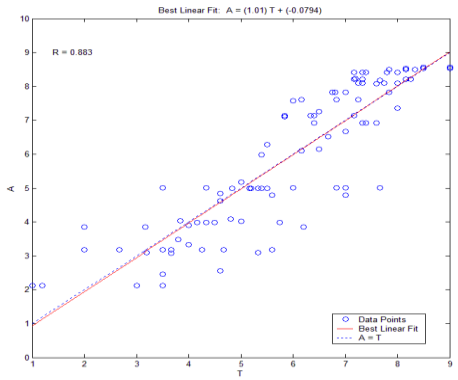

Figure 16. The regression analysis of two hundred people CQ values

The correlation coefficient *R* between the system outputs and the corresponding experts' desired values is calculated, *R*=0.883. After training the system with these data, the final *R* is close to 1. Based on the results of the validation, the cultural experts compared the CIDSS results with their own. These experts concluded that the cross-cultural business decisions recommended by CIDSS are similar to the ones suggested by a human expert.

To date, in the CQ domain, no research on CQ has been empirically computerized. This computational model is first created with soft-computing technology.

We also add CIDSS to self-awareness CQ training programs as an important means of improving the capacity of individuals and organizations to overcome these cross-cultural challenges. It is critical that employees be able to interact effectively with their clients, users, vendors, and other professionals from different cultures in today's global workforce. This new work environment requires employees to acquire new competencies and unique capabilities in order to work effectively beyond traditional cross-cultural training. Within this context, the CIDSS provides important insights about personal capabilities, as well as information on the user's own CQ in culturally diverse situations. Users can get two evaluation (self- and observer evaluations) questionnaires available in the CIDSS in order to compare their results. Figs. 17 and 18 present two parts of a user's results of the self-evaluation questionnaire in the CIDSS. For example, the self-evaluation questionnaire that evaluates the user's CQ is presented in the system as follows:

Result 1: After inputting the answers of the questionnaire to a user's response in the CIDSS, the system provides feedback. If a user's evaluation achieves a high score (e.g., greater than 8), the system displays the following message:

```
========================================
Current time is Fri Jan 04 18:12:02 2013
========================================
Your the newest result  is  :
9.5.
Congratulation!! The CQ Evaluation is excellent !!
```

Figure 17. Result 1- High score: Greater than 8

Result 2: When the evaluation results are lower than 6, the system accordingly gives useful suggestions for personal self-development as required. The CIDSS presents recommendations as follows:

```
========================================
Current time is Fri Jan 04 18:14:44 2013
========================================
Your the newest results are :
4.9.
*****************
   In the future trainning,
  the Systems suggest you that
  you should pay more attenttion to the following aspects
  to improve your CQ ability:

A)In Behavioral
 1) altering your facial expressions when a cross-cultural
interaction requires it.

B)In Motivational
 1) confident socializing with locals in a culture that is
unfamiliar to you.
 2) interacting with people from different cultures.

C)In Metacognitive
 1) the accuracy of cultural knowledge  with people from
different cultures.
```

Figure 18. Result 2- Low score: Lower than 6

This process allows the system first to evaluate the users to identify their problems in the CQ domain. The system then offers several precise recommendations to users based on the results of the evaluation. Moreover, the system uses natural language to give users recommendations in order to provide the users with a stress-free and friendly evaluation environment.

Organizations could also use the CIDSS (both self- and observer evaluations) to train employees for expatriate purposes. At this point, the CIDSS serves as an efficient team of top CQ experts who accompany individuals or organizations that want to have training or insights on how to increase their efficiency in culturally diverse settings.

VIII. CONCLUSION

To keep up with the pace of globalization, international business and traditional BI need to deal with two major issues: how to adapt to cultural diversity and how to deal with "soft data" or natural language in order to make human-like business decisions.

In order to address these issues, this research attempts to build a "culturally aware" system, which helps users make decisions in cross-cultural business activities, and enables users to solve cultural problems that would otherwise have to be solved by cultural experts. Organizations can also use the system to evaluate and train employees by providing them with specific suggestions to improve their weaknesses and develop their cultural skills for expatriate assignments. This latter point is of particular importance in modern learning theories.

The other noteworthy points in this research are the following: (1) this research treats four CQ dimensions as an integrated and interdependent body. As a result, the CQ theories are more complete, more efficient and more precise in their applications. (2) This research fills that gap between CQ and AI. We have made a contribution in the application of AI by computerizing CQ. Consequently, this inventive research provides the opportunity for delving into new research areas and expands the range of intelligence in the field of AI. (3) Furthermore, this research simplifies the work of researchers by freeing them from heavy, complex, repetitive tasks normally carried out manually in the process of CQ studies.

There are some limitations in this research; one of them is that it is confined to CQ domain. In the future, there are still many aspects to improve such as developing a more user friendly interfaces in the commercial version of CIDSS, collecting more multicultural data, integrating CIDSS with other existing systems. Although the limitations, adapting to cultural diversity is a big challenge for the international business and traditional BI where this research has attempted to give an effective answer.

REFERENCES

[1] Z. X. Wu, R. Nkambou, and J. Bourdeau, "Cultural Intelligence Decision Support System for Business Activities," The Second International Conference on Business Intelligence and Technology, BUSTECH 2012, Nice, France, 2012.

[2] J. S. Tan, "Cultural intelligence and the global economy," Leadership in Action, 24, pp.19–21, 2004

[3] Z. H. Gao and C. P. Li, "Research on Cultural Intelligence: Review and Prospect," Advances in Psychological Science, Vol. 17, No. 1, pp.180–188, 2009

[4] S. Ang, and L. Van Dyne, "Handbook of Cultural Intelligence," 1st ed. M.E. Sharpe. Armonk 2008, 2010

[5] M. Janssens and J. M. Brett, "Cultural intelligence in global teams: A fusion model of collaboration," Group and Organization Management, 31, pp.124–153, 2006

[6] Z. X. Wu, R. Nkambou, and J. Bourdeau, "The Application of AI to Cultural Intelligence, " The 2012 World Congress in Computer Science Computer Engineering and Applied Computing-ICAI 2012, The International Conference on Artificial Intelligence, Las Vegas, U.S.A. 2012

[7] H. Cohen and C. Lefebvre, "Handbook of Categorization in Cognitive Science," Elsevier, Amsterdam, NL. 2005

[8] G. Hofstede, "Culture's consequences: International Differences in Work Related Values". Beverly Hills: Sage. 1980.

[9] G. Hofstede, "Cultures and Organizations: Software of the Mind", New York: McGraw Hill. 1997

[10] F. L. Schmidt and J. E. Hunter, "Select on Intelligence," In E. A. Locke, Ed, The Blackwell HandBook of Organizational Principles. Oxford: Blackwell. 2000

[11] R.Sternberg and K.D. Douglas, "What is Intelligence?" , Contemporary Viewpoints on Its nature and definition, Ablex publishing corporation, 355 Chestnut Street, Norwood, NewJersey 07648, 1986

[12] P.C. Earler, and S. Ang, "Cultural intelligence: Individual interactions across cultures," Stanford, CA: Stanford University Press, 2003

[13] P.C. Earley and E. Mosakowski, "Cultural intelligence," Harvard Business Review, 82, pp.139–146, 2004.

[14] B. Peterson, "Cultural intelligence: A guide to working with people from other cultures," Yarmouth. ME: Intercultural Press, 2004.

[15] G. Hofstede, "Cultures and Organizations: Software of the Mind," McGraw-Hill, New York, 1991

[16] R. Brisling, R.Worthley, and B. MacNab, "Cultural intelligence: understanding behaviors that serve people's goals," Group and Organization Management, 2006

[17] D. C. Thomas and K. Inkson, "Cultural Intelligence People Skills for a Global Workforce," Consulting to Management, 16 (1). pp. 5-9, March, 2005

[18] D. C. Thomas, "Domain and development of cultural intelligence: The importance of mindfulness," Group and Organization Management, 31, pp.78–99, 2006

[19] K.Y. Ng and P. C. Earley, "Culture + intelligence: Old constructs, new frontiers," Group and Organization Management, 31, pp. 4–19, 2006

[20] J. P. Johnson, T. Lenartowicz, and S. Apud, "Cross-cultural competence in international business: Toward a definition and a model," Journal of International Business Studies, 37, pp. 525–543, 2006

[21] P. C. Earley and S. Ang, "Cultural intelligence: Individual interactions," Stanford, CA: Stanford University Press, 2003

[22] D. C. Thomas, "Domain and development of cultural intelligence: The importance of mindfulness," Group and Organization Management, 31, pp.78–99, 2006

[23] S.Ting-Toomey, "Communicating across cultures," NewYork. Guilford, 1999

[24] S. Ang, L.Van Dyne, C.K.S. Koh, K. Y. Ng, K.Templer, J. C. Tay, and N. A. Chandrasekar, "Cultural Intelligence: Its Measurement and Effects on Cultural Judgment and Decision Making, Cultural Adaptation, and Task Performance," Management and Organization Review 3 335–371, 2007

[25] L. Ottavi, "Cultural Intelligence in the Globalized Work Environment, " December 1, 2009

[26] G. Hofstede, "The cultural relativity of organizational practices and theories," Journal of International Business Studies, 1983

[27] F. Trompenaars and C. Hampden-Turner, "Riding the waves of culture: Understanding cultural diversity in business," London: Nicholas Brealey Publishing, 1997

[28] T. Kern and L. P. Willcocks, "Exploring information technology outsourcing relationships: Theory and practice," Journal of Strategic Information Systems, 2000

[29] S. Ang, L.Van Dyne, C.K.S. Koh, and K. Y. Ng, "The Measurement of Cultural Intelligence," Paper presented at the 2004 Academy of Management Meetings Symposium on Cultural Intelligence in the 21st Century, New Orleans, L.A. 2004

[30] G. Huber, "A theory of the effects of advanced information technologies on organizational design, intelligence, and decision-making, " Academy of Management Review, 1990

[31] S. Ang and C. I. Andrew, "Cultural Intelligence and Offshore Outsourcing Success: A Framework of Firm-Level Intercultural Capability," Journal compilation, Decision Sciences Institute, Decision Sciences Volume 39, Number 3, 2008

[32] M. Negnevitsky, "Artificial Intelligence: A Guide to Intelligent Systems," ISBN 0-321-20466-2, British Library Cataloguing-in-Publication Data, 2nd Edition, 2005

[33] E.H. Mamdani and S. Assilian, "An Experiment in Linguistic Synthesis with a Fuzzy Logic Controller," International Journal of Man–Machine Studies, 1975

[34] J.S.R. Jang, C.T. Sun, and E. Mizutani, "Neuro-Fuzzy and Soft Computing: A Computational Approach to Learning and Machine Intelligence," Prentice Hall, Englewood Cliffs, NJ 1997

[35] P. Y. K, Chau, "Expert systems and professional services marketing," Journal of Professional Services Marketing, vol.7, no.2, pp.79-86. 1991

[36] M. Steinberg and R. E. Plank, "Implementing Expert Systems into Business Marketing Practice," The Journal of Business and Industrial Marketing, vol.5, no.2, pp.15-26, 1990

[37] J. F. Noubel, "Intelligence Collective : la révolution invisible," The Transitioner.org. 2007

Modelling of Mechanical Properties for Integrated Casting and Rolling Processes Using Dedicated Extra-High Temperature Solutions Platform

Marcin Hojny
Dept. of Applied Computer Science and Modelling
AGH University of Science and Technology
A. Mickiewicza Av. 30, 30-059 Kraków, Poland
e-mail: mhojny@metal.agh.edu.pl

Miroslaw Glowacki
Dept. of Applied Computer Science and Modelling
AGH University of Science and Technology
A. Mickiewicza Av. 30, 30-059 Kraków, Poland
e-mail: glowacki@metal.agh.edu.pl

***Abstract*—The main subject of the current paper is the modelling of mechanical properties of carbon steels at a temperature which exceeds the typical hot rolling temperature range as well as a new methodology of such investigation was developed. The method requires high accuracy model of semi-solid steel deformation. Hence, it requires a dedicated hybrid analytical-numerical model of deformation of steel with variable density. The newly developed methodology allows to compute curves depending on both temperature and strain rate. In aim to verify the new modified methodology, a number of experimental tests using Gleeble 3800 thermo-mechanical simulator were done. The comparison between numerical and experimental results are presented in the first part of the paper. The developed methodology allows reliable numerical simulation of deformation of semi-solid steel samples and calculation of realistic flow curve parameters. In the second part of the paper, the newest results of mechanical properties prediction of 11SMn30 grade steel as well as an example numerical and experimental results are presented.**

Keywords-strain-stress curve; semi-solid steel testing; extra-high deformation temperature; numerical analysis; inverse method

I. INTRODUCTION

Due to the global energy crisis in recent years, more and more new production technologies require energy preservation and environmental protection. The integrated casting and rolling technologies are newest efficient and very profitable ways of hot strip production. Only few companies all over the world are able to manage such processes. The technical staff of a plant located in Cremona, Italy is working on new methods of flat steel manufacturing for several years now. The ISP (Inline Strip Production) and AST (Arvedi Steel Technologies) technologies, which are developed in Cremona, are distinguished by very high rolling temperature. The main benefits of both methods are related to very low rolling forces and favourable field of temperature. However, certain problems particular to such metal treatment arise. The central parts of slabs are mushy and the solidification is not yet finished while the deformation is in progress. This results in changes in material density and occurrence of characteristic temperatures having great influence on the plastic behaviour of the material [1] [2] [3] [4] [5]. The nil strength temperature (NST), strength recovery temperature (SRT), nil ductility temperature (NDT) and ductility recovery temperature (DRT) have effect on steel plastic behaviour and limit plastic deformation [5]. The nil strength temperature (NST) is the temperature level at which material strength drops to zero, while the steel is being heated above the solidus temperature. Another temperature associated with NST is the strength recovery temperature (SRT). At this temperature the cooled material regains strength greater than 0.5 N/mm^2. Nil ductility temperature (NDT) represents the temperature at which the heated steel loses its ductility. The ductility recovery temperature (DRT) is the temperature at which the ductility of the material (characterised by reduction of area) reaches 5% while it is being cooled. Over this temperature, the plastic deformation is not allowed at any stress tensor configuration.

The most important steel property having crucial influence on metal flow paths is the yield stress. In the literature of the past years, one can find papers regarding experimental results [6] and modelling [7] of non-ferrous metals. Both the mentioned contributions focus mainly on tixotrophy. Thixoforming process is one member of a family of semi-solid forming processes and it possesses characteristics of both casting and forging. The first results regarding steel deformation at extra high temperature were only presented in the past few years [8]. This stems from the fact that level of liquidus and solidus temperatures of steel is very high in comparison with non-ferrous metals. It causes serious experimental problems contrary to deformation tests for non-ferrous metals which are much easier. Rising abilities of thermo-mechanical simulators such as the Gleeble 3800 and development of new methods of identification of mechanical properties allow investigations leading to strain-stress relationships for semi-solid steels, as well. This problem became a subject of research done by authors of the presented paper for several years now. As a result a computer system supporting the investigation of mushy steel has been developed. The current paper presents the modified methodology, which allows the calculation of

the real stress-strain relationships for a wide range of temperatures and strain rate. In Section II, the modified methodology of stress-strain curves is described. Section III presents a mathematical model, while Section IV presents experimental verification of the developed methodology. In Section V, the newest results of strain-stress prediction for simulations of rolling process are presented. Finally, in the last section, the main conclusions and future work are shortly described.

II. THE NEW METHODOLOGY

The old version of steel examination methodology, denoted as variant no. 1, was based on both tension and compression tests [12] [13]. The temperature range was divided into two sub-ranges: lower – below NDT – and higher – above this temperature. The usual experimental procedure based on tensile tests, which is valid for cold and low-level hot deformation was applied for the lower temperature range. The resulting yield curves were described by modified Voce formula using approximation of experimental data [11].

A special technique of testing was developed for temperatures higher than NDT due to several serious experimental problems. The deformation process has been divided into two main stages. The first one – a very small preliminary compression and the second one – the ultimate compression. The preliminary deformation was designed to eliminate clearances in the testing equipment. The coefficients of the Voce formula were calculated using inverse solutions. This was the only acceptable method due to strong strain inhomogeneity of semi-sold steel. This approach allowed to compute strain-stress curves depending on only one additional parameter – the temperature. The newly developed methodology (denoted as variant no. 2) allows the computation of curves depending on both temperature and strain rate. The tension tests has been replaced by compression ones and the Voce formula was replaced by more adequate equation. Contrary to the old version of the method the newly developed one allows the computation of curves depending on both temperature and strain rate. Figure 1 schematically presents the modified methodology. More details concerning the experimental work were published in [14]. The presented approach allows to compute realistic yield stress curves depending on strain, temperature and strain rate in temperature range from 1200°C to NDT and above. The objective function of the inverse analysis was defined as a square root error of discrepancies between calculated (F_c) and measured (F_m) loads at several subsequent steps of the compression process. The experimental values of the deformation forces were collected by the Gleeble 3800 equipment while the theoretical ones (F_c) were calculated with the help of a sophisticated solver facilitating accurate computation of strain, stress and temperature fields for materials with variable density.

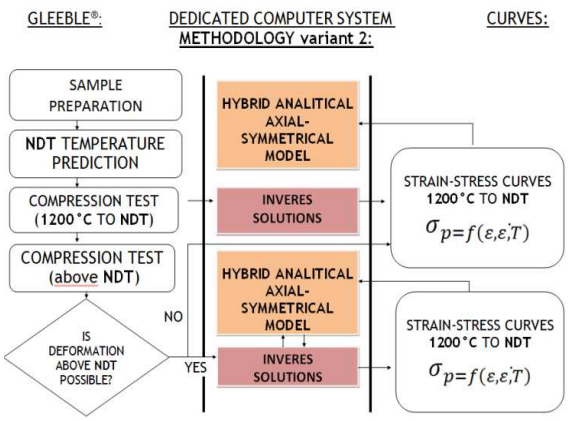

Figure 1. Flowchart of the integrated testing methodology of flow stress investigation of semi-solid steel.

This solver is the least visible but the most powerful part of the computer aided testing system developed by the authors called Def_Semi_Solid. The heart of the solver is based on a hybrid analytical-numerical mushy steel deformation model described in the next section. The Def_Semi_Solid solver was included into Extra-High Temperature Solutions Platform (EHTS Platform) in order to support modelling of plastic deformation of materials at very high temperature levels (Figure 2). The solutions platform consists of two independent tools: Def_Semi_Solid v.5.0 – complete 2D modelling toolset dedicated for Gleeble® 3800 thermo-mechanical simulator with integrated Pre&Postprocessor and DEFFEM 3D – vertical application toolset including three modules: DEFFEM solver (still in development) full three dimensional multiscale thermo-mechanical solver for new methodology purposes, DEFFEM inverse and DEFFEM pre&postprocessor. The last two modules were tested in real industrial tests during modelling of TIG welding process of Inconel super alloy and stamping processes. Those modules supported of boundary condition identification as well as strain-stress curves based on industrial results. More details concerning modelling of mentioned processes with DEFFEM inverse module support can be found in [9] [10] [15].

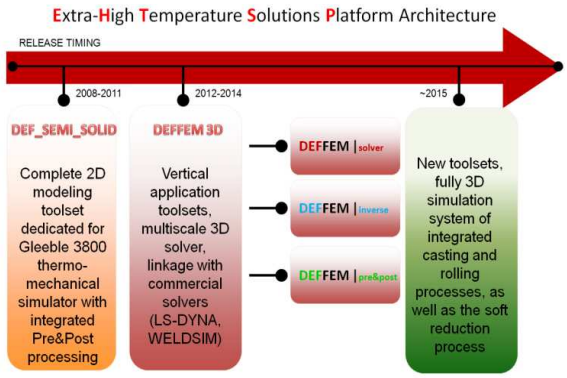

Figure 2. Architecture of extra-high temperature solutions platform.

The newest version of Def_Semi_Solid system is equipped with full automatic installation unit (Figure 3) and new graphical interface. It allows the computer aided testing of mechanical properties of steels at very high temperature using Gleeble 3800 physical simulators to avoid problems which arise by traditional testing procedures. The first module allows the establishment of new projects or working with previously existing ones (Figure 4). The integral parts of each project are: input data for a specific compression/tension test as well as the results of measurements and optimization. In the current version of the program the module permits application of a number of database engines (among other standard MSAcces, dBASE IV and Paradox 7-8 for PC-based systems) and allows the implementation of material databases and procedures of automatic data verification. The next module (the solver) gives user the possibility of managing the working conditions of the simulation process. The inverse analysis can be turned off or on using this part of the system.

Figure 3. The main window of the newest version of Def_Semi_Solid system.

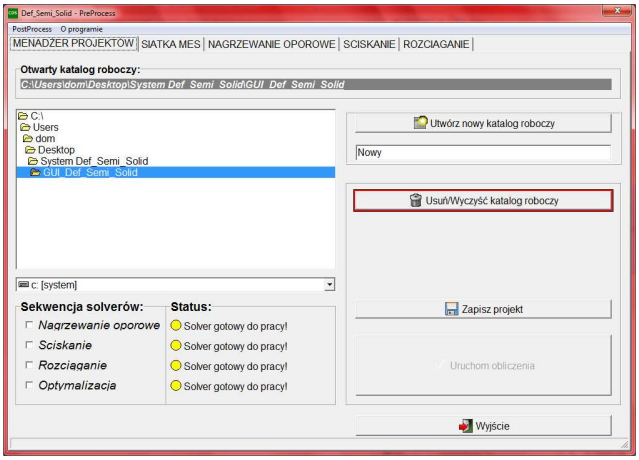

Figure 4. The Pre-processor of the newest version of Def_Semi_Solid system.

The last module (DSS/Post module) is dedicated to the visualisation of the numerical results and printing the final reports. In the current version the possibility of visualization was significant improved. The main are: shading options using OpenGL mode (2D and 3D) as shown in Figure 5 and possibility make a full contour map (2D and 3D) as shown in Figure 6.

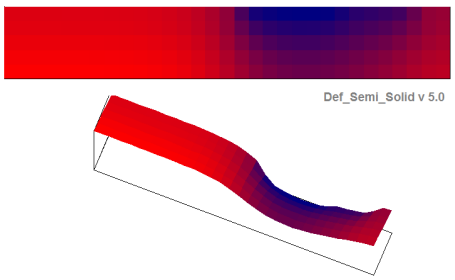

Figure 5. The Post-processor of the newest version of Def_Semi_Solid system (shading option 2D and 3D).

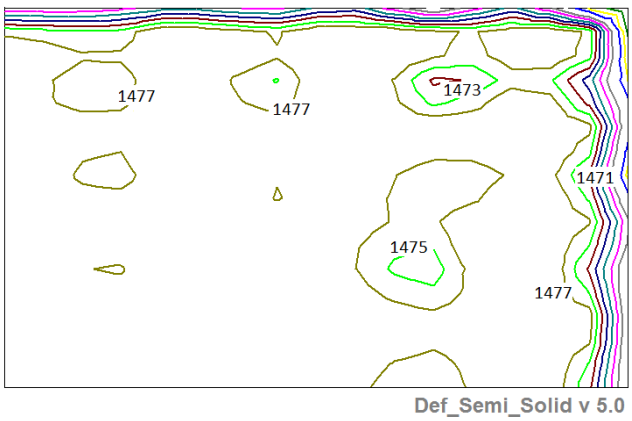

Figure 6. The Post-processor of the newest version of Def_Semi_Solid system (contour option).

III. MATHEMATICAL MODEL

A mathematical model of the compression process has been developed using the theory of plastic flow [11]. The principle of the upper assessment, calculus of variations, approximation theory, optimization and numerical methods for solving partial differential equations were used [16]. The following assumptions were established:

- Deformation and stress state are axial-symmetrical;
- Deformed material is isotropic but inhomogeneous;
- The material behaviour is rigid-plastic – the relationship between the stress tensor and strain rate tensor is calculated according to the Levy-Mises flow law [11], which is given as:

$$\sigma_{ij} - \frac{1}{3}\sigma_{kk}\delta_{ij} = \frac{2}{3}\frac{\sigma_p}{\dot{\varepsilon}_i}\dot{\varepsilon}_{ij} \quad (1)$$

Rigid-plastic model was selected due to its very good accuracy at the strain field during the hot deformation and sufficient correctness of calculated deviatoric part of the stress field. Moreover, the elastic part of each stress tensor component is very low at temperatures close to solidus line and can in practice be neglected in calculations of strain distribution. The limits for plastic metal behaviour are defined according to Huber-Mises-Hencky yield criterion:

$$\sigma_{ij}\sigma_{ij} = 2\left(\frac{\sigma_p}{\sqrt{3}}\right)^2 \quad (2)$$

In (1) and (2), σ_{ij} denotes the stress tensor components, σ_{kk} represents the mean stress, δ_{ij} is the Kronecker delta [11], σ_p indicates the yield stress, $\dot{\varepsilon}_i$ is the effective strain rate, and $\dot{\varepsilon}_{ij}$ denotes strain rate tensor components. The components are given by an equation:

$$\dot{\varepsilon}_{ij} = \frac{1}{2}\left(\nabla_i v_j + \nabla_j v_i\right) \quad (3)$$

In cylindrical coordinate system $Or\theta z$ the solution is a vector velocity field defined by the distribution of three coordinates $\boldsymbol{v} = (v_r, v_\theta, v_z)$. The field is a result of optimization of a power functional, which can be written in general form as the sum of power necessary to run the main physical phenomena related to plastic deformation. Due to the axial-symmetry of the sample the circumferential component of the velocity field can be neglected and the functional is usually formulated as:

$$J[\boldsymbol{v}] = \dot{W} = \dot{W}_\sigma + \dot{W}_\lambda + \dot{W}_f \quad (4)$$

Component $\dot{W}_\sigma$ occurring in (4) represents the plastic deformation power, $\dot{W}_\lambda$ is the power which is a penalty for the departure from mass conservation condition, $\dot{W}_f$ denotes the friction power and $\boldsymbol{v} = (v_r, v_z)$ describes the reduced velocity field distribution.

Rigid-plastic formulation of metal deformation problem requires the condition of mass conservation in the deformation zone. In case of solids and liquids with a constant density, this condition can be simplified to the incompressibility condition. Such a condition is generally satisfied with sufficient accuracy during the optimization of functional (4). In most solutions a slight, but noticeable loss of volume is observed. The loss occurs because the incompressibility condition imposed on the solution is not completely satisfied in numerical form. It is negligible in case of traditional computer simulation of deformation processes although in some embodiments more accurate methods are used to restore the volume of metal subjected to the deformation. In contrast, in the presented case the density of semi-solid materials varies during the deformation process and these changes result in a physically significant change in the volume of a body having constant mass. The size of the volume loss due to numerical errors is comparable with changes caused by fluctuation in the density of the material.

A further problem specific to the variable density continuum is power $\dot{W}_\lambda$, which occurs in functional (4). It is used in most solutions and has a significant share of total power. Even when the iterative process approaches the end, this power component is still significant, especially if the convergence of the optimization procedures is insufficient. In case of discretization of the deformation area (e.g., using the finite element method) if one focuses solely on the $\dot{W}_\lambda$ a number of possible locally optimal solutions appear. They are related to a number of possible directions of movement of discretization nodes providing the volume preservation of the deformation zone. Each of these solutions creates a local optimum for $\dot{W}_\lambda$ power and thus for the entire functional (4). This makes it difficult to optimize because of lack of uniform direction of fall of total power which leads to global optimum. The material density fluctuation causes further optimization difficulties, resulting from additional replacement of incompressibility condition with a full condition of mass conservation.

The proposed solution requires high accuracy in ensuring the incompressibility condition for the solid material or mass conservation condition for the semi-solid areas. This stems from the fact that the errors resulting from the breach of these conditions can be treated as a volume change caused by the steel density variation in the semi-solid zone. High accuracy solution is required also due to large differences in yield stress for the individual subareas of the deformation zone. In the discussed temperature range they appear due to even slight fluctuations in temperature. In presented solution the second component of functional (4) is left out and mass conservation condition is given in analytical form constraining the radial (v_r) and longitudinal (v_z) velocity field components. The functional takes the following shape:

$$J[\boldsymbol{v}] = \dot{W}_\sigma + \dot{W}_t \quad (5)$$

In case of functional (5), the numerical optimisation procedure converges faster than the one for functional (4) due to the reduced number of velocity field parameters (only radial components are optimisation parameters) and the lack of numerical form of mass conservation condition. The accuracy of the proposed hybrid solution is higher also due to negligible volume loss caused by numerical errors, which is very important for materials with variable density.

As mentioned before, the solution of the problem is a velocity field in cylindrical coordinate system in axial-symmetrical state of deformation. Optimization of metal flow velocity field in the deformation zone of semi-variational problem requires the formulation according to equation (5). The radial velocity distribution $v_r(r, \theta, z)$ and the longitudinal one $v_z(r, \theta, z)$ are so complex that such wording in the global coordinate system poses considerable difficulties. These difficulties are the result of the mutual dependence of these velocities. Therefore, the basic formulation will be written for the local cylindrical coordinate system $Or\theta z$ with a view to the future discretization of deformation area using one of the dedicated methods. In addition, one will find that the deformation of

cylindrical samples is characterized by axial symmetry. As demonstrated by experimental studies conducted using semi-solid samples the symmetry may be disturbed only as a result of unexpected leakage of liquid phase [16].

Such experiments, however, are regarded as unsuccessful and not subject to numerical analysis. Establishment of the axial symmetry, with the exception of cases of physical instability can be considered valid also for the process of compression or tensile test of semi-solid samples, allows one to simplify the model because of the identical strain distribution at any axial sample cross-section. Therefore, considerations will be carried out in Orz coordinates for the sample cross-section using one of the planes containing the sample axis. Components of power functional given by (5) have been formulated in accordance with the general theory of plasticity by relevant equations. The plastic power for the deformation zone having volume of V is given by the subsequent relation:

$$\dot{W}_\sigma = \int_V \sigma_i \dot{\varepsilon}_i \, dV \tag{6}$$

where σ_i is the effective stress and $\dot{\varepsilon}_i$ denotes the effective strain. The plastic deformation starts when the rising effective stress reaches yield stress limit σ_p ($\sigma_i = \sigma_p$) according to yield criterion given by equation (2). Effective strain occurring in (6) is calculated on the basis of the strain tensor components $\dot{\varepsilon}_{ij}$ according to following relationship:

$$\dot{\varepsilon}_i = \sqrt{\frac{2}{3}\dot{\varepsilon}_{ij}\dot{\varepsilon}_{ij}} \tag{7}$$

The components are given by (3). The second component of functional (5) is responding for friction. To compute friction power on the boundary S of area V a model given by the subsequent equation was used:

$$\dot{W}_t = \int_S m \frac{\sigma_p}{\sqrt{3}} \|\overline{\boldsymbol{v}}\| dS \tag{8}$$

In (8), m is the so called friction factor, which is usually experimentally selected and $\overline{\boldsymbol{v}}$ is a relative velocity vector of metal and tool $\overline{\boldsymbol{v}} = \boldsymbol{v} - \boldsymbol{v_t}$. In case of tensile test, the samples are permanently fixed in jaws of a physical simulator and friction must not be taken into account. However, compression test requires sharing the friction power which is significant.

For the solid zones the incompressibility condition can be described by universal operator equation independently of the mechanical state of the deformation process:

$$\nabla \mathbf{v} = 0 \tag{9}$$

Because the semi-solid zone is characterized by density change due to still ongoing progress of steel solidification, the condition of incompressibility is inadequate to reflect changes and was replaced with the mass conservation condition, which describes the following modified operational equation:

$$\nabla \mathbf{v} - \frac{1}{\rho}\frac{\partial \rho}{\partial t} = 0 \tag{10}$$

The basis for the optimization of functional (5) is the velocity field determined by appropriate system of velocity functions in the concerned area. These functions are then the source of deformation field and other physical quantities affecting the power functional formulation. Obtaining an accurate real velocity field requires the use of velocity functions depending on a number of variational parameters. The functions should be flexible enough to map the field throughout the whole volume of the deformation zone. Analytical description of each component of the velocity field with a single function in the whole area of deformation is not preferred. This approach creates difficulties especially in areas not subjected to the deformation where the velocity function should remain constant. Therefore, the solution to the problem of semi-solid metal flow was based on a specific method.

In the case of deformation of axial-symmetrical bodies, the incompressibility condition is given by following differential equation:

$$\frac{\partial v_r}{\partial r} + \frac{v_r}{r} + \frac{\partial v_z}{\partial z} = 0 \tag{11}$$

For the semi-solid area, (11) is replaced by the mass conservation condition due to existing density changes. The longitudinal velocity has been calculated as an analytical function of radial velocity using this condition. In cylindrical coordinate system the condition has been described with an equation:

$$\frac{\partial v_r}{\partial r} + \frac{v_r}{r} + \frac{\partial v_z}{\partial z} - \frac{1}{\rho}\frac{\partial \rho}{\partial \tau} = 0 \tag{12}$$

Equation (11) is a special case of (12) and therefore the proposed solution will consider the dependence (12) as more general. In (12) ρ is the temporary material density and τ is the time variable. The proposed variational formulation makes the longitudinal velocity dependent on the radial one. Condition (12) allows for the calculation of $\partial v_z/\partial z$ derivative as a function of $\partial v_r/\partial r$ after analytical differentiation of radial velocity distribution function $v_r(r,z)$. Hence, the longitudinal velocity is calculated as a result of analytical integration according to following equation:

$$v_z = -\int \left(\frac{\partial v_r}{\partial r} + \frac{v_r}{r} - \frac{1}{\rho}\frac{\partial \rho}{\partial \tau}\right) dz \tag{13}$$

In this case, the velocity field depends only on one function – the radial velocity distribution.

Heat exchange between solid metal and environment, and its flow inside the metal is controlled by a number of factors. During phase transformation two additional phenomena have to be taken into account. Note that in the process of deformation of steel at temperature of liquid to solid phase transformation there are two sources of heat changes. On the one hand, heat is generated due to the state transformation. On the other hand, it is secreted as a result of plastic deformation. In addition, steel density variations also cause changes of body temperature.

Thermal solution has a major impact on simulation results, since the temperature has strong effect on remaining variables. This is especially evident if the specimen temperature is close to solidus line when the body consist of both solid and semi-solid regions. In such case, the affected phenomena are: plastic flow of solid and mushy materials, stress evolution and density changes. The theoretical temperature field is a solution of Fourier-Kirchhoff equation with appropriate boundary conditions [16].

The most general form of the Fourier-Kirchhoff equation in any coordinate system can be written in operator form as follows:

$$\nabla^T(\mathbf{\Lambda}\,\nabla T) + Q = c_p\rho\left(\boldsymbol{v}^{\boldsymbol{T}}\nabla T + \frac{\partial T}{\partial \tau}\right) \tag{14}$$

where T is the temperature distribution in the controlled volume and $\mathbf{\Lambda}$ denotes the symmetrical second order tensor called heat transformation tensor. In case of thermal inhomogeneity, the whole tensor has to be considered. Q represents the rate of heat generation (or consumption) due to the phase transformation, due to plastic work done and due to electric current flow (resistance heating of the sample is usually applied). Finally, c_p describes the specific heat, ρ the steel density, $\boldsymbol{v}$ the velocity vector of specimen particles and τ the elapsed time.

For axial-symmetrical case, (14) can be simplified. The following form of Fourier-Kirchhoff equations for isotropic, axially-symmetric heat flow was applied in the presented solution:

$$\lambda\left(\frac{\partial^2 T}{\partial r^2} + \frac{1}{r}\frac{\partial T}{\partial r} + \frac{\partial^2 T}{\partial z^2}\right) + Q = \rho c_p \frac{\partial T}{\partial \tau} \tag{15}$$

Equation (15) needs to be solved with appropriate initial and boundary conditions. Combined Hankel's boundary conditions have been adopted for the presented model.

One of the most important parameters of the solution is the density. Its changes have influence on the mechanical part of the presented model. The knowledge of effective density distribution is very important for modelling the deformation of porous materials. Density changes of liquid, solid-liquid and solid materials are ruled over three phenomena: solid phase formation, laminar liquid flow through porous material and thermal shrinkage. Total density changes can be calculated according to following equation:

$$\frac{\partial \rho}{\partial \tau} = (\rho_s X_s + \rho_l X_l)\left(\frac{\partial_s}{\partial_l} - 1\right)\frac{\partial X_l}{\partial_\tau} + \rho_l X_l div\,\vartheta + (\beta_S \rho_S X_s + \beta_l \rho_l X_l)\frac{\partial T}{\partial \tau} \tag{16}$$

where X is the fraction and β the linear expansion coefficient. Indexes l and s denote the liquid and solid phases, respectively.

IV. Example Results - New Methodology Validation

The experimental work was done in Institute for Ferrous Metallurgy in Gliwice, Poland using Gleeble 3800 thermo-mechanical simulator (Figure 7).

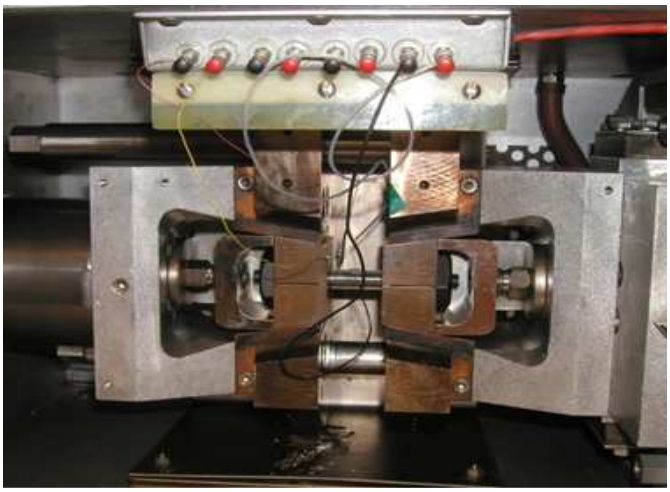

Figure 7. The standard Gleeble 3800 equipment allowing deformation is semi-solid state (right before running process).

The steel used for the experiments was the C45 grade steel having 0.45% of carbon content. In all cases, experiments were performed according to the following schedule:

- initial stage: sample preparation divided into several sub stages (e.g., thermocouple assembly); die selection, etc,
- stage 2: melting procedure,
- stage 3: deformation process.

It is good practice to test materials in isothermal conditions [11]. Unfortunately, this is not possible for semi-solid steel. Nevertheless, the condition should be as close to isothermal as possible due to the very high sensitivity of material rheology to even small variations of temperature. The basic reason for uneven temperature distribution inside the sample body on the Gleeble 3800 simulator is the contact with hot copper handles presented in Figure 8.

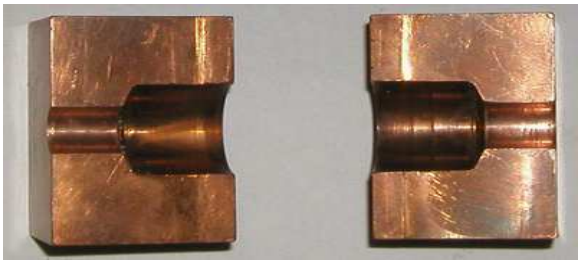

Figure 8. The short contact zone handles used in experiments (hot handle).

The estimated liquidus and solidus temperature levels of the investigated steel are: 1495°C and 1410°C, respectively. Thermal solution of the theoretical model has crucial influence on simulation results, since the temperature has strong effect on remaining parameters. The resistance sample heating and contact of the sample with cold cooper handles cause non-uniform distribution of temperature inside heated material, especially along the sample. The semi-solid conditions in central parts of the sample cause even greater temperature gradient due to latent heat of transformation. Such non-uniform temperature distribution is the source of significant differences in the microstructure and hence in material rheological properties.

During the experiments, samples were heated to 1430°C and after maintaining at constant temperature were cooled down to the required deformation temperature. In case of heating, the heat generated is usually not known because the Gleeble 3800 equipment uses an adaptive procedure for resistive heating controlled by temperature instead of current flow. Hence, the actual heat generated by current flow (in fact the rate of heat generation Q) has to be calculated using inverse procedure. In this case, the objective function (F) was defined as a norm of discrepancies between calculated (T_c) and measured (T_m) temperatures at a checkpoint (steering thermocouple position: TC4 in Figure 9) according to the following equation:

$$F(\mathrm{Q}) = \int_{\tau_0}^{\tau_i} [T_c(Q,r,z,T) - T_m(r,z,T)]d\tau \qquad (17)$$

where τ is the time variable, Q is the rate of heat generation.

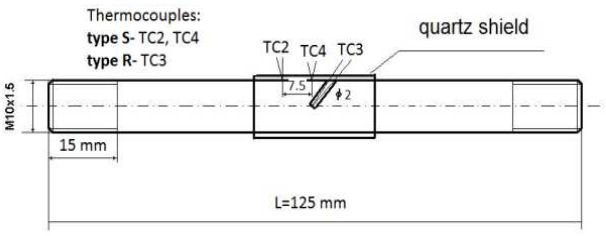

Figure 9. Samples used for the experiments. TC2, TC3 and TC4 thermocouples.

In the final stage of physical test, the temperature difference between core of the sample (TC3 thermocouple position) and its surface (TC4 thermocouple position) can be significant. In all cases the core temperature was higher than surface temperature. Differences between these two reach around 30°C for cold handle (handle with long contact zone) and about 40°C for hot handle. The results of numerical simulation are in agreement with experiments. In Figure 10 and Figure 11 the temperature distribution after 3 and 6 seconds of heating process are shown. One can observe increasing gradient of temperature near the die-sample interface.

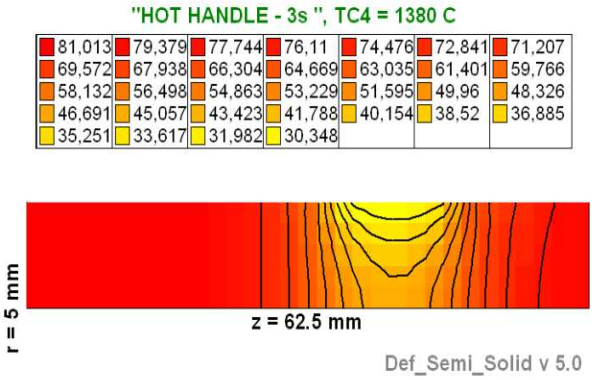

Figure 10. Temperature distribution after 3 seconds of heating.

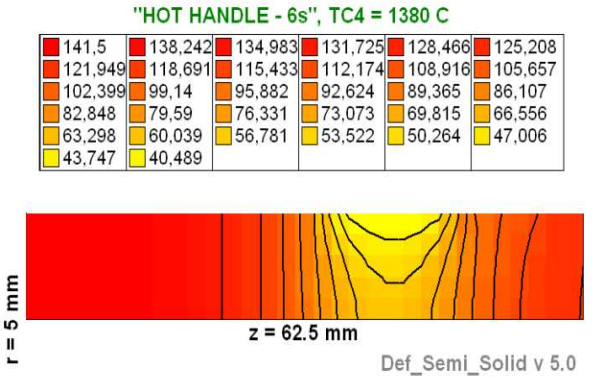

Figure 11. Temperature distribution after 6 seconds of heating.

Figure 12 presents the final temperature distributions in the cross section of sample tested at 1380°C right before deformation (variant with hot handle). One can observe major temperature gradient between die-sample contact surface (physical contact sample with tool). However, difference between experimental and theoretical core temperatures for hot handles was only 3°C (calculated core temperature was equal to 1417°C and measured one was equal to 1420°C).

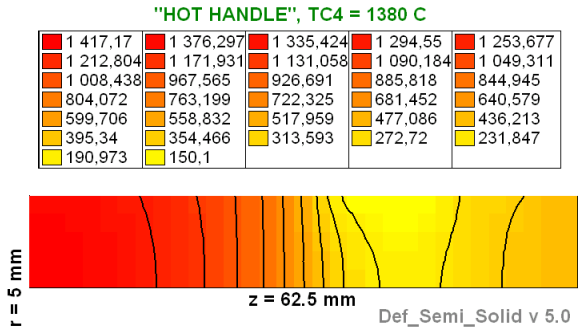

Figure 12. Distribution of temperature in the cross section of sample tested at temperature 1380°C right before deformation (variant with hot handle).

The micro and macrostructure of the tested samples were investigated as well. Figure 13 shows microstructure right before deformation for both central and boundary regions of the heating zone. Microstructure of the cooled samples consists of pearlite (the darkest phase), bainite (grey phase mainly near the borders of grains) and the bright ferrite. This is a result of phase composition, wide melting zone and almost two times lower rate of cooling of central parts of the sample (in the case of hot handles).

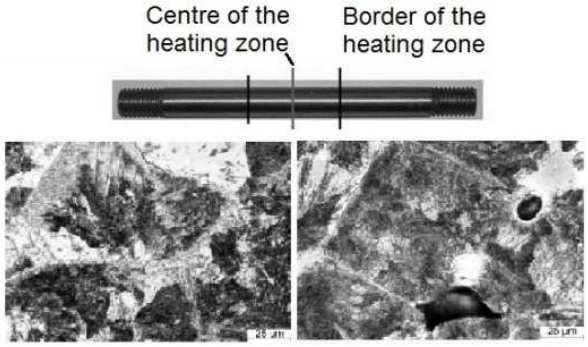

Figure 13. Microstructure of the central and boundary regions of sample right before deformation. Variant with cold handle. Magnification: 400x.

Figure 14 shows macrostructure of the central part of cross-sections of samples right before deformation. Liquid phase particles were observed. Experimental and numerical results can be compared taking into consideration the temperature gradient within the sample. This shows that the mathematical model of resistance heating is consistent with the experimental data.\

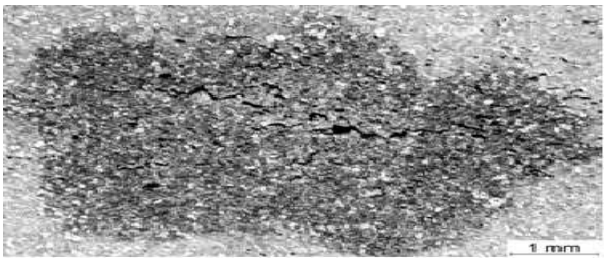

Figure 14. Macrostructure of the sample central part right before deformation. Variant with cold handle. Magnification: 10x.

Compression and tension tests were performed, according to the given methodology. During experiments die displacement, force and temperature changes in the deformation zone were recorded. The computer simulations were performed as well. All series of tests and computer simulations were done using long contact zone between samples and simulator jaws (cold handle). The deformation zone had the initial height of 62.5 mm. The sample diameter was 10 mm. The samples were melted at 1430°C and then cooled to deformation temperature. During the tests each sample was subjected to 10 mm reduction of height. Results of each test were used for inverse analysis to compute yield stress curve parameters. Figure 15 shows strain-stress curves at several strain rate levels for temperature 1300°C. The relationships were calculated using presented experimental methodology.

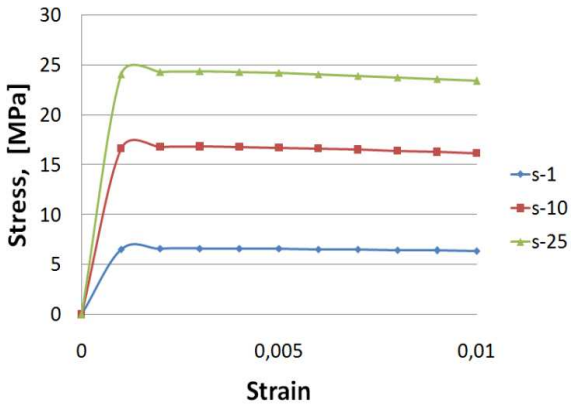

Figure 15. Stress-strain curves at several strain rate levels for temperature 1300°C.

Comparison between the calculated and measured loads are presented in Figure 16, showing quite good agreement.

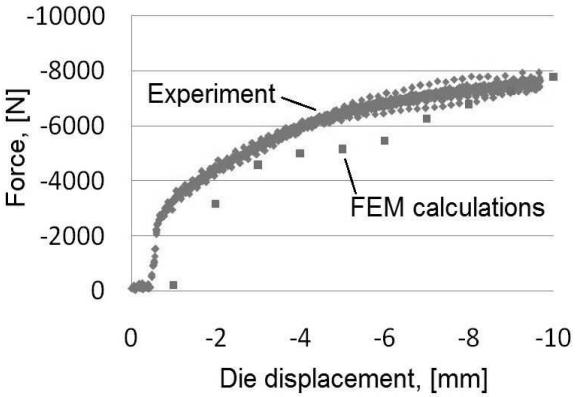

Figure 16. Comparison between measured and predicted loads at temperature 1380°C (new methodology).

Shape of a sample after experiment at 1300°C is presented in Figure 17.

Figure 17. Example final shape of the sample after deformation at 1300°C.

Comparison between the measured and calculated maximal diameters of samples allow rough verification of the developed computer aided experimental methodology. Results of such comparison are presented in Table 1. The table shows results for samples which have been subjected to deformation at several levels of temperature, i.e., 1300°C, 1350°C and 1380°C. Good agreement between the real diameter and its calculated value is observed. The relative mean square error between both the values is equal to 2.76%.

TABLE I. COMPARISION OF THE MEASURED AND CALCULATED MAXIMAL DIAMETERS OF SAMPLES DEFORMED AT DIFFERENT TEMPERATURE

Test	Experiment	Simulations
1300°C	15.3 mm	15.6 mm
1350°C	15.3 mm	15 mm
1380°C	17.8 mm	18.2 mm
Relative mean square error: 2.76%		

Figure 18 compares measured loads with those computed using the methodology previously used by the authors. One can see that the mean square error in this case is significantly greater than its equivalent for the newly developed method.

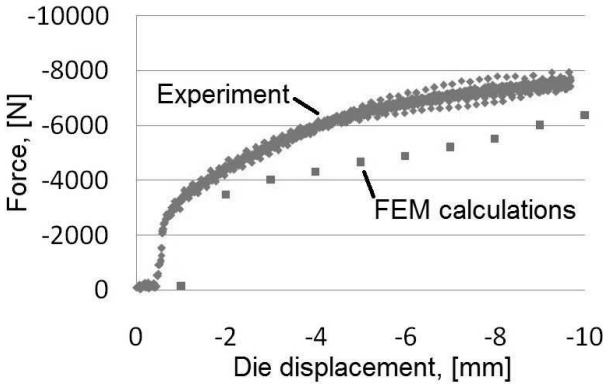

Figure 18. Comparison between measured and predicted loads at temperature 1380°C (old methodology).

The main reason for that is the lack of strain rate dependency of yield stress in the old model. The results obtained taking into account the strain rate as a parameter of the flow curve are more accurate for temperatures exceeding the NDT level.

V. EXAMPLE RESULTS OF INVESTIGATION OF 11SMN30 GRADE STEEL

In this section, the newest results of investigation of 11SMn30 grade steel are presented. The investigation procedures were analogous to those applied in case of C45 grade steel described in the previous chapter and based on new methodology. The long contact zone handles are used during all physical tests made using Gleeble 3800 thermo-mechanical simulator. The liquidus and solidus temperature of 11SMn30 grade steel are 1518°C and 1439°C, respectively. The average NST temperature for the selected steel was 1410±15°C. In order to determine the nil ductility temperature (NDT) a number of experiments were done. All the tests indicate a common temperature of 1425°C. The estimated ductility recovery temperature was 1400°C. At this temperature the sample's reduction of area was around 5% and rose very fast with the temperature drop. The predictions of strain-stress relationships were based on compression tests. The sample were melted at 1430°C and then deformed after dynamic cooling to selected temperature levels between 1200°C and NDT. The temperature program used for all experimental tests are presented in Figure 19.

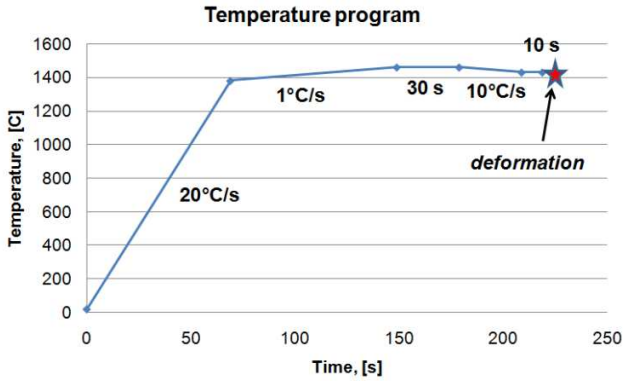

Figure 19. Temperature program used for all experimental tests.

For dynamic cooling and deformation processes in some regions of the sample the remainder of liquid phase can be observed at temperatures lower than NDT. We must remember that for cold handles the core temperature is higher about 35°C than nominal test temperature. Due to significant strain inhomogeneity inverse analysis is the only method allowing appropriate calculation of coefficients of yield stress functions at any temperature higher than NDT. The objective function was defined as a norm of discrepancies between calculated (F^c) and measured (F^m) loads in a number of subsequent stages of the compression according to the following equation:

$$\varphi(x) = \sum_{i=1}^{n} [F_i^c - F_i^m]^2 \qquad (18)$$

The theoretical forces F^c were calculated with the help of sophisticated FEM solver facilitating accurate computation of strain, stress and temperature fields for materials with variable density. As written before, experiments for temperatures higher than NDT are difficult. Several serious experimental problems arise. Apart from problems with keeping temperature constant and uniform during the whole experimental procedure there are also difficulties concerning interpretation of the measurement results. The inhomogeneity in strain distribution and distortion of the central part of the sample lead to poor accuracy of the stress fields calculated using traditional methods which are usually good for lower temperatures. Hence, the application of the developed FEM software is necessary in order to ensure appropriate interpretation of experimental data but experimental procedure has still to be carried out with great caution. More details concerning the applied inverse model can be found in [12].

Figure 20 presents an example graph of stress versus strain curve at temperature of 1400°C for the several strain rates levels. The presented curves are plotted using the calculated coefficients for temperature levels observed in the samples' cross-sections. The formula itself can be written in the following form:

$$\sigma_p = A\varepsilon^n \exp(B\varepsilon)\dot{\varepsilon}^m \exp(-CT) \qquad (19)$$

where: A, n, b, C are calculated coefficients and ε, $\dot{\varepsilon}$, T are strain, strain rate and temperature, respectively.

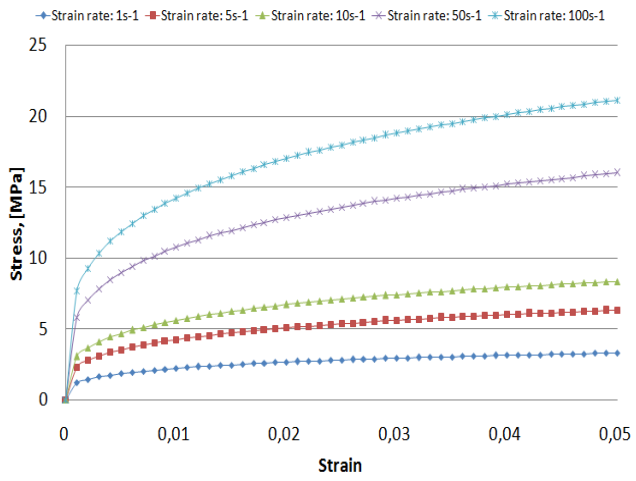

Figure 20. Flow stress vs strain at temperature 1400°C and several strain rate levels.

The comparison between the calculated and measured loads are presented in Figures 21-26, showing quite good agreement between both loads.

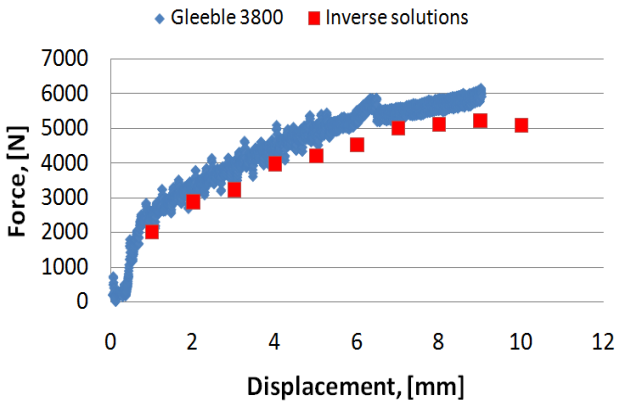

Figure 21. Comparison between measured and predicted loads at temperature 1350°C (medium-dynamic process).

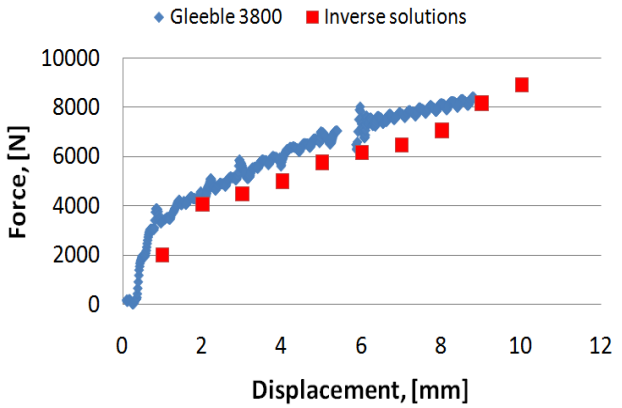

Figure 22. Comparison between measured and predicted loads at temperature 1350°C (high-dynamic process).

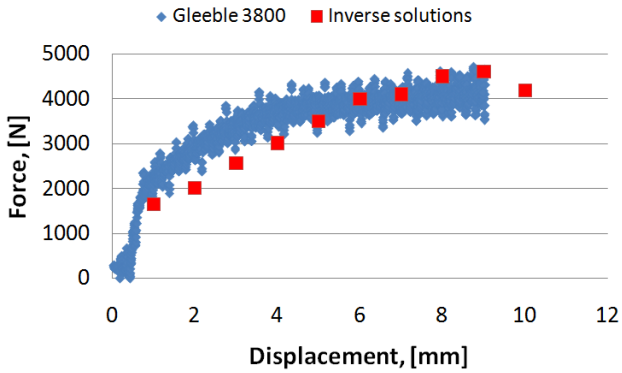

Figure 23. Comparison between measured and predicted loads at temperature 1400°C (medium-dynamic process).

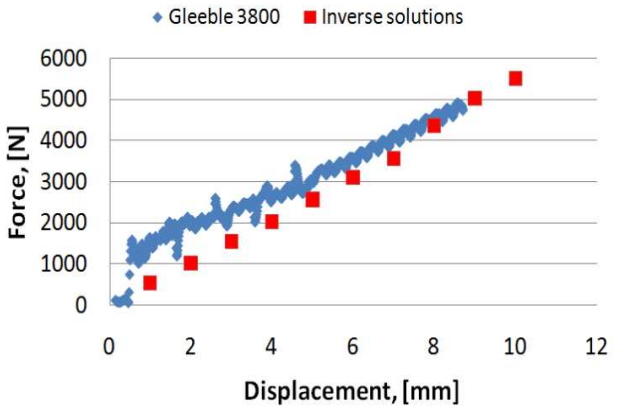

Figure 24. Comparison between measured and predicted loads at temperature 1400°C (high-dynamic process).

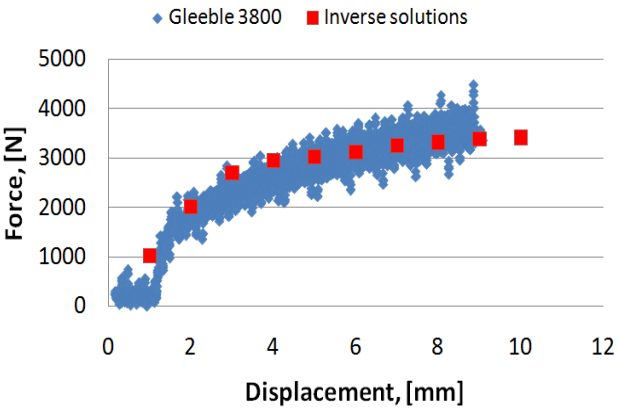

Figure 25. Comparison between measured and predicted loads at temperature 1420°C (medium-dynamic process).

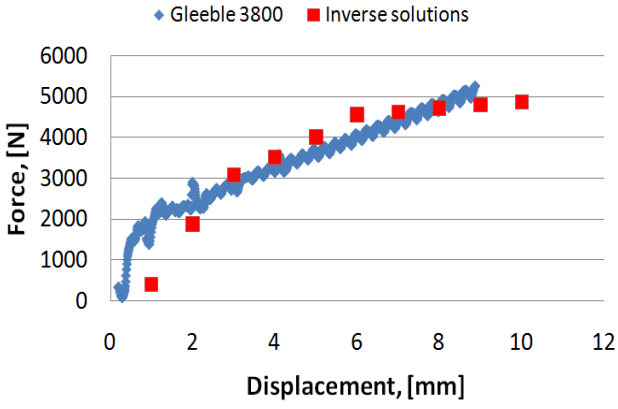

Figure 26. Comparison between measured and predicted loads at temperature 1420°C (high-dynamic process).

The verification of the model was done by comparing numerical and experimental results. The developed yield stress curves were used for example simulations of compression of cylindrical samples with mushy central part. The length of the potential deformation zone of the sample was 30 mm (the rest was mounted in the testing equipment jaws), but only a part of it has been subjected to the deformation due to huge temperature gradient along the sample. Samples were melted at 1430°C and then subjected to the deformation at nominal test temperature with height reduction of 10 mm. In Figure 27, the final temperature distribution in the cross-section of the sample just before the deformation at 1425°C is presented. Taking into account the value of NDT temperature, solidus temperature as well as the temperature difference between the surface and central part of the sample one can assume existence of mushy zone in the sample volume.

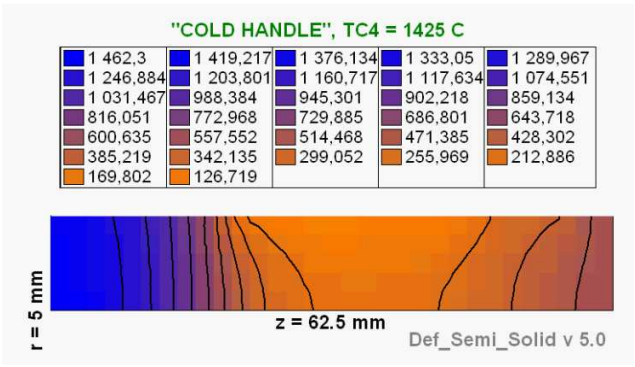

Figure 27. Initial temperature distribution (right before the deformation at 1425°C) in the ¼ part of sample cross-section.

The non-uniform temperature distribution in the sample cross-section has a great influence on the strain field and deformation zone size and shape. The inhomogeneity of the strain field leads to inhomogeneous stress distribution. The analysis of the strain shows its maximum values in the central region of the sample. In the Figures 28-33, example strain distribution in the cross section of the deformed samples at several temperatures are presented. The one can observe that strain level is higher for high-dynamic process. On the other hand, the level of strain increases with increasing test temperature for both processes: medium and high-dynamic.

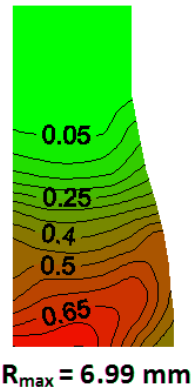

Figure 28. Strain distribution in the ¼ cross-section of the sample deformed at 1350°C for the medium-dynamic process.

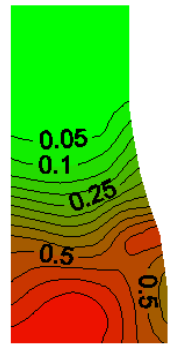

Figure 29. Strain distribution in the ¼ cross-section of the sample deformed at 1400°C for the medium-dynamic process.

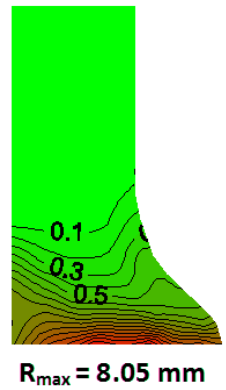

Figure 30. Strain distribution in the ¼ cross-section of the sample deformed at 1420°C for the medium-dynamic process.

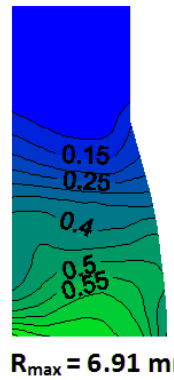

Figure 31. Strain distribution in the ¼ cross-section of the sample deformed at 1350°C for the high-dynamic process.

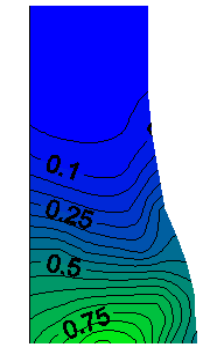

Figure 32. Strain distribution in the ¼ cross-section of the sample deformed at 1400°C for the high-dynamic process.

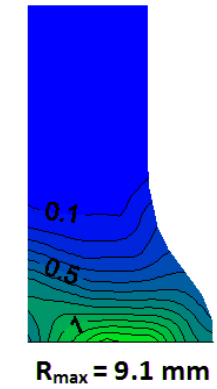

Figure 33. Strain distribution in the ¼ cross-section of the sample deformed at 1420°C for the high-dynamic process.

Example shape of a sample after experiment at 1420°C is presented in Figure 34. Visible cracks formed during virtually all attempts carried out in the temperature ranges close NDT temperature. The proposed mathematical model of steel deformation in semi-solid state does not take into account this phenomena. The authors have run further investigations leading to development of crack propagation model, which will be implemented into developed FEM system.

Figure 34. Example final shape of the sample after deformation at 1420°C with visible crack propagation (medium-dynamic process).

Finally, the verifications of the model were done. Two main comparative criteria were used for the verification:
-comparison between the measured and calculated maximum sample radii,
-comparison between the measured and calculated length of zone, which is not subjected to the deformation.
Figures 35-36 and Figures 37-38 show example application of the 1st and 2nd criterion, respectively. The figures confirm quite good agreement between theoretical and experimental results.

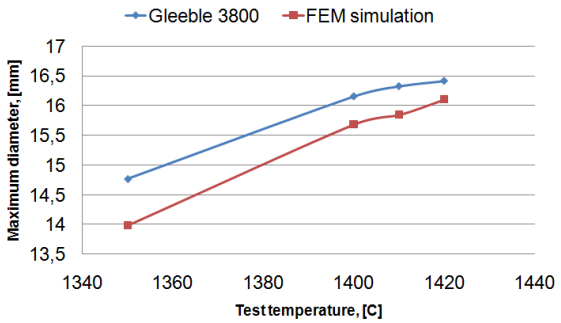

Figure 35. The comparison of the measured and calculated maximum diameters of the sample – deformation in temperature range 1350°C to 1420°C (medium-dynamic process).

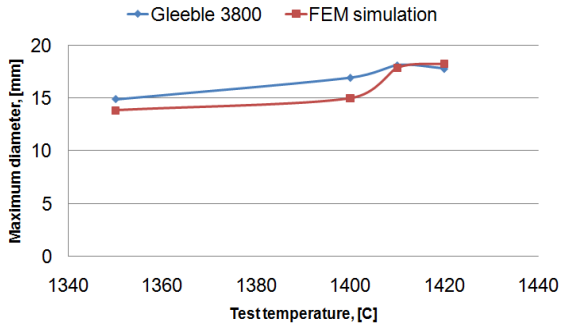

Figure 36. The comparison of the measured and calculated maximum diameters of the sample – deformation in temperature range 1350°C to 1420°C (high-dynamic process).

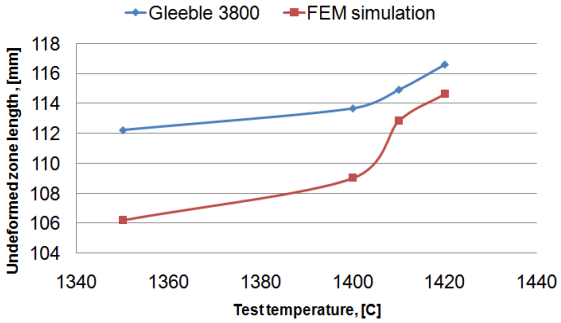

Figure 37. The comparison of the measured and calculated length of zone, which was not subjected to the deformation – experiment in temperature range 1350°C to 1420°C (medium-dynamic process).

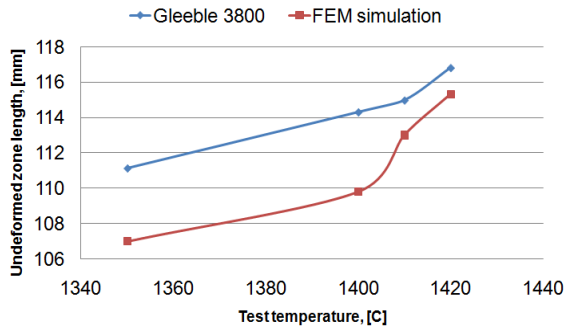

Figure 38. The comparison of the measured and calculated length of zone, which was not subjected to the deformation – experiment in temperature range 1350°C to 1420°C (high-dynamic process).

VI. Conclusion And Future Work

The investigations reported in the current paper have shown that temperature distribution inside the controlled semi-solid volume is strongly heterogeneous and non-uniform. Axial-symmetrical model does not take into account all the physical phenomena accompanying the deformation. Finally, the error of the predicted strain-stress curves can still be improved. The proposed solution of the presented problem is application of both fully three-dimensional solution and more adequate solidification model taking into consideration evolution of forming steel microstructure. Therefore, the study of multiscale modelling of mechanical properties is the main target of the future work. Contrary to the current model, the new approach should allow to better capture the physical principles of semi-solid steel deformation in micro-scale. Additionally, the methodology should allow to transfer the characteristics of the material behaviour between the micro- and macro-scale. As a consequence, the final results should be more precise and accurate. Modelling of deformation of steel samples at extra-high temperatures involves a number of issues. One of them is the difficulty of calculating of thermal and mechanical material properties. Another most important problem is the right interpretation of the results of compression tests that provide data for flow stress calculation. The presented testing methodology allows reliable numerical simulation of deformation of semi-solid steel samples and calculation of realistic flow curve parameters. The presented research was focused on mechanical properties of investigated semi-solid steel. Compression tests carried out for semi-solid materials could only be interpreted using inverse analysis. Temperature strain and strain rate as parameters of the flow curve provide accurate results of computer simulation of semi-solid steel behaviour.

The authors have run further investigations leading to development of fully three-dimensional simulation system of integrated casting and rolling processes, as well as the soft reduction process, that are part of strip casting technology. Like the model presented in the hereby paper,

the spatial one focus on three main aspects: thermal, mechanical and density changes. All of them are dependent on each other

ACKNOWLEDGMENT

The project has been supported by the Polish National Science Centre, Decision number: DEC-2011/03/D/ST8/04041

REFERENCES

[1] M. Glowacki and M. Hojny, "Computer-aided investigation of mechanical properties for integrated casting and rolling processes using hybrid numerical-analytical model of mushy steel deformation," in Proceedings of the Sixth International Conference on Advanced Engineering Computing and Applications in Sciences (ADVCOMP 2012), 2012.

[2] D. Senk, F. Hagemann, B. Hammer, and R. Kopp, “Umformen und Kühlen von direkt gegossenem,” Stahlband, Stahl und Eisen, vol. 120, 2000, pp. 65-69.

[3] H.G. Suzuki and S. Nishimura, “Physical simulation of the continuous casting of steels,” Proceedings of Physical Simulation of Welding, Hot Forming and Continuous Casting, Canmet Canada, May 2-4, 1988, pp. 166-191.

[4] A. Gołdasz, Z. Malinowski, and B. Hadała, " Study of heat balance in the rolling process of bars," Archives of Metallurgy and Materials, vol. 54, 2009, pp. 685–694.

[5] T. Telejko, Z. Malinowski, and M. Rywotycki, " Analysis of heat transfer and fluid flow in continuous steel casting," Archives of Metallurgy and Materials, vol. 54, 2009, pp. 837–844.

[6] R. Kopp, J. Choi, and D. Neudenberger, "Simple compression test and simulation of an Sn–15% Pb alloy in the semi-solid state," J. Mater. Proc. Technol.,vol. 135, 2003, pp. 317-323, doi: 10.1016/S0924-0136(02)00863-4.

[7] M. Modigell, L. Pape, and M. Hufschmidt,"The Rheological Behaviour of Metallic Suspensions," Steel Research Int., vol. 75, 2004, pp. 506–512.

[8] Y.L. Jing, S. Sumio, and Y. Jun, "Microstructural evolution and flow stress of semi-solid type 304 stainless steel," J. Mater. Proc. Technol., vol. 161, 2005, pp. 396–406, doi: 10.1016/j.jmatprotec.2004.07.063.

[9] M. Hojny, "Application of an integrated CAD/CAM/CAE/IBC system in the stamping process of a bathtub 1200 S," Archives of Metallurgy and Materials, vol. 55, 2010, pp. 713–723.

[10] M. Paćko, M. Dukat, T. Śleboda, and M. Hojny ,"The analysis of multistage deep drawing of AA5754 aluminum alloy," Archives of Metallurgy and Materials, vol. 55, 2010, pp. 1173–1184. DOI: 10.2478/v10172-010-0021-5.

[11] M. Hojny and M. Glowacki," Computer modelling of deformation of steel samples with mushy zone," Steel Research Int., vol. 79, 2008, pp. 868-874. DOI: 10.2374/SRI08SP083.

[12] M. Głowacki and M. Hojny,"Inverse analysis applied for determination of strain-stress curves for steel deformed in semi-solid state," Inverse Problems in Science and Engineering, vol. 17, 2009, pp.159–174. DOI: 10.1080/17415970802082757.

[13] M. Hojny and M. Glowacki, "The methodology of strain – stress curves determination for steel in semi-solid state," Archives of Metallurgy and Materials, vol. 54, 2009, pp. 475–483.

[14] M. Hojny and M. Glowacki, "The physical and computer modeling of plastic deformation of low carbon steel in semi-solid state," Journal of Engineering Materials and Technology, vol. 131, 2009, pp. 041003.1-041003.7, DOI: 10.1115/1.3184034.

[15] M Hojny and M. Głowacki ,"Computer aided methodology of strain-stress curve construction for steels deformed at extra high temperature," High Temperature Materials and Processes, vol. 28, 2009, pp. 245–252. DOI: 10.1515/HTMP.2009.28.4.245.

[16] M. Hojny and M. Glowacki, "Modeling of strain-stress relationship for carbon steel deformed at temperature exceeding hot rolling range," Journal of Engineering Materials and Technology, vol. 133, 2011, pp. 021008.1-021008.7, DOI: 10.1115/1.4003106.

www.iariajournals.org

International Journal On Advances in Intelligent Systems

ICAS, ACHI, ICCGI, UBICOMM, ADVCOMP, CENTRIC, GEOProcessing, SEMAPRO, BIOSYSCOM, BIOINFO, BIOTECHNO, FUTURE COMPUTING, SERVICE COMPUTATION, COGNITIVE, ADAPTIVE, CONTENT, PATTERNS, CLOUD COMPUTING, COMPUTATION TOOLS, ENERGY, COLLA, IMMM, INTELLI, SMART, DATA ANALYTICS

issn: 1942-2679

International Journal On Advances in Internet Technology

ICDS, ICIW, CTRQ, UBICOMM, ICSNC, AFIN, INTERNET, AP2PS, EMERGING, MOBILITY, WEB

issn: 1942-2652

International Journal On Advances in Life Sciences

eTELEMED, eKNOW, eL&mL, BIODIV, BIOENVIRONMENT, BIOGREEN, BIOSYSCOM, BIOINFO, BIOTECHNO, SOTICS, GLOBAL HEALTH

issn: 1942-2660

International Journal On Advances in Networks and Services

ICN, ICNS, ICIW, ICWMC, SENSORCOMM, MESH, CENTRIC, MMEDIA, SERVICE COMPUTATION, VEHICULAR, INNOV

issn: 1942-2644

International Journal On Advances in Security

ICQNM, SECURWARE, MESH, DEPEND, INTERNET, CYBERLAWS

issn: 1942-2636

International Journal On Advances in Software

ICSEA, ICCGI, ADVCOMP, GEOProcessing, DBKDA, INTENSIVE, VALID, SIMUL, FUTURE COMPUTING, SERVICE COMPUTATION, COGNITIVE, ADAPTIVE, CONTENT, PATTERNS, CLOUD COMPUTING, COMPUTATION TOOLS, IMMM, MOBILITY, VEHICULAR, DATA ANALYTICS

issn: 1942-2628

International Journal On Advances in Systems and Measurements

ICQNM, ICONS, ICIMP, SENSORCOMM, CENICS, VALID, SIMUL, INFOCOMP

issn: 1942-261x

International Journal On Advances in Telecommunications

AICT, ICDT, ICWMC, ICSNC, CTRQ, SPACOMM, MMEDIA, COCORA, PESARO, INNOV

issn: 1942-2601